### **MDAG.com Internet Case Study 33**

## Thirty-One Years of Monitoring Minesite-Drainage Chemistry, During Operation and After Closure: The Bell Minesite, British Columbia, Canada

by K.A. Morin and N.M. Hutt

© 2010 Kevin A. Morin and Nora M. Hutt www.mdag.com/case\_studies/cs33.html

### **TABLE OF CONTENTS**

List of Tables	2
List of Figures	2
Abstract	4
1. INTRODUCTION	8
2. HISTORY OF THE BELL MINESITE  2.1 Pre-Operation  2.2 Operation  2.3 Closure  1	9 9
3. GEOLOGY, LAYOUT, AND MINESITE COMPONENTS	
5. LONG-TERM TRENDS IN FREQUENTLY ANALYZED DRAINAGE-CHEMISTRY PARAMETERS	
6. THE 2010 EMPIRICAL DRAINAGE-CHEMISTRY MODEL (EDCM) FOR THE BELL MINESITE	34
7. CONCLUSION	13
8. REFERENCES	4
Acknowledgments	16

APPENDIX A. Scatterplots, Histograms, Best-Fit Equations, and Standard Deviations for the 2010 Bell Empirical Drainage-Chemistry Model (EDCM)
<u>List of Tables</u>
3-1. Rock units and their estimated mined tonnages at Bell Mine
6-1. The 2010 Empirical Drainage-Chemistry Model (EDCM) for the Bell Minesite 3'
<u>List of Figures</u>
<ul> <li>3-1. Photograph of Bell Mine after closure, looking northeast towards Hagan Arm, with the safety berm and Collection Pond CP1-3 for the tailings impoundment in the lower centre</li></ul>
5-1. Histogram of pH at the Bell Minesite
Bell Minesite
5-5. Long-term temporal trend in aqueous pH and other concentrations in the pit, at the pit sump during operation and in the surficial pit-lake water after closure
5-8. Long-term temporal trend in aqueous pH and other concentrations in CP 1-3 below Dam 1
below Dam 1

#### Abstract

This Internet Case Study from MDAG.com compiles and reviews more than three decades of drainage-chemistry monitoring data at the Bell Minesite. These data ranged from mid operation in 1978, and include 17 years of closure to 2009. Based on this information, long-term trends in frequently analyzed parameters are shown, and an Empirical Drainage-Chemistry Model (EDCM) statistically linking parameters is created. We are grateful to Xstrata Copper for providing, through Pacific Booker Minerals, all data as one database, saving a great deal of time typing data from government-submitted annual reports.

Bell Mine formally opened in 1972 and closed in 1992, with two extended periods of inactivity. Rock was mined from a single pit, and delivered to various dumps, tailings-impoundment dams, and mine roads. Most ore rock was delivered to the mill for processing, and the resulting discharge was slurried to the tailings impoundment. However, some ore rock was reportedly used in tailings-dam construction in early years of mining, and minor quantities of low-grade ore rock were occasionally delivered to dumps and the low-grade stockpile through the years.

As a result, Bell Mine is now comprised of several minesite components, which have distinct hydrologic and hydrogeologic characteristics. Approximately 150,000,000 metric tonnes (97,000,000 m³) of geologic materials were mined at the site, of which tailings (ore rock) comprised approximately half, and the remaining two quarters were placed in the tailings dams and in rock dumps, respectively.

Long-term trends in frequently analyzed parameters showed that drainage chemistry was generally steady, and thus in local equilibrium, at some monitoring stations. However, pH and other parameters were changing at other stations due to remedial activities or natural geochemical evolution. Predictions made at the time of closure in 1992 indicated some locations would eventually evolve to acidic conditions many decades after closure, and this is apparently starting to happen.

Seasonal variability in recent years could not be assessed at many locations, because drainage samples were analyzed only once a year. At stations with more frequent analyses, seasonal variability occurred within definable long-term ranges of steady or gradually increasing or decreasing average concentrations.

For the 2010 Bell EDCM, scatterplots, histograms, best-fit equations, and standard deviations were compiled in Appendix A of this MDAG case study. The results are compiled in Table A below.

Table A. The 2010 Empirical Drainage-Chemistry Model (EDCM) for the Bell Minesite <sup>1</sup>			
Parameter <sup>2</sup>	<u>Conditions</u>	<u>Equation</u>	log(Std <u>Dev)</u>
	Net Acidity > +407.0 mg/L	pH = -0.950298*log(Acidity) + 5.77986	NA
11	+202.87 < NA < +407.0 mg/L	pH = -3.63689*log(Net Acidity) + 12.79111	NA
pН	-72.54≤NA≤+202.87 mg/L	pH = -0.0083512*(Net Acidity) + 6.09421	NA
	Net Acidity < -72.54 mg/L	pH = +1.43741*log(-Net Acidity) + 4.02560	NA
	pH < 3.3	log(Acidity) = -1.05232*pH + 6.08223	0.39142
Acidity	$3.3 \leq pH \leq 6.0$	log(Acidity) = -0.27496*pH + 3.51704	0.32292
	pH > 6.0	log(Acidity) = -0.49283*pH + 4.82426	0.31224
Alkalinity	pH ≥ 4.0	log(Alkalinity) = +0.69570*pH - 2.80060	0.35848
	Rock dumps and related drainages	$\log(SO4) = -0.022428*pH + 3.40071$	0.33829
Sulphate	Tailings and rock dams, pH<3.0	$\log(SO4) = -1.10924*pH + 6.69650$	0.32026
	Tailings and rock dams, pH≥3.0	$\log(SO4) = -0.027802*pH + 3.45219$	0.15797
Conductivity		log(Cond) = +0.70745*log(SO4) + 1.10225	0.1007
TDS	NA	NA	NA
Hardness		log(Hardness) = +0.98380*log(SO4) - 0.00500	0.17639
Fluoride	NA	NA	NA
Chloride	NA	NA	NA
Nitrate		Typically below detection; <3 mg/L before closure in 1992 and <2 mg/L after closure	NA
Nitrite		Typically below detection; <3 mg/L before closure in 1992 and <0.6 mg/L after closure	NA
Ammonia		Typically below detection; <2 mg/L	NA
Al-D		log(Al-D) = -0.82805*pH + 4.89619	0.64112
Sb-D	Near-neutral pH	Typically below detection; <0.0001 mg/L	NA
4.5	pH < 4.0	$\log(As-D) = -1.94657*pH + 4.69773$	0.96847
As-D	pH ≥ 4.0	log(As-D) = -3.08856 (0.0008155 mg/L)	0.50975
Ba-D		$\log(\text{Ba-D}) = -0.97620*\log(\text{SO4}) + 1.30754$	0.36521
n -	pH < 4.0	log(Be-D) = -0.77446*pH + 0.79682	0.35975
Be-D	pH ≥ 4.0	Near or below detection; <0.005 mg/L	NA

Parameter <sup>2</sup>	Conditions	<u>Equation</u>	log(Std <u>Dev)</u>
	Before closure in 1992	Near or below detection; < 1.1 mg/L	NA
Bi-D	After closure in 1992-2000	Near or below detection; <0.3 mg/L	NA
	After closure in 2001-2009	Near or below detection; <0.001 mg/L	NA
B-D		Typically below detection; <0.2 mg/L	NA
Cd-D	Near-neutral pH	Near or below detection; <0.0002 mg/L	NA
Ca-D		$\log(\text{Ca-D}) = +0.80815*\log(\text{SO4}) - 0.19749$	0.17105
C. D	pH < 4.0	log(Cr-D) = -1.83617*pH + 4.34466	0.58217
Cr-D	$pH \ge 4.0$	Near or below detection; <0.001 mg/L	NA
Co-D	Excluding 2009 data	$\log(\text{Co-D}) = -0.37796 * \text{pH} + 1.30330$	0.37595
	pH < 3.0	log(Cu-D) = -1.17265*pH + 5.37432	0.37011
Cu-D	$3.0 \leq pH \leq 5.5$	log(Cu-D) = -0.48982*pH + 3.32581	0.43962
	pH > 5.5	log(Cu-D) = -1.04518*pH + 6.38030	0.81956
E- D	pH < 4.0	log(Fe-D) = -1.55584*pH + 6.48218	0.6119
Fe-D	$pH \ge 4.0$ , oxidized Eh	log(Fe-D) = -0.48131*pH + 2.18405	0.66123
Pb-D		log(Pb-D) = -2.03560 (0.009213 mg/L)	0.62098
Li-D		Li-D < 0.1 mg/L	NA
Mg-D		log(Mg-D) = +0.98155*log(SO4) - 0.85568	0.18773
Mn-D		$\log(\text{Mn-D}) = -0.29027 * \text{pH} + 2.20133$	0.45138
Hg-D		Always below detection; <0.0005 mg/L	NA
Mo-D		log(Mo-D) = -1.19379 (0.0640  mg/L)	0.27549
Ni-D		log(Ni-D) = -0.45906*pH + 1.69877	0.40611
n n	pH < 5.0	$\log(P-D) = -0.95927*pH + 3.77252$	0.80015
P-D	$pH \ge 5.0$	log(P-D) = -1.02381 (0.09467 mg/L)	0.55378
K-D	Near-neutral pH	K-D < 75 mg/L	NA
So D	pH < 4.0	log(Se-D) = -1.4000*pH + 2.29897	NA
Se-D	$pH \ge 4.0$	Se-D < 0.0005 mg/L	NA
c: D	pH < 5.0	log(Si-D) = -0.30121*pH + 2.21879	0.23253
Si-D	$pH \ge 5.0$	$\log(\text{Si-D}) = -0.075708*pH + 1.10057$	0.19275
Ag-D		None; at/below detection; <0.0001 mg/L	NA

Parameter <sup>2</sup>	<u>Conditions</u>	<u>Equation</u>	log(Std <u>Dev)</u>
N. D	For rock piles and related drainages	$\log(\text{Na-D}) = +0.80747*\log(\text{SO4}) - 1.59772$	0.17161
Na-D	For tailings and related rock dams	$\log(\text{Na-D}) = +0.11537 * \text{pH} + 0.79938$	0.18605
	For rock piles and related drainages, with SO4≥1700 mg/L	log(Sr-D) = +1.43125*log(SO4) - 4.42770	0.17029
Sr-D	For rock piles and related drainages, with SO4<1700 mg/L	log(Sr-D) = +0.79763*log(SO4) - 2.38082	0.13069
	For tailings and related rock dams, with SO4 < 7000 mg/L	log(Sr-D) = +2.09647*log(SO4) - 6.25106	0.1963
Te-D		None; below detection; <0.001 mg/L	NA
Tl-D		None; below detection; <0.0001 mg/L	NA
m D	pH < 3.5	log(Th-D) = -2.0*pH + 3.7	NA
Th-D pH ≥ 3.5		<0.0005 mg/L	NA
Sn-D		None; below detection; <0.001 mg/L	NA
Ti-D, maximum		log(Max Ti-D) = -0.14162*pH - 0.89881	0.17712
W-D		NA	NA
U-D		log(U-D) = +1.27549*log(SO4) - 7.20752	0.21187
V D	pH < 3.5	$\log(V-D) = -1.500*pH + 3.2500$	NA
V-D	pH ≥ 3.5	None; typically below detection; <0.01 mg/L	NA
	pH < 3.0	log(Zn-D) = -1.08849*pH + 3.56852	0.34748
Zn-D	$3.0 \le pH \le 6.0$	$\log(\text{Zn-D}) = -0.15634 * \text{pH} + 0.77207$	0.40923
	pH > 6.0	log(Zn-D) = -0.98600*pH + 5.75002	0.77426
Zr-D	pH < 4.0	log(Zr-D) = -1.500*pH + 3.0000	NA
∠l-D	pH ≥ 4.05	None; typically below detection; <0.001 mg/L	NA

<sup>&</sup>lt;sup>1</sup> Based on data through 2009; non-minesite data like Babine Lake was not used; master parameters from which others were predicted were pH, sulphate, conductivity for sulphate only, and net acidity (acidity - alkalinity) for pH only; all concentrations are mg/L except pH (pH units) and conductivity (μS/cm); acidity, alkalinity, net acidity, and hardness are mg CaCO<sub>3</sub>/L; all logarithmic values are base 10.

<sup>&</sup>lt;sup>2</sup> "-D" indicates the information applies only to the dissolved (filtered) form.

#### 1. INTRODUCTION

A major issue for minesite-drainage chemistry is: how does drainage chemistry at a particular minesite or minesite component change through time, during operation and after closure? Although a relatively simple question, there are many ways to answer this (Morin and Hutt, 1997 and 2001).

If remedial activities such as removal of net-acid-generating rock or lime addition to acidic water are carried out, then, yes, drainage chemistry can change. Of greater interest here, though, are natural or non-remediation-induced changes. Over decades, how does pH, for example, evolve when not forced by ongoing human activity?

Because dozens of natural elements and related parameters (like hardness) appear on many water-quality guidelines around the world, changes in pH are not the only drainage-chemistry concerns at minesites. The more important and encompassing question is: how do aqueous concentrations of dozens of elements change through time, during operation and after closure? Obviously, each element can have a unique answer at each minesite or minesite component, but correlations among elements and parameters can simplify the work.

Based on detailed earlier work (Morin and Hutt, 1993a, 1997, 2000a, and 2001; Morin, 1994; Morin et al., 1993a, 1995a, 1995b, and 2001), aqueous equilibrium concentrations of some elements correlate with "master parameters" like pH, sulphate, and acidity. Under this concept, a change in a master parameter can trigger changes in many aqueous concentrations. Accordingly, our attention here focusses on: is a value for a master parameter, like pH, at one location associated with similar aqueous concentrations found at another location with a similar master-parameter value? If so, then as a master parameter changes at any location around a site, corresponding changes in dozens of other elements and parameters can also be estimated. In this way, concerns in spatial and temporal trends for dozens of elements can be simplified to trends for a few master parameters.

A compilation of correlations with master parameters, with temporal variabilities expressed as standard deviations, is called Empirical Drainage-Chemistry Models (EDCMs). To have reasonable confidence in an EDCM, hundreds to thousands of chemical analyses are often needed (Morin and Hutt, 1993a, 1997, 2000a, and 2001; Morin, 1994; Morin et al., 1993, 1995a, 1995b, and 2001; Day et al., 1996). Few minesites have such readily available databases containing decades of drainage-chemistry monitoring at many locations. Thus, there are few meaningful EDCMs. Unfortunately, there are even some inherently unreliable ones based on only a few dozen analyses per minesite (Day and Rees, 2006).

For the existing EDCMs, some elements were frequently to always below detection. In these cases, correlations with those elements could not be reliably assessed within the EDCM framework.

This MDAG case study compiles and reviews more than three decades of drainage-chemistry monitoring, during operation and after closure, at the Bell Minesite in British Columbia, Canada (Sections 2 through 4). From this information, spanning 1978 through 2009, long-term trends are shown for frequently analyzed parameters (Section 5), and an EDCM is created (Section 6). This work builds on earlier studies for the original closure plan and subsequent studies (Morin and Hutt, 1993b and 2000b).

#### 2. HISTORY OF THE BELL MINESITE

Bell Mine is located on the Newman Peninsula of Babine Lake, at coordinates 126° 15'W and 55°N. It is approximately 15 km north of the Village of Granisle, British Columbia, Canada.

### 2.1 Pre-Operation

This area of Babine Lake was initially explored in 1913 for veins with lead and zinc mineralization (BC Minfile, 2010). As a result, showings on the west shore of the peninsula (where Bell Mine is located) were staked by Mr. C. Newman in about 1913. Two adits, 12 and 20 metres long, were subsequently driven northeasterly at lake level.

Reconnaissance geophysics and anomalously elevated copper, from a soil geochemical survey in 1962, led Noranda Exploration Company to an area 800 metres northeast of the old adits (BC Minfile, 2010). This area and its claims were then restaked by Noranda. Detailed soil sand silt sampling was carried out in 1963 and 3 short drill holes put down, just short of the ore zone. The first drill hole put down in 1964 intersected the ore zone and during 1964 and 1965, 12,176 metres feet of diamond drilling were done in 132 holes. This work indicated 136,050,000 tonnes of ore averaging 0.5% copper, of which 46,000,000 tons averaging 0.5% copper could be mined by open pit. By 1967, mineable reserves of 42 million tonnes of ore had been defined grading 0.50 per cent copper, 0.35 grams per tonne gold and 1.0 grams per tonne silver, within an overall geological ore reserve of 116 million tonnes grading 0.48 per cent copper, 0.35 grams per tonne gold, 1.0 grams per tonne silver and less than 0.005 per cent molybdenum.

Design work for mining and milling began in 1966, but was suspended the following year (Minfile, 2010). Further exploration work, from 1966 through 1969, included geophysical and geochemical surveys and 17,677 metres of diamond drilling.

#### 2.2 Operation

In May 1970, Noranda Mines Limited began construction of facilities for a production rate of 10,000 tons per day (Morin and Hutt, 1993b). The mill was put into operation in October 1972. Mill capacity was increased in subsequent years. About one sixth of the mined rock graded 0.3 to 0.45 per cent copper ("low grade") and was stockpiled for later processing.

A strike closed the mine for a 29-week period during 1976. This was the first of two relatively long temporary closures of Bell Mine, with the other starting in 1982.

An October 1978, agreement to sell the property to Granby Mining Corporation, operator of the nearby Granisle Minesite, failed to receive approval of the Foreign Investment Review Agency. As a result, the sale agreement was terminated.

A \$20 million mine-mill expansion begun in May 1979 resulted in the mill capacity being

raised from 13,000 to 15,400 tonnes per day in the latter half of 1980. Open pit reserves at that time were reported as 40,384,000 tonnes with 0.52 per cent copper and 0.38 grams per tonne gold. With the purchase in November 1979, of the Granisle Minesite, about 8 kilometres to the southeast, both operations were combined to form the Babine Division of Noranda Mines Limited.

Due to low copper prices, both Bell and Granisle Mines closed in 1982, with Granisle closing permanently on July 2. Although reopening was considered for a few years afterwards, Granisle, unlike Bell Mine, never reopened due to lower ore grades. Bell Mine re-opened in 1985, and by the late 1980's mill production had increased to 19,000 tonnes per day. The mill operated under provincial permit PE1505 using reclaimed water from the tailings pond and additional fresh water from Babine Lake.

#### 2.3 Closure

Noranda estimated that the mine would close in June 1992 due to depleted ore reserves. The mine formally closed on April 12, 1992, about 20 years after initial mining.

Total ore production from 1972 to 1992 was 77,146,088 tonnes yielding 38,319,730 grams of silver, 12,885,964 grams of gold and 304,795,539 kilograms copper. Tonnages are discussed further in Section 3 of this MDAG case study.

Buildings have been removed from the minesite, and reclamation and revegetation are now in advanced stages. Poor-quality water is pumped to the pit from a series of collection ponds, and water-quality monitoring continues today.

#### 3. GEOLOGY, LAYOUT, AND MINESITE COMPONENTS

The climatic conditions at Bell Mine are typical of the continental climate of central British Columbia with long cold winters and cool summers. Average annual precipitation at the minesite is 513 mm, with snow accounting for about half as water equivalent. The topography of the site is rolling with maximum relief of roughly 120 meters. Because Bell Mine is located on and occupies much of a peninsula in Babine Lake, all runoff and groundwater at the minesite originate from precipitation (Figures 3-1 and 3-2). This simplifies local hydrology and hydrogeology.

The Bell Deposit is a porphyry copper deposit where plutonic rock intruded volcanic sediments. Following the intrusion, several episodes of hydrothermal alteration occurred, locally causing the consumption of some minerals and the formation of others. For example, a "halo" of pyrite was formed around the orebody, extending beneath the current location of Babine Lake. Another alteration episode resulted in the formation of carbonate minerals, but to a lesser extent than the pyrite halo. These alteration events are important to drainage chemistry, because they cut across rock types and thus pyrite formed in several rock types. Sulphide minerals identified at Bell Mine include pyrite, minor molybdenite, minor sphalerite, minor galena, chalcopyrite, minor bornite, chalcocite, and trace arsenopyrite. Carbonate minerals include calcite, ankerite, and siderite.

The geological studies at Bell Mine have identified seven primary rock types plus the relatively small 16 Ore Zone at the northwest wall of the pit (Tables 3-1 and 3-2). BFP (Biotite Feldspar Porphyry) was the dominant ore type.

At Bell Mine, mine rock was delivered to various dumps, tailings-impoundment dams, and mine roads (Figures 3-3 and 3-4, and Tables 3-3 and 3-4). Most ore rock was delivered to the mill for processing, and the resulting discharge was slurried to the tailings impoundment. However, some ore rock was reportedly used in tailings-dam construction in early years of mining, and minor quantities of low-grade ore rock were occasionally delivered to dumps and the low-grade stockpile through the years.

As a result, Bell Mine is now comprised of several minesite components (Figures 3-1 to 3-4, and Table 3-3 and 3-4), which have distinct hydrologic and hydrogeologic characteristics. A quantitative inventory of geologic materials showed that an estimated 97,000,000 m<sup>3</sup> of geologic materials were mined at the site, of which tailings comprised approximately half.

The Overburden Dump is composed of clay till with an estimated volume of  $3,000,000 \text{ m}^3$ . Mine rock in the remaining four dumps, including some cap rock and clay till, represents about  $23,800,000 \text{ m}^3$  or 37,120,000 tonnes. An additional 37,400,000 tonnes of rock are found in tailings dams.



Figure 3-1. Photograph of Bell Mine after closure, looking northeast towards Hagan Arm, with the safety berm and Collection Pond CP1-3 for the tailings impoundment in the lower centre.

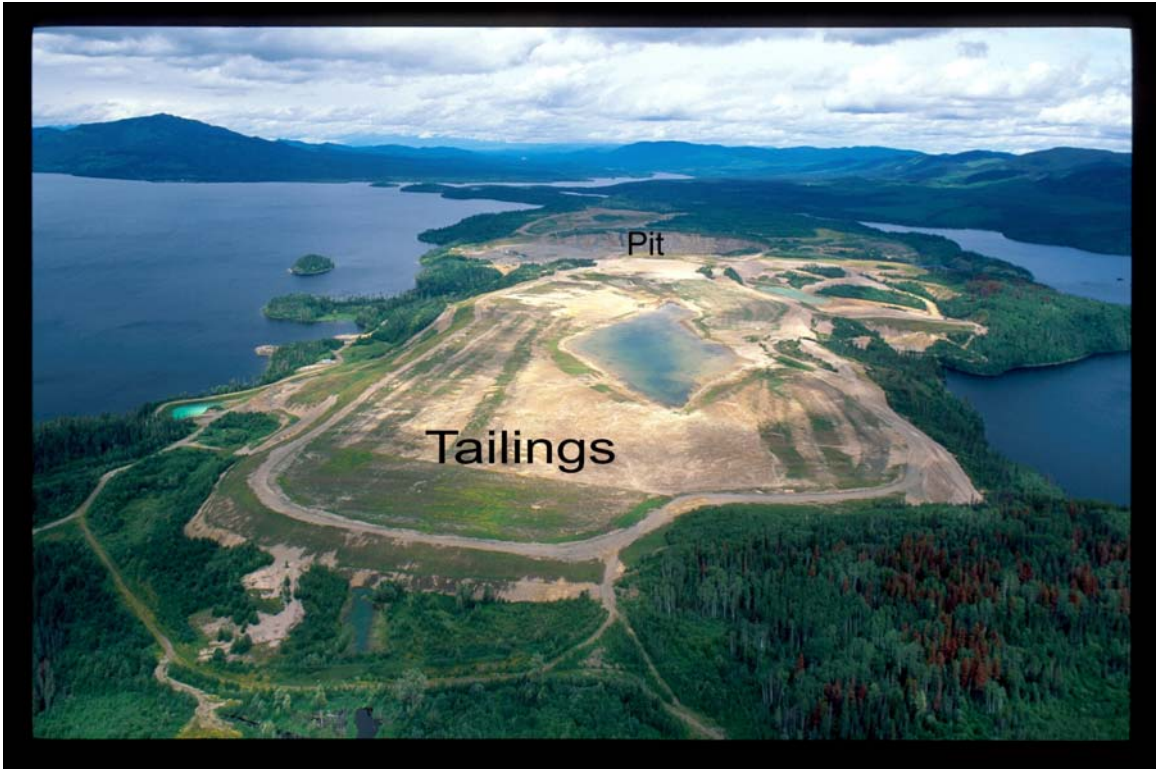


Figure 3-2. Photograph of Bell Mine after closure, looking north towards the pit, with the remnant tailings pond in the in the lower centre.

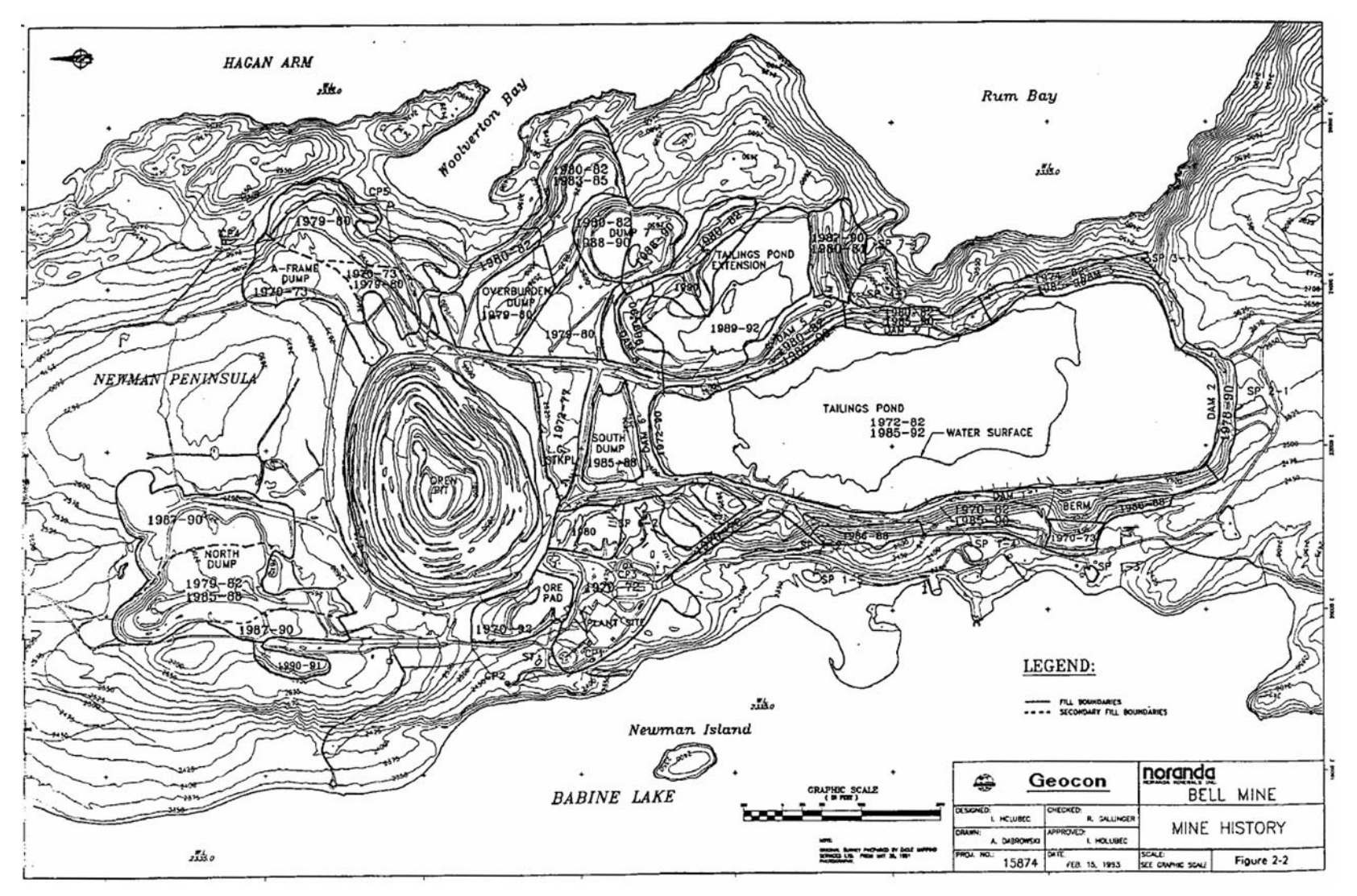


Figure 3-3. Map of Bell Mine from the original 1993 closure plan, showing minesite components and their years of active dumping and construction.

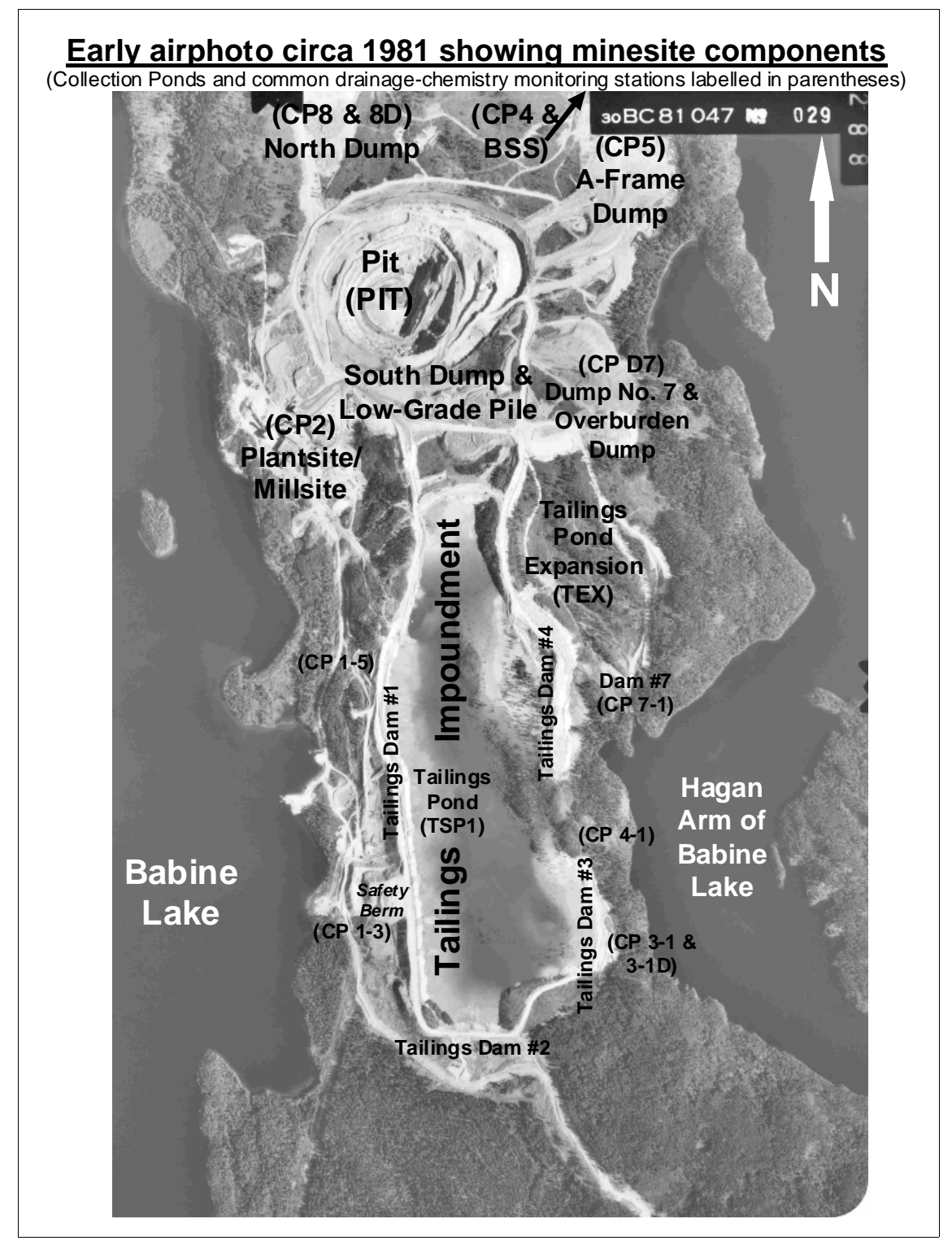


Figure 3-4. An airphoto taken around midpoint of Bell Mine's operating years, showing minesite components, and labelling (in parentheses) the common drainage-chemistry monitoring stations.

Table 3-1. Rock units and their estimated mined tonnages at Bell Mine (from Morin and Hutt, 1993b)				
Rock Unit	<u>Description</u>	Estimated Tonnage Delivered to Dump and Dams		
BFP (Biotite Feldspar Porphyry)	Dominant ore type; quartz, sericite, pyrite	6266000		
BBFP	Biotite and plagioclase phenocrysts in aphanitic matrix of intermediate composition	6266000		
RHYODACITE	Quartz, sericite, pyrite	15665000		
QFP (Quartz Feldspar Porphyry)	White sericite-pyrite rock	6,266,000		
SEDIMENTARY ROCK	Siltstones: clay, quartz, calcite, pyrite	15665000		
TUFF (COMBINED)	Similar to rhyodacites	12532000		
ANDESITE	no description	minor		
16 ZONE	no description	minor		

Table 3-2. General mineralogy of Bell Mine rock units (from Morin and Hutt, 1993b)						
	Quartz/silica (%)	Sericite/clay (%)	Pyrite (%)	Copper (%)	Calcite (%)	Secondary precipitants
Rhyodacite	70	20	10	0.17		jarosite, hematite, melanterite
Sedimentary	25	60	8	0.14	7	
Tuff	high	high	~10	~0.2		
BBFP (waste)			3	0.14		
QFP			6	0.08	some	
BFP (waste)	high	high	8	0.2		

Table 3-3. Minesite components receiving rock or tailings at the Bell Minesite (from Morin and Hutt, 1993b)			
<u>Component</u>	Estimated Volume (m³)	Estimated Weight (tonnes) <sup>1</sup>	
No. 7 Dump (D7)	5960000	9300000	
North Dump (ND)	6040000	9420000	
A-Frame Dump (AF)	4520000	7050000	
South Dump (SD)	7280000	11360000	
Overburden Dump	3000000	4680000	
Mine rock in tailings dams	24000000	37400000	
Tailings (two areas, TP/TEX)	45000000	71100000	
<sup>1</sup> As metric tonnes, calculated from an average bulk density of 1.56 t/m <sup>3</sup> based on data for			

mine rock, cap rock, and clay till and 1.58 t/m³ for tailings in the Closure Plan.

Table 3-4. Average rock-unit composition of Bell Mine rock dumps (from Morin and Hutt, 1993b)					
	<u>North</u>	A-Frame	<u>South</u>	Low Grade	Ore <sup>1</sup>
Rhyodacite (%)	10%	70%	25%	40%	55%
QFP (%)			72.5%		
BFP (%)	25%	25%		3.5%	40%
BBFP (%)	25%			20%	
Tuff (%)		5%	2.5%	36.5%	5%
Sedimentary (%)	40%				
TOTAL	100%	100%	100%	100%	100%
Pyrite	2.5%	2.4%	2.8%	3.2%	5.9%
Copper	0.12%	0.21%	0.13%	0.24%	0.57%
Calcite	some	none	low-moderate	very low	none - slight
Secondary minerals	gypsum, limonite, chalcanthite?	limonite, hematite	limonite, magnetite, [molybdenite]	limonite, malachite?, magnetite	

One-time temperature profiles in drillholes within the rock dumps and dams, during warm days in the early 1990's, did not detect any internal temperatures above 30°C. It was not clear if the elevated temperatures around 25-30°C, detected within 6 m below surface, were mostly attributable to sulphide oxidation or solar heating. One drillhole, in Tailings Dam #1 near CP 1-3 (Figures 3-3 and 3-4), was above 25°C to a depth of about 12 m, and was more likely due to sulphide oxidation. Despite these limited one-time drillhole temperatures, thermal venting from various dumps, attributable to sulphide oxidation, had been reported during winter months by employees. Thus, elevated internal temperatures may have been more widespread than detected by the drillholes.

# 4. THE DRAINAGE-CHEMISTRY DATABASE FOR THE BELL MINESITE THROUGH 2009

The Bell Minesite is currently owned by Xstrata Copper. Monitoring data for minesite-drainage chemistry and water quality are maintained in a single database, for various stations (in parentheses in Figure 3-4). This database contains data extending back to June 1976 for Babine Lake shoreline, and to January 1978 for the minesite, more than 30 years.

Monitoring data for Bell Mine are regularly provided to government and regulatory agencies in annual reports. However, Xstrata Copper was very helpful by providing the single database to us through Pacific Booker Minerals, so that manual typing of annual data was not necessary.

The Bell database was checked and corrected for noticeable errors, through statistics and scatterplots. For example:

- measured pH ranged from 0.3 (unlikely) to 2486 (basically impossible in natural waters);
- electrical conductivity normally reported as  $\mu S/cm$  was apparently divided by 10, 100, or 1000 on some dates, perhaps reflecting mS/cm for the 1000-times factor; and
- analyses for total dissolved solids (TDS) were apparently combined with total suspended solids (TSS).

Obvious corrections were made, but uncertain corrections were simply deleted. Other possible errors, like incorrect entries of trace-element concentrations, were not checked, and would require original analytical certificates.

Other important aspects of the database are as follows.

- First, detection limits tended to decrease (but not consistently) by up to orders of magnitude through the decades, although detection limits in a particular year sometimes varied by sample. For elements frequently close to or below detection, this made interpretations difficult (Section 6).
- Second, analyses of some elements did not always include one or more of the "master parameters" (Sections 5 and 6), so that the number of individual analyses did not always match the number of data pairs for correlations.
- Third, acidity can be a master parameter at some minesites, like the nearby Granisle Minesite (Morin and Hutt, 2010), but few acidity analyses were made outside the period of 1987 to 1991 during closure studies. Thus, acidity could not be used as a master parameter at Bell Mine.
- Fourth, in recent years, drainages from some stations were only analyzed once a year, precluding an assessment of seasonal variability for them.
- Fifth, due to insufficient analyses, trends could not be assessed for chloride (7 values) and fluoride (1 value).
- Sixth, total organic carbon (TOC) is not addressed in detail here, but ranged from 0.83 to 60 mg/L, with an average of 7 mg/L.

# 5. LONG-TERM TRENDS IN FREQUENTLY ANALYZED DRAINAGE-CHEMISTRY PARAMETERS

As asked in Section 1 of this MDAG case study, how does drainage chemistry at a particular minesite or minesite component change through time, during operation and after closure? Obviously, remedial activities can force a change. At the Bell Minesite, disruptive remedial activities are ongoing, but were most intensive around closure, in the late 1980's and early 1990's. However, where left relatively undisturbed, how did minesite-drainage chemistry with its dozens of elements and parameters evolve at the Bell Minesite?

For the Bell Minesite, only a few elements (dissolved copper, iron, zinc, and sulphate) and parameters (pH) were measured frequently and regularly for at least 15 years. For example, in the Bell database, there are approximately 5700 measurements of dissolved copper and pH, and more than 4700 analyses of dissolved zinc. A few other elements and parameters, like dissolved calcium, acidity, and electrical conductivity were also measured more than 1000 times, but only over a shorter period of a few or several years. This Section focusses on those long-term few to delineate geochemical evolution. Through correlations, however, changes in pH and sulphate (long-term "master parameters") are indicative of changes in the others, which is discussed in more detail in Section 6.

Before discussing the long-term trends, some concepts require clarification: equilibrium and bimodal pH distributions. First, in this MDAG case study, "equilibrium" encompasses thermodynamic equilibrium, metastable equilibrium, dynamic equilibrium, pseudo-equilibrium, and emergence, which cause aqueous concentrations to fluctuate around an annual average within a definable and repeating standard deviation. Second, minesites with both acidic and near-neutral drainages typically display a bimodal distribution of pH at preferred acidic and near-neutral ranges. The causes for this distribution and the preferred ranges, such as equilibrium, are discussed in Morin and Hutt (2008). The Bell Minesite database shows a subdued bimodal distribution (Figure 5-1), with the acidic peak relatively lower than the nearby Granisle Minesite (Figure 5-2).

Bell Minesite monitoring stations with long-term data did not show many long-term stable trends in pH at some stations (combined together in Figure 5-3 and discussed separately below). This was in contrast to the nearby Granisle Minesite, with more stable and less variable pH at many stations (Morin and Hutt, 2010). Aqueous sulphate was more stable (Figure 5-4), probably due to gypsum solubility.

The pit walls at Bell Mine contained both net-neutralizing and net-acid-generating rock (Morin and Hutt, 1993b). As a result, the pH of the pit sump during operation was variable between roughly 6.0 and 8.0 (Figure 5-5), with one anomalous value near 4.6 in 1989. Immediately after closure, pit-sump pH began falling and reached its lowest pH of 3.6 in early 1993.

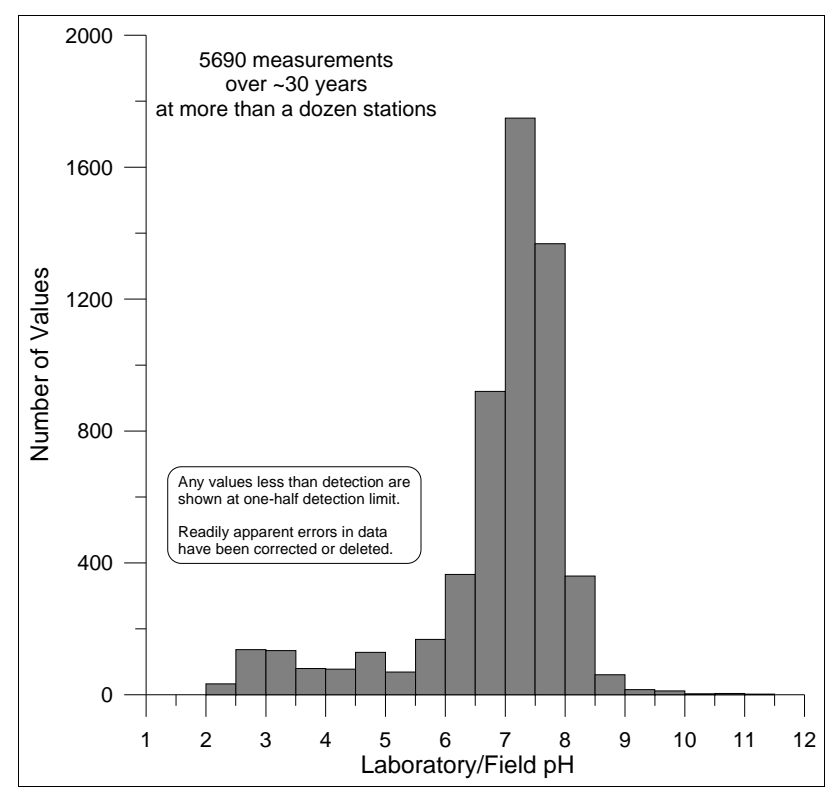


Figure 5-1. Histogram of pH at the Bell Minesite (5690 values).

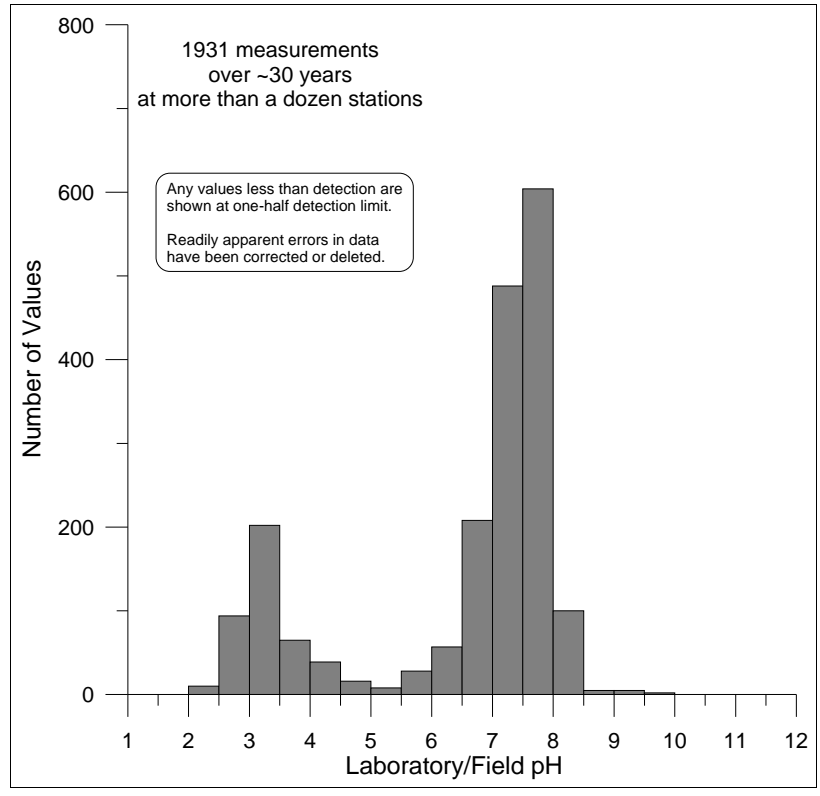


Figure 5-2. Histogram of pH at the Granisle Minesite (1931 values).

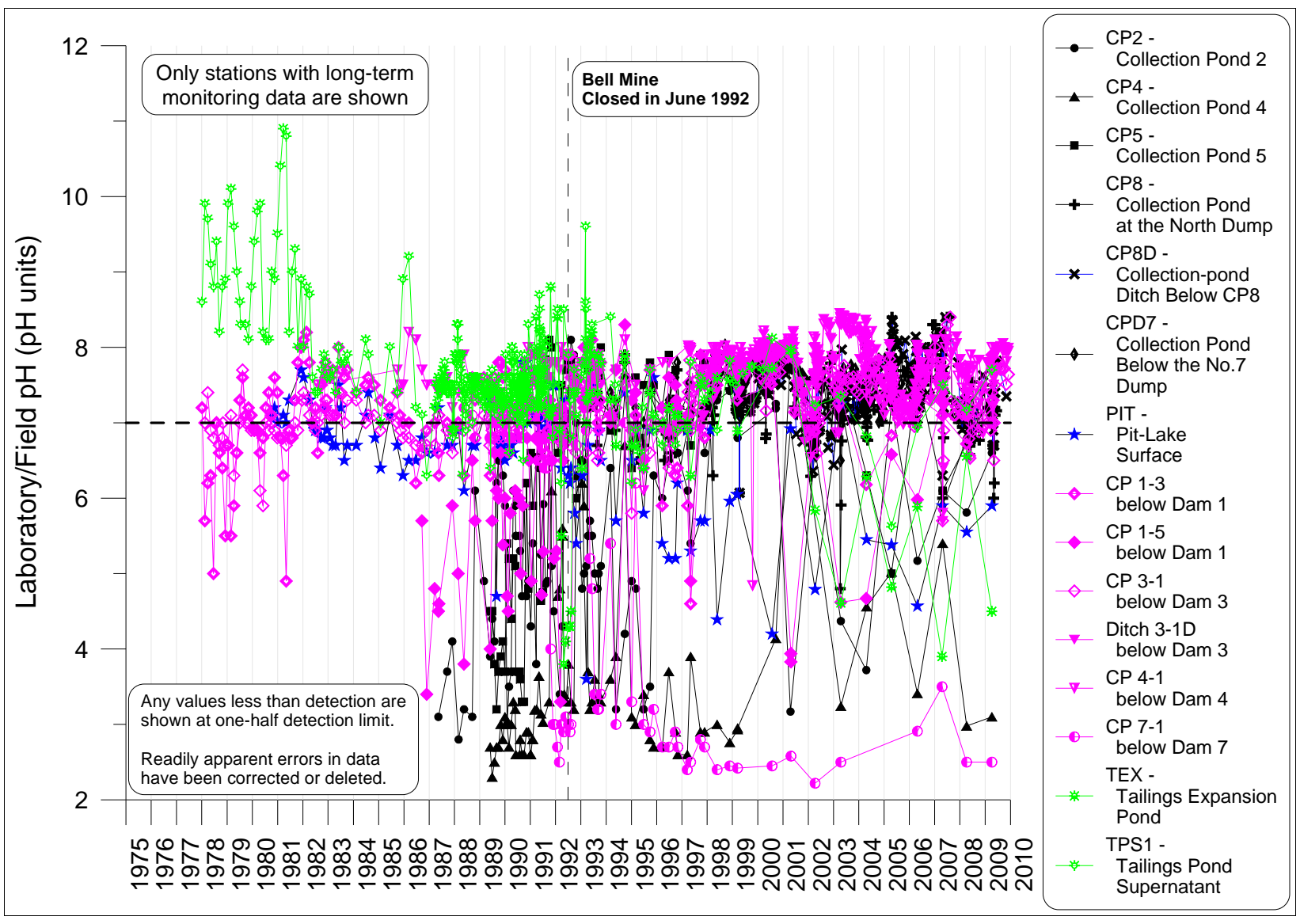


Figure 5-3. Long-term temporal trends in aqueous pH at various monitoring stations at the Bell Minesite.

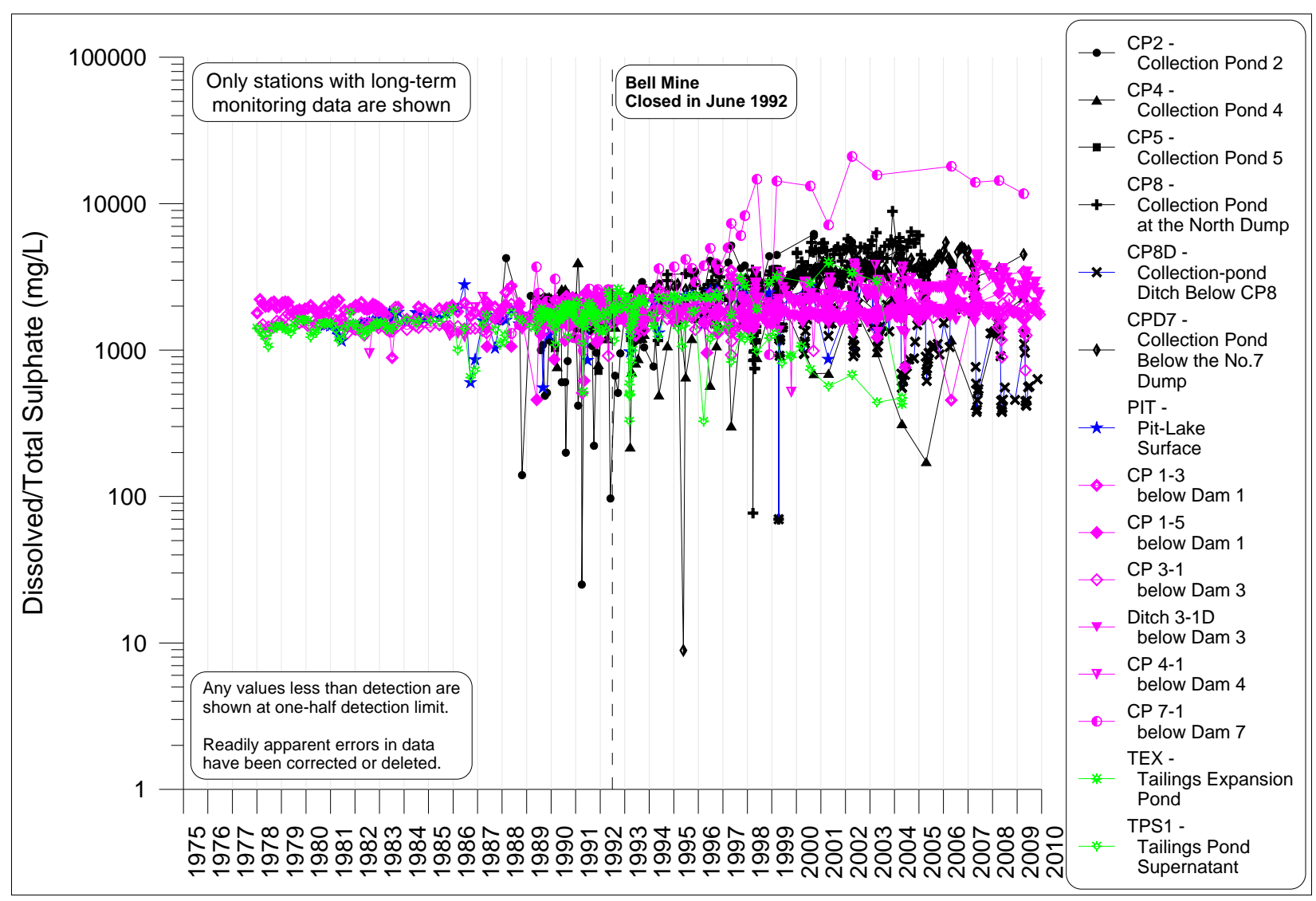


Figure 5-4. Long-term temporal trends in aqueous sulphate at various monitoring stations at the Bell Minesite.

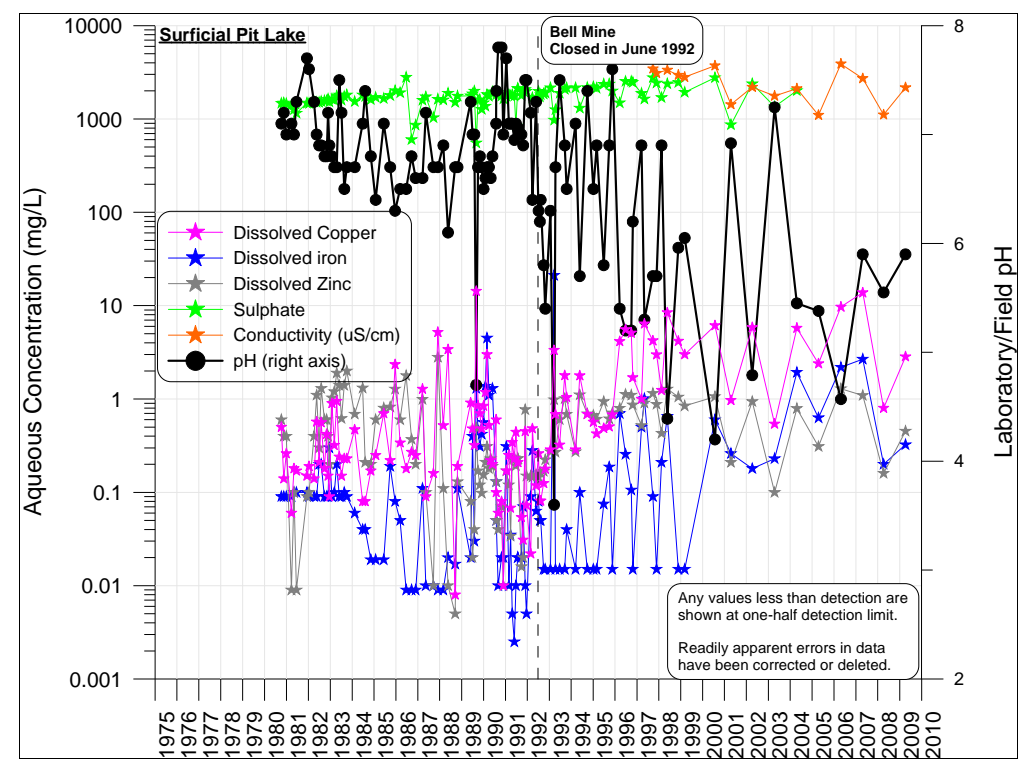


Figure 5-5. Long-term temporal trend in aqueous pH and other concentrations in the pit, at the pit sump during operation and in the surficial pit-lake water after closure.

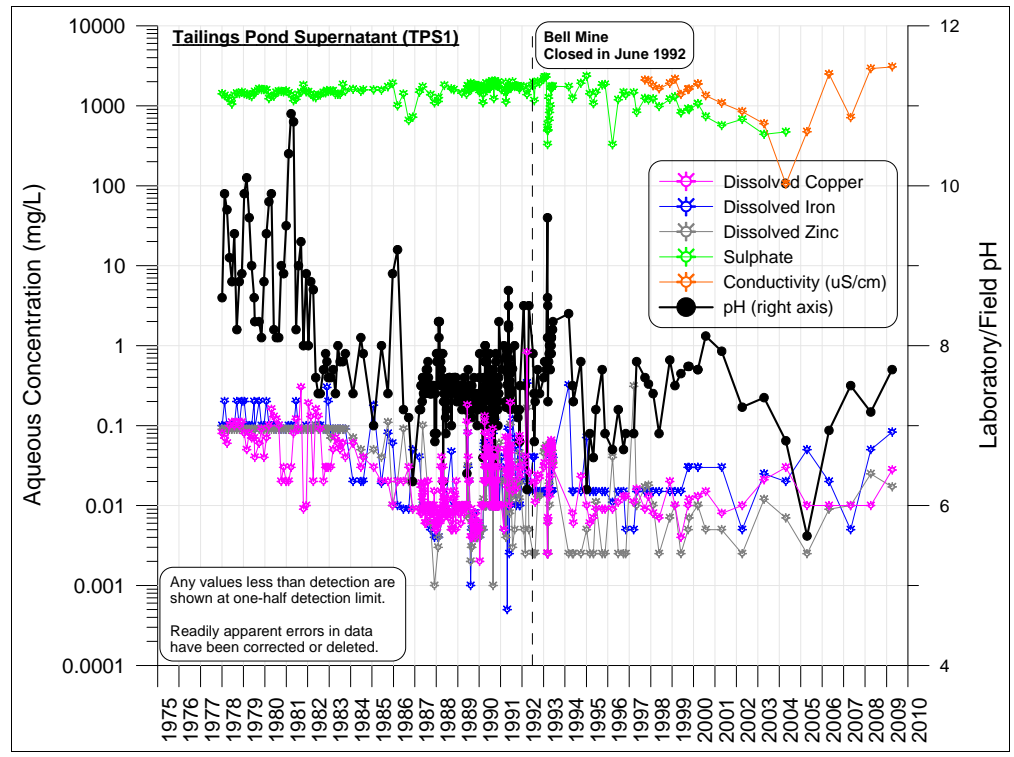


Figure 5-6. Long-term temporal trend in aqueous pH and other concentrations in the tailings pond.

Since then, near-neutral high-copper and acidic water have been pumped into the pit as it fills. As a result, the pH of the pit lake is predicted to fall to 2.7 after several decades as more drainages become acidic. The monitoring data since closure has been primarily for the surficial pit-lake water affected daily by variable precipitation, local runoff, and pumping. Thus, surficial pH has been variable after 1993 (Figure 5-5), but more generally acidic than during operation. This was accompanied by generally higher concentrations of dissolved copper and zinc, and variable but generally steady sulphate, conductivity, and dissolved zinc. Recent seasonal variability in surficial pit-lake pH cannot be assessed, because samples were analyzed only once annually in the last decade.

During operation, the tailings pond received effluent from the mill, as well as poor-quality drainages and ARD from the minesite. Water was recirculated to the mill, and any excess was discharged into Babine Lake. Because of this, the tailings pond was used during operation as a water-treatment facility, with pH actively managed by lime to raise pH as needed and to lower copper levels to meet discharge criteria. This can be seen in some early pH values around 10.0 and later pH management during late operation around pH 7.0-8.0 (Figure 5-6).

After closure, the tailings pond received only direct precipitation and seepage from surrounding higher tailings beaches. In recent years, the tailings pond has also occasionally received some pumpage from seepage collection pond CP 3-1 (Figure 3-4) as its drainage quality declined (discussed below). These inputs have increased the variability in pond pH after closure (Figure 5-6), often between 6.5 and 8.0. The exception is the lowest pH of 5.6 measured in April 2005, probably reflecting the input of dilute precipitation and snowmelt rather than concentrated ARD. However, the once-a-year sampling since 2000 cannot reasonably show seasonal variability as earlier data did.

In the tailings pond, detection limits for dissolved metals were lower after 1983 (note the horizontal bars in Figure 5-6 at 0.1 mg/L before 1984, representing half the detection limit). Since 1993, dissolved copper and zinc have been generally steady within definable ranges; dissolved iron may be gradually increasing; and sulphate with its surrogate indicator of conductivity show a decrease through 2004 and then an increase.

The rock dams surrounding the tailings impoundment contain net-acid-generating rock (Morin and Hutt, 1993b), and thus the chemistry of tailings seepage passing through the dams can be altered to lower pH and higher aqueous concentrations. The surrounding seepage collection ponds with long-term monitoring records are CP 1-3 and 1-5 below Dam 1, CP3-1 and the ditch below it (3-1D) below Dam 3, and CP 4-1 below Dam 4 (Figures 3-4 and 5-7). During operation, CP 1-5 had the lowest and most acidic pH (Figure 5-7). After closure and with less seepage from the tailings, pH in CP 1-5 became more consistent with the tailings pond around pH 7, but CP 1-5 and 1-3 still occasionally received ARD with pH below 5.0. Concentrations of dissolved metals generally changed inversely with pH (Figures 5-8 and 5-9), and this correlation with pH is discussed in more detail in Section 6.

The 1993 closure plan predicted Dam 1 would become consistently net acidic sometime between 1999 and 2030 (Morin and Hutt, 1993b), with a mean prediction of 2014. At this time, there are no clear signs of impending net acidity at CP 1-3 and 1-5 (Figures 5-8 and 5-9), but the elevated conductivity and sulphate in recent years indicate concentrations may be increasing.

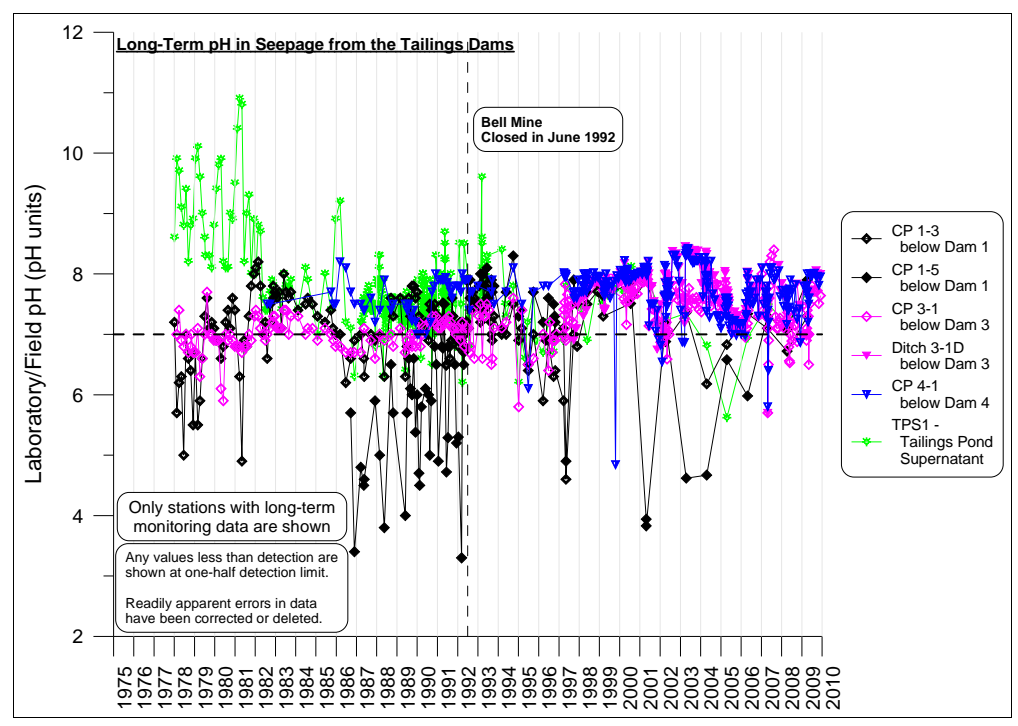


Figure 5-7. Long-term temporal trend in aqueous pH in seepage collection ponds along the east side (Dam 1) and west side (Dams 3 and 4) of the tailings impoundment.

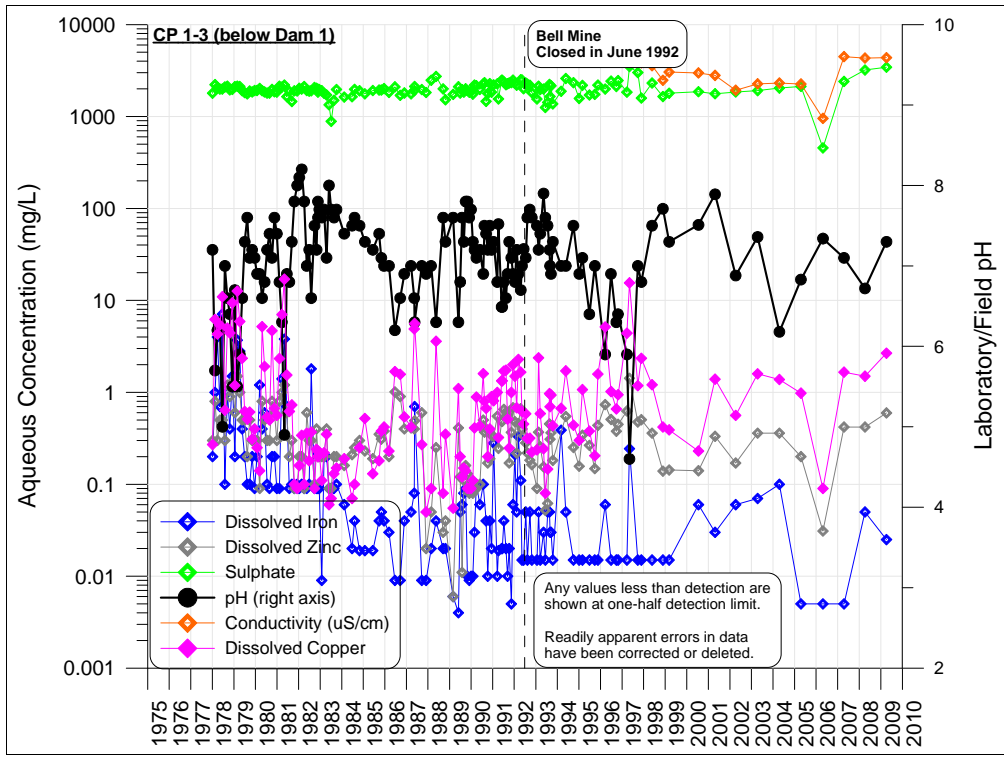


Figure 5-8. Long-term temporal trend in aqueous pH and other concentrations in CP 1-3 below Dam 1.

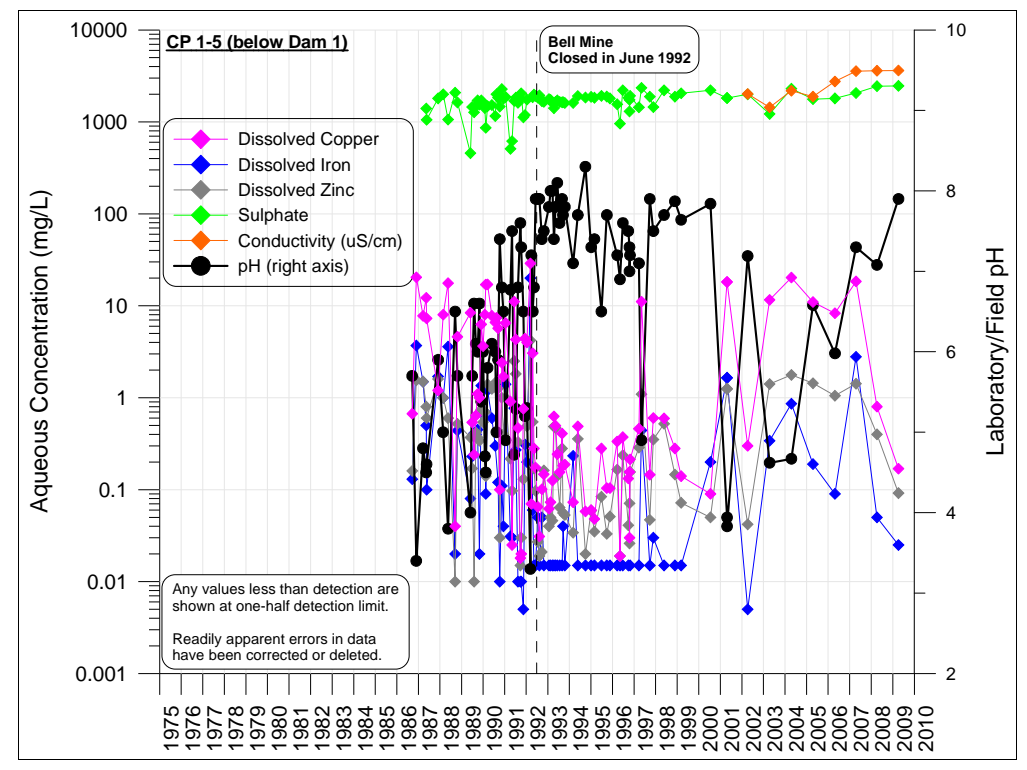


Figure 5-9. Long-term temporal trend in aqueous pH and other concentrations in CP 1-5 below Dam 1.

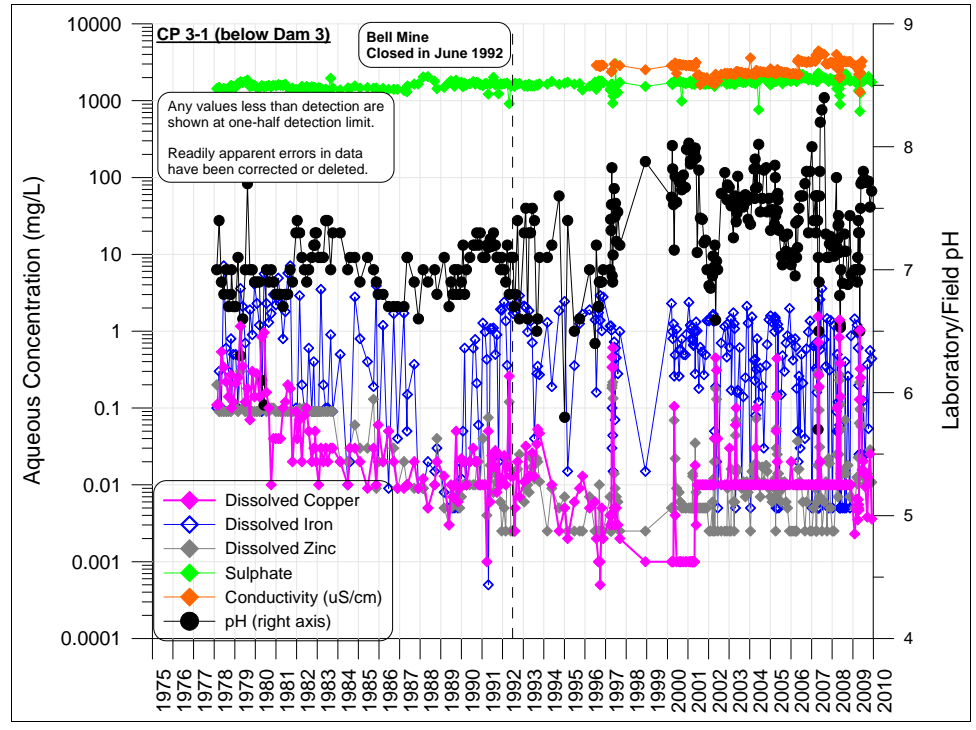


Figure 5-10. Long-term temporal trend in aqueous pH and other concentrations in CP 3-1 below Dam 3.

On the east side of the tailings impoundment around Dams 3 and 4 (Figure 3-4), pH has been measured more frequently after closure than on the west side (Figure 5-7). Also, on the east side, pH has not been as low since closure and was typically above 7.0. However, seepage collection pond CP 3-1 has produced some acidic pH values (Figure 5-10). This is part of a long-term, gradually downward pH trend in recent years, associated with occasionally higher concentrations of dissolved copper. As a result, in recent years, water from CP 3-1 has sometimes been pumped into the tailings pond, rather than released into Babine Lake through the discharge ditch at 3-1D (Figure 5-11). The 1993 closure plan predicted Dam 3 would become consistently acidic between 2009 and 2047, with a mean prediction of 2029.

Also on the east side, below Dam 4, CP 4-1 has produced one acidic pH below 6.0, in 2007 (Figure 5-12). This was not associated with a major peak in dissolved metals, but with an increase in sulphate and conductivity. Levels then returned to previous ranges, so no consistent ARD is expected at CP 4-1 soon.

To the east of the tailings impoundment (Figure 3-4), the Tailings Expansion Pond (TEX) was built in the last years of operation, in the hope that operation would continue and more tailings would be placed in it. A major confining dam for TEX is Dam 7. When Bell Mine closed in June 1992, only a small amount of tailings had been placed in TEX, but acid generation and metal leaching had started. Although pH was erratic but near neutral in TEX during operation and for years after closure (Figure 5-13), it became consistently more acidic in 2002 with annually measured pH averaging around 5.5. This was accompanied by generally increasing trends in dissolved elements and conductivity.

Meanwhile, the seepage collection pond CP 7-1 below Dam 7 began releasing the strongest ARD seen at Bell Mine (Figure 5-14). After a commonly observed warning trend of highly variable pH through 1995 accompanied by increasing sulphate, pH fell almost consistently below 3.0, except for the one measurement in 2007 of 3.5.

At its worst, pH in CP 7-1 was 2.15, and maximum concentrations were 21,000 mg/L for dissolved sulphate, 228 mg/L of dissolved copper, 2520 mg/L of dissolved iron, and 19.7 mg/L of dissolved zinc (other elements were not analyzed as frequently after closure). The last two annual pH measurements were 2.50 and 2.58. Although variable, the ARD at CP 7-1 has been generally stable within definable ranges since 1998. Thus, this drainage is not quickly evolving into stronger or weaker ARD at this time.

The A-Frame Waste-Rock Dump lies to the east-northeast of the pit (Figure 3-4), and was one of the first minesite components constructed along with Tailings Dam 1 (Figure 3-3). Drainage from the A-Frame Dump was also the first reported ARD at Bell Mine, apparently detected a few years after initial mining. These acidic conditions reportedly precluded the processing of the low-grade ore placed there. Collection ponds CP4 and CP5 collect A-Frame drainage, where it is then pumped to the pit. During operation, CP4 produced the most acidic ARD with pH as low as 2.3 in 1989 (Figure 5-15). However, associated concentrations were notably lower than the worst for CP 7-1 after closure, except dissolved copper reaching a maximum of 600 mg/L. Towards the end of operation, some pH measurements in CP 4 reached near-neutral levels (Figure 5-15).

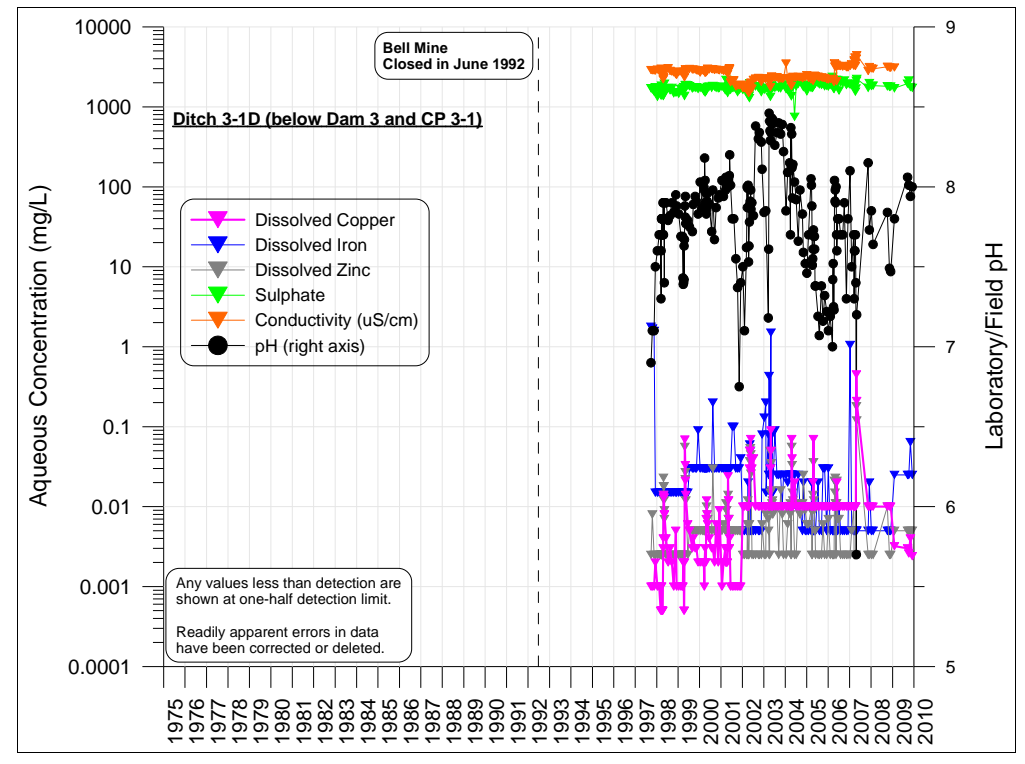


Figure 5-11. Long-term temporal trend in aqueous pH and other concentrations in Ditch 3-1D below Dam 3 and CP 3-1.

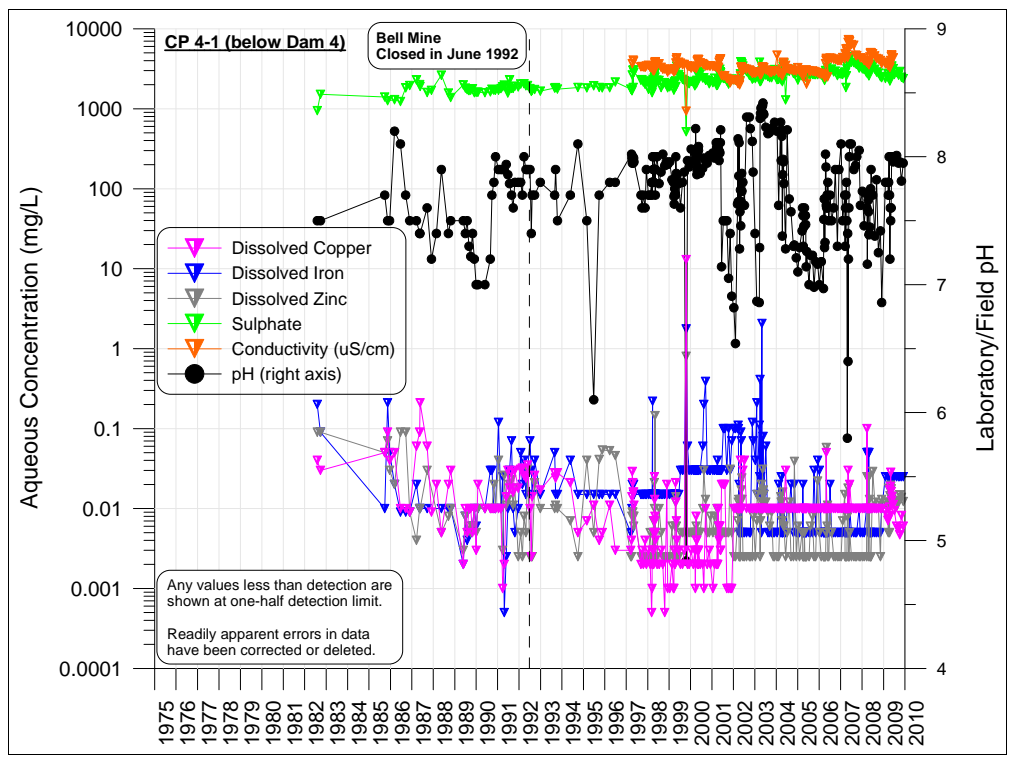


Figure 5-12. Long-term temporal trend in aqueous pH and other concentrations in CP 4-1 below Dam 4.

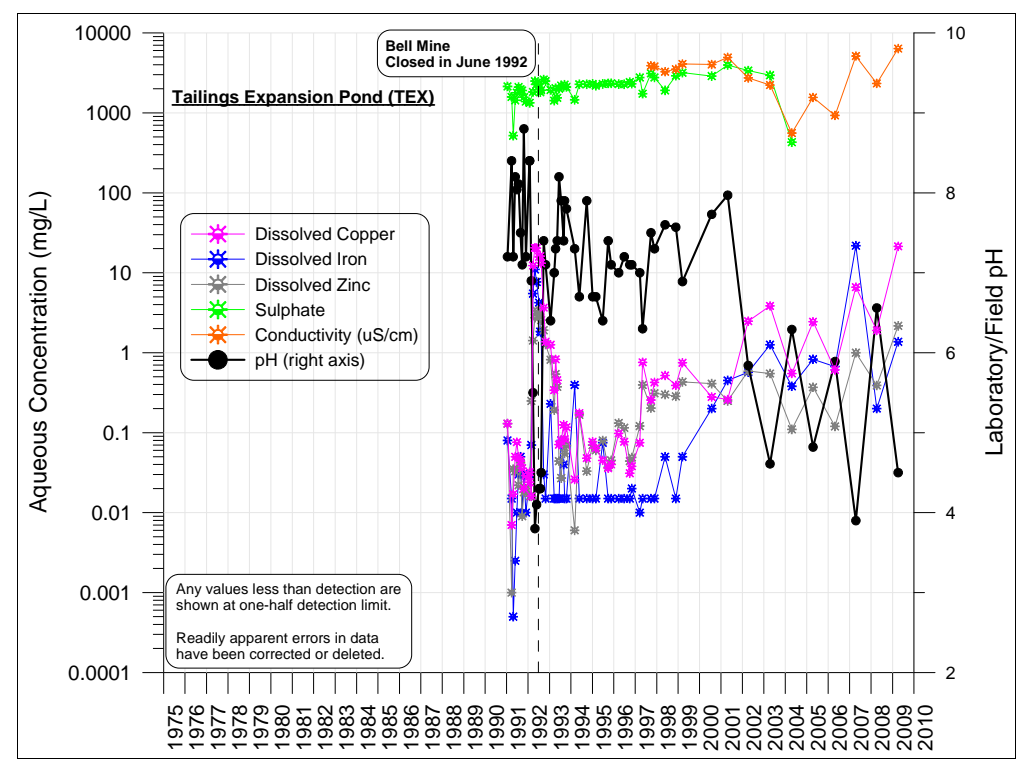


Figure 5-13. Long-term temporal trend in aqueous pH and other concentrations in the Tailings Pond Expansion (TEX) area.

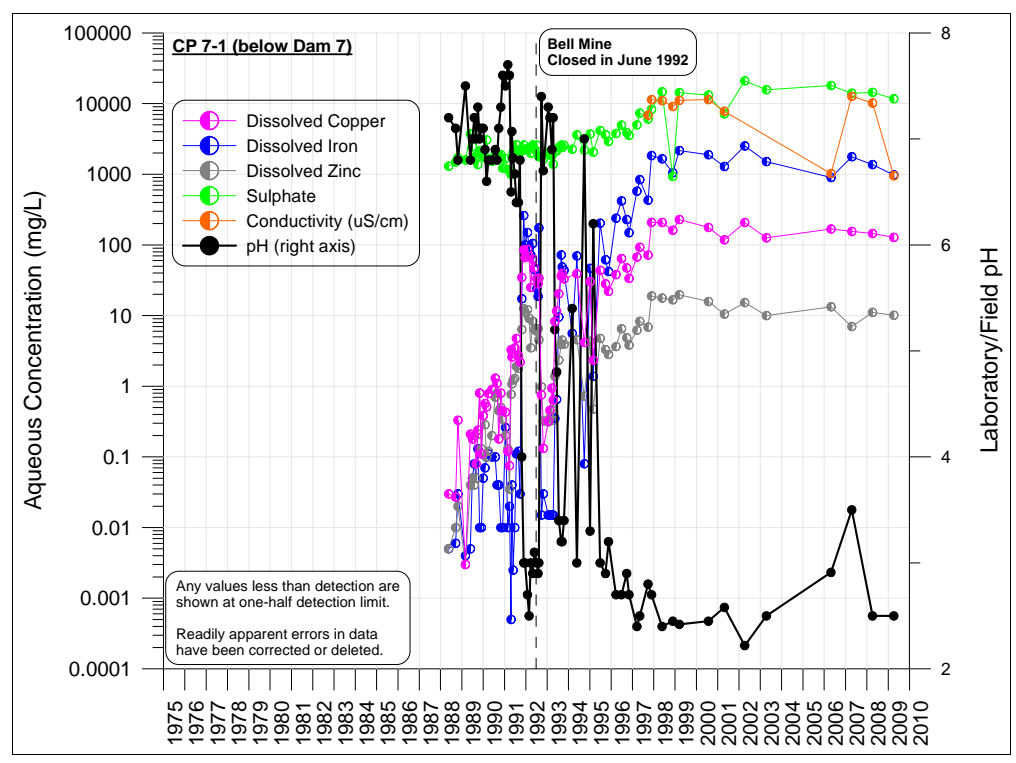


Figure 5-14. Long-term temporal trend in aqueous pH and other concentrations in CP 7-1 below Dam 7 and TEX.

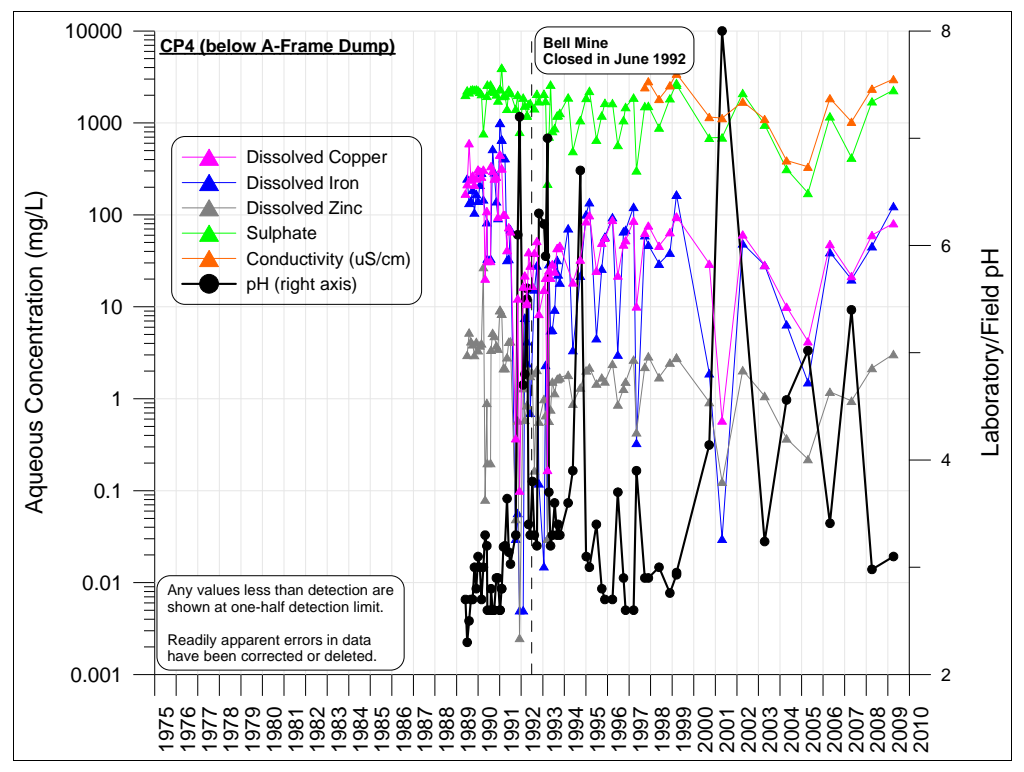


Figure 5-15. Long-term temporal trend in aqueous pH and other concentrations in CP4 below the A-Frame Dump.

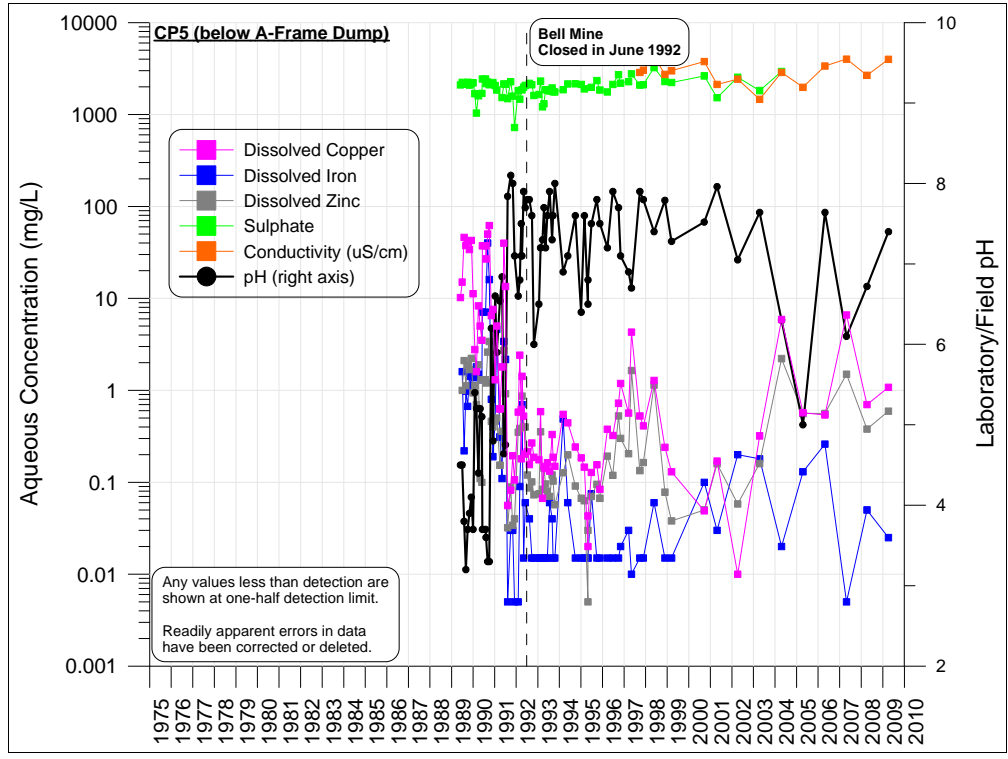


Figure 5-16. Long-term temporal trend in aqueous pH and other concentrations in CP5 below the A-Frame Dump.

However, after closure, CP4 became acidic below pH 3 again (Figure 5-15). Based on oncea-year measurements, CP4 has averaged around pH 4, with the last two years producing pH 3.0 and 3.1. Other parameters have generally varied inversely with pH, which is discussed further in Section 6 of this MDAG case study.

Compared to CP4, acidic CP5 also became near neutral around closure (Figure 5-16), but remained so for about a decade after closure. This may be the result of the resloping, soil capping, and remedial activity above CP5. However, starting with the annual sample in 2004, CP5 has occasionally produced more acidic pH and higher concentrations of dissolved copper and zinc. Conductivity may also show a recent, gradual upward trend.

Waste-rock dump D7 lies to the east-southeast of the pit (Figure 3-4). The closure plan predicted its drainage would become acidic between 2002 and 2047 (Morin and Hutt, 1993b), with a mean prediction of 2023. Since closure through 2006, the seepage collection pond CPD7 below this dump has typically produced water between pH 7.0 and 8.0 (Figure 5-17), with some intervals down to approximately 6.5. However, in 2007, the single annual pH value was below 6.0, accompanied by spikes in dissolved copper and zinc, but pH recovered the following two years. This, combined with a gradual trend of increasing sulphate and conductivity in the last decade, suggests the drainage from D7 Dump is evolving towards ARD.

At closure, a substantial amount of broken ore and waste rock could be found around the millsite and plantsite (Figure 3-4). As a result, pH in the downgradient collection pond CP2 was occasionally as low as 3.0 (Figure 5-18). Around closure, remedial activities removed much of the loose rock from this area, and pH up to around 8 was measured in CP2. However, after closure, pH again fell to acidic levels, additional remediation was undertaken through roughly 2000, and pH again improved to near-neutral levels. Since then, each annual measurement of pH has been notably different, but with a general trend towards near-neutral levels. This highlights the difficulties and the long-term delay that can arise upon remediation of net-acid-generating materials.

In the last 15 years at CP2 (Figure 5-18), dissolved metals generally displayed an inverse pattern during sharp pH changes. This inverse correlation with pH is discussed further in Section 6. Overall, dissolved metals and conductivity in CP2 showed generally increasing levels in the last 15 years, so drainage chemistry is expected to worsen, with the water pumped to the pit.

CP8 is located north of the North Dump (Figure 3-4), and monitors its drainage. The 1993 closure plan predicted the North Dump drainage would become acidic between 2007 and 2042 (Morin and Hutt, 1993b), with a mean prediction of 2023. Although the ditch (CP8D) that carries released water from CP8 has typically been between pH 6.5 and 8.5 (Figure 5-19), the pond itself (with water pumped to the pit when unacceptable for release to CP8D) has had a few measurements around 6.0 and lower to 4.8 (Figure 5-20). These were measured early in the annual periods, suggesting a spring "flushing" of some ARD, which included some peaks of dissolved metals. Furthermore, since 2007, pH has generally fallen from above 7.5 to around 7.0. Combined with general trends of increasing conductivity and sulphate, this suggests North Dump drainage is actively becoming acidic.

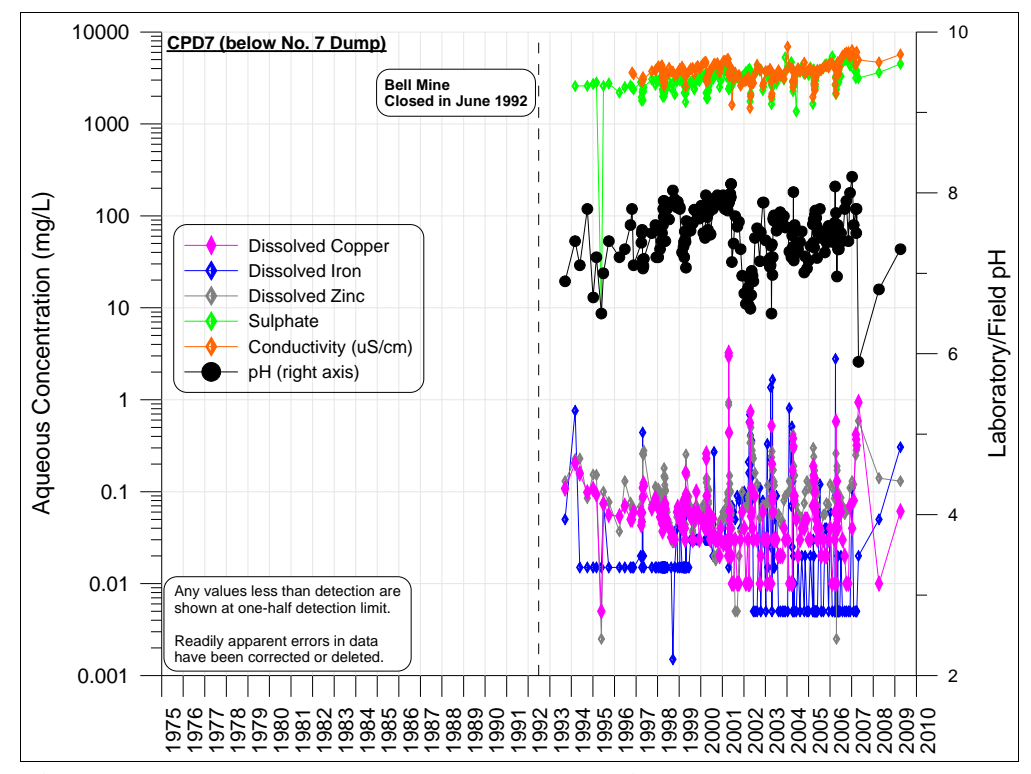


Figure 5-17. Long-term temporal trend in aqueous pH and other concentrations in CPD7 below the No. 7 Dump.

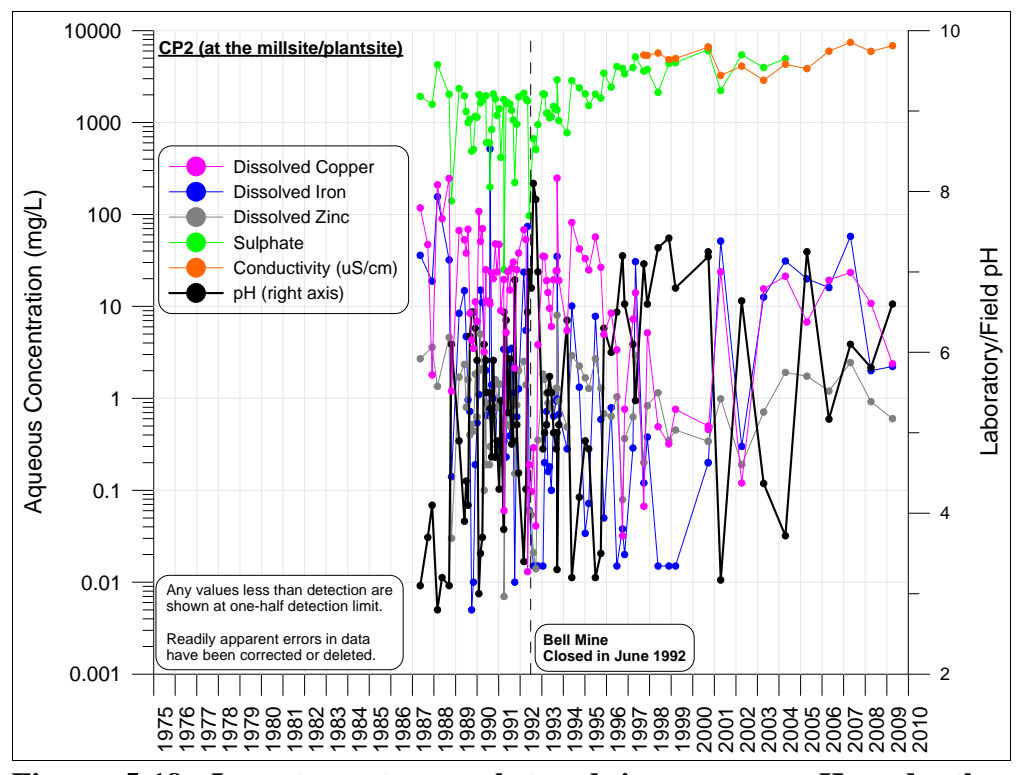


Figure 5-18. Long-term temporal trend in aqueous pH and other concentrations in CP2 at the millsite and plantsite.

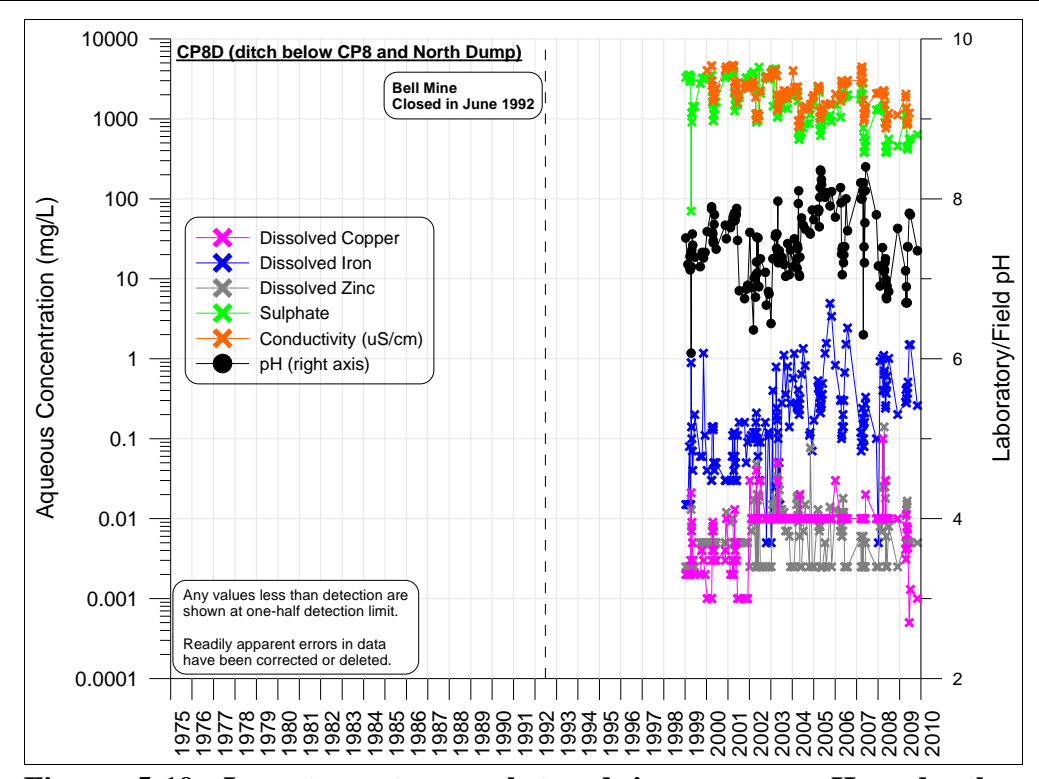


Figure 5-19. Long-term temporal trend in aqueous pH and other concentrations in Ditch CP8D below the A-Frame Dump and CP8.

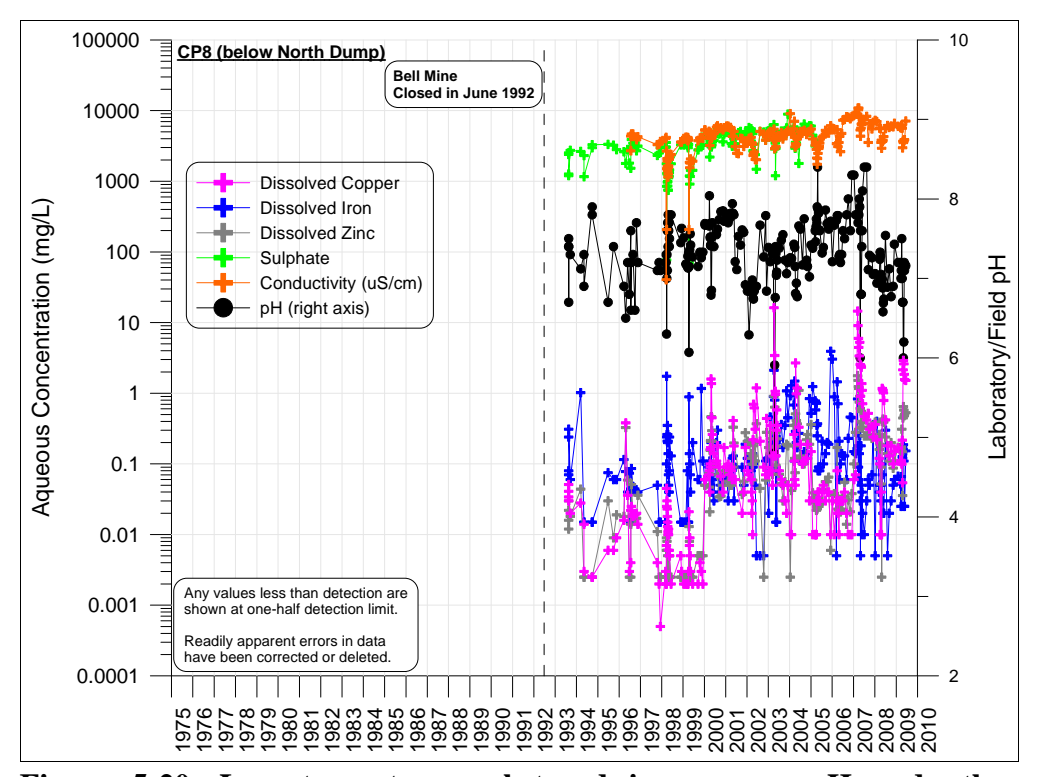


Figure 5-20. Long-term temporal trend in aqueous pH and other concentrations in CP8 below the North Dump.

# 6. THE 2010 EMPIRICAL DRAINAGE-CHEMISTRY MODEL (EDCM) FOR THE BELL MINESITE

#### 6.1 Introduction to EDCMs

In this study, "equilibrium" encompasses thermodynamic equilibrium, metastable equilibrium, dynamic equilibrium, pseudo-equilibrium, and emergence, which allows aqueous concentrations to vary significantly from season to season but to remain within defined ranges over years and decades. Section 5 showed that drainage chemistry at the Bell Minesite is in general equilibrium at some locations, within long-term definable ranges. At other locations, aqueous concentrations and parameters were still evolving, sometimes with an inverse correlation between pH and the others. This provided an opportunity to geochemically "link" the frequently measured elements and parameters with each other and with less frequently measured ones, based on correlations and equilibrium groupings. The result was the 2010 Empirical Drainage-Chemistry Model (EDCM) for the Bell Minesite (Section 1 and Appendix A), which provides estimates of elemental concentrations based on a specified value of a master parameter.

Where equilibrium exists at a minesite, some correlations will typically be seen with parameters like aqueous pH, acidity, or sulphate. These then become "independent variables" (or "master" parameters) for estimating other elements and parameters. Acidity analyses were mostly limited to 1987 through 1991 for the Bell Minesite (Section 4), so acidity is not used here as a master parameter, but net acidity (acidity minus alkalinity) vs. pH is discussed in Appendix A.

Correlations may be seen within the entire database as a whole, or only with certain sampling stations, or only with certain times. However, this often requires hundreds to thousands of analyses (Morin and Hutt, 1993a, 1997, 2000a, and 2001; Morin, 1994; Morin et al., 1993, 1995a, 1995b, and 2001). Any major temporal changes in the master parameters should be checked before proceeding to statistical calculations, which was done in Section 5 of this MDAG case study for the Bell Minesite.

Once reasonable correlations are obtained with the master parameters, "best-fit" equations provide an average value of the dependent parameter from a value of the master parameter (Appendix A). If an entire database is used, this best-fit equation is often synonymous with the site-wide annual average, and thus the equation will provide the average concentration at this minesite. The accompanying standard deviation characterizes the seasonal or spatial variability around the long-term annual average, or the long-term trend.

The seasonal fluctuations in equilibrium concentrations are caused by natural processes like temperature variations, as well as artificial factors like analytical error and filtration effects. Each factor contributes to the standard deviation based on its weighting factor:

$$(log\ standard\ deviation)^2 = weight_{factor1}*variation_{factor1} + \ weight_{factor2}*variation_{factor2} + \ \dots \ (Eq.\ 6-1)$$

In a complex open system like a minesite, the weighting factors and variations of all significant factors cannot be identified. So, while Equation 6-1 mathematically explains the source of the

seasonal and spatial variability of equilibrium concentrations, the standard deviation remains an empirically observed site-specific value.

EDCMs allow estimates of variable concentrations over very short periods that may not have been monitored. For example, with a best-fit equation of  $[\log_{10}(\text{dissolved copper}) = -0.327*pH + 2.666]$  and a standard deviation of 0.692 log10 cycles, the average annual equilibrium concentration at pH 5.0 is:

log(avg. annual Cu-D, mg/L) = 
$$= -0.327 \text{pH} + 2.666$$
$$= -0.327*5.0 + 2.666$$
$$= +1.03$$
 (Eq. 6-2)

Average annual equilibrium copper = 10.7 mg/L

Standard probability tables applied to one year indicate the maximum equilibrium concentration of one-month duration would be 1.73 log standard deviations above the average annual equilibrium concentration (best-fit line). Thus, the corresponding maximum one-month-duration concentration of dissolved copper at pH 5.0 is:

log(max. one-month-duration copper) =
$$= -0.327 \text{pH} + 2.666 + (1.73*0.692)$$

$$= -0.327*5.0 + 2.666 + (1.73*0.692)$$

$$= +2.65$$
(Eq. 6-3)

Maximum one-month-duration equilibrium copper each year = 169 mg/L

As explained earlier, equilibrium concentrations reflect site-specific factors, and thus can deviate from globally expected levels derived from stock mineral solubility or other global

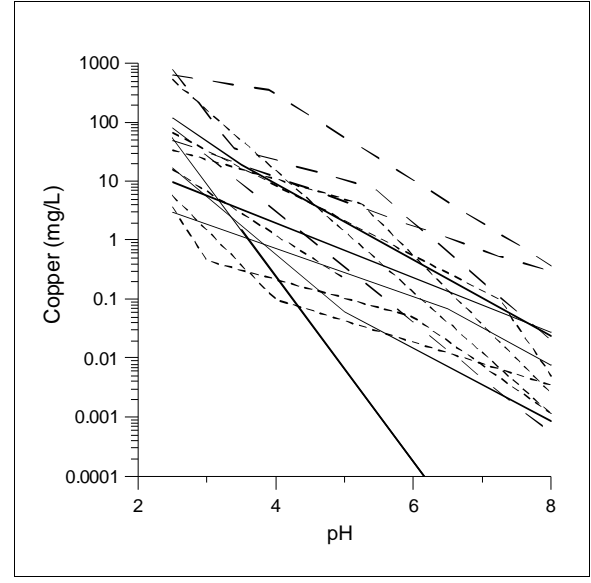


Figure 6-1. Compiled Empirical Drainage-Chemistry Models from 15 minesites and minesite components for dissolved copper vs. pH (from Morin and Hutt, 2007).

characteristics. A compilation of EDCMs for 15 minesites and minesite components showed that average annual equilibrium copper concentrations were quantitatively unique to each minesite (Morin and Hutt, 2007), but followed similar qualitative patterns with pH (Figure 6-1). Depending on pH, average equilibrium copper concentrations among the sites differed by up to three orders of magnitude. Furthermore, for eight months each year, equilibrium copper concentrations statistically remained within plus-and-minus one standard deviation of the annual average. This was a total span of one order of magnitude (a factor of 10) for the average site, but varied from 0.4 to 1.6 orders of magnitude among the sites. For four months every year, concentrations were outside (above and below) this range around the annual average. Similar observations were made for zinc, lead, and nickel.

Therefore, equilibrium concentrations are site-specific and seasonally variable, sometimes by more than one order of magnitude. However, average annual equilibrium concentrations remain about the same year after year, if pH and other master parameters remain relatively constant.

#### 6.2 The 2010 Bell EDCM

Based on Section 6.1, an EDCM for the Bell Minesite, covering data from 1978 through 2009, was created (Appendix A and Table 6-1). For example, nearly 5500 analyses were available for dissolved copper from all the monitoring stations on the Bell Minesite. Copper showed some correlation with the master parameter of pH (Figure 6-2), but was mostly independent of sulphate (Figure 6-3).

The best-fit correlation of dissolved copper with pH consisted of three segments (Figure 6-4). Below pH 3.0, the slope of the best-fit equation was -1.17265 and the logarithmic standard deviation was 0.37011 log cycles. Above pH 5.5, the slope was similar, but the standard deviation was much larger due to the greater vertical "spread" of datapoints in this range in Figure 6-4.

Other elements and parameters are discussed in Appendix A and summarized in Table 6-1.

Table 6-1. The 2010 Empirical Drainage-Chemistry Model (EDCM) for the Bell Minesite<sup>1</sup> (see also Appendix A)

Minesite <sup>1</sup> (see also Appendix A)				
Parameter <sup>2</sup>	<u>Conditions</u>	<u>Equation</u>	log(Std <u>Dev)</u>	
рН	Net Acidity > +407.0 mg/L	pH = -0.950298*log(Acidity) + 5.77986	NA	
	+202.87 < NA < +407.0 mg/L	pH = -3.63689*log(Net Acidity) + 12.79111	NA	
	-72.54≤NA≤+202.87 mg/L	pH = -0.0083512*(Net Acidity) + 6.09421	NA	
	Net Acidity < -72.54 mg/L	pH = +1.43741*log(-Net Acidity) + 4.02560	NA	
Acidity	pH < 3.3	log(Acidity) = -1.05232*pH + 6.08223	0.39142	
	$3.3 \leq pH \leq 6.0$	log(Acidity) = -0.27496*pH + 3.51704	0.32292	
	pH > 6.0	log(Acidity) = -0.49283*pH + 4.82426	0.31224	
Alkalinity	pH ≥ 4.0	log(Alkalinity) = +0.69570*pH - 2.80060	0.35848	
Sulphate	Rock dumps and related drainages	log(SO4) = -0.022428*pH + 3.40071	0.33829	
	Tailings and rock dams, pH<3.0	$\log(SO4) = -1.10924 * pH + 6.69650$	0.32026	
	Tailings and rock dams, pH≥3.0	$\log(SO4) = -0.027802*pH + 3.45219$	0.15797	
Conductivity		log(Cond) = +0.70745*log(SO4) + 1.10225	0.1007	
TDS	NA	NA	NA	
Hardness		log(Hardness) = +0.98380*log(SO4) - 0.00500	0.17639	
Fluoride	NA	NA	NA	
Chloride	NA	NA	NA	
Nitrate		Typically below detection; <3 mg/L before closure in 1992 and <2 mg/L after closure	NA	
Nitrite		Typically below detection; <3 mg/L before closure in 1992 and <0.6 mg/L after closure	NA	
Ammonia		Typically below detection; <2 mg/L	NA	
Al-D		log(Al-D) = -0.82805*pH + 4.89619	0.64112	
Sb-D	Near-neutral pH	Typically below detection; <0.0001 mg/L	NA	
	pH < 4.0	$\log(As-D) = -1.94657*pH + 4.69773$	0.96847	
As-D	pH ≥ 4.0	log(As-D) = -3.08856 (0.0008155 mg/L)	0.50975	
Ba-D		log(Ba-D) = -0.97620*log(SO4) + 1.30754	0.36521	
<b>-</b> -	pH < 4.0	log(Be-D) = -0.77446*pH + 0.79682	0.35975	
Be-D	pH ≥ 4.0	Near or below detection; <0.005 mg/L	NA	

Parameter <sup>2</sup>	Conditions	<u>Equation</u>	log(Std <u>Dev)</u>
Bi-D	Before closure in 1992	Near or below detection; < 1.1 mg/L	NA
	After closure in 1992-2000	Near or below detection; <0.3 mg/L	NA
	After closure in 2001-2009	Near or below detection; <0.001 mg/L	NA
B-D		Typically below detection; <0.2 mg/L	NA
Cd-D	Near-neutral pH	Near or below detection; <0.0002 mg/L	NA
Ca-D		$\log(\text{Ca-D}) = +0.80815*\log(\text{SO4}) - 0.19749$	0.17105
Cr-D	pH < 4.0	log(Cr-D) = -1.83617*pH + 4.34466	0.58217
	$pH \ge 4.0$	Near or below detection; <0.001 mg/L	NA
Co-D	Excluding 2009 data	$\log(\text{Co-D}) = -0.37796 * \text{pH} + 1.30330$	0.37595
	pH < 3.0	log(Cu-D) = -1.17265*pH + 5.37432	0.37011
Cu-D	$3.0 \leq pH \leq 5.5$	log(Cu-D) = -0.48982*pH + 3.32581	0.43962
	pH > 5.5	log(Cu-D) = -1.04518*pH + 6.38030	0.81956
E- D	pH < 4.0	log(Fe-D) = -1.55584*pH + 6.48218	0.6119
Fe-D	$pH \ge 4.0$ , oxidized Eh	log(Fe-D) = -0.48131*pH + 2.18405	0.66123
Pb-D		log(Pb-D) = -2.03560 (0.009213 mg/L)	0.62098
Li-D		Li-D < 0.1 mg/L	NA
Mg-D		log(Mg-D) = +0.98155*log(SO4) - 0.85568	0.18773
Mn-D		$\log(\text{Mn-D}) = -0.29027 * \text{pH} + 2.20133$	0.45138
Hg-D		Always below detection; <0.0005 mg/L	NA
Mo-D		log(Mo-D) = -1.19379 (0.0640 mg/L)	0.27549
Ni-D		log(Ni-D) = -0.45906*pH + 1.69877	0.40611
n n	pH < 5.0	$\log(P-D) = -0.95927*pH + 3.77252$	0.80015
P-D	$pH \ge 5.0$	log(P-D) = -1.02381 (0.09467 mg/L)	0.55378
K-D	Near-neutral pH	K-D < 75 mg/L	NA
So D	pH < 4.0	log(Se-D) = -1.4000*pH + 2.29897	NA
Se-D	$pH \ge 4.0$	Se-D < 0.0005 mg/L	NA
c: D	pH < 5.0	log(Si-D) = -0.30121*pH + 2.21879	0.23253
Si-D	$pH \ge 5.0$	$\log(\text{Si-D}) = -0.075708*pH + 1.10057$	0.19275
Ag-D		None; at/below detection; <0.0001 mg/L	NA

Parameter <sup>2</sup>	Conditions	Equation Equation	log(Std <u>Dev)</u>
Na-D	For rock piles and related drainages	$\log(\text{Na-D}) = +0.80747*\log(\text{SO4}) - 1.59772$	0.17161
	For tailings and related rock dams	log(Na-D) = +0.11537*pH + 0.79938	0.18605
	For rock piles and related drainages, with SO4≥1700 mg/L	log(Sr-D) = +1.43125*log(SO4) - 4.42770	0.17029
Sr-D	For rock piles and related drainages, with SO4<1700 mg/L	log(Sr-D) = +0.79763*log(SO4) - 2.38082	0.13069
	For tailings and related rock dams, with SO4 < 7000 mg/L	log(Sr-D) = +2.09647*log(SO4) - 6.25106	0.1963
Te-D		None; below detection; <0.001 mg/L	NA
Tl-D		None; below detection; <0.0001 mg/L	NA
D	pH < 3.5	log(Th-D) = -2.0*pH + 3.7	NA
Th-D	pH ≥ 3.5	<0.0005 mg/L	NA
Sn-D		None; below detection; <0.001 mg/L	NA
Ti-D, maximum		log(Max Ti-D) = -0.14162*pH - 0.89881	0.17712
W-D		NA	NA
U-D		log(U-D) = +1.27549*log(SO4) - 7.20752	0.21187
V.D	pH < 3.5	$\log(V-D) = -1.500*pH + 3.2500$	NA
V-D	pH ≥ 3.5	None; typically below detection; <0.01 mg/L	NA
	pH < 3.0	log(Zn-D) = -1.08849*pH + 3.56852	0.34748
Zn-D	$3.0 \leq pH \leq 6.0$	$\log(\text{Zn-D}) = -0.15634 * \text{pH} + 0.77207$	0.40923
	pH > 6.0	$\log(\text{Zn-D}) = -0.98600 * \text{pH} + 5.75002$	0.77426
Zr-D	pH < 4.0	log(Zr-D) = -1.500*pH + 3.0000	NA
21-17	$pH \ge 4.05$	None; typically below detection; <0.001 mg/L	NA

 $<sup>^1</sup>$  Based on data through 2009; non-minesite data like Babine Lake was not used; master parameters from which others were predicted were pH, sulphate, conductivity for sulphate only, and net acidity (acidity - alkalinity) for pH only; all concentrations are mg/L except for pH (pH units) and conductivity ( $\mu$ S/cm); acidity, alkalinity, net acidity, and hardness are mg CaCO<sub>3</sub>/L; all logarithmic values are base 10.

<sup>&</sup>lt;sup>2</sup> "-D" indicates the information applies only to the dissolved (filtered) form.

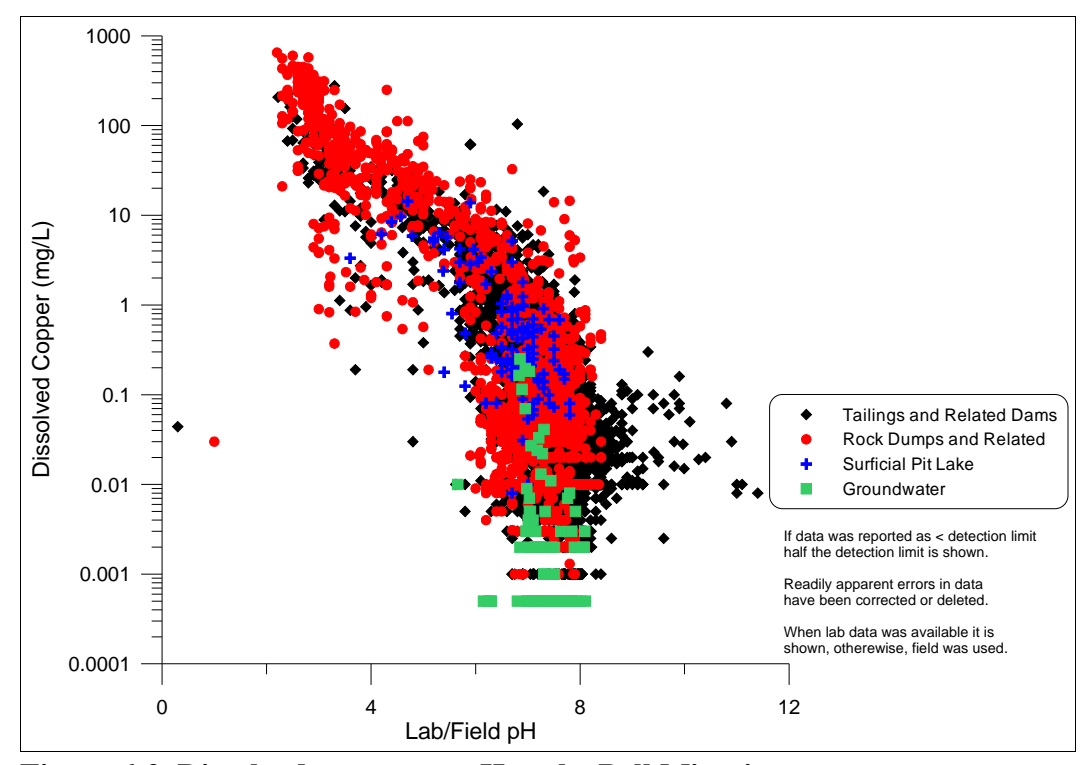


Figure 6-2. Dissolved copper vs. pH at the Bell Minesite.

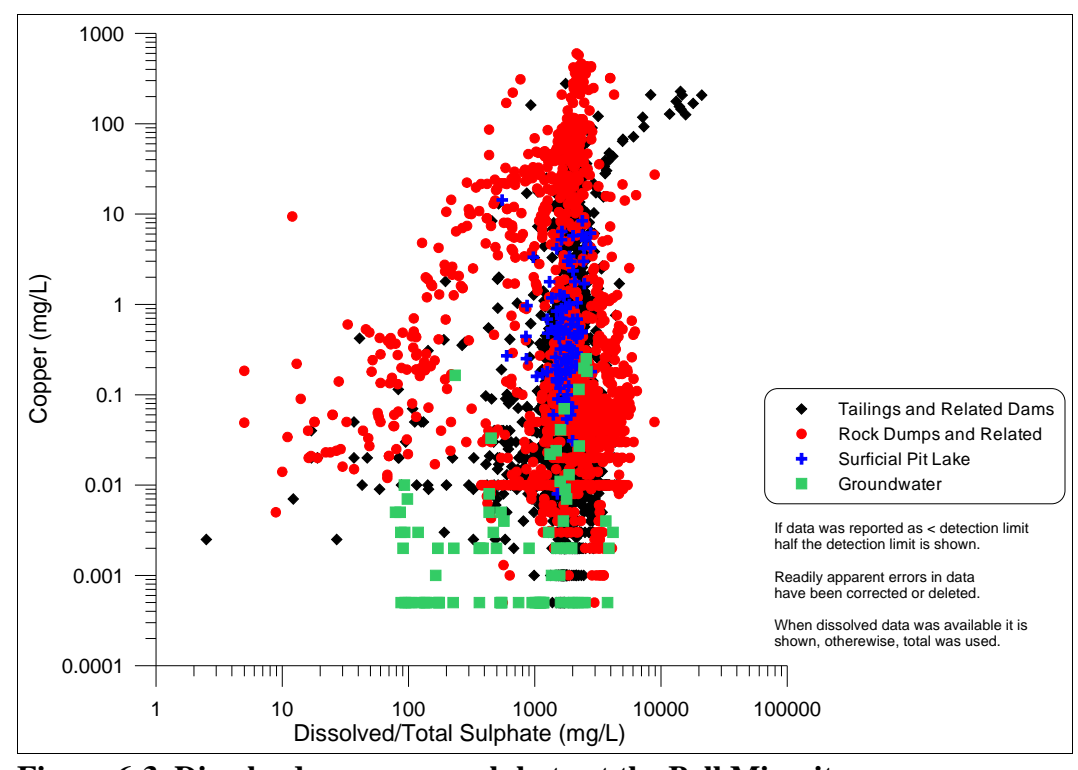


Figure 6-3. Dissolved copper vs. sulphate at the Bell Minesite.

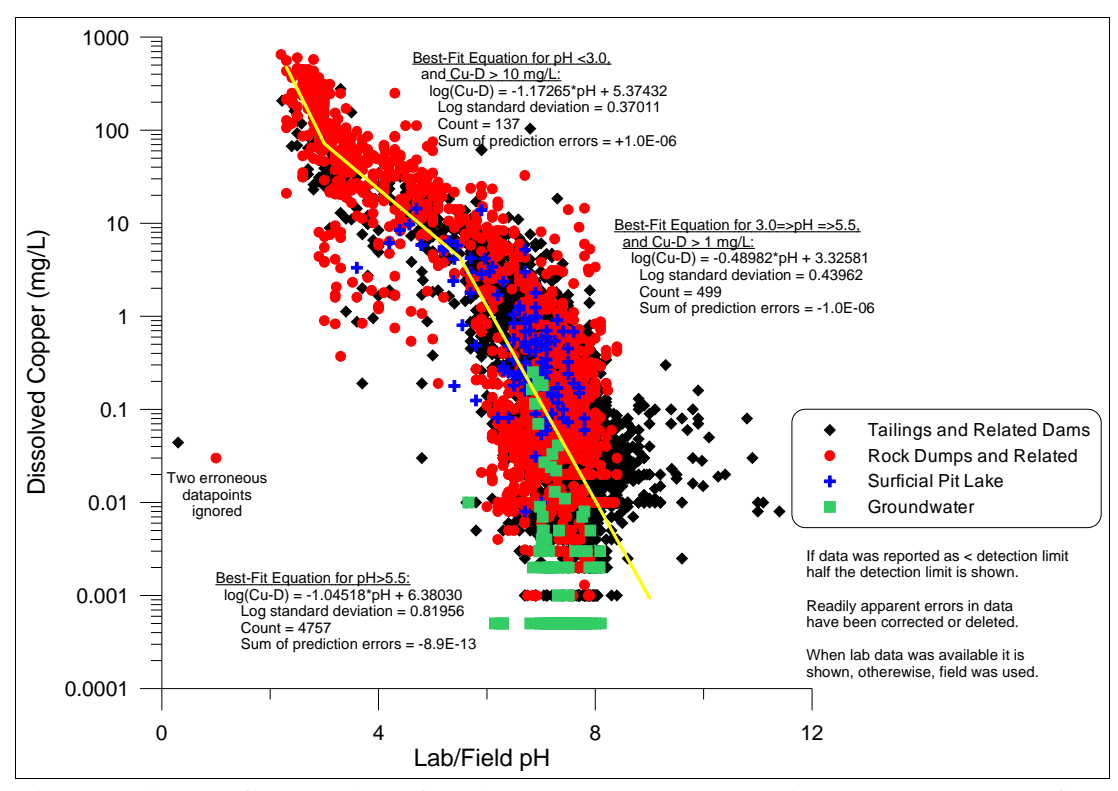


Figure 6-4. Best-fit equations for dissolved copper vs. pH in the 2010 Bell EDCM.

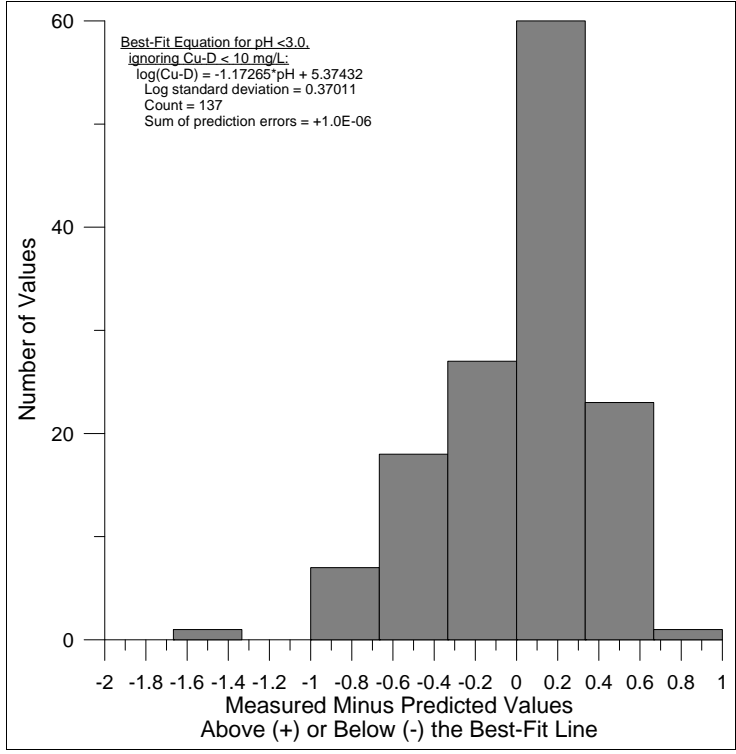


Figure 6-5. Statistical distribution of (measured-calculated) datapoints around the best-fit equation for dissolved copper below pH 3.0.

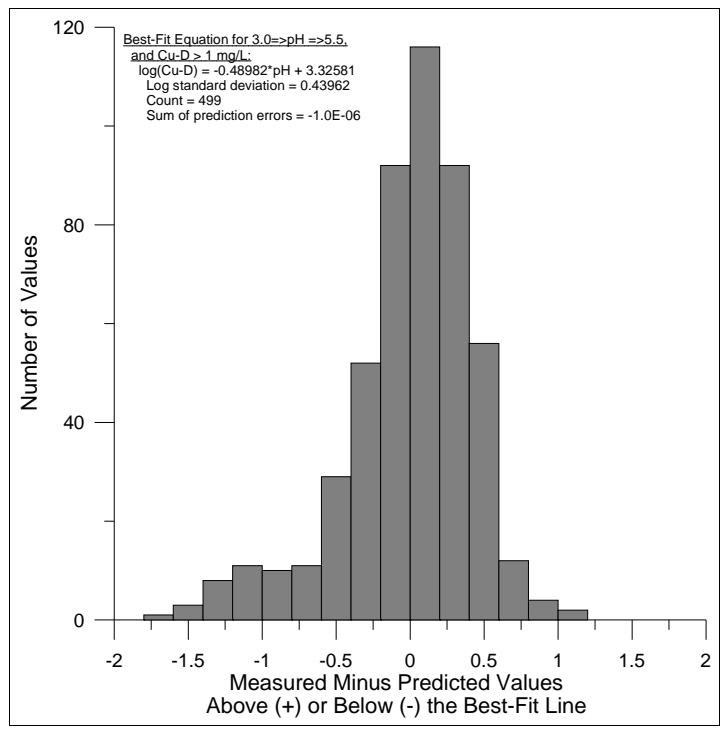


Figure 6-6. Statistical distribution of (measured-calculated) datapoints around the best-fit equation for dissolved copper between pH 3.0 and 5.5.

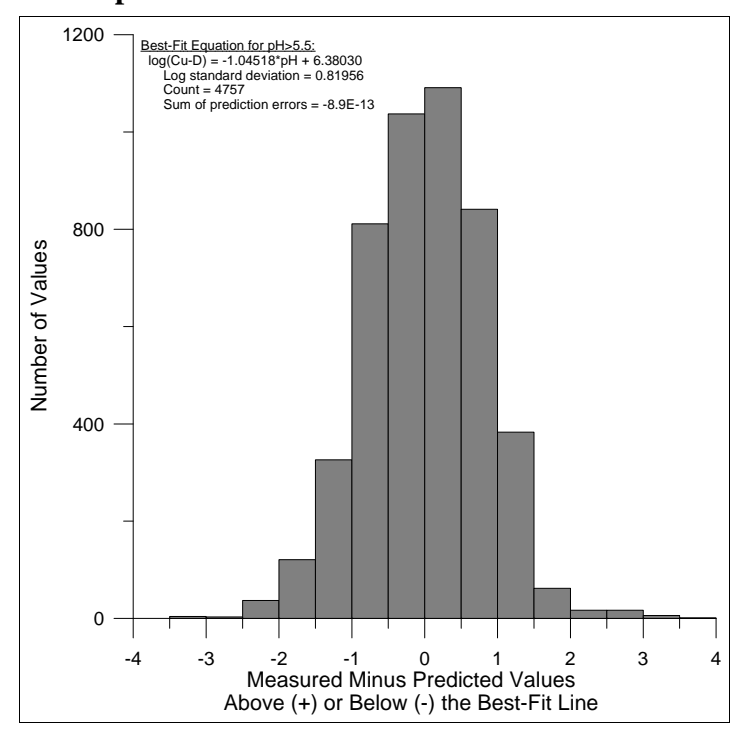


Figure 6-7. Statistical distribution of (measured-calculated) datapoints around the best-fit equation for dissolved copper above pH 5.5.

## 7. CONCLUSION

In conclusion, this MDAG case study has compiled and reviewed more than three decades of drainage-chemistry monitoring data at the Bell Minesite. These data ranged from mid operation through 17 years of closure.

From this information, long-term trends in frequently analyzed parameters were shown and discussed in Section 5. This showed that drainage chemistry was generally steady and thus in local equilibrium at some monitoring stations, but pH and other parameters were changing at others due to remedial activities or natural geochemical evolution. Seasonal variability in recent years could not be assessed at many locations, because drainage samples were analyzed only once a year. At stations with more frequent analyses, seasonal variability occurred within definable long-term ranges of steady or gradually increasing or decreasing average concentrations.

Then, an Empirical Drainage-Chemistry Model (EDCM) statistically linking master and dependent parameters was created in Section 6 and Appendix A. The EDCM is summarized in Table 6-1.

We are grateful to Xstrata Copper for providing, through Pacific Booker Minerals, all data as one database, saving a great deal of time typing data from government-submitted annual reports.

## 8. REFERENCES

- British Columbia Minfile Website. 2010. Bell Mine. Information accessed in 2010, at http://minfile.gov.bc.ca/Summary.aspx?minfilno=093M++001.
- Day, S., and B. Rees. 2006. Geochemical controls on waste-rock dump seepage chemistry at several porphyry mines in the Canadian Cordilleran. IN: Proceedings of the 7th International Conference on Acid Rock Drainage, St. Louis, MO, USA, March 26 30, 2006.
- Day, S.D., T. Higgs, and M. Paine. 1996. Guide for Predicting Water Chemistry from Waste Rock Piles. Canadian MEND Report 1.27.1a, July 1996.
- Morin, K.A. 1994. Prediction of water chemistry in open pits during operation and after closure. IN: Proceedings of the Eighteenth Annual British Columbia Mine Reclamation Symposium, Vernon, British Columbia, April 11-14, p. 72-86.
- Morin, K.A., and N.M. Hutt. 2010. Twenty-Nine Years of Monitoring Minesite-Drainage Chemistry, During Operation and After Closure: The Granisle Minesite, British Columbia, Canada. www.mdag.com/case\_studies/cs34.html.
- Morin, K.A., and N.M. Hutt. 2008. Bimodal Distribution of pH at Minesites with Acid Rock Drainage. MDAG Internet Case Study #28, www.mdag.com/case\_studies/cs28.html
- Morin, K.A., and N.M. Hutt. 2007. Scaling and Equilibrium Concentrations in Minesite-Drainage Chemistry. MDAG Internet Case Study #26, www.mdag.com/case\_studies/cs26.html
- Morin, K.A., and N.M. Hutt. 2001. *Environmental Geochemistry of Minesite Drainage: Practical Theory and Case Studies, Digital Edition.* MDAG Publishing (www.mdag.com), Surrey, British Columbia. ISBN: 0-9682039-1-4.
- Morin, K.A., and N.M. Hutt. 2000a. Case studies in metal solubility at minesites. Presented at the 7th Annual British Columbia Metal Leaching/ARD Workshop, Vancouver, November 29-30.
- Morin, K.A., and N.M. Hutt. 2000b. Bell Mine Update of Environmental Geochemistry. Report for Noranda Inc., dated June 4, 2000.
- Morin, K.A., and N.M. Hutt. 1997. *Environmental Geochemistry of Minesite Drainage: Practical Theory and Case Studies*. MDAG Publishing (www.mdag.com), Surrey, British Columbia. ISBN: 0-9682039-0-6.
- Morin, K.A., and N.M. Hutt. 1993a. The use of routine monitoring data for assessment and prediction of water chemistry. IN: Proceedings of the 17th Annual Mine Reclamation Symposium, Port Hardy, British Columbia, May 4-7, p.191-201. Mining Association of British Columbia.

- Morwijk Enterprises Ltd. 1993b. Bell 92 Closure Plan, Support Document E, Mine Rock and Tailings Geochemistry and Prediction of Water Chemistry. Dated April 23, 1993.
- Morin, K.A., N.M. Hutt, and S. Hutt. 2001. A compilation of empirical drainage-chemistry models (EDCMs). IN: Proceedings of Securing the Future, International Conference on Mining and the Environment, Skellefteå, Sweden, June 25-July 1, Volume 2, p. 556-565. The Swedish Mining Association.
- Morin, K.A., N.M. Hutt, and I.A. Horne. 1995a. Prediction of future water chemistry from Island Copper Mine's On-Land Dumps. IN: Proceedings of the 19th Annual British Columbia Mine Reclamation Symposium, Dawson Creek, B.C., June 19-23, p. 224-233.
- Morin, K.A., N.M. Hutt, and R. McArthur. 1995b. Statistical assessment of past water chemistry to predict future chemistry at Noranda Minerals' Bell Mine. IN: Proceedings of the Conference on Mining and the Environment, Sudbury, Ontario, May 28 June 1, Volume 3, p.925-934.
- Morin, K.A., I.A. Horne, and D. Flather. 1993. The appropriate geochemical monitoring of toe seepage from a mine-rock dump. IN: Proceedings of the 17th Annual Mine Reclamation Symposium, Port Hardy, British Columbia, May 4-7, p.119-129. Mining Association of British Columbia.
- Noranda Minerals Inc. [Noranda]. 1993. The Mines of Babine Lake. A booklet describing the history of Granisle and Bell Minesites.

## Acknowledgments

We thank Pacific Booker Minerals Inc., owner of the Morrison Project currently seeking environmental approvals, for this opportunity to compile and interpret decades of monitoring data for the Bell Minesite. Valuable lessons can be learned from drainage chemistry at a particular minesite spanning operation and closure, from 1978 through 2009.

We also thank to Xstrata Copper, who provided the monitoring data normally submitted in individual annual reports to government agencies, as one integrated database. This saved a great deal of typing!

MDAG.com Internet Case Study #33: 31 Years of Minesite-Drainage Chemistry: Bell Mi	nesite Page 47
APPENDIX A. Scatterplots, Histograms, Best-Fit Equations, and Standard the 2010 Bell Empirical Drainage-Chemistry Model (EDCM	d Deviations for )

Appendix A1. Acidity

Notes:

Because acid rock drainage (ARD) is an important aspect of minesite-drainage chemistry at the Bell Minesite, the balance between acidity and alkalinity (Appendices A2 and A3) is critical for understanding and predicting pH, which in turn correlates with many other aqueous elements. Laboratory or field pH, with more than 5400 values back to 1977 (32 years of pH data), is one of the frequently analyzed parameters at the Bell Minesite, in addition to sulphate, dissolved copper, dissolved iron, and dissolved zinc.

A scatterplot of acidity with pH (Figure A1-1) shows a better correlation across the measured range than with sulphate (Figure A1-2), which shows little correlation around 2000 mg/L.

The best-fit correlation of acidity with pH contains three segments (Figure A1-3). The (measured-calculated) datapoints around these three segments generally form lognormal distributions (Figures A1-4 to A1-6). The standard deviations of these distributions range from 0.312 to 0.391 log10 cycles.

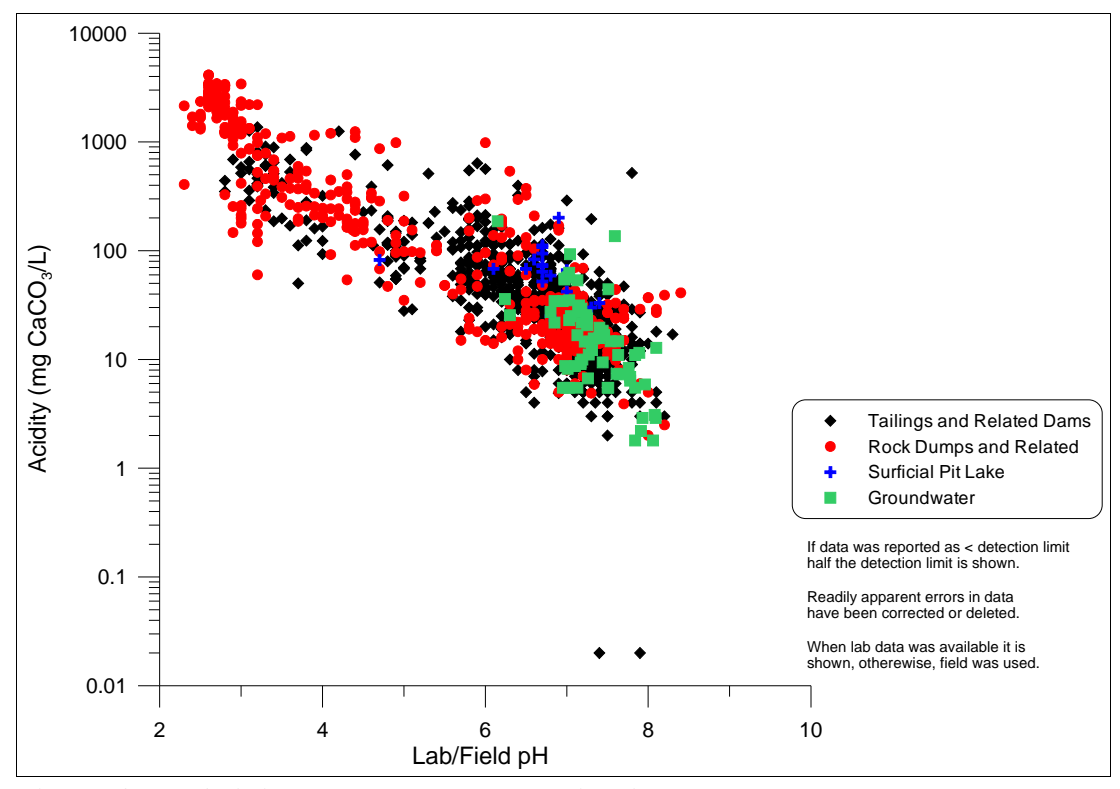


Figure A1-1. Acidity vs. pH at the Bell Minesite.

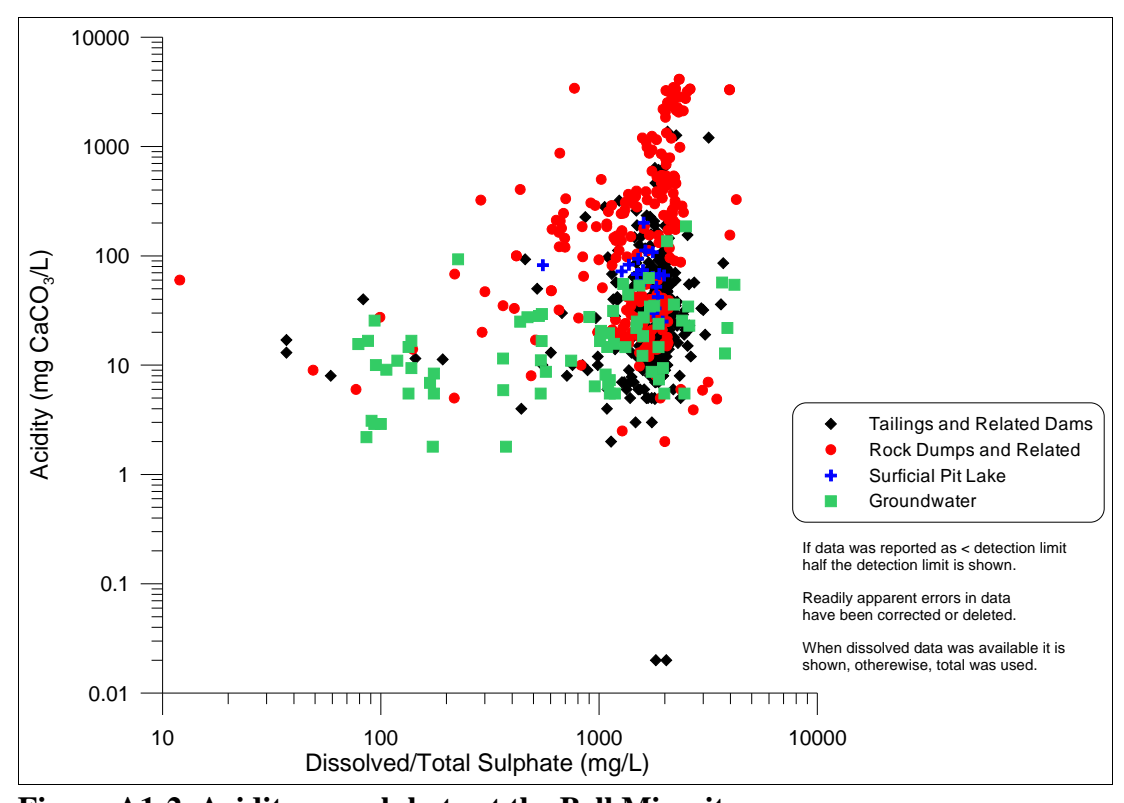


Figure A1-2. Acidity vs. sulphate at the Bell Minesite.

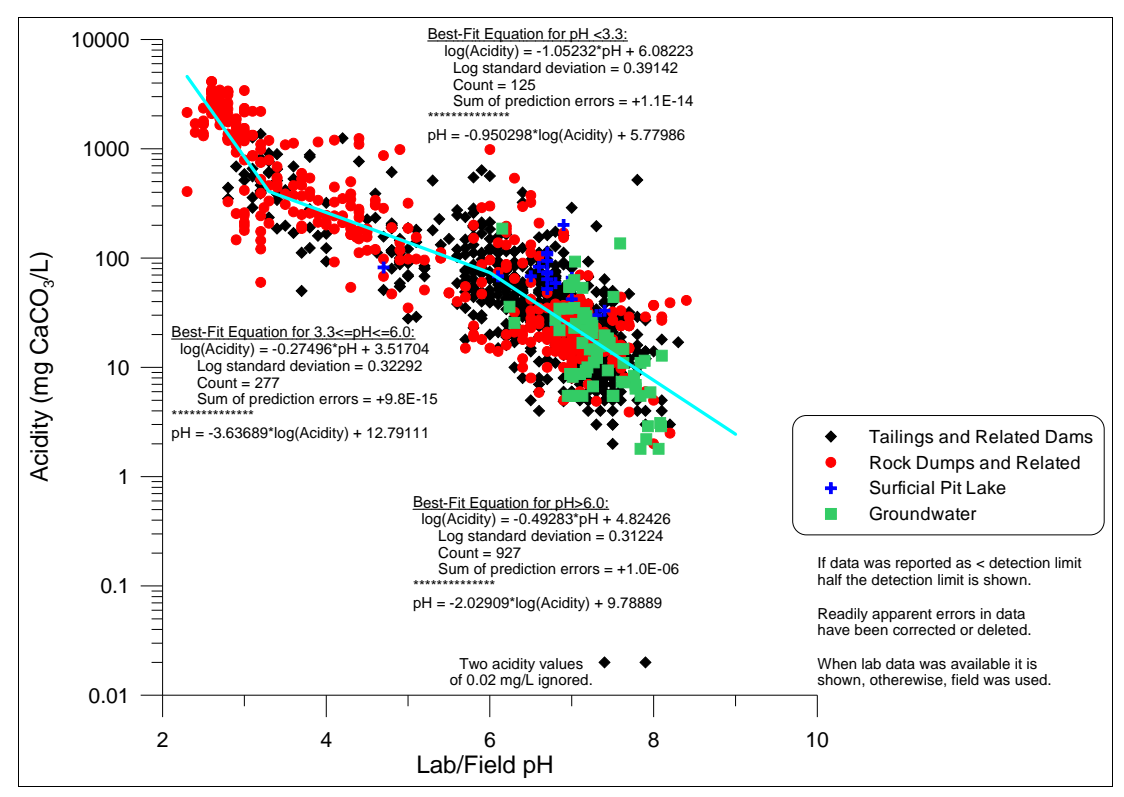


Figure A1-3. Best-fit equations for acidity vs. pH in the 2010 Bell EDCM.

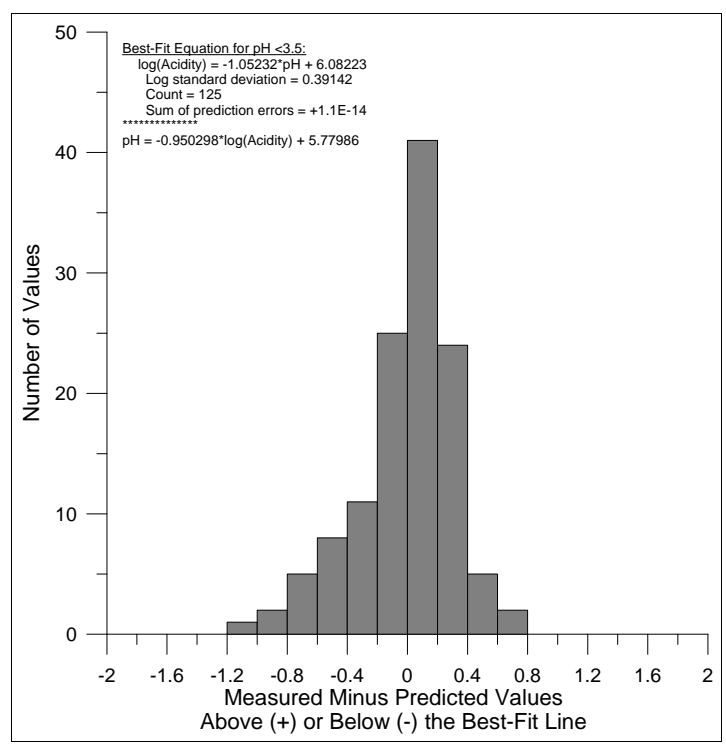


Figure A1-4. Statistical distribution of (measured-calculated) datapoints around the best-fit equation for acidity below pH 3.3.

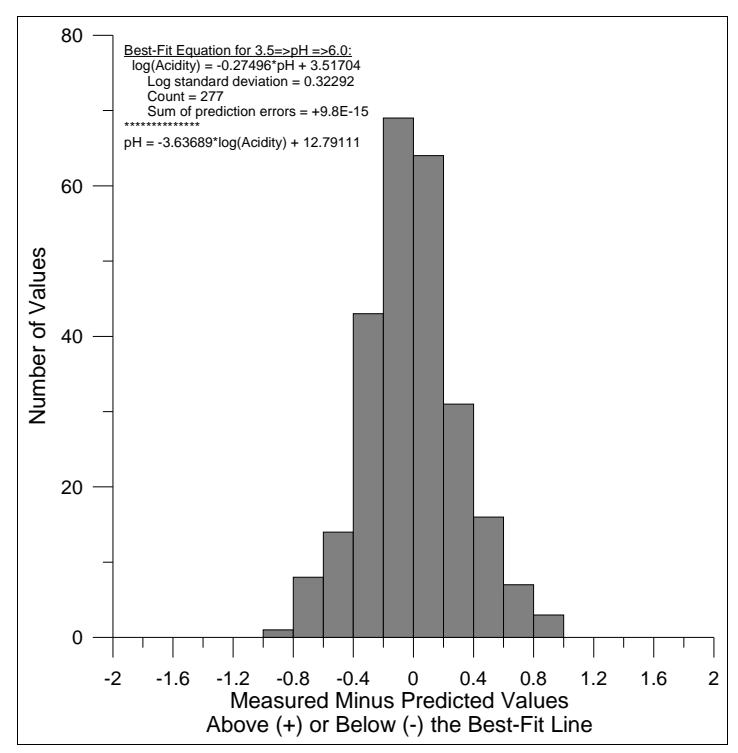


Figure A1-5. Statistical distribution of (measured-calculated) datapoints around the best-fit equation for acidity between pH 3.3 and 6.0.

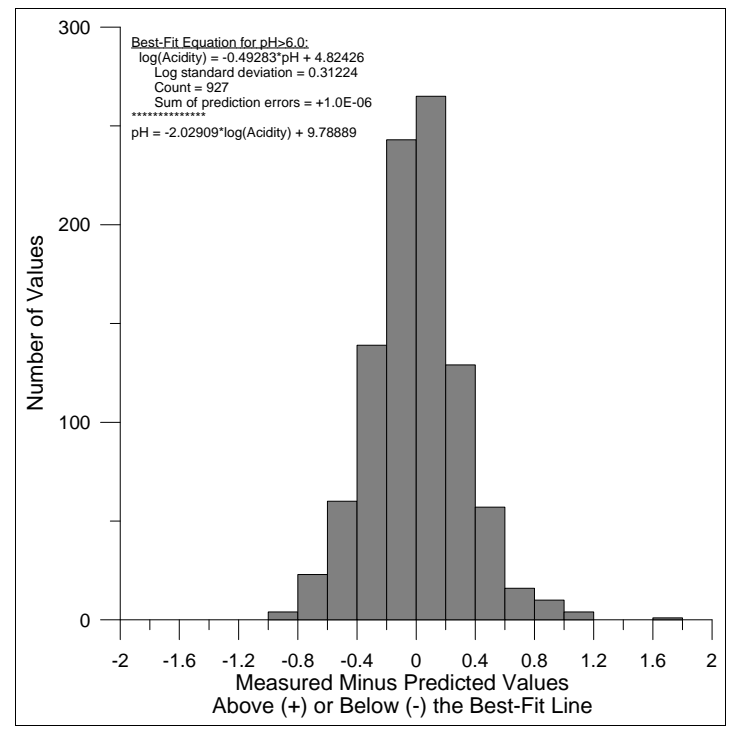


Figure A1-6. Statistical distribution of (measured-calculated) datapoints around the best-fit equation for acidity above pH 6.0.

Appendix A2. Alkalinity

Notes:

Because acid rock drainage (ARD) is an important aspect of minesite-drainage chemistry at the Bell Minesite, the balance between acidity and alkalinity (Appendices A1 and A3) is critical for understanding and predicting pH, which in turn correlates with many other aqueous elements. A scatterplot of alkalinity with pH (Figure A2-1) shows a better correlation across the measured range than with sulphate (Figure A2-2), which shows little correlation.

The best-fit correlation of alkalinity with pH has a slope of +0.69570 (Figure A2-3). The (measured-calculated) datapoints around this correlation resembles lognormal (Figure A2-4), with a standard deviation of 0.35848 log10 cycles.

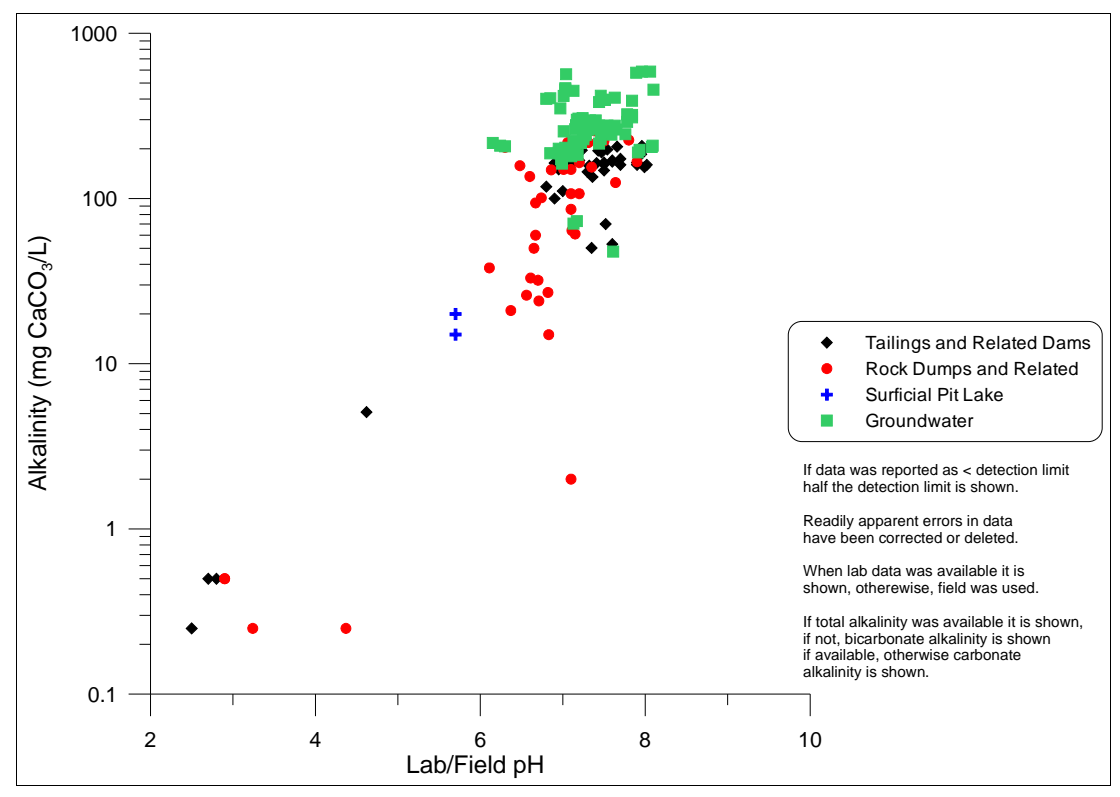


Figure A2-1. Alkalinity vs. pH at the Bell Minesite.

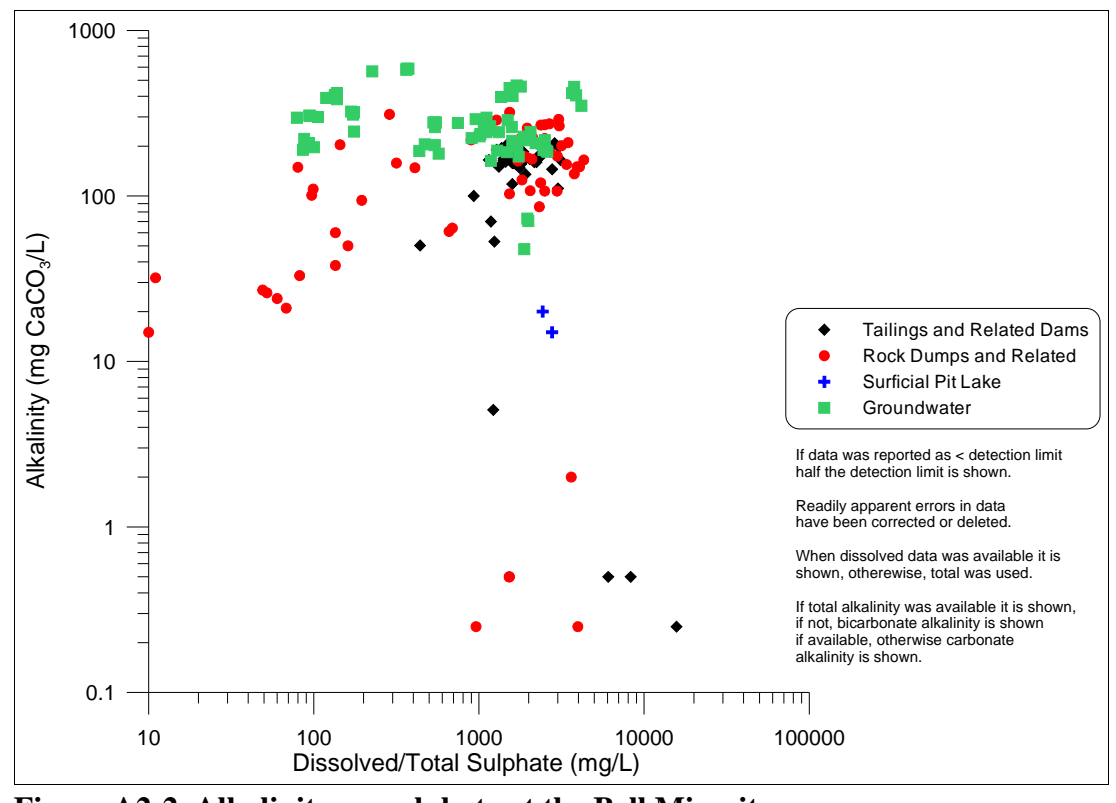


Figure A2-2. Alkalinity vs. sulphate at the Bell Minesite.

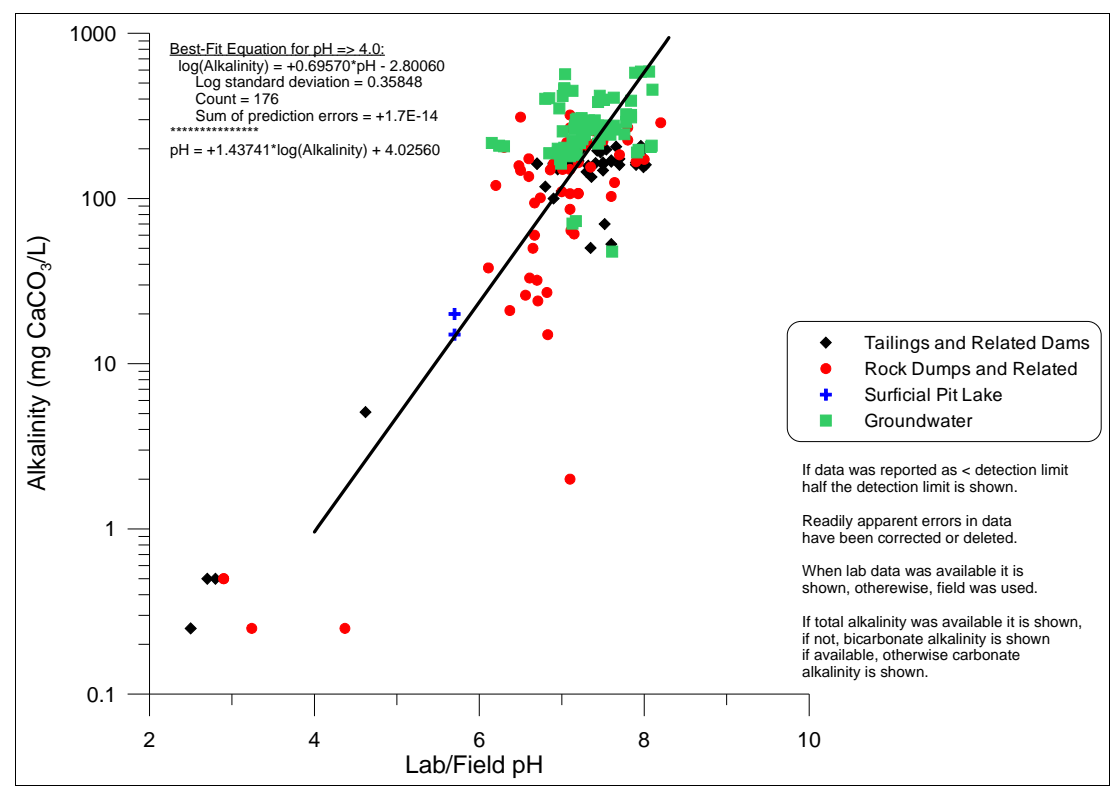


Figure A2-3. Best-fit equations for alkalinity vs. pH in the 2010 Bell EDCM.

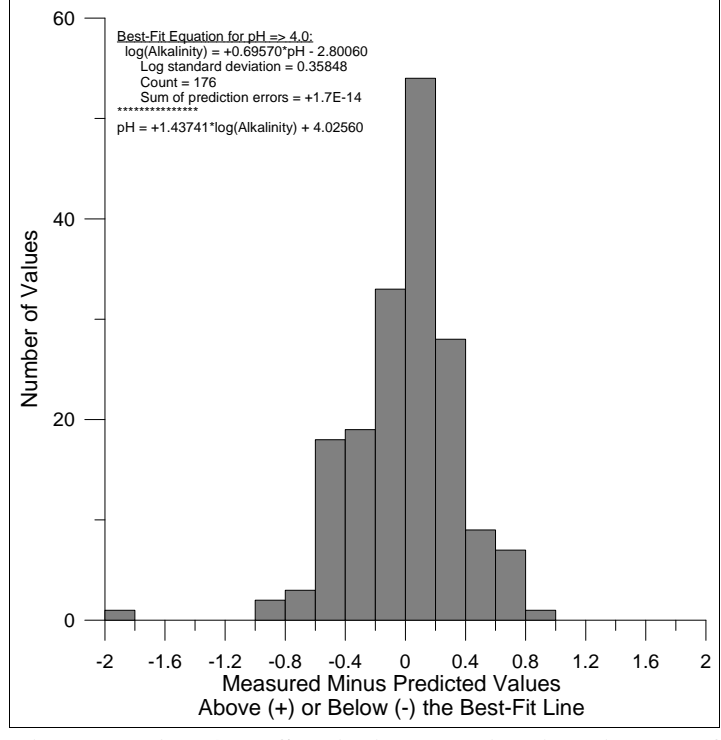


Figure A2-4. Statistical distribution of (measured-calculated) datapoints around the best-fit equation for alkalinity.

Appendix A3. Net Acidity

Notes:

Because acid rock drainage (ARD) is an important aspect of minesite-drainage chemistry at the Bell Minesite, the balance between acidity and alkalinity (Appendices A1 and A2) is critical for understanding and predicting pH, which in turn correlates with many other aqueous elements. Here, net acidity is determined from the two, with Net Acidity = Acidity - Alkalinity (Figures A3-1 and A3-2).

Below pH 4.4, acidity significantly exceeds alkalinity, so the acidity equations (Appendix A1) are used directly for net acidity below pH 4.4 (Figures A3-1 and A3-2). Above pH 6.7, alkalinity significantly exceeds acidity, so the alkalinity equation (Appendix A2) is used directly above pH 6.7. Between 4.4 and 6.7, a straight line combines the two to represent net acidity in this range (Figure A3-3).

The statistical characterizations of (measured-calculated) values above and below the best-fit net-acidity lines are taken directly as those for acidity (Appendix A1) and alkalinity (Appendix A2). No similar statistics are available for the straight line between 4.4 and 6.7 due to the general lack of datapoints.

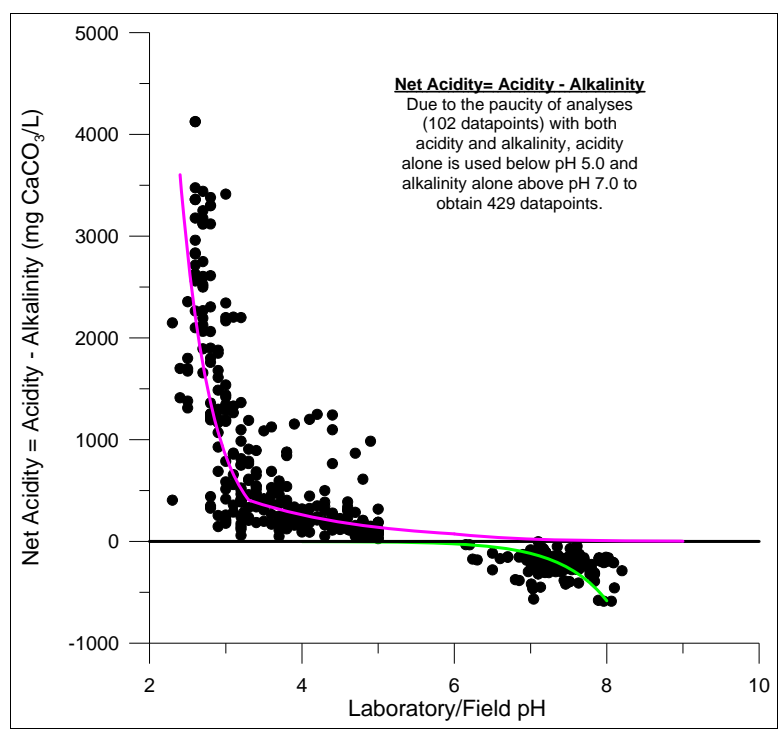


Figure A3-1. Net Acidity vs. pH at the Bell Minesite.

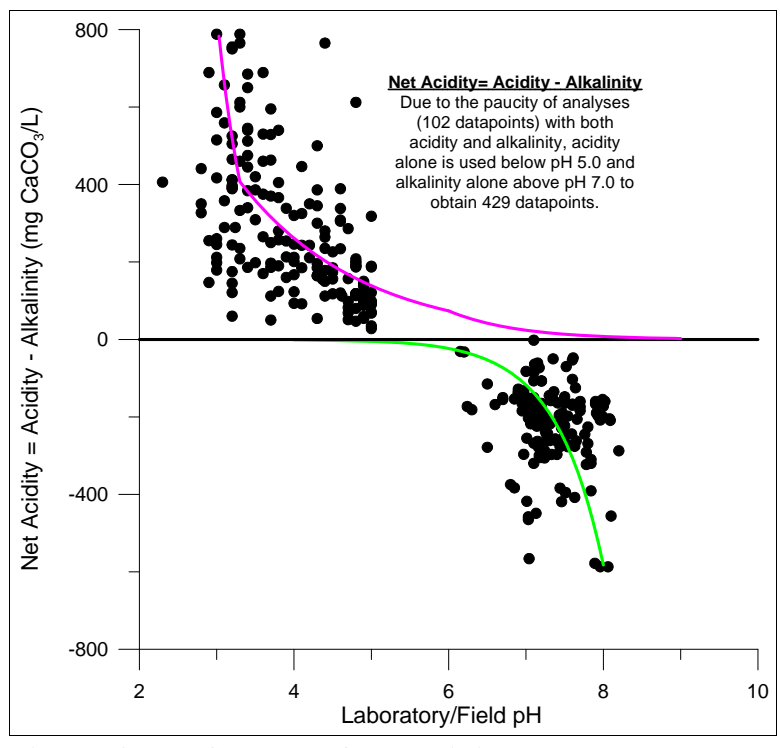


Figure A3-2. Closeup of net acidity vs. pH at the Bell Minesite.

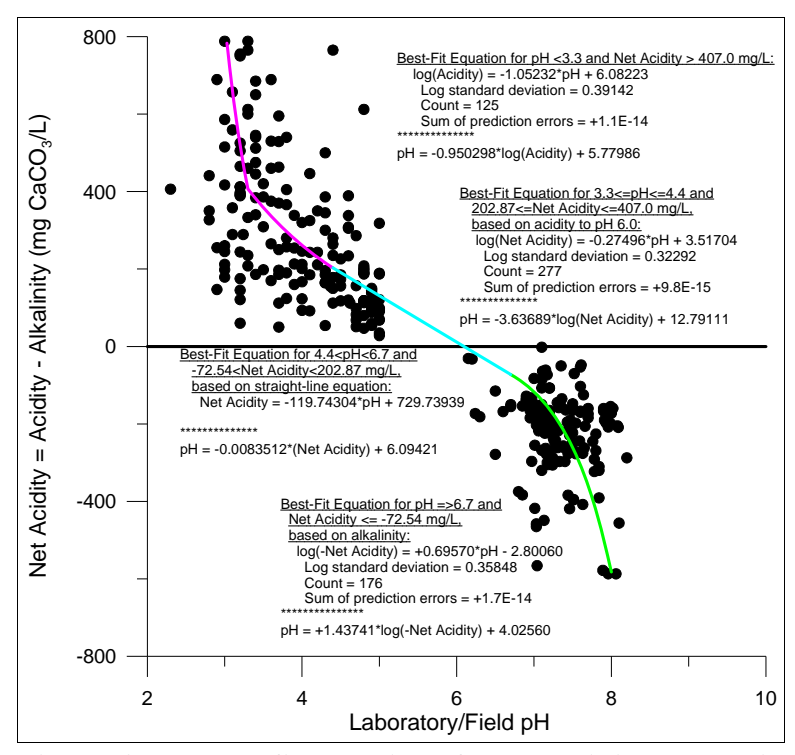


Figure A3-3. Best-fit equations for net acidity vs. pH in the 2010 Bell EDCM.

Appendix A4. Sulphate

Notes:

Acid rock drainage (ARD) is the result of sulphide oxidation, and thus sulphate can be an important aqueous parameter. For the Bell Minesite, some aqueous elements correlate better with sulphate than with pH, justifying its consideration as a master parameter. Dissolved or total sulphate, with more than 4000 values back to 1977 (32 years of data), is one of the frequently analyzed parameters at the Bell Minesite, in addition to pH, dissolved copper, dissolved iron, and dissolved zinc.

The correlation of sulphate with the other master parameter of pH (Figure A4-1) shows little correlation, and the best-fit correlation for tailings and related dams with a slope of about -0.028 is close to that for rock dumps and related drainages with a slope of -0.022 (Figure A4-2). The exception is below pH 3.0, where the tailings correlation changes to a steeper slope of -1.1 (Figure A4-3).

The distributions of (measured-calculated) datapoints above and below the two segments for tailings and dams are generally lognormal (Figures A4-4 and A4-5). This is also the case for datapoints around the rock-dump best-fit equation (Figure A4-6).

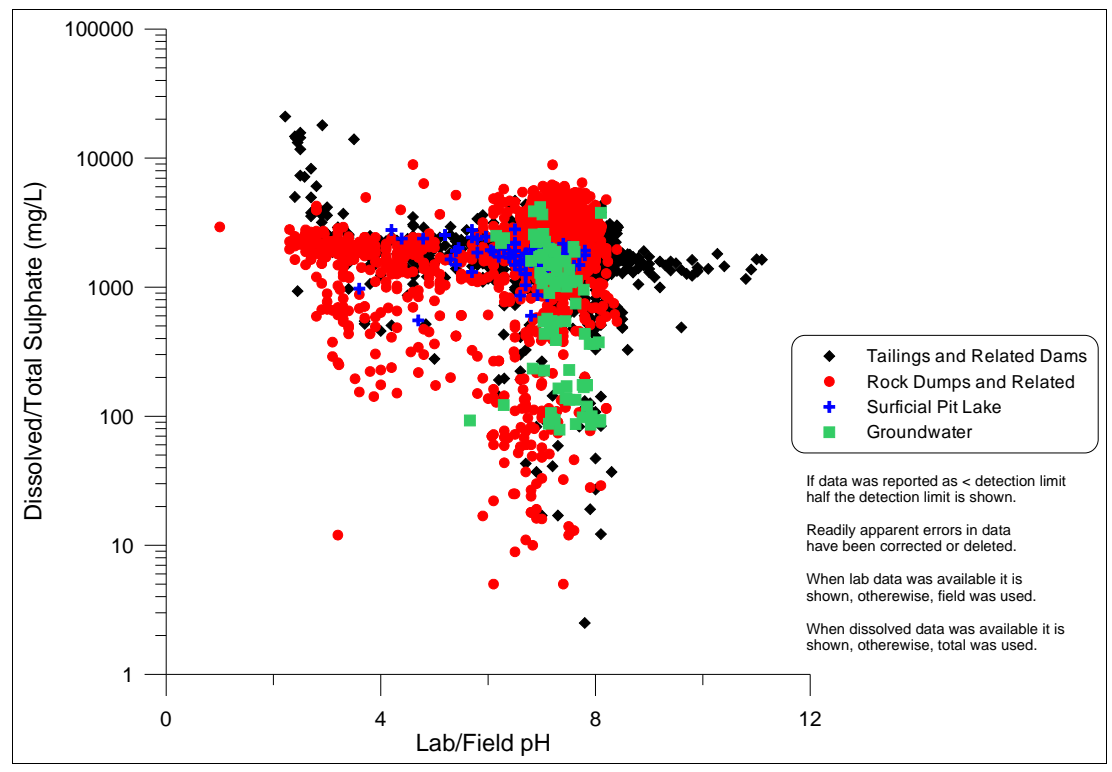


Figure A4-1. Sulphate vs. pH at the Bell Minesite.

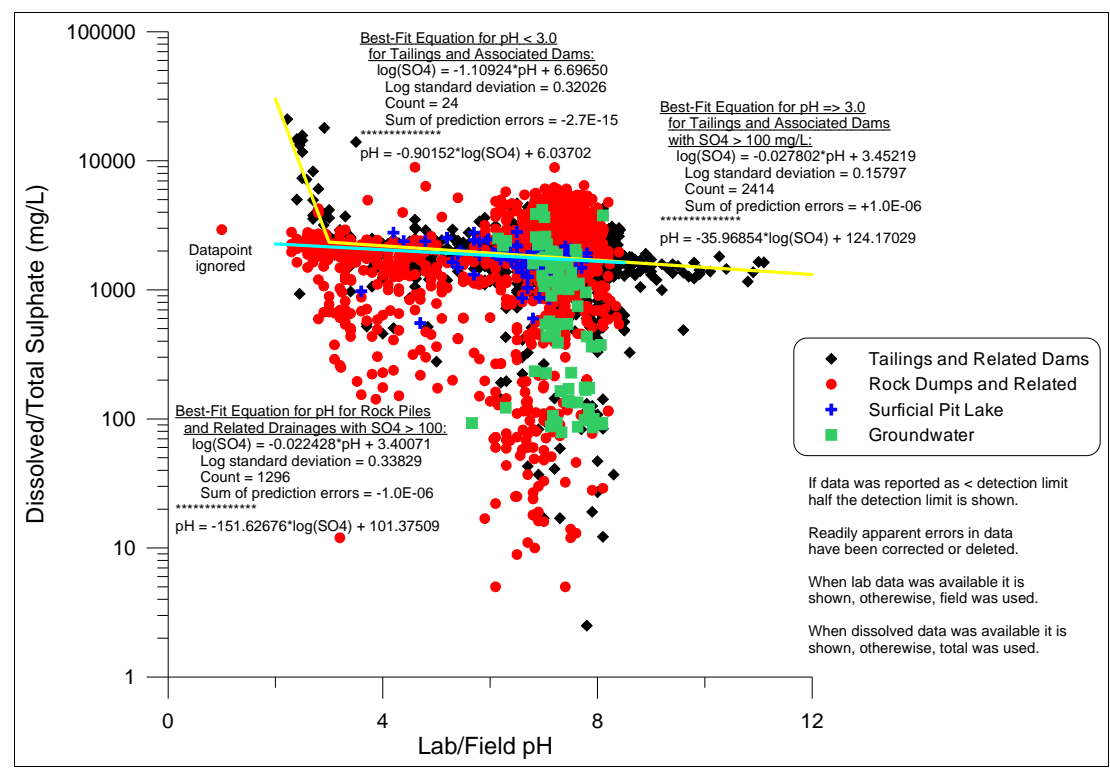


Figure A4-2. Best-fit equations for sulphate vs. pH in the 2010 Bell EDCM (see also Figure A4-3).

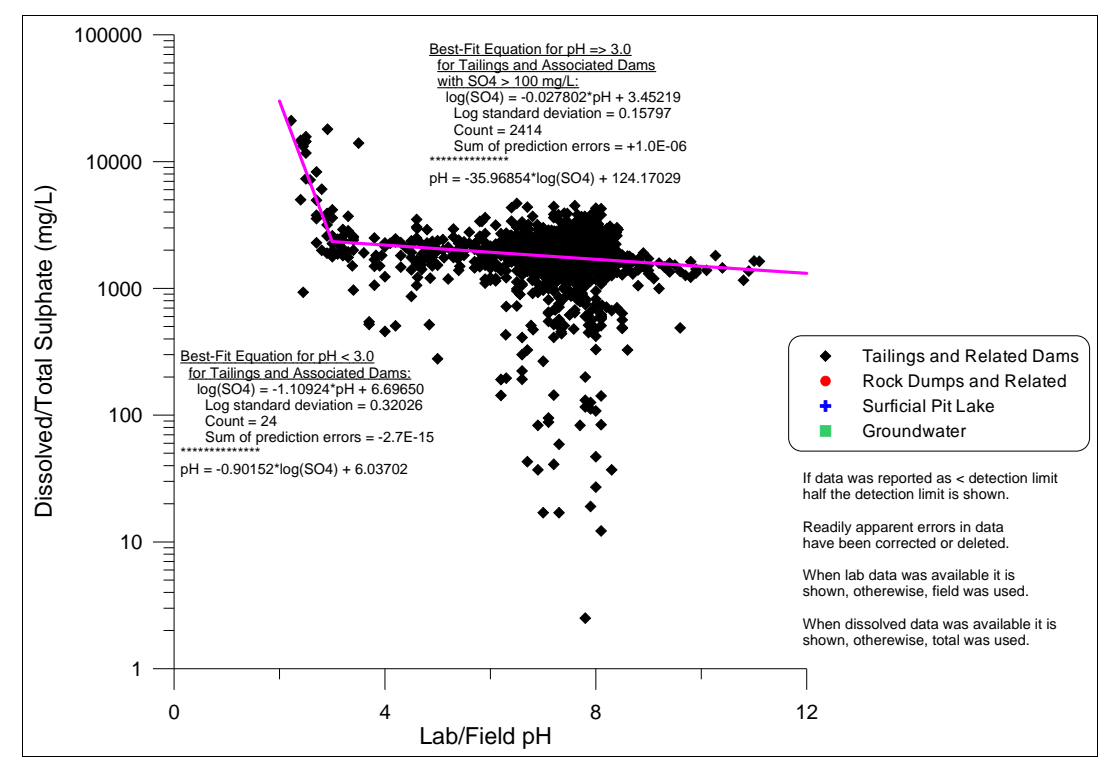


Figure A4-3. Best-fit equations for sulphate vs. pH in the 2010 Bell EDCM only for tailings and related dams (see also Figure A4-2).

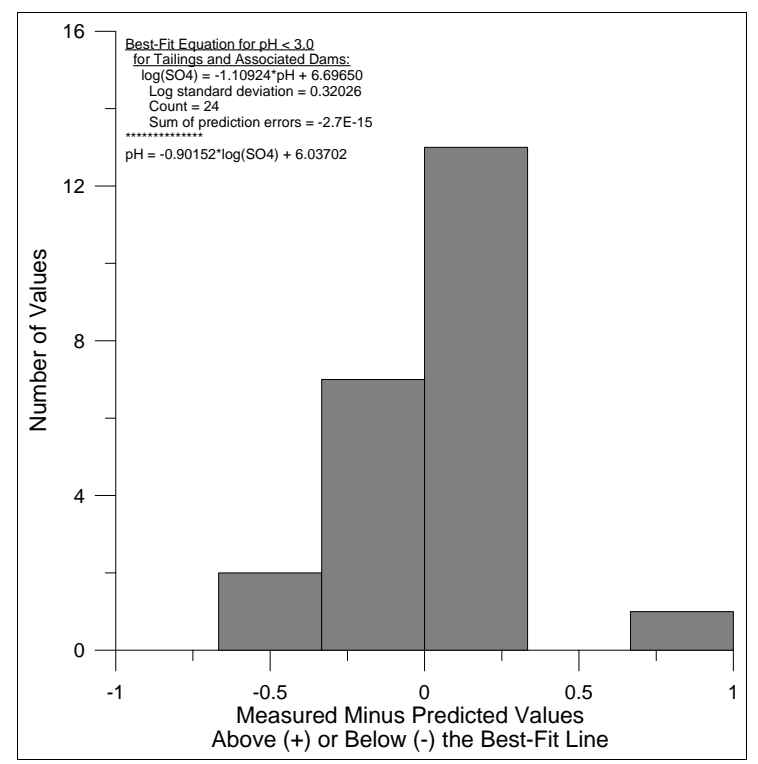


Figure A4-4. Statistical distribution of (measured-calculated) datapoints around the best-fit equation for sulphate below pH 3.0 for tailings and related dams.

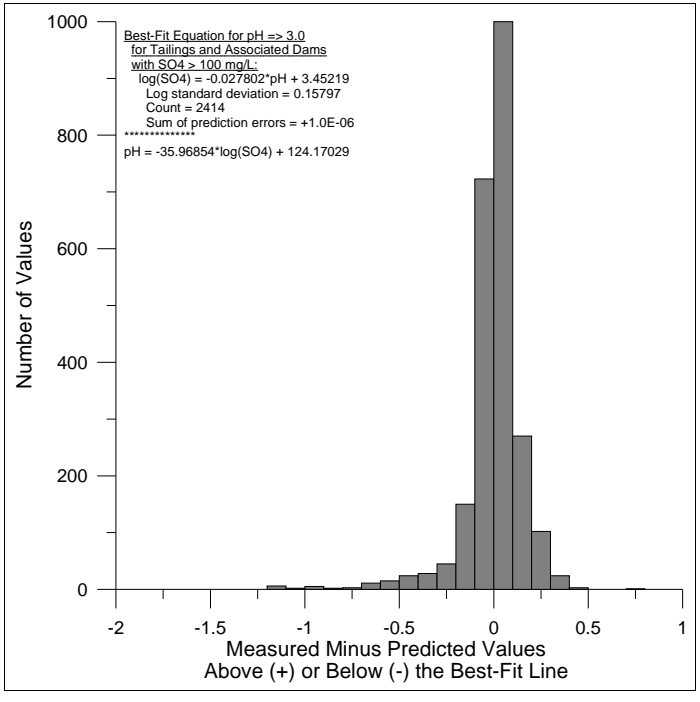


Figure A4-5. Statistical distribution of (measured-calculated) datapoints around the best-fit equation for sulphate at and above pH 3.0 for tailings and related dams.

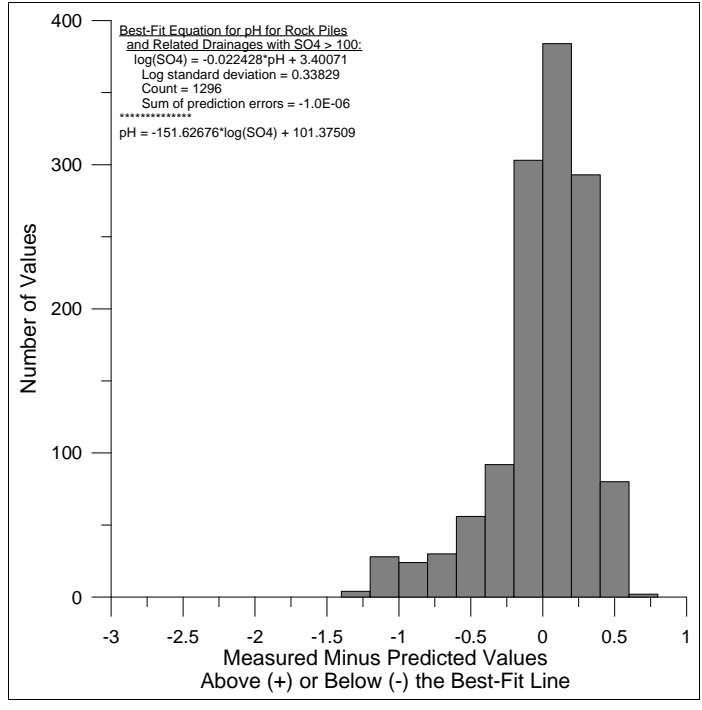


Figure A4-6. Statistical distribution of (measured-calculated) datapoints around the best-fit equation for sulphate in the rock dumps and related drainages.

Appendix A5. Conductivity

Notes:

Electrical conductivity is a relatively fast and easy measurement to make. There were more than 1400 measurements of laboratory or field conductivity in the Bell database.

Conductivity best reflected aqueous concentrations of sulphate (Figure A5-1), rather than pH (Figure A5-2). The correlation of conductivity with sulphate was good (Figure A5-3), with (measured-calculated) datapoints distributed around the best-fit equation in a general lognormal pattern (Figure A5-4) with a standard deviation of 0.10070 log10 cycles.

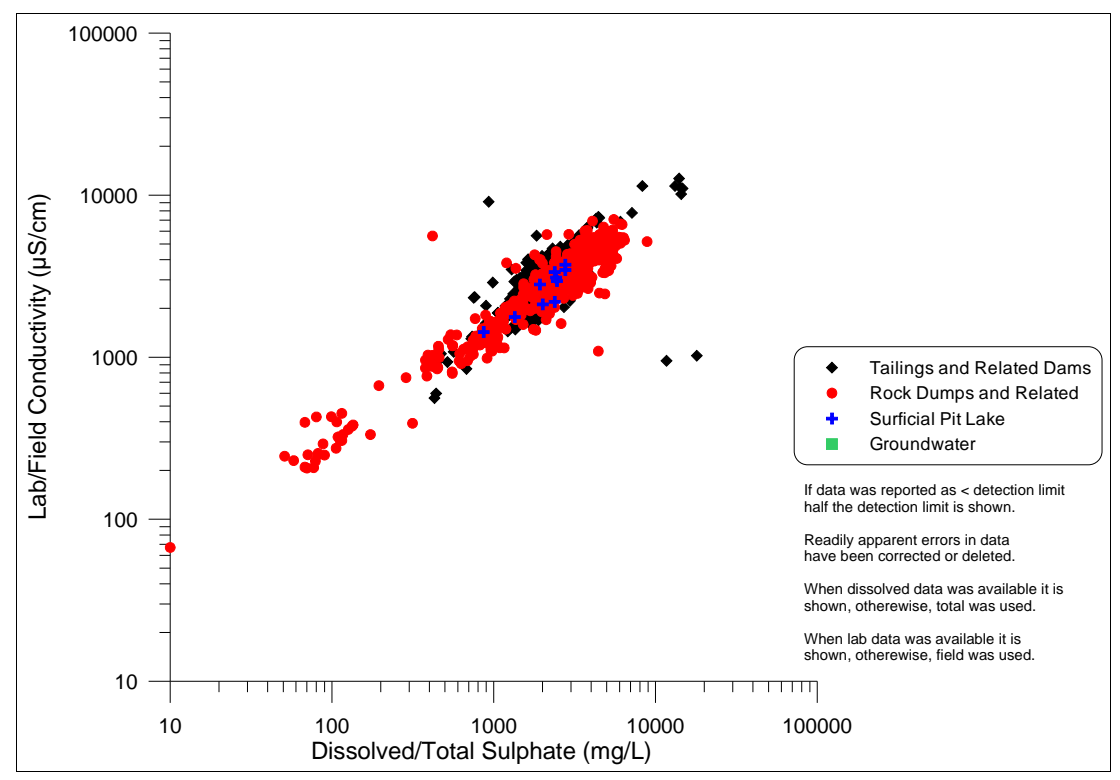


Figure A5-1. Electrical conductivity vs. sulphate at the Bell Minesite.

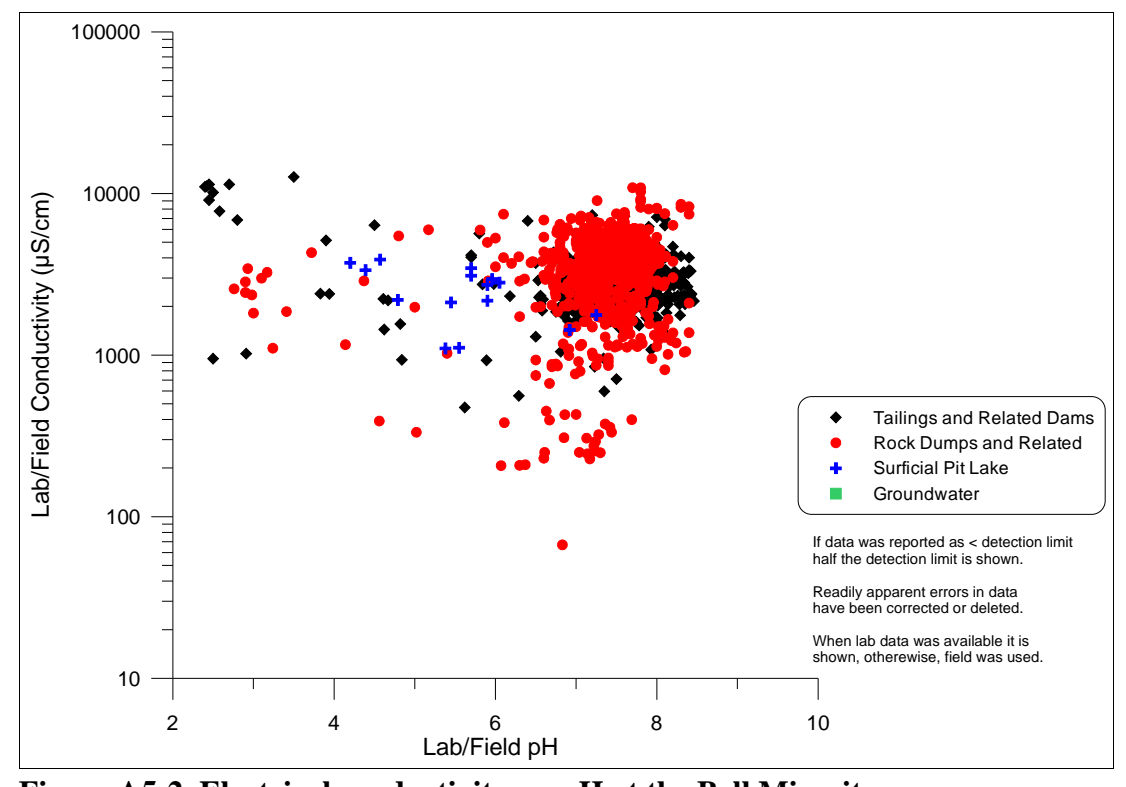


Figure A5-2. Electrical conductivity vs. pH at the Bell Minesite.

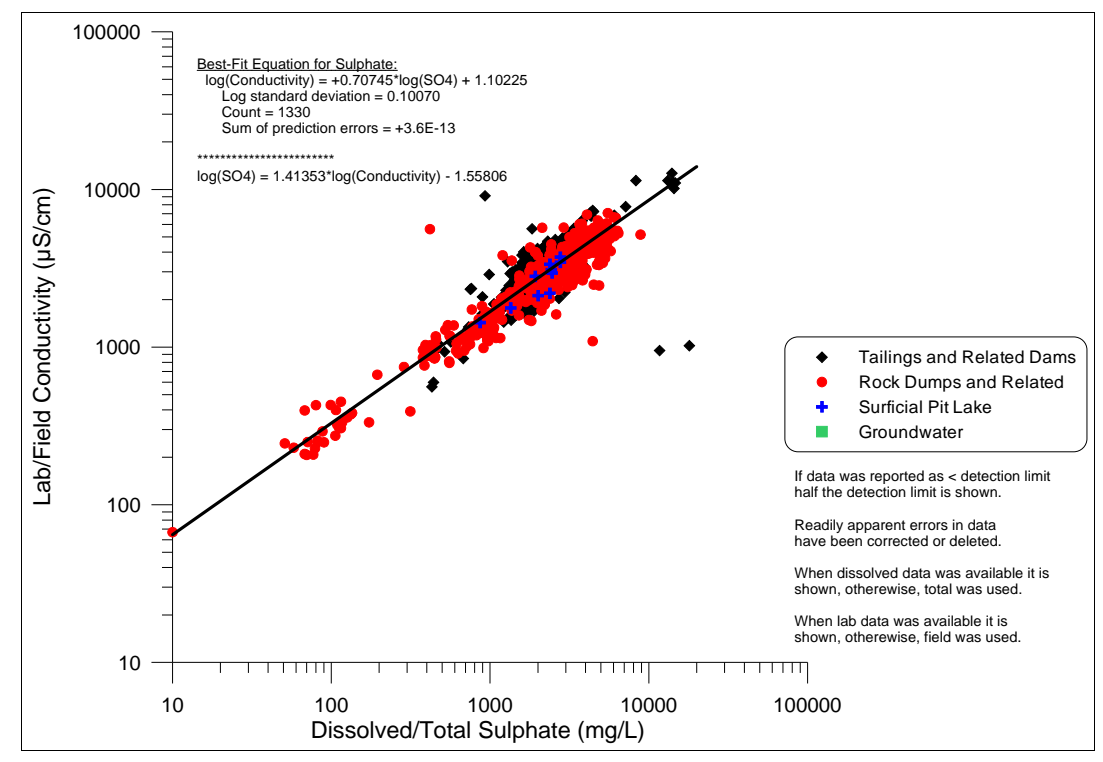


Figure A5-3. Best-fit equation for electrical conductivity vs. sulphate in the 2010 Bell EDCM.

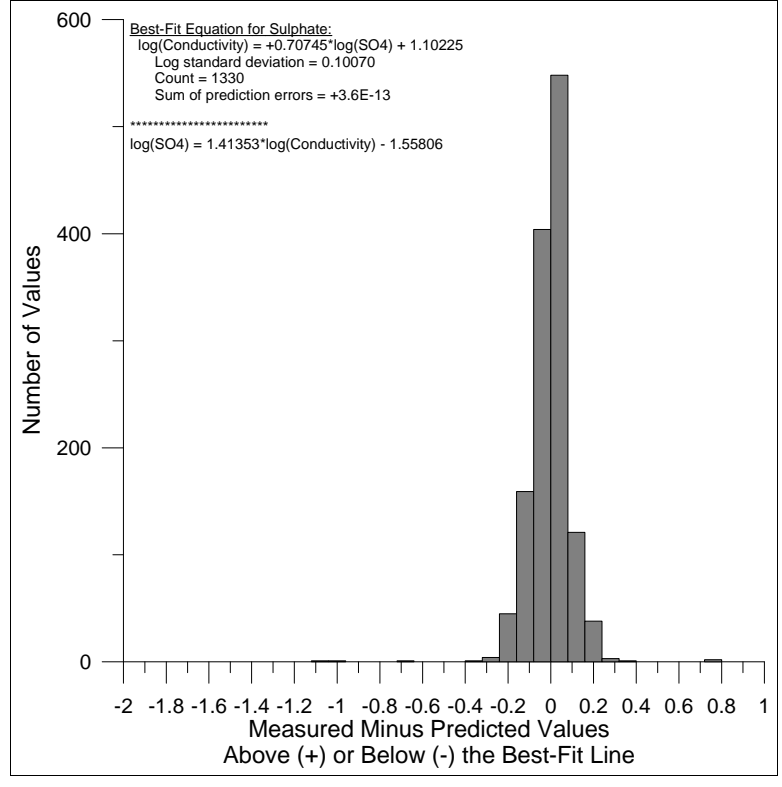


Figure A5-4. Statistical distribution of (measured-calculated) datapoints around the best-fit equation for conductivity.

Appendix A6. Hardness

Notes:

Hardness is typically a combination of calcium and magnesium, which are shown separately below. However, it is addressed separately here, because some water-quality guidelines change with hardness.

Hardness correlates much better with sulphate (Figure A6-2) than pH (Figure A6-1). With 2482 datapoints, the best-fit equation has a slope near 1.0 (Figure 6-3). These datapoints also generally form a lognormal distribution above and below the best-fit equation (Figure A6-4), with a standard deviation of roughly 0.18 log cycles.

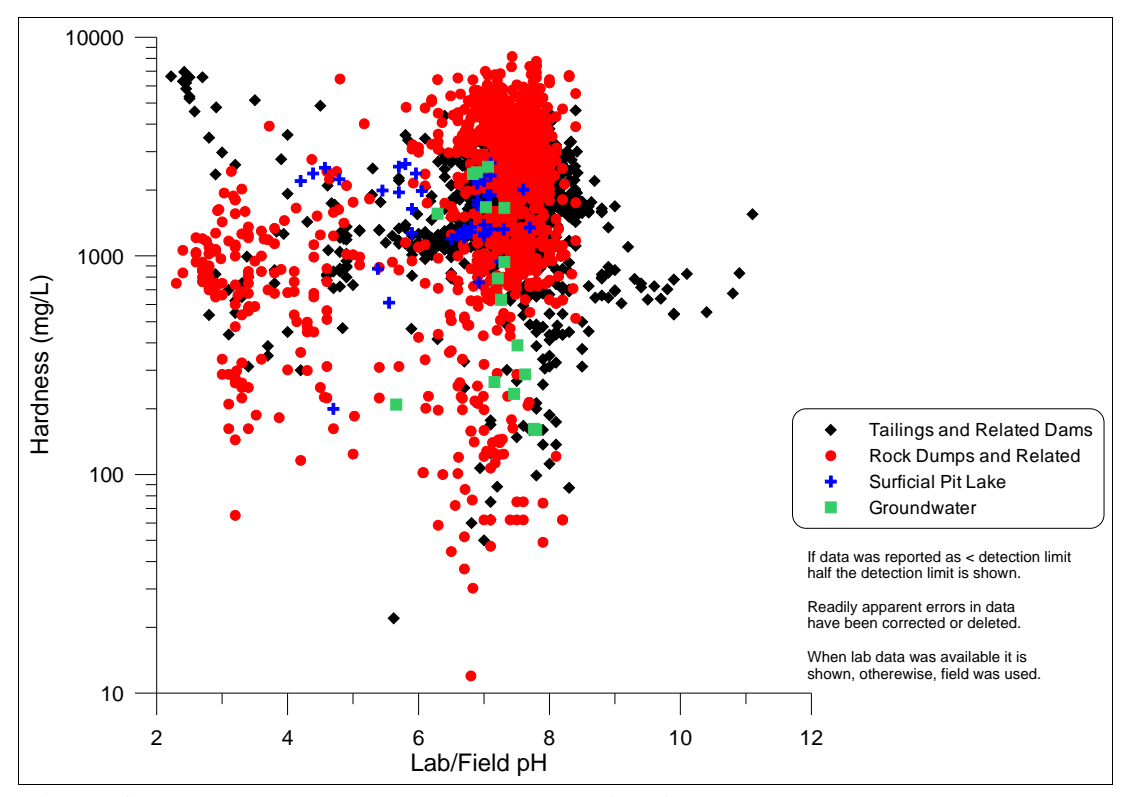


Figure A6-1. Hardness vs. pH at the Bell Minesite.

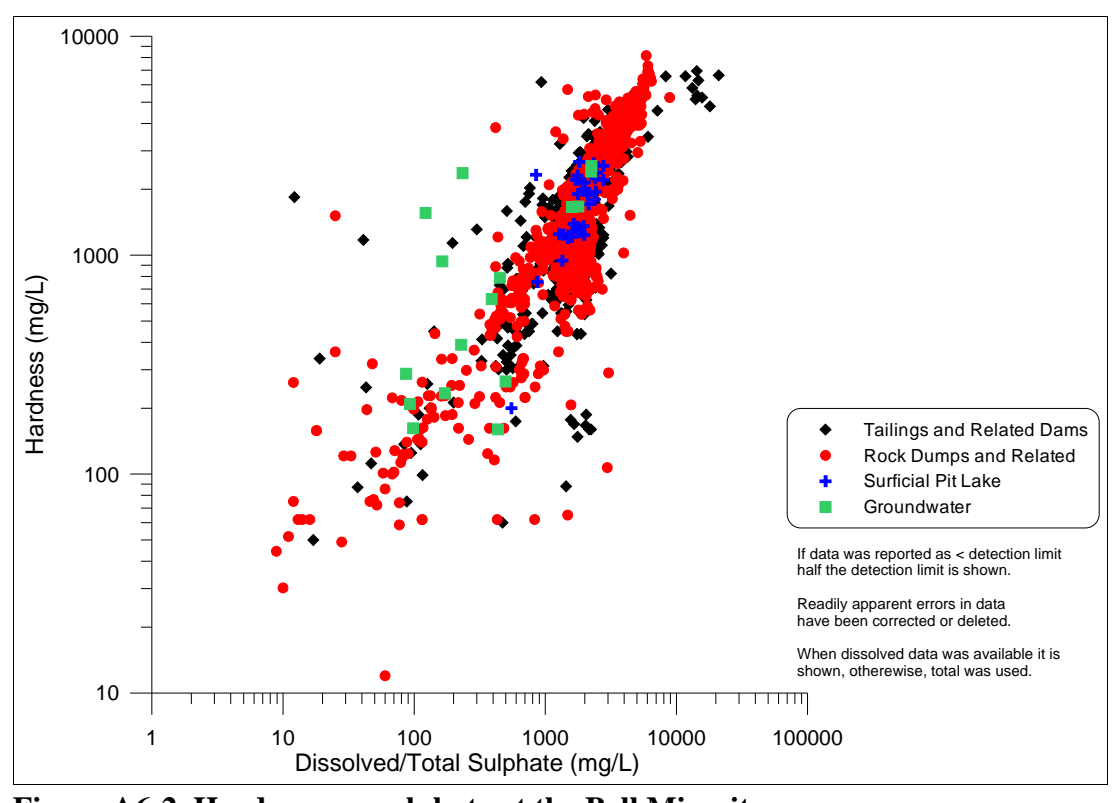


Figure A6-2. Hardness vs. sulphate at the Bell Minesite.

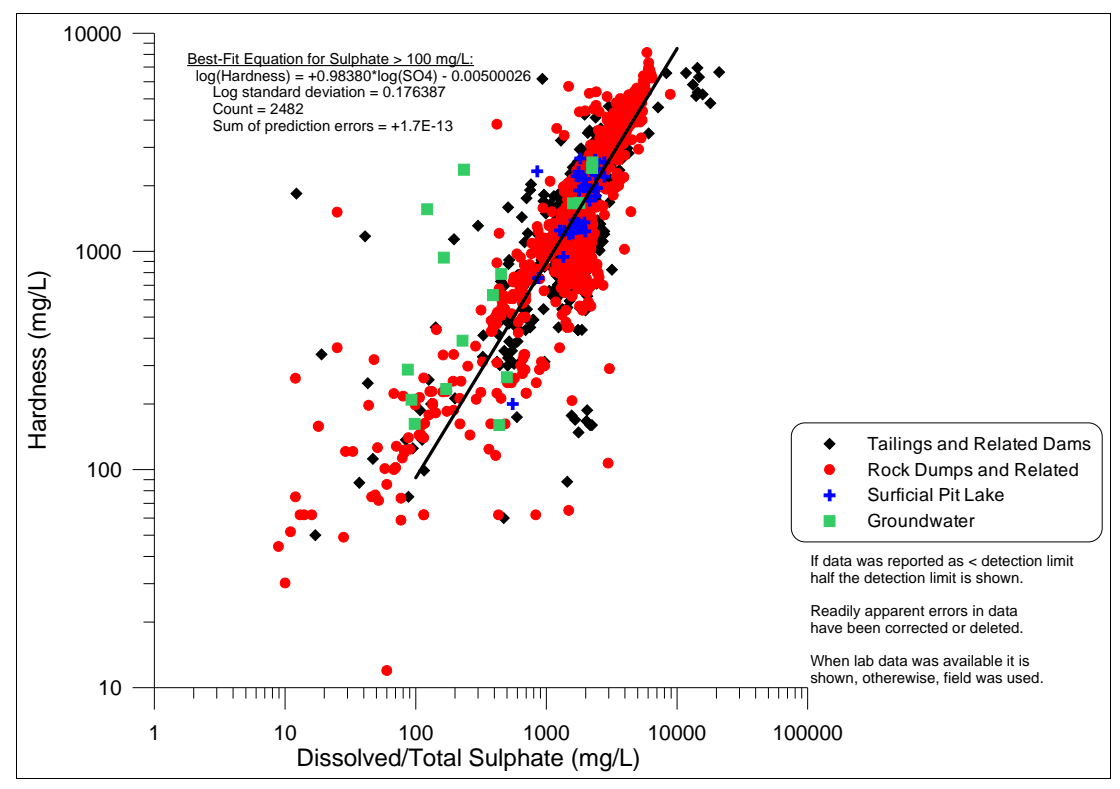


Figure A6-3. Best-fit equations for hardness vs. sulphate in the 2010 Bell EDCM.

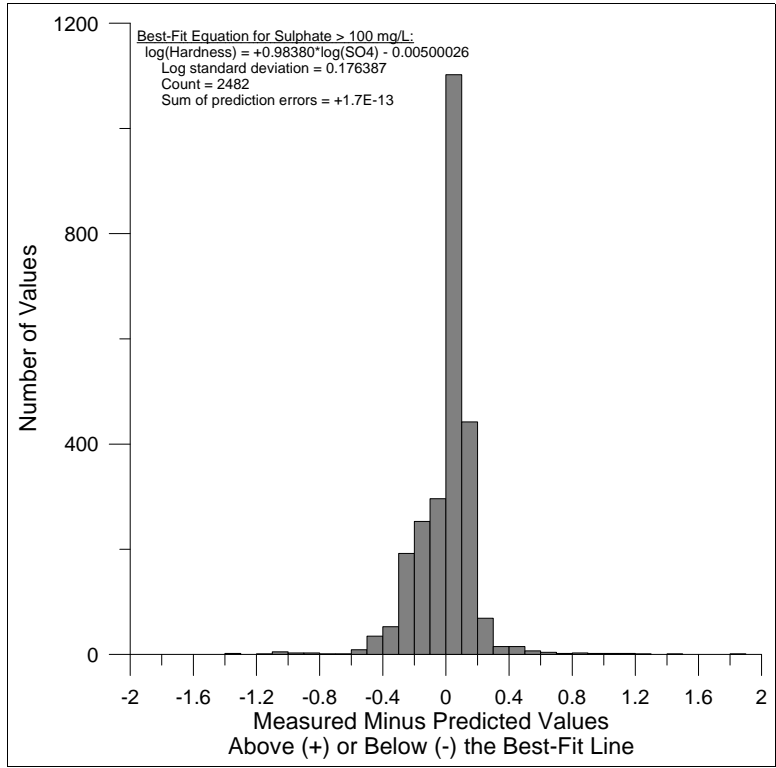


Figure A6-4. Statistical distribution of (measured-calculated) datapoints around the best-fit equation for hardness.

Appendix A7. Nitrate

Notes:

Nitrate, with more than 200 analyses in the Bell database, does not show any strong correlation with pH (Figure A7-1) or sulphate (Figure A7-2), but a general decrease through time. Therefore, nitrate is set at <3 mg/L before closure in 1992 and <2 mg/L afterwards (Figure A7-3).

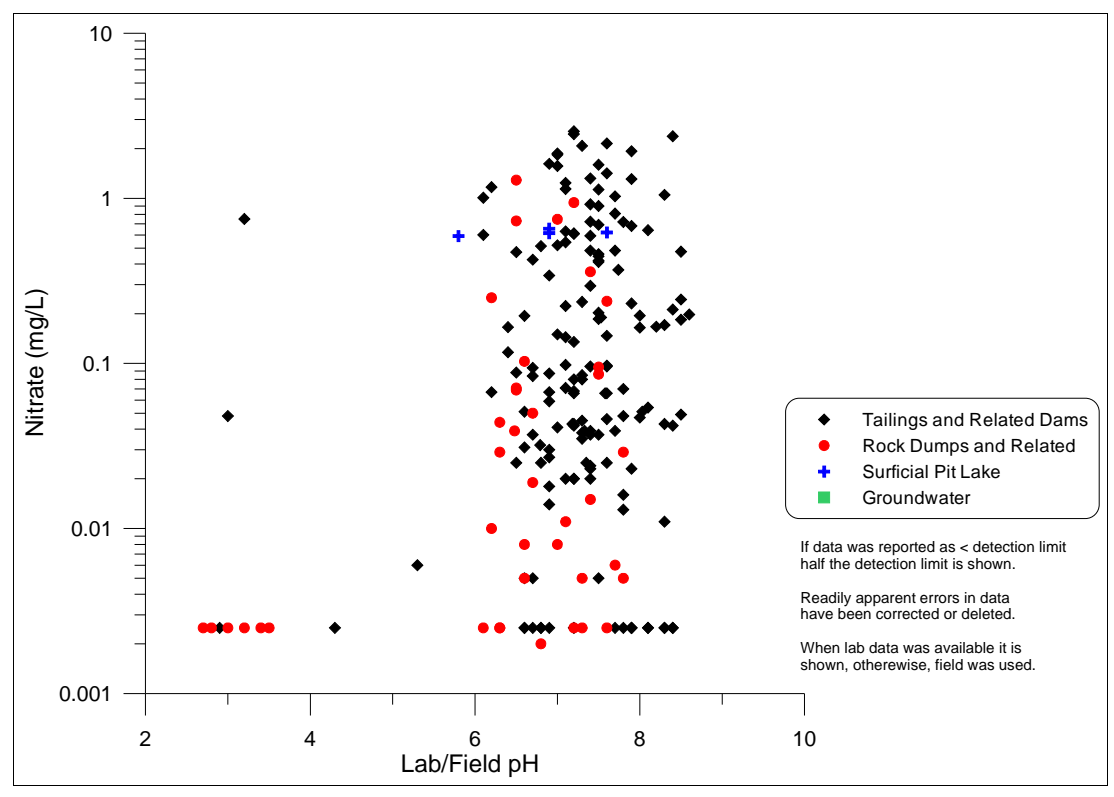


Figure A7-1. Nitrate vs. pH at the Bell Minesite.

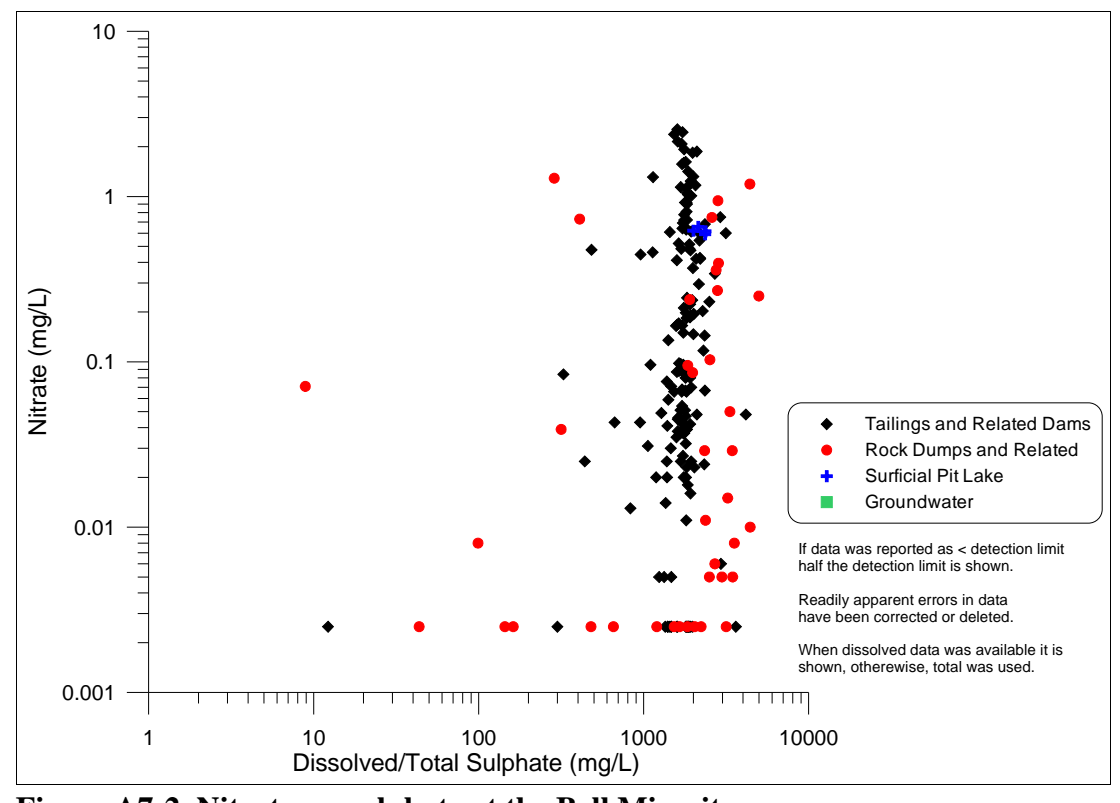


Figure A7-2. Nitrate vs. sulphate at the Bell Minesite.

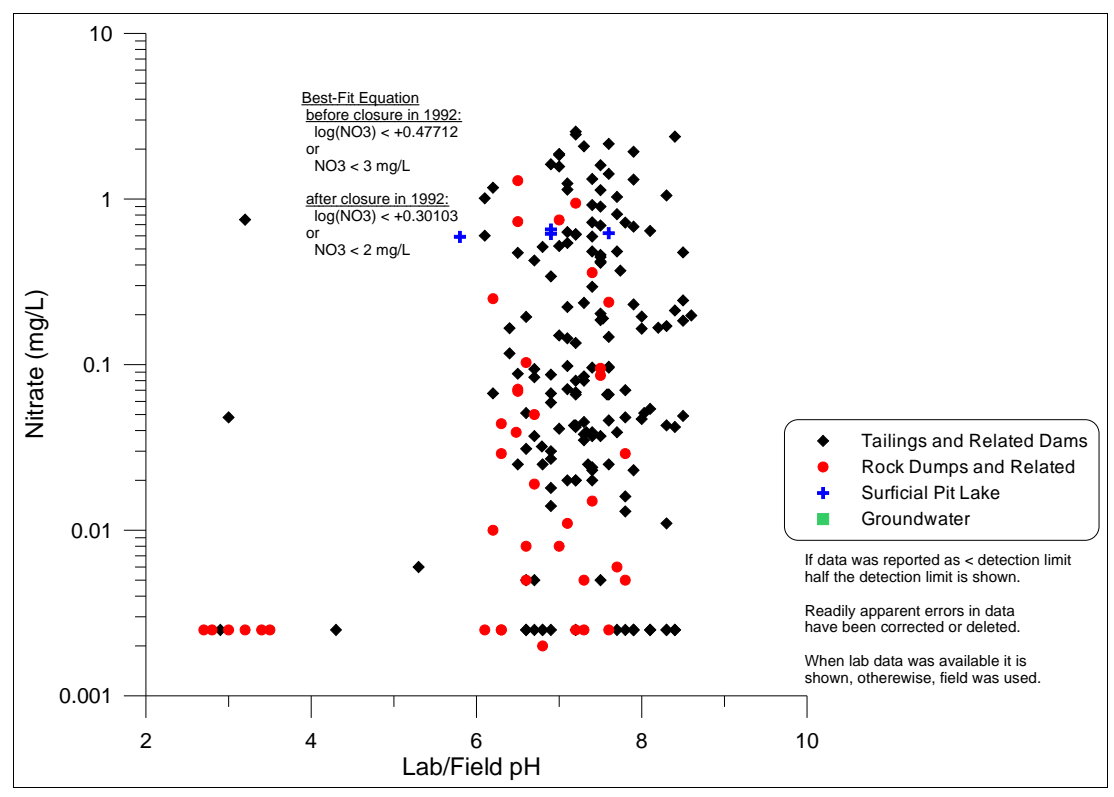


Figure A7-3. Best-fit equation for nitrate in the 2010 Bell EDCM.

Appendix A8. Nitrite

Notes:

Nitrite, with more than 200 analyses in the Bell database, does not show any strong correlation with pH (Figure A8-1) or sulphate (Figure A8-2), but a general decrease through time. Therefore, nitrite is set at <3 mg/L before closure in 1992 and <0.6 mg/L afterwards (Figure A8-3).

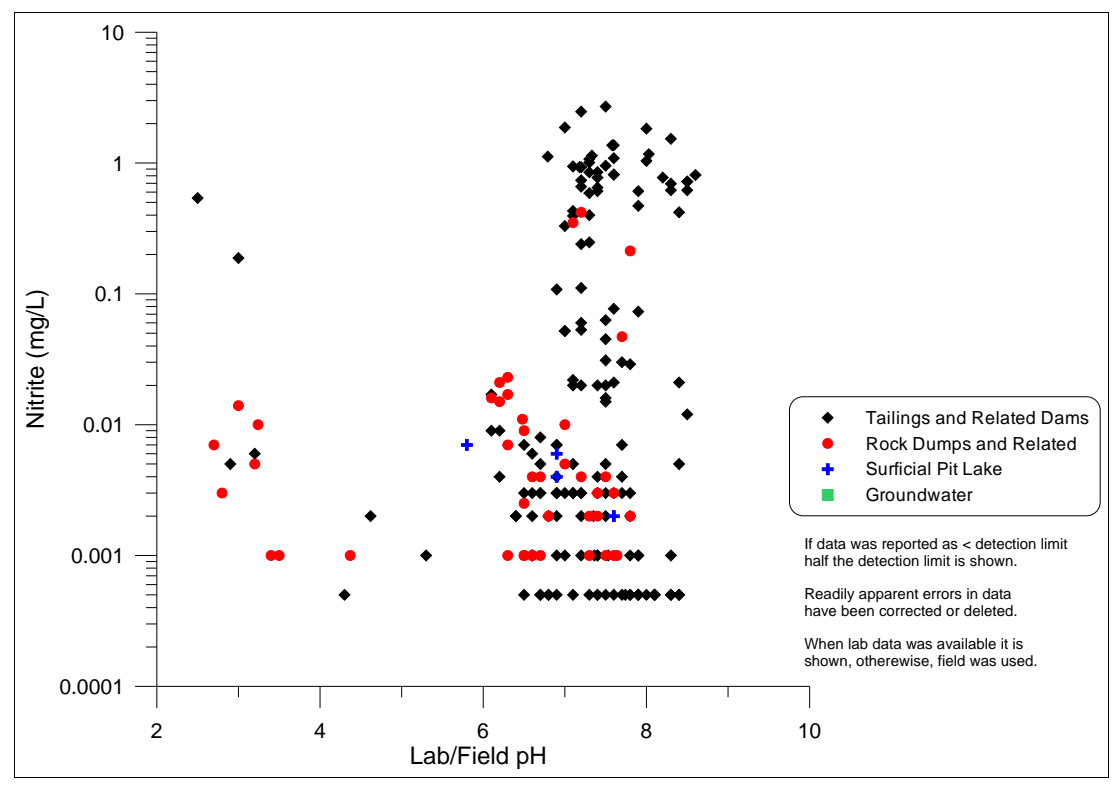


Figure A8-1. Nitrite vs. pH at the Bell Minesite.

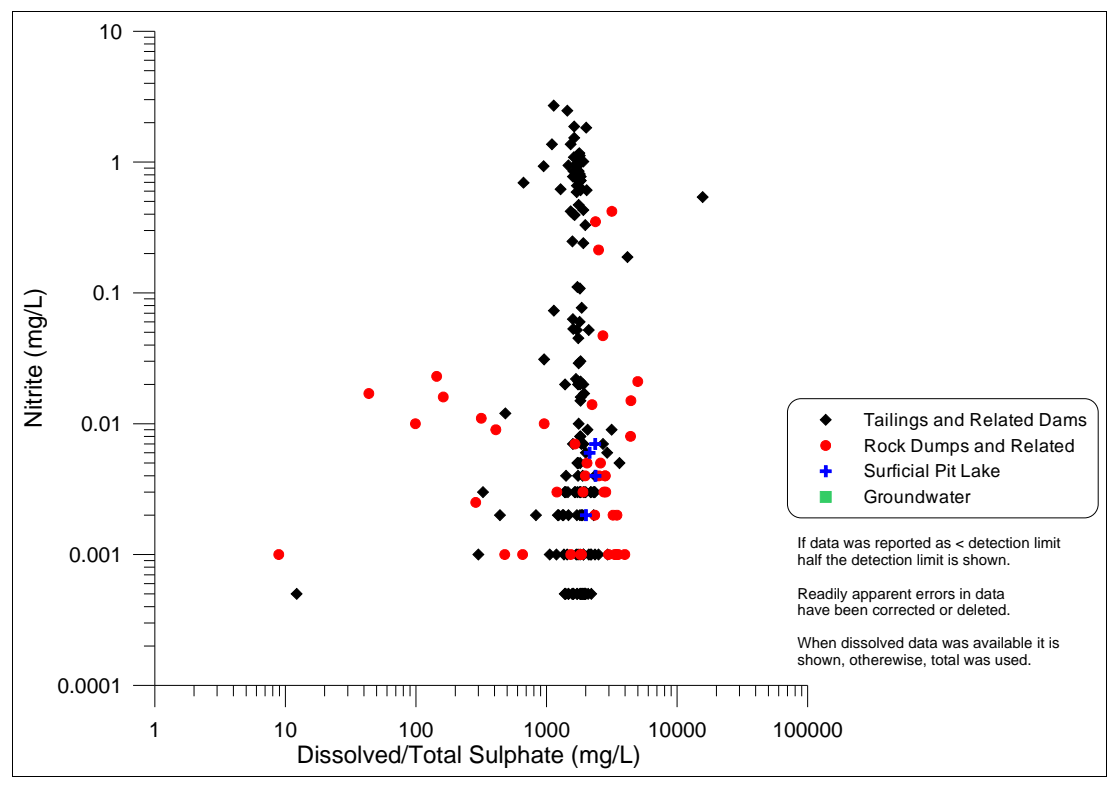


Figure A8-2. Nitrite vs. sulphate at the Bell Minesite.

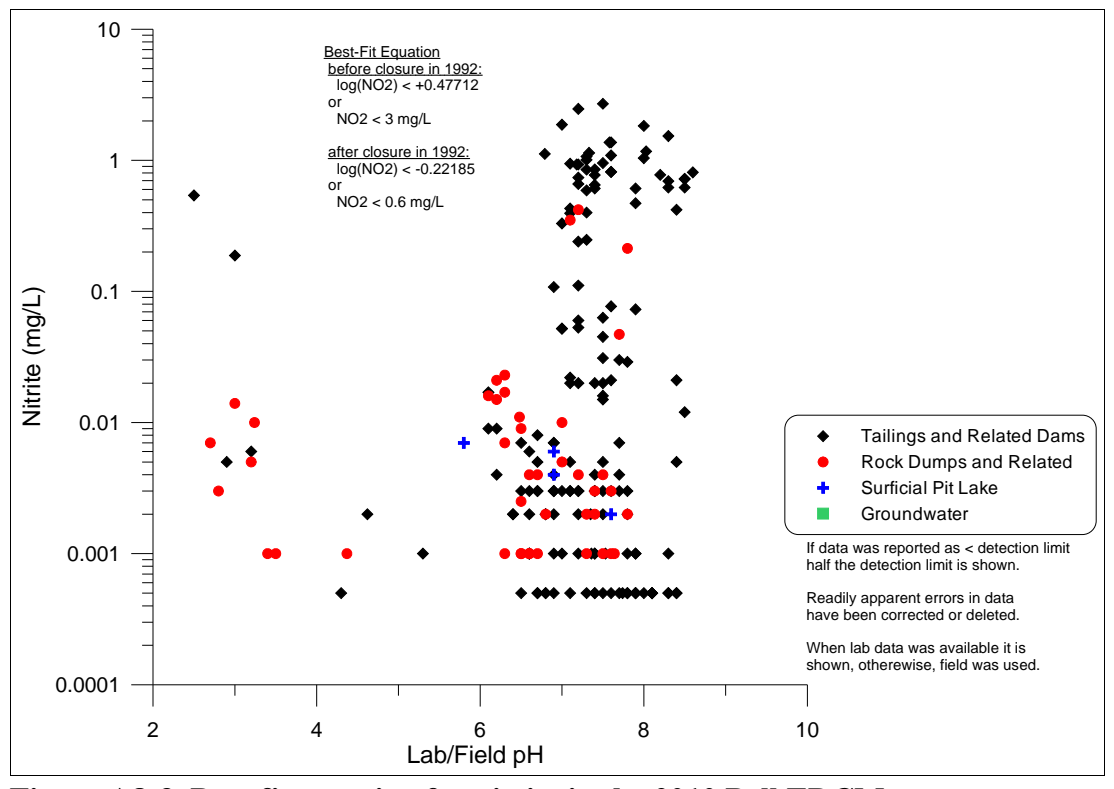


Figure A8-3. Best-fit equation for nitrite in the 2010 Bell EDCM.

Appendix A9. Ammonia

Notes:

Ammonia, with roughly 70 analyses in the Bell database only for groundwater, does not show any strong correlation with pH (Figure A9-1) or sulphate (Figure A9-2). Therefore, ammonia is simply set at <2 mg/L (Figure A9-3).

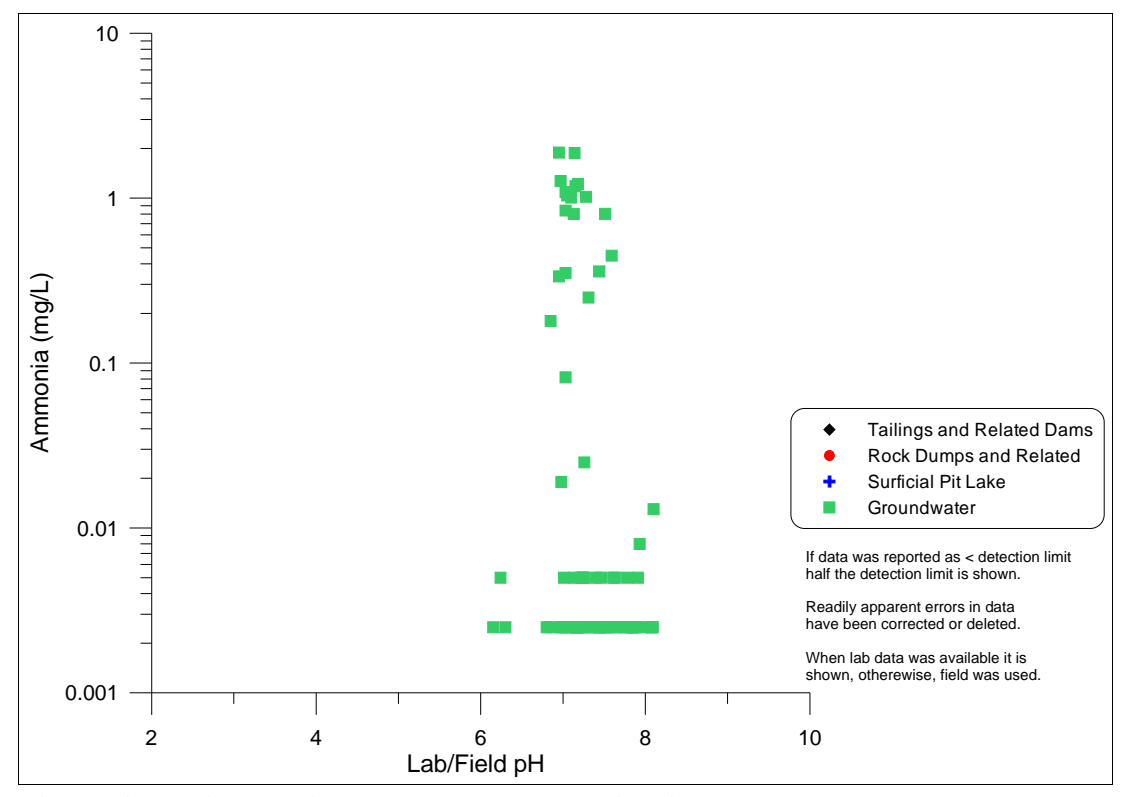


Figure A9-1. Ammonia vs. pH at the Bell Minesite.

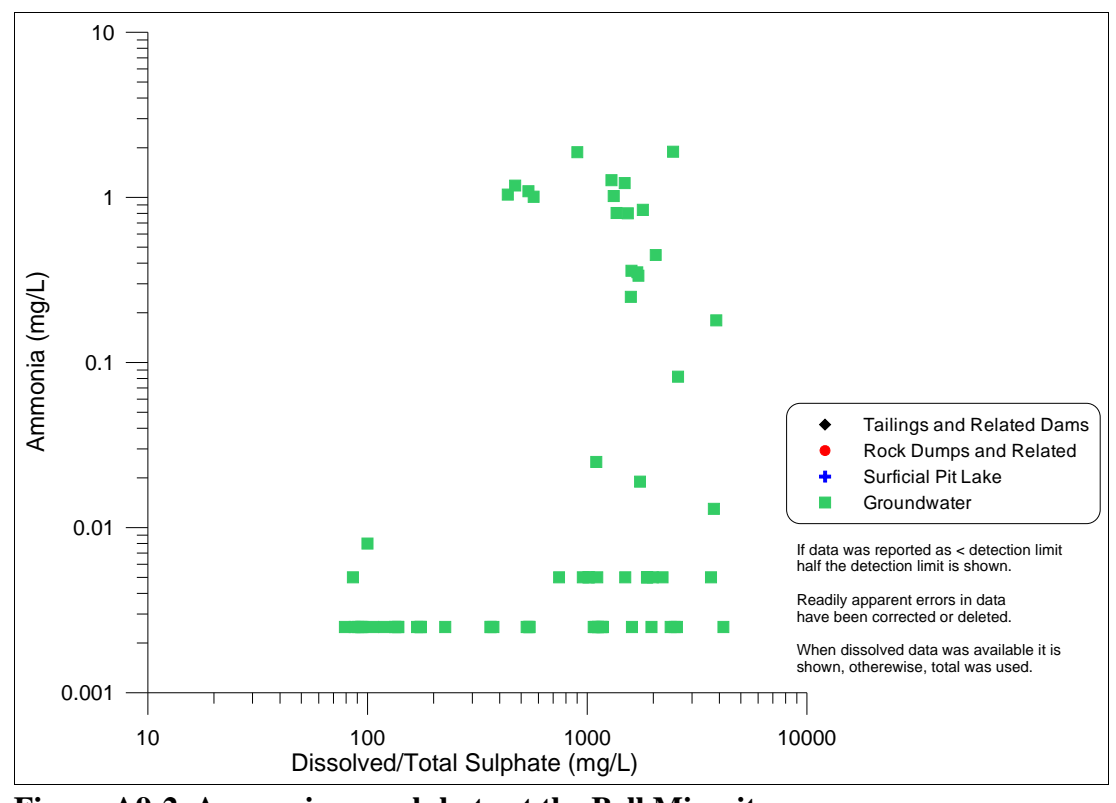


Figure A9-2. Ammonia vs. sulphate at the Bell Minesite.

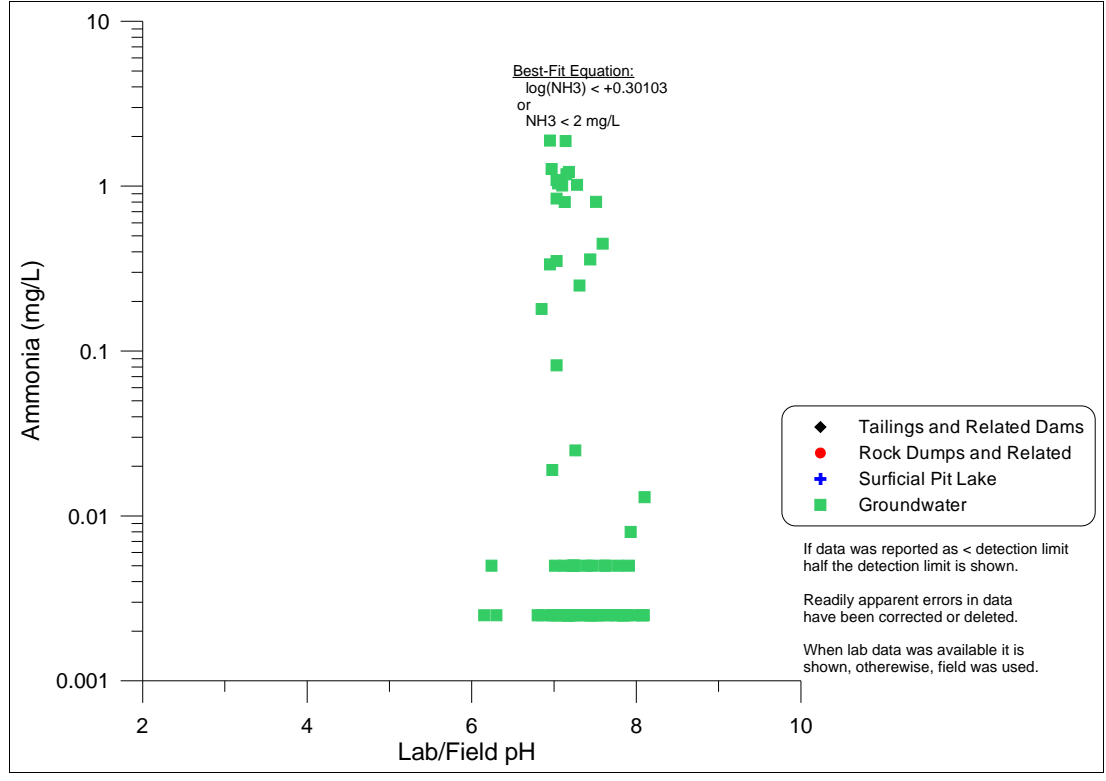


Figure A9-3. Best-fit equation for ammonia in the 2010 Bell EDCM.

Appendix A10. Dissolved Aluminum (Al-D)

Notes:

Dissolved aluminum shows some correlation with the master parameters of pH (Figure A10-1) and sulphate (Figure A10-2), with Al-D concentrations below roughly 1 mg/L more independent of these.

A best-fit equation based on 845 pairs of Al-D and pH has a slope of about -0.83 (Figure A10-3). The distribution of these datapoints above and below this equation is generally lognormal (Figure A10-4), with a standard deviation of 0.64 log cycles.

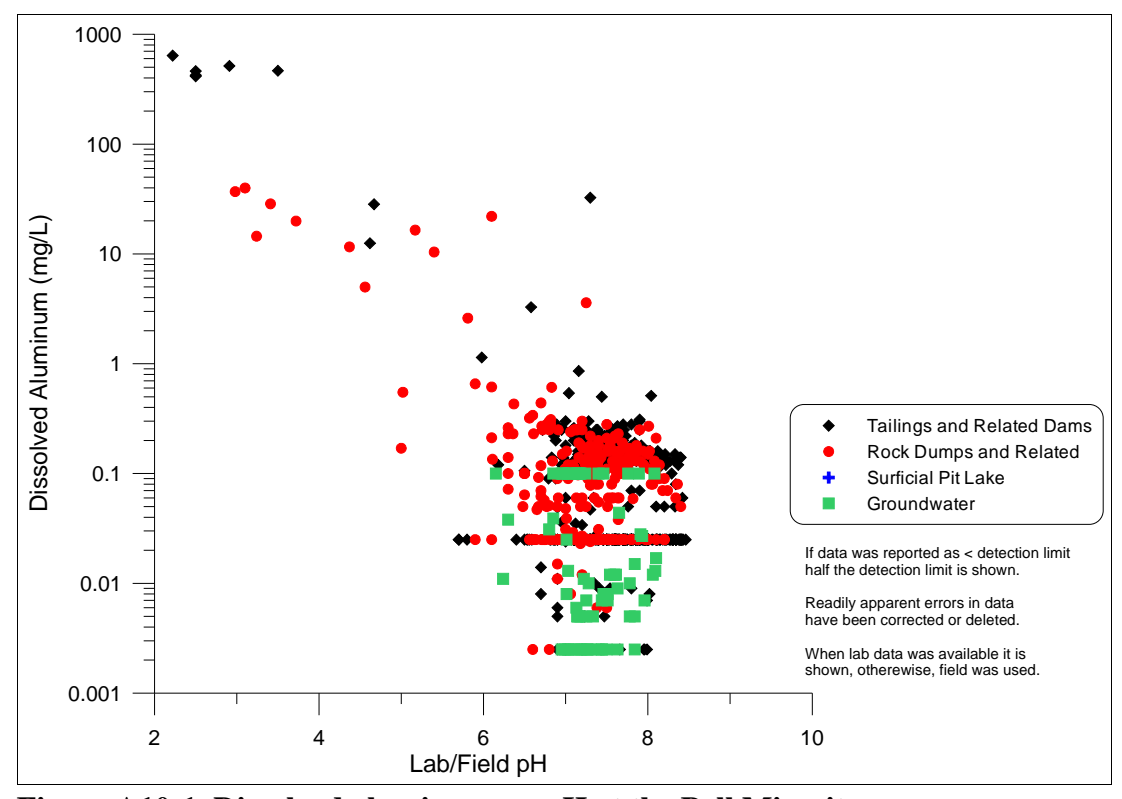


Figure A10-1. Dissolved aluminum vs. pH at the Bell Minesite.

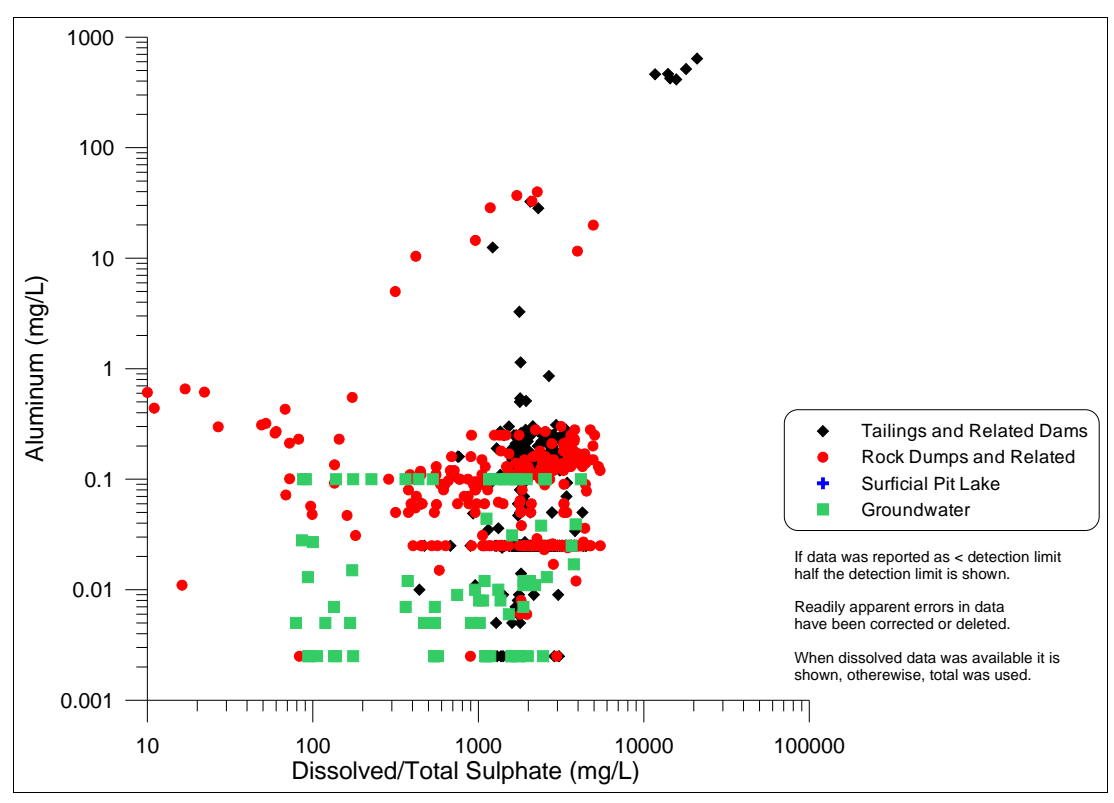


Figure A10-2. Dissolved aluminum vs. sulphate at the Bell Minesite.

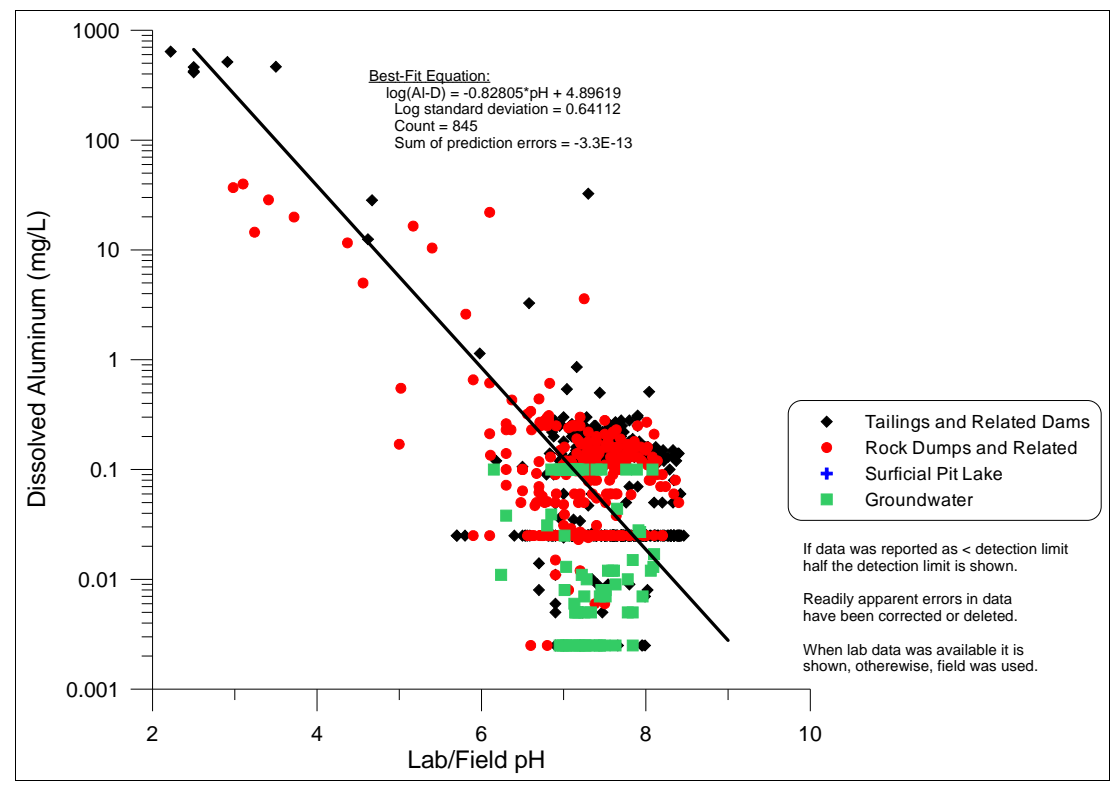


Figure A10-3. Best-fit equation for dissolved aluminum vs. pH in the 2010 Bell EDCM.

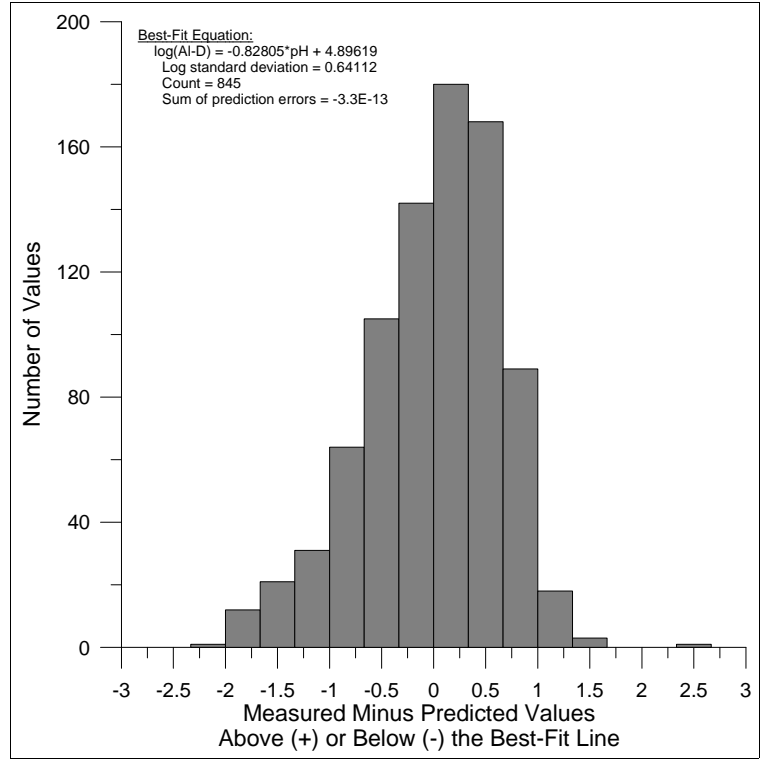


Figure A10-4. Statistical distribution of (measured-calculated) datapoints around the best-fit equation for dissolved aluminum.

Appendix A11. Dissolved Antimony (Sb-D)

Notes:

In the Bell Minesite database, the 98 analyses of dissolved antimony were in near-neutral waters (Figure A11-1), so trends with pH cannot be assessed. Furthermore, the analytical results were at or below various detection limits, hiding any trends with sulphate (Figure A11-2). Thus, dissolved antimony was simply set to below the lowest detection limit, <0.0001 mg/L (Figure A11-3).

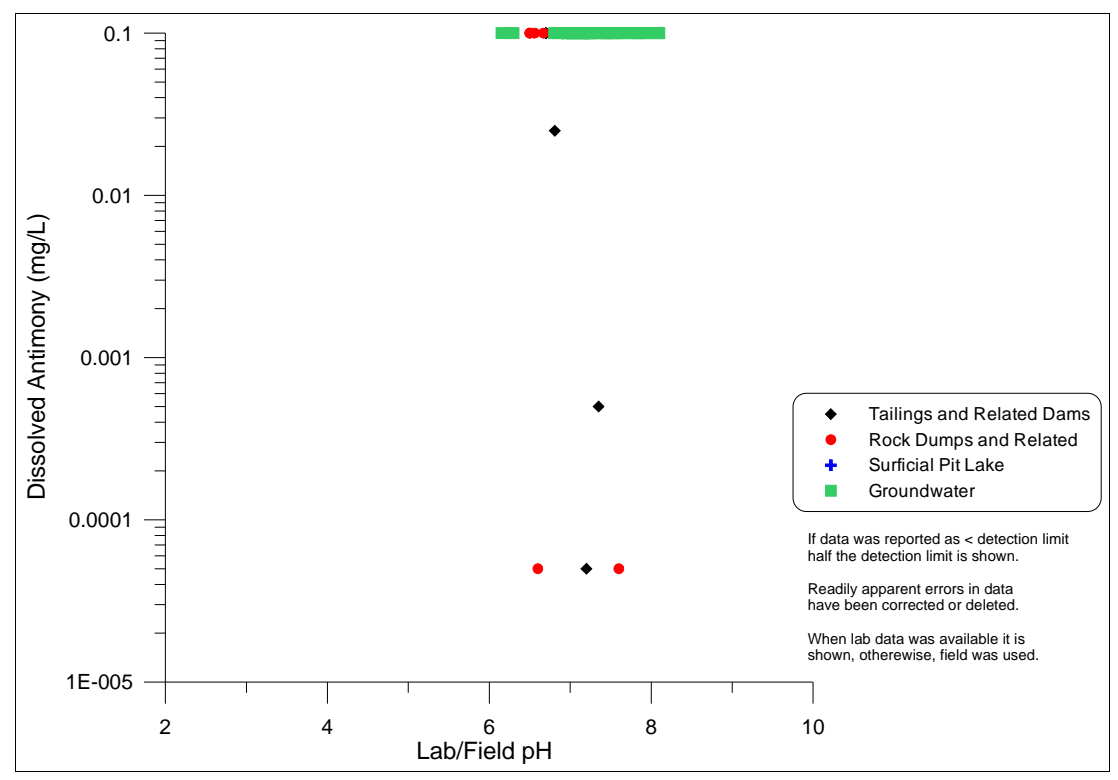


Figure A11-1. Dissolved antimony vs. pH at the Bell Minesite.

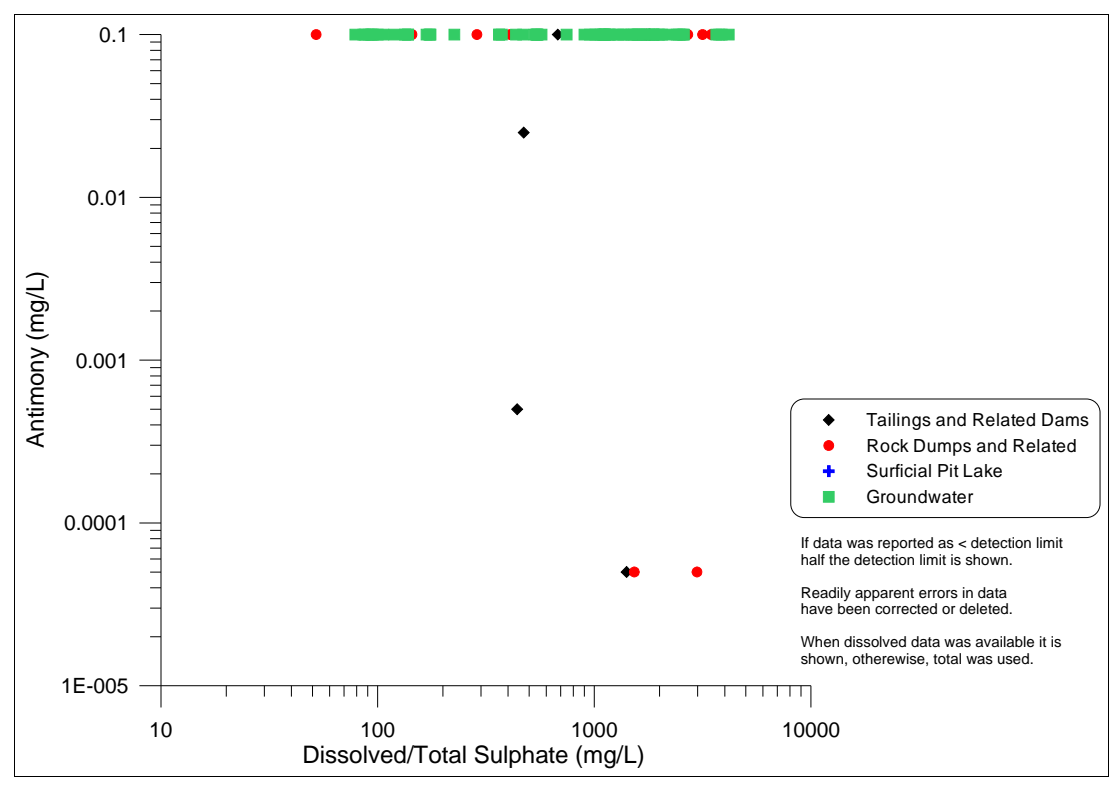


Figure A11-2. Dissolved antimony vs. sulphate at the Bell Minesite.

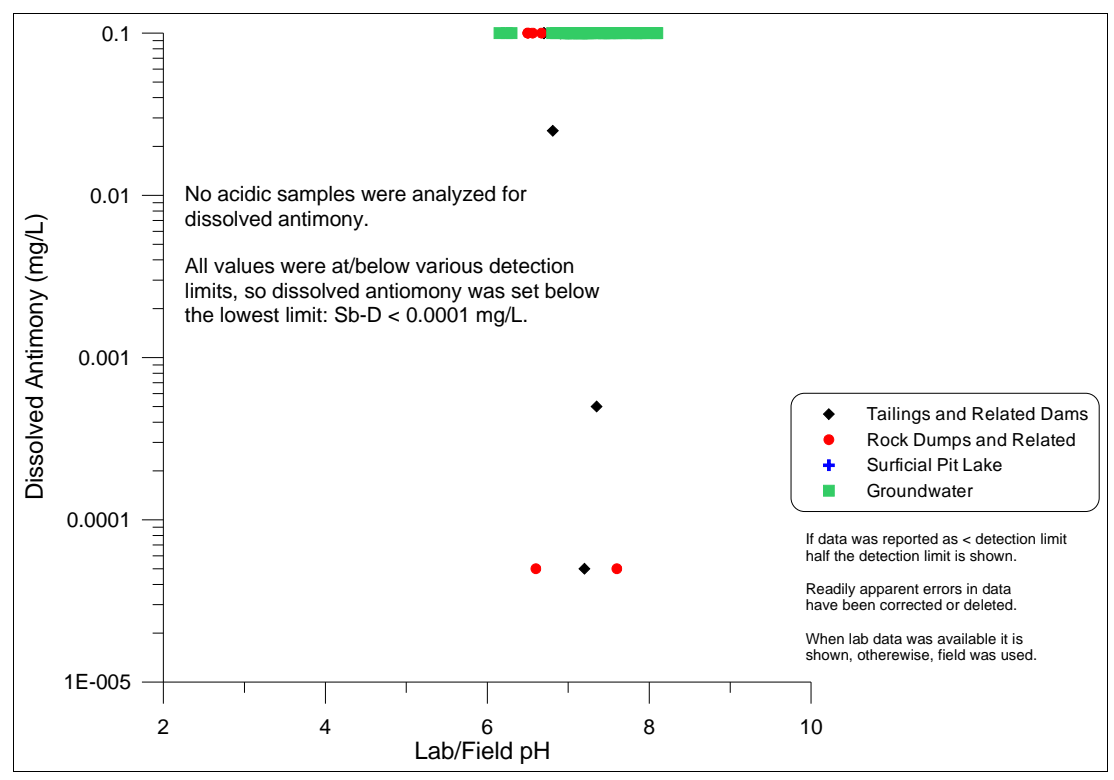


Figure A11-3. Best-fit equation for dissolved antimony in the 2010 Bell EDCM.

Appendix A12. Dissolved Arsenic (As-D)

Notes:

Of the 802 analyses of dissolved arsenic in the Bell Minesite database, only 72 had detectable levels. As a result, trends with pH (Figure A12-1, with half detection limits seen as horizontal bands) and sulphate (Figure A12-2) are not readily apparent.

Ignoring data at and below detection limits, a best-fit trend with pH consists of two segments (Figure A12-3), but with the acidic segment below pH 4 represented by only 11 datapoints. Above pH 4, the detectable arsenic was considered independent of pH (and sulphate).

Below pH 4.0, the 11 datapoints are too few to suggest a statistical distribution (Figure A12-4), but with a standard deviation of 0.97 log cycles if lognormal statistics apply. Above 4.0, the datapoints display a general lognormal distribution with a standard deviation of 0.51 log cycles (Figure A12-5).

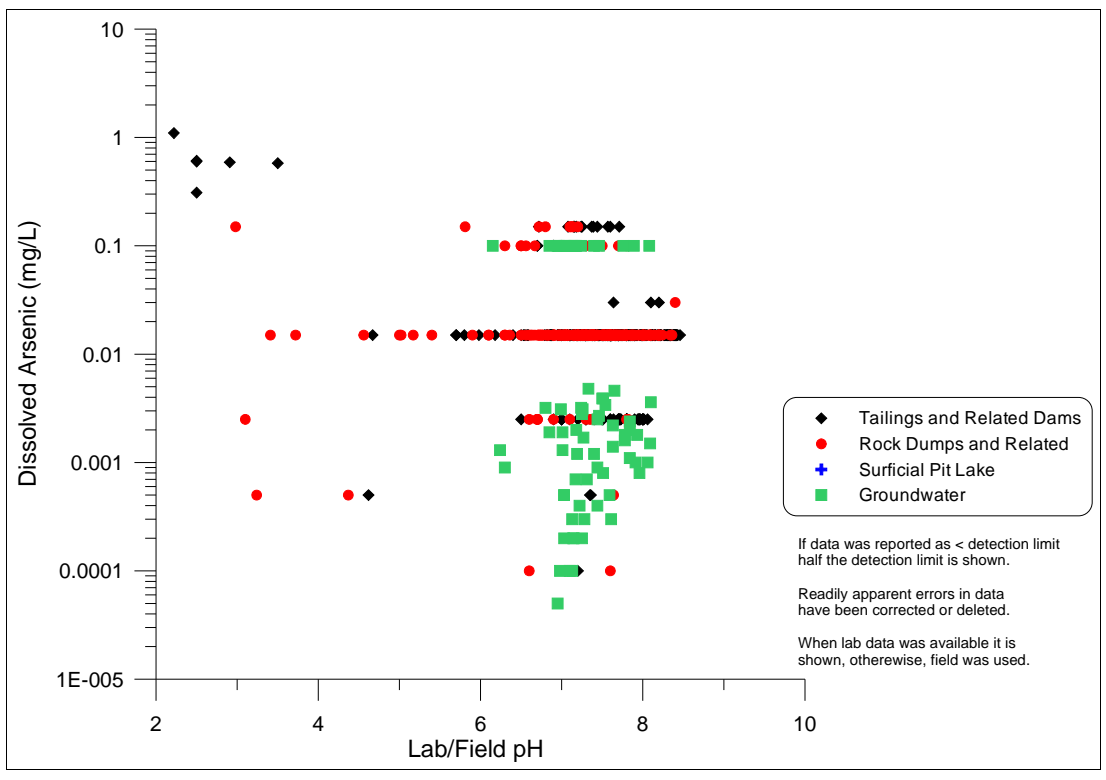


Figure A12-1. Dissolved arsenic vs. pH at the Bell Minesite.

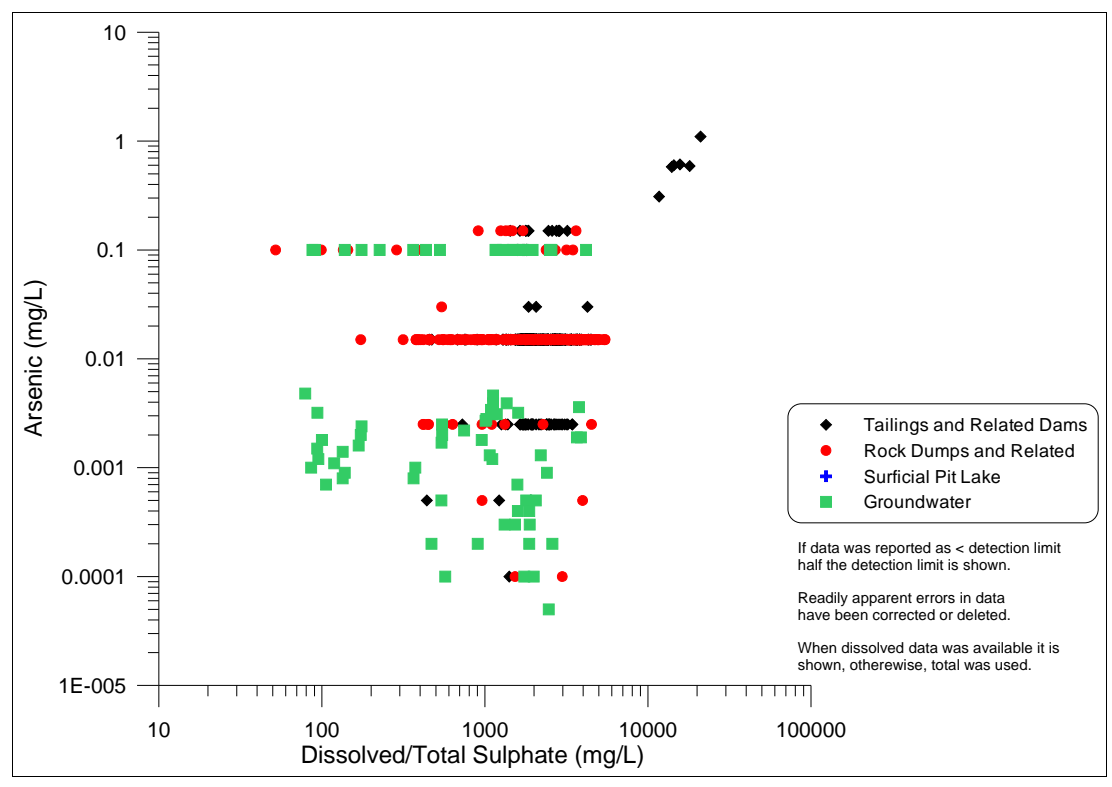


Figure A12-2. Dissolved arsenic vs. sulphate at the Bell Minesite.

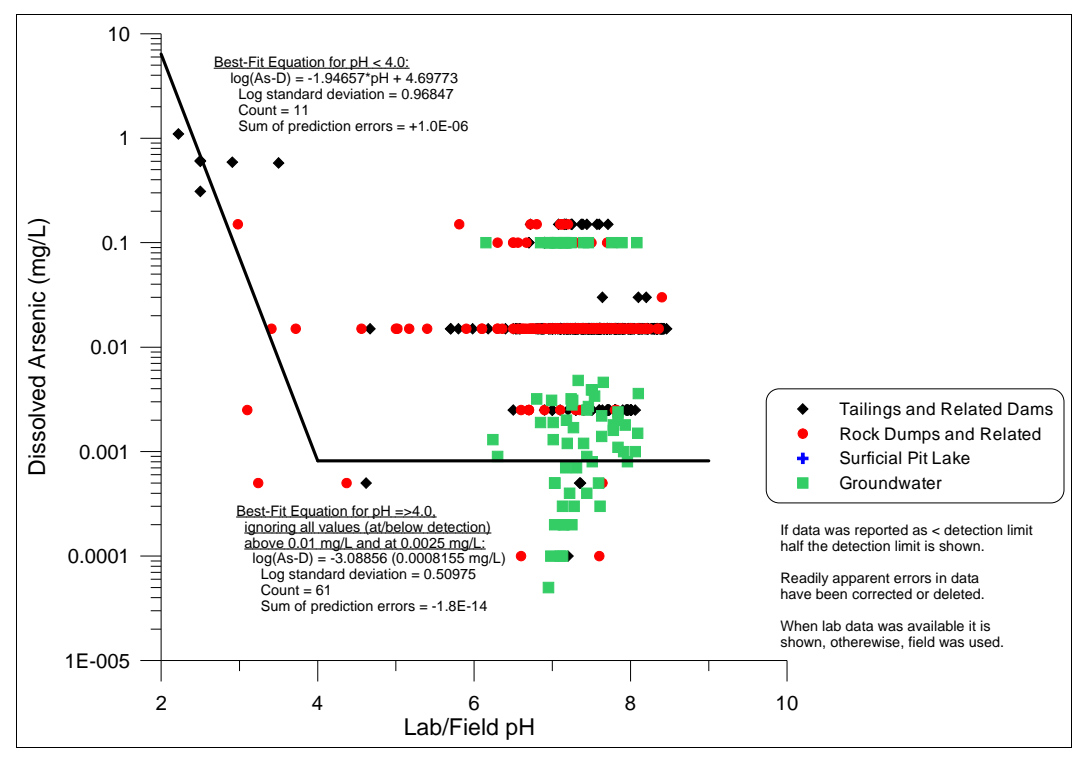


Figure A12-3. Best-fit equations for dissolved arsenic vs. pH in the 2010 Bell EDCM.

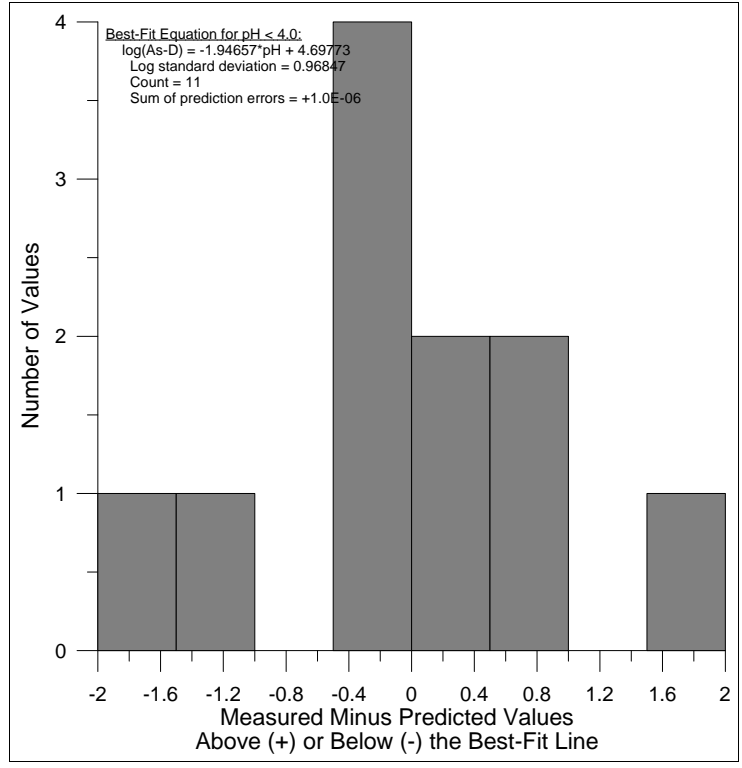


Figure A12-4. Statistical distribution of (measured-calculated) datapoints around the best-fit equation for dissolved arsenic below pH 4.0.

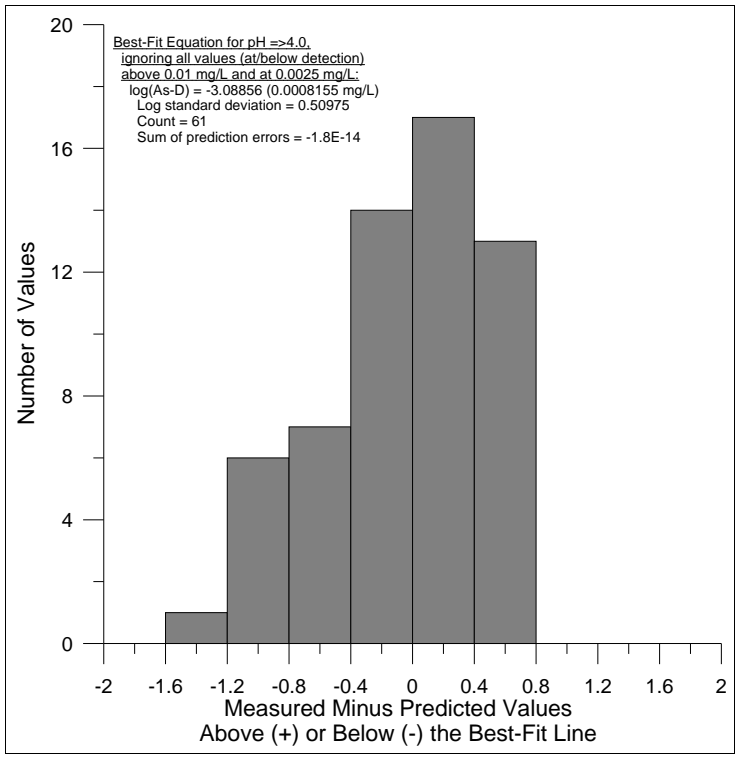


Figure A12-5. Statistical distribution of (measured-calculated) datapoints around the best-fit equation for dissolved arsenic above pH 4.0.

Appendix A13. Dissolved Barium (Ba-D)

Notes:

Dissolved barium shows little correlation with pH (Figure A13-1), but some correlation with sulphate (Figure A13-2). The best-fit equation of dissolved barium with sulphate has a slope of nearly -1.0 (Figure A13-3). The datapoints above and below this line generally display a lognormal distribution (Figure A13-4) with a standard deviation of 0.36521 log cycles.

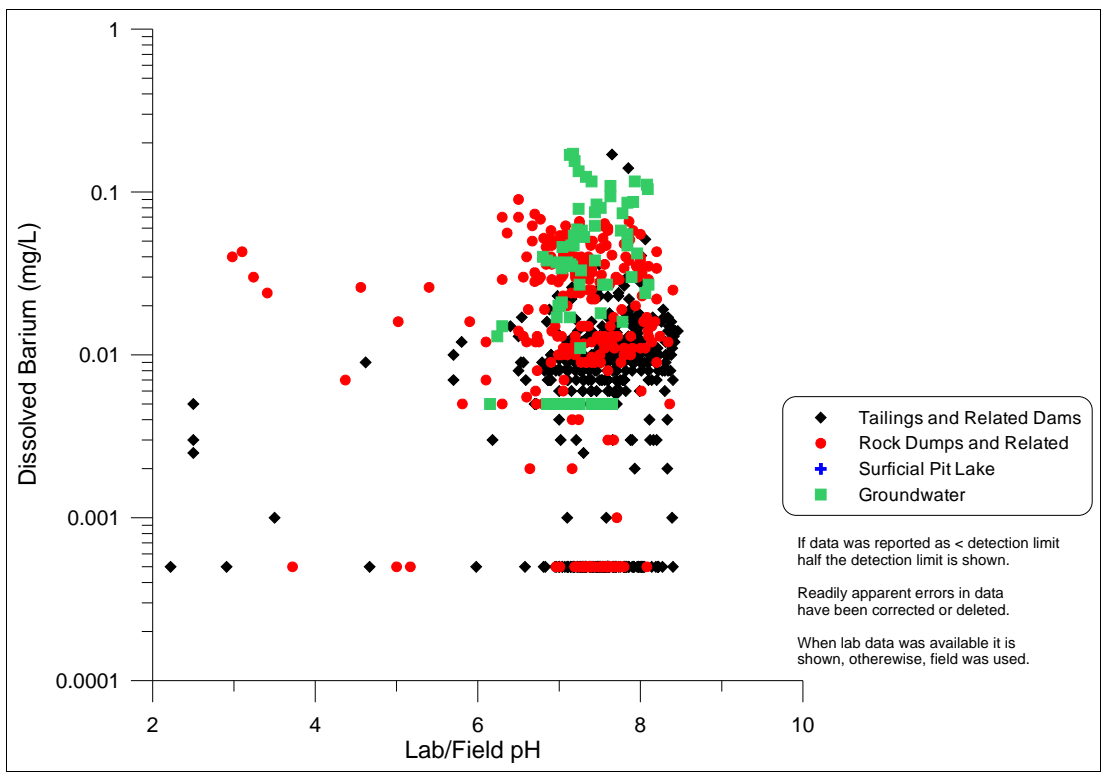


Figure A13-1. Dissolved barium vs. pH at the Bell Minesite.

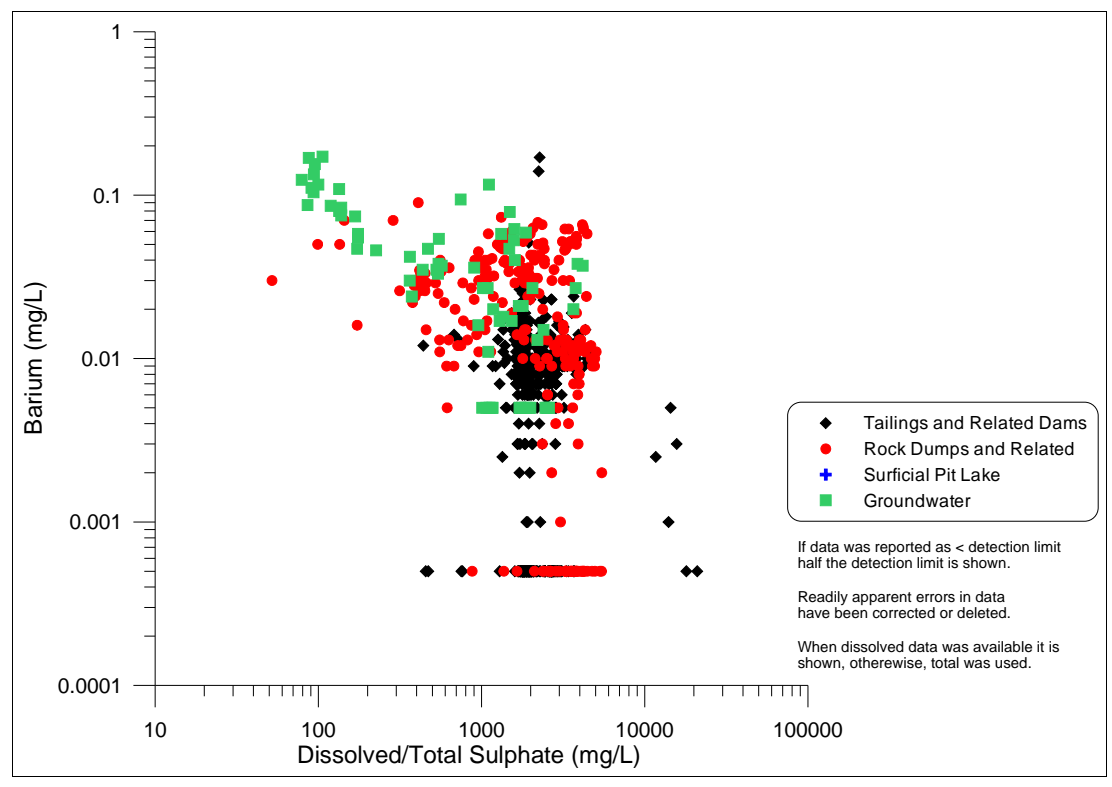


Figure A13-2. Dissolved barium vs. sulphate at the Bell Minesite.

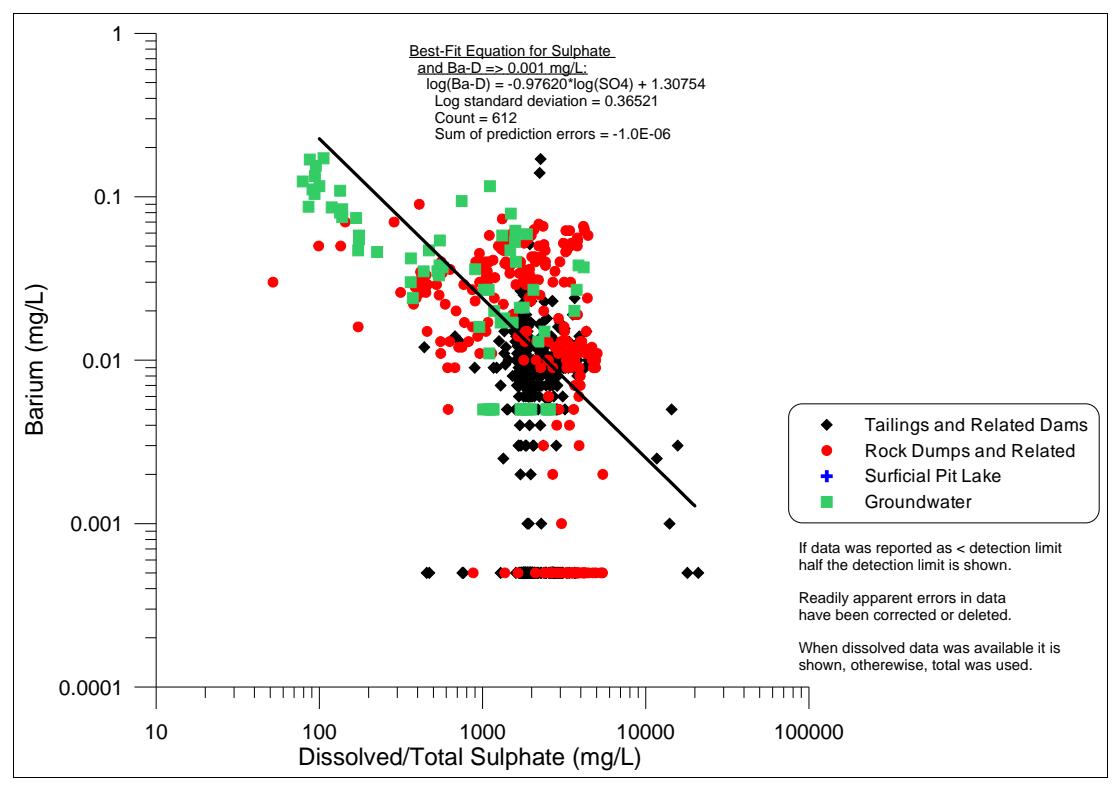


Figure A13-3. Best-fit equation for dissolved barium vs. sulphate in the 2010 Bell EDCM.

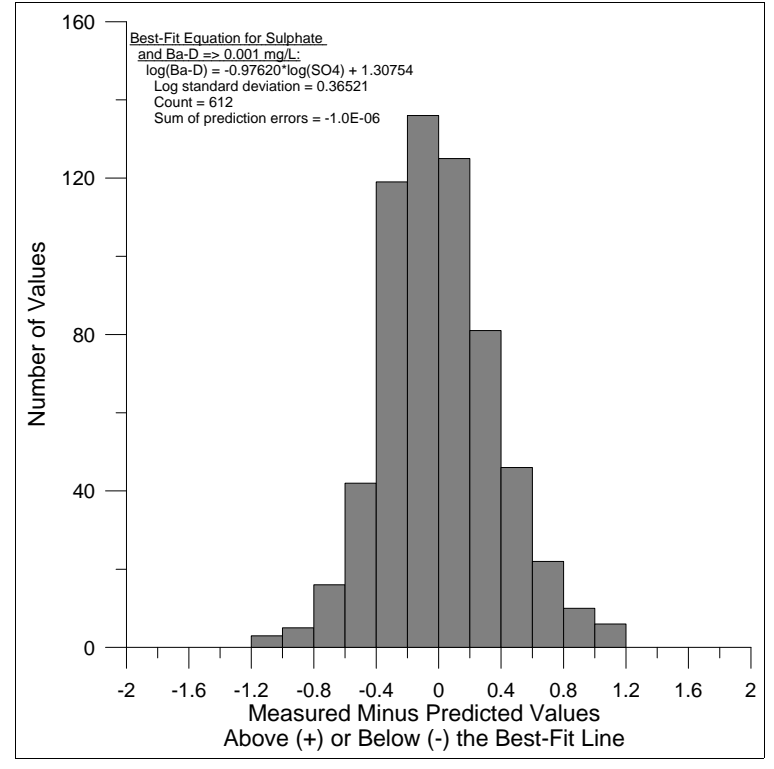


Figure A13-4. Statistical distribution of (measured-calculated) datapoints around the best-fit equation for dissolved barium.

Appendix A14. Dissolved Beryllium (Be-D)

Notes:

Nearly all of the roughly 800 analyses of dissolved beryllium were near or below various detection limits. Thus, trends with pH (Figure A14-1) and sulphate (Figure A14-2) are not readily apparent. However, below pH 4.0, the highest concentrations were taken as representative, and thus a correlation based on only seven datapoints was defined (Figure A14-3). These seven datapoints may be lognormally distributed around the acidic best-fit equation (Figure A14-4), with a standard deviation of about 0.36 log cycles. Above pH 4, dissolved beryllium was set at <0.005 mg/L.

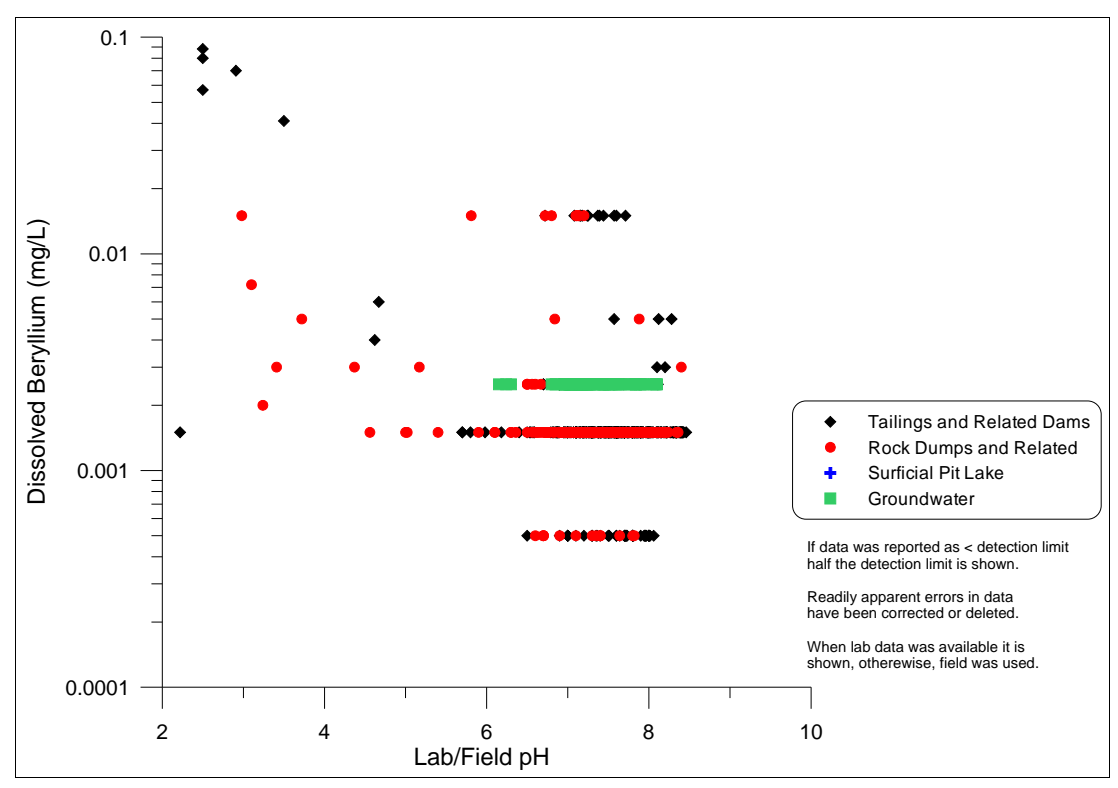


Figure A14-1. Dissolved beryllium vs. pH at the Bell Minesite.

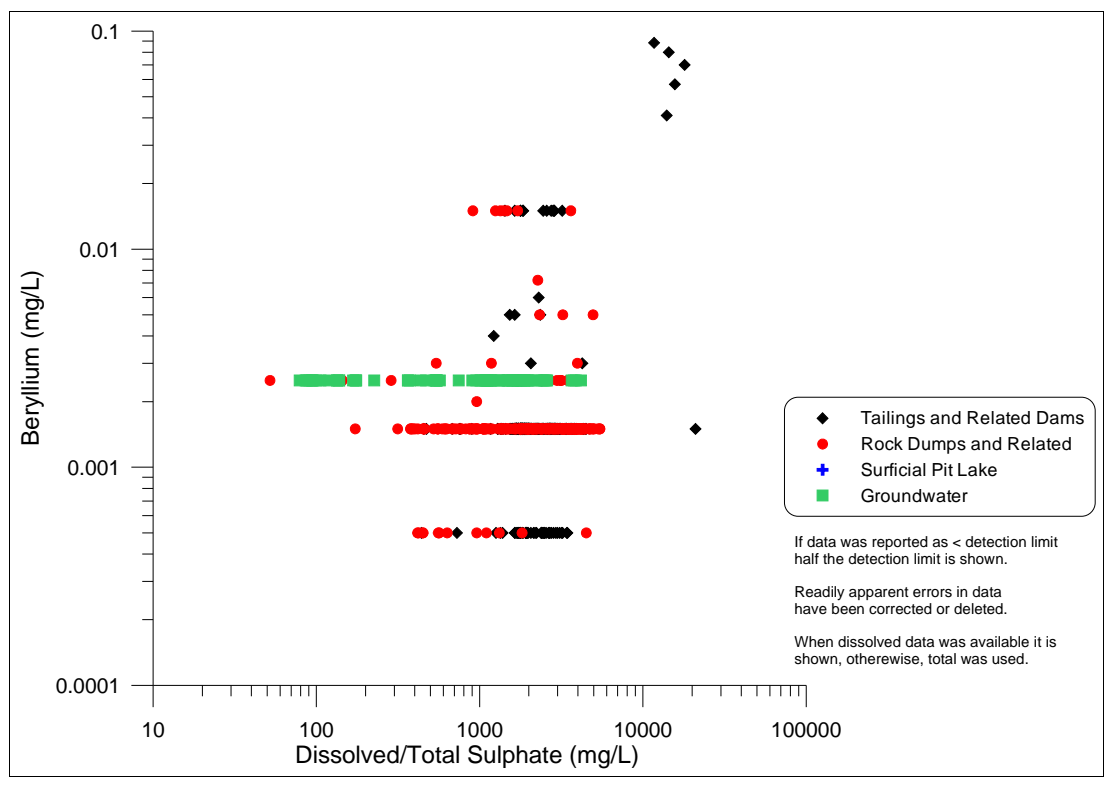


Figure A14-2. Dissolved beryllium vs. sulphate at the Bell Minesite.

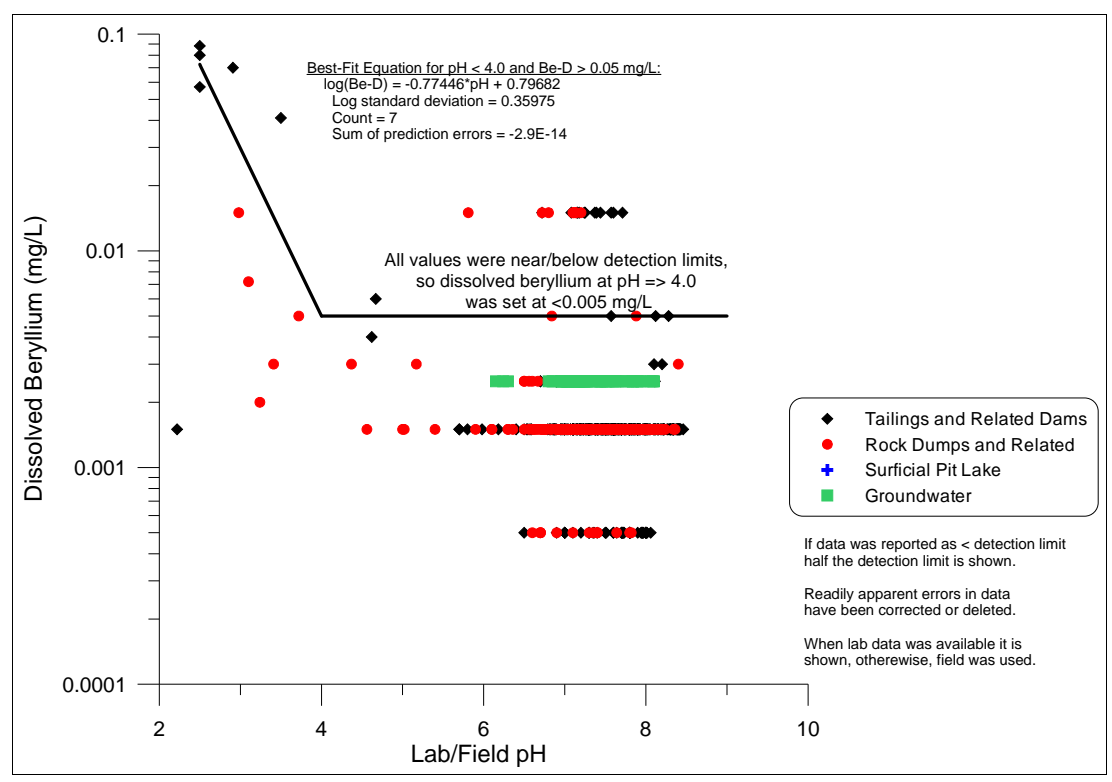


Figure A14-3. Best-fit equations for dissolved beryllium vs. pH in the 2010 Bell EDCM.

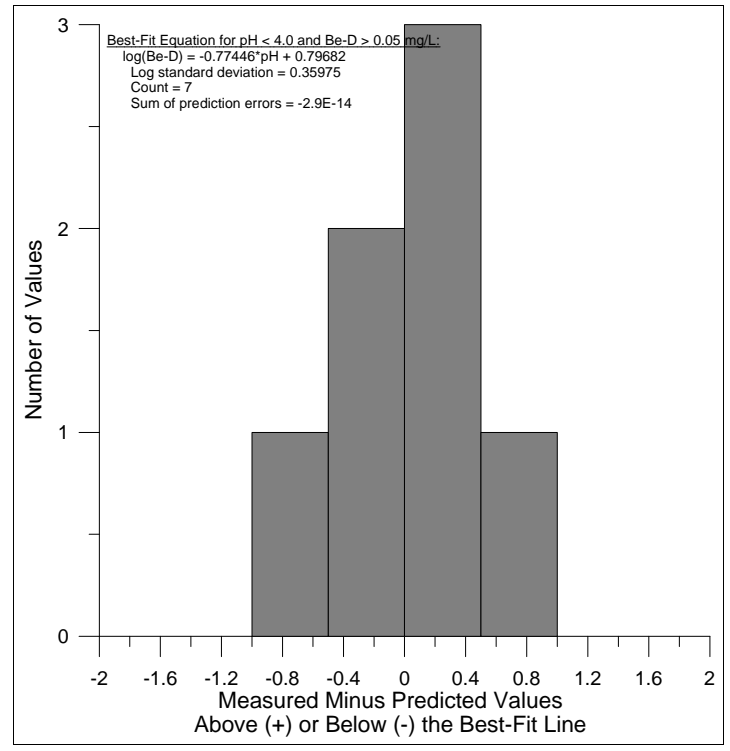


Figure A14-4. Statistical distribution of (measured-calculated) datapoints around the best-fit equation for dissolved beryllium below pH 4.0.

Appendix A15. Dissolved Bismuth (Bi-D)

Notes:

Because all measured concentrations of dissolved bismuth were at or below various detection limits, there are no apparent correlations with pH (Figure A15-1) or sulphate (Figure A15-2). Therefore, dissolved bismuth was set below its highest detection limit through time (Figure A15-3), with the latest period of 2001-2009 at <0.001 mg/L.

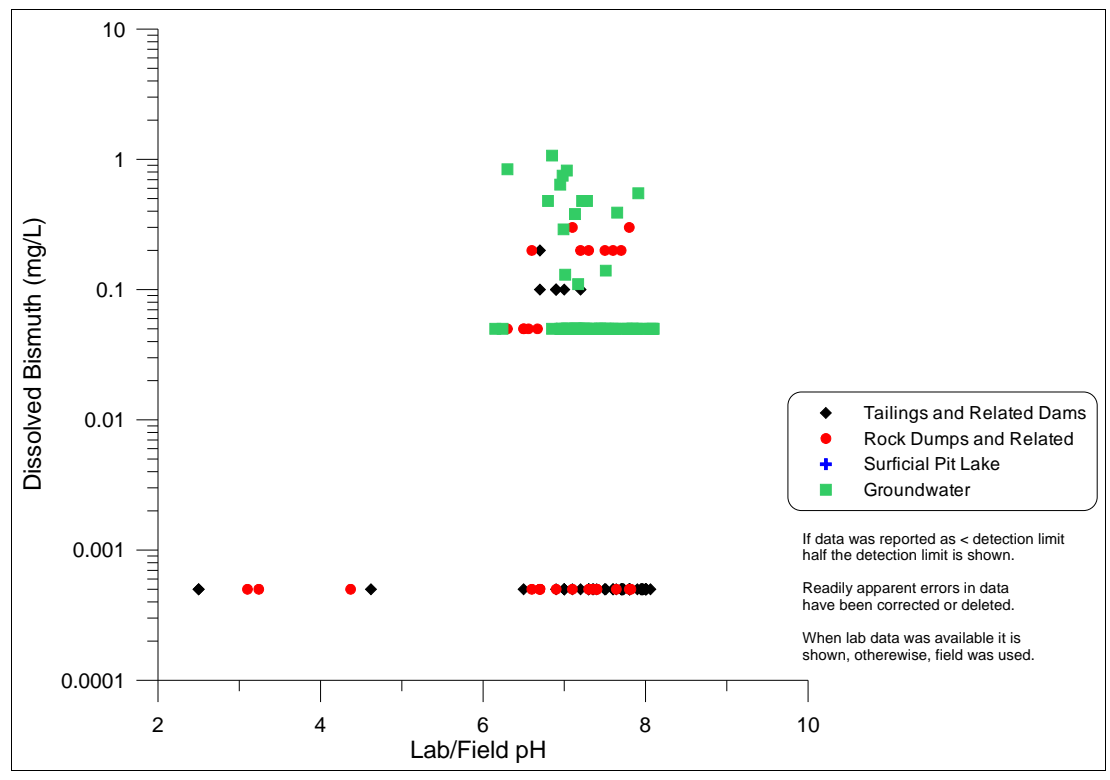


Figure A15-1. Dissolved bismuth vs. pH at the Bell Minesite.

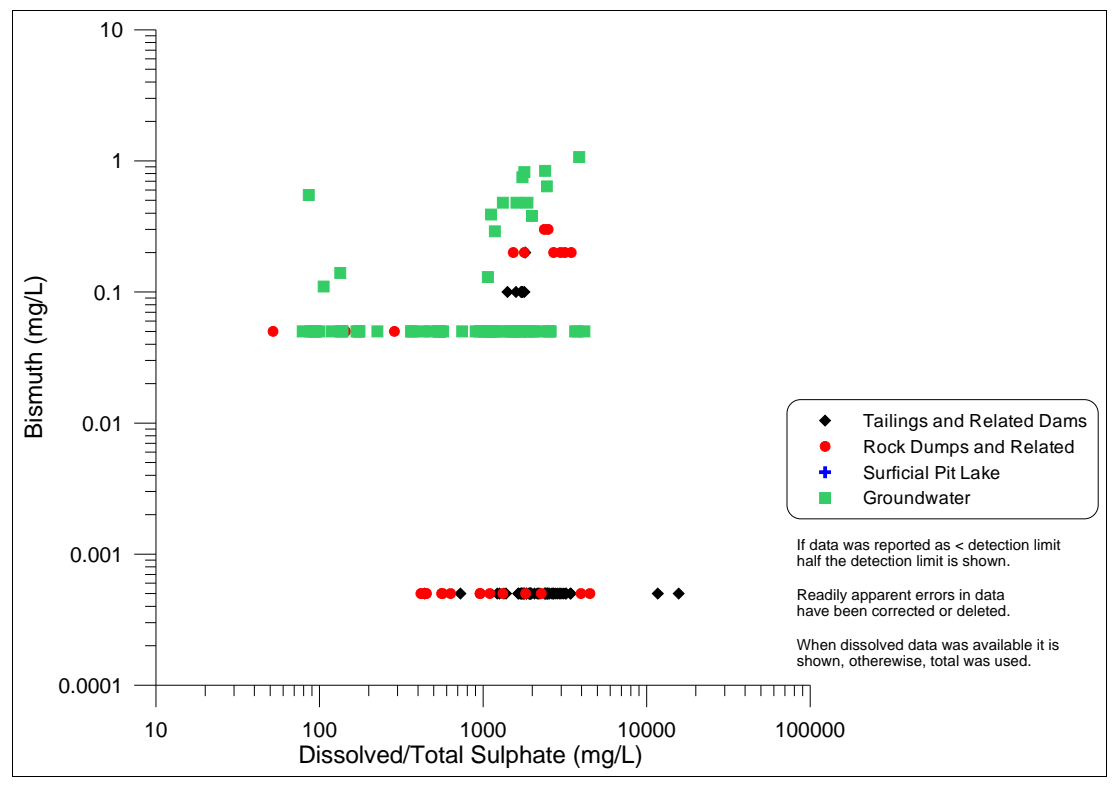


Figure A15-2. Dissolved bismuth vs. sulphate at the Bell Minesite.

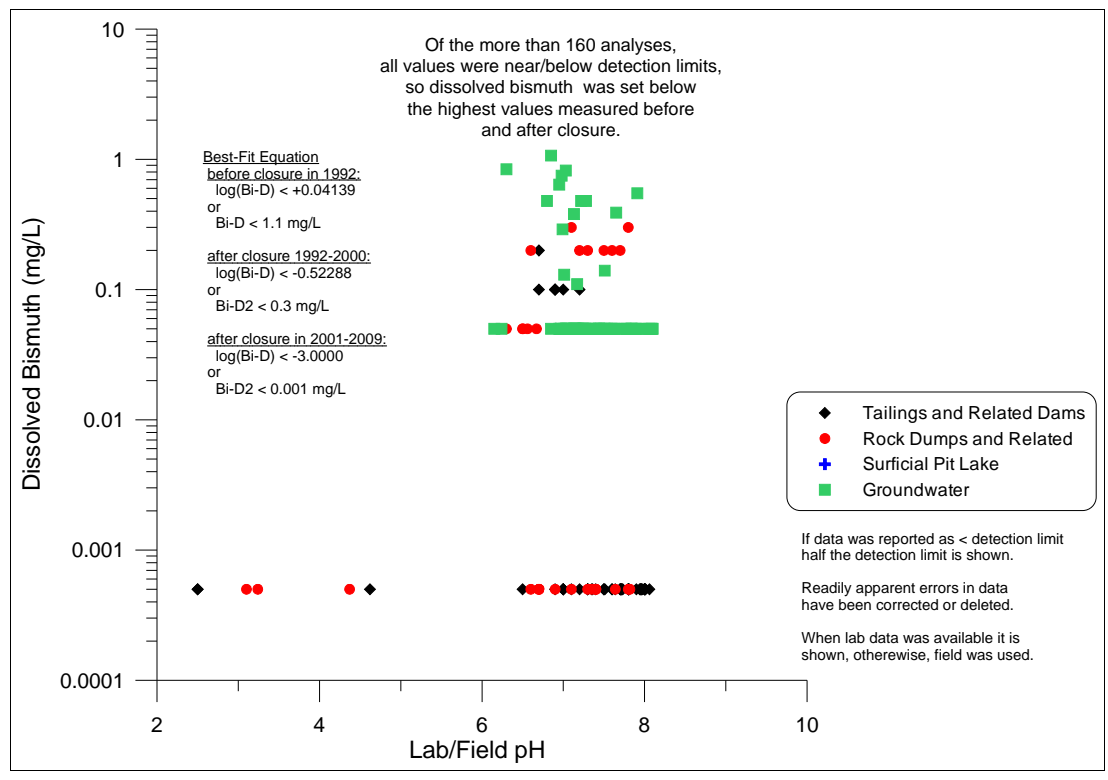


Figure A15-3. Best-fit equations for dissolved bismuth in the 2010 Bell EDCM.

Appendix A16. Dissolved Boron (B-D)

Notes:

Most of the more than 700 analyses of dissolved boron were at or below various detection limits, and thus no correlations were readily apparent with pH (Figure A16-1) or sulphate (Figure A16-2). Thus, ignoring two anomalously high values, dissolved boron was simply set at <0.2 mg/L (Figure A16-3).

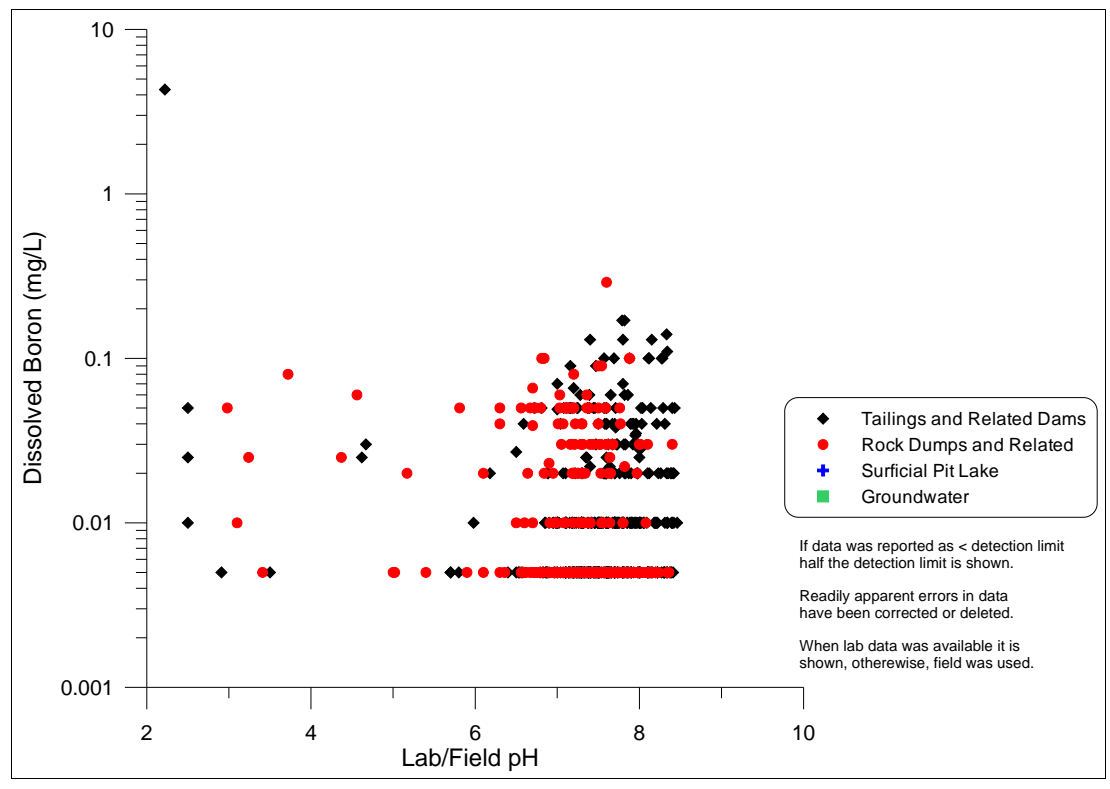


Figure A16-1. Dissolved boron vs. pH at the Bell Minesite.

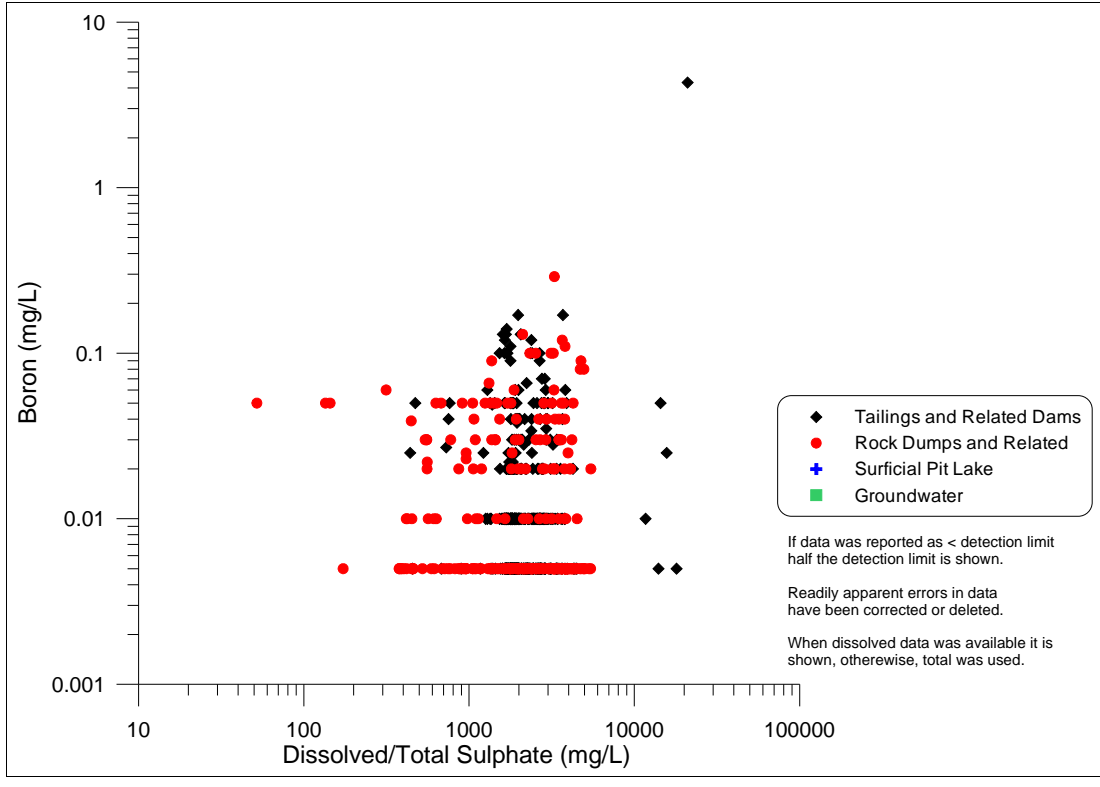


Figure A16-2. Dissolved boron vs. sulphate at the Bell Minesite.

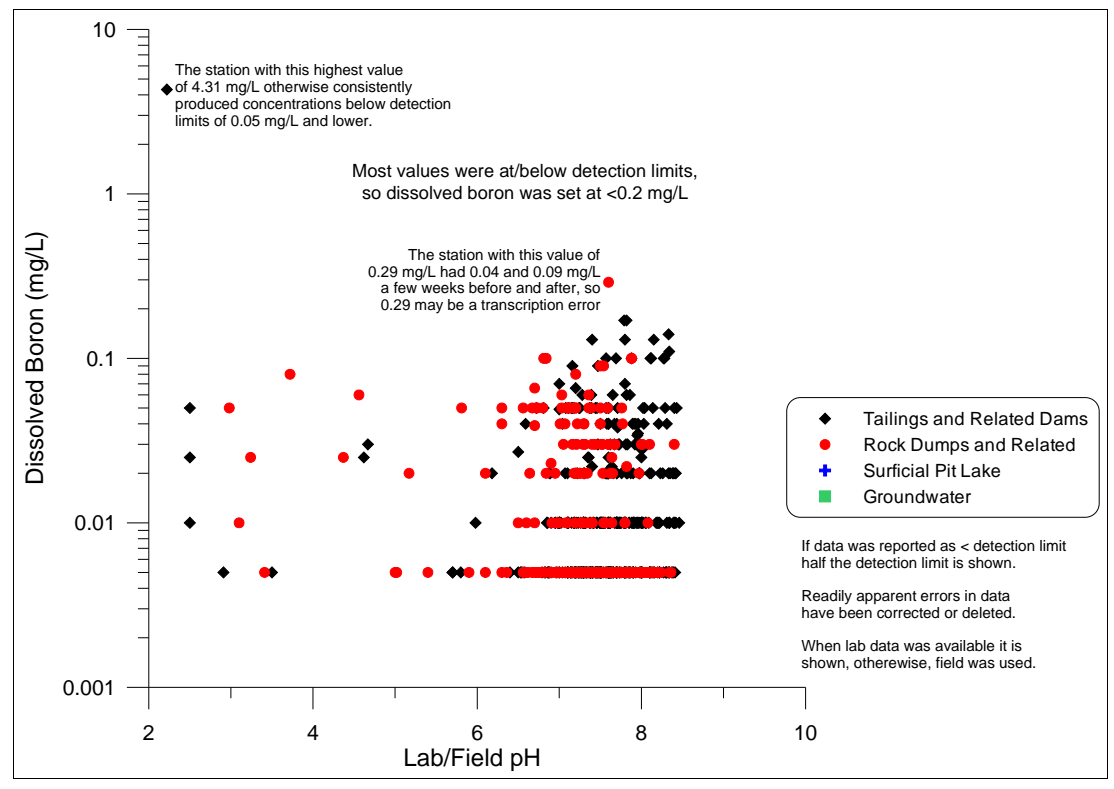


Figure A16-3. Best-fit equation for dissolved boron in the 2010 Bell EDCM.

Appendix A17. Dissolved Cadmium (Cd-D)

Notes:

Dissolved cadmium was analyzed 98 times, but only in near-neutral drainages where it was near or below various detection limits. As a result, no correlation with pH could be defined (Figure A17-1). Also, no correlation with sulphate is apparent (Figure A17-2). Thus, dissolved cadmium was set at <0.0002 mg/L in near-neutral Bell Minesite drainages (Figure A17-3).

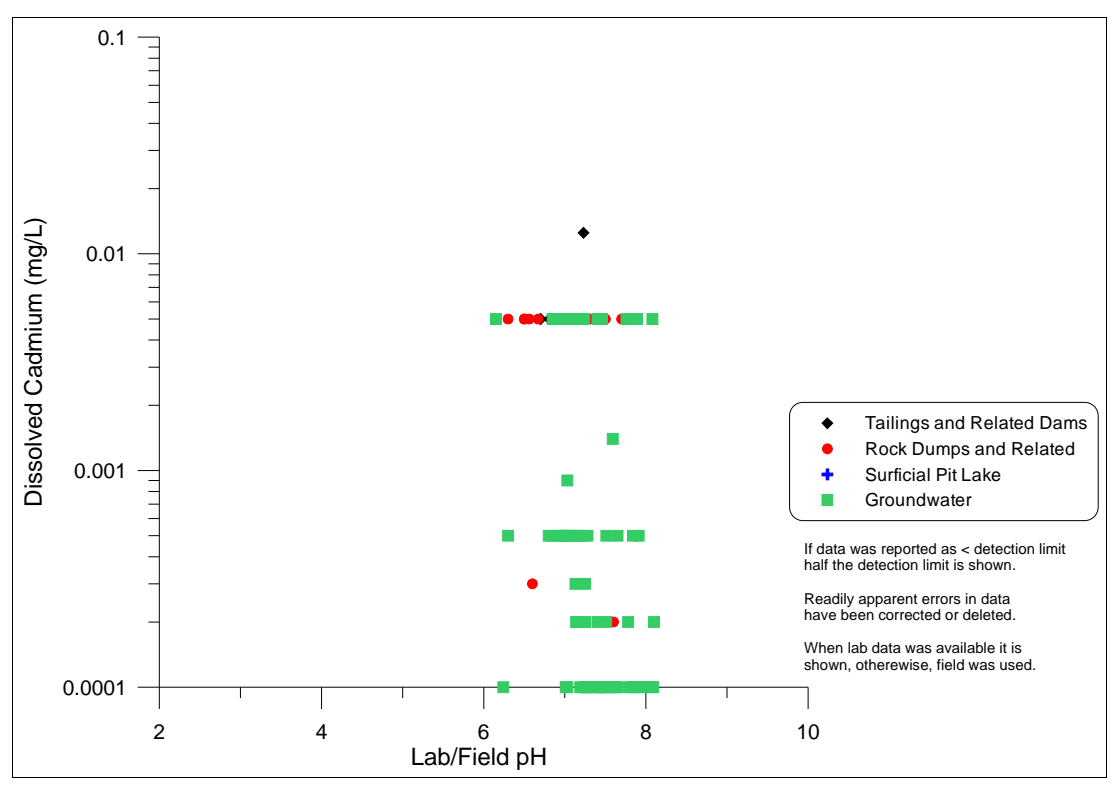


Figure A17-1. Dissolved cadmium vs. pH at the Bell Minesite.

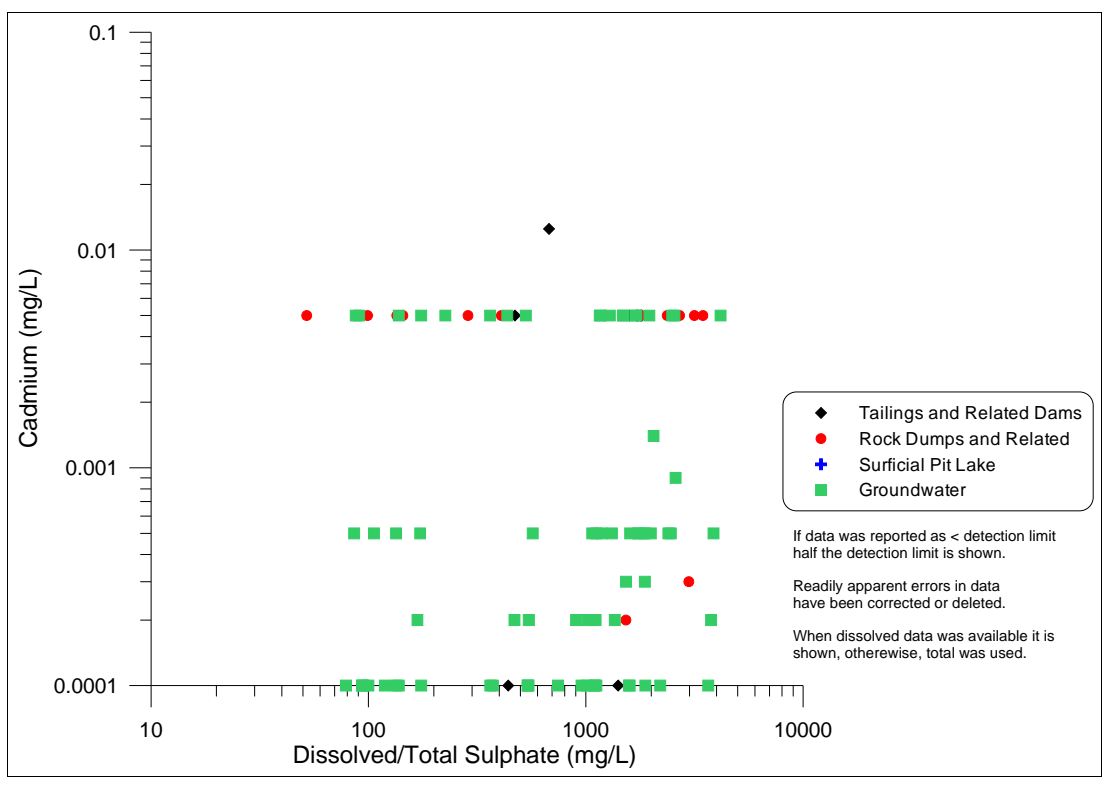


Figure A17-2. Dissolved cadmium vs. sulphate at the Bell Minesite.

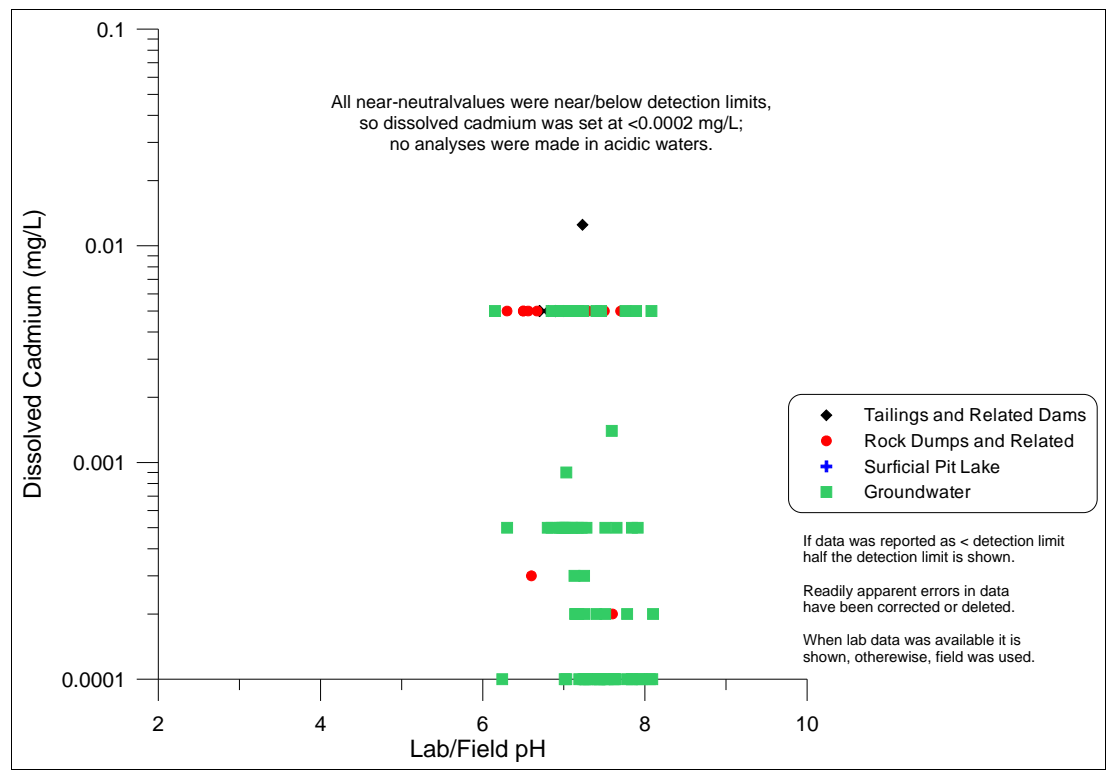


Figure A17-3. Best-fit equation for dissolved cadmium in the 2010 Bell EDCM.

Appendix A18. Dissolved Calcium (Ca-D)

Notes:

Dissolved calcium is predominantly independent of pH (Figure A18-1), but correlates with sulphate (Figure A18-2). The best-fit equation for all drainages (1460 datapoints) has a slope of approximately +0.81 (Figure A18-3), although the rock-dump drainages at higher sulphate are generally below but parallel to this line (somewhat lower calcium concentrations). The datapoints form a general lognormal distribution around this best-fit equation (Figure A18-4).

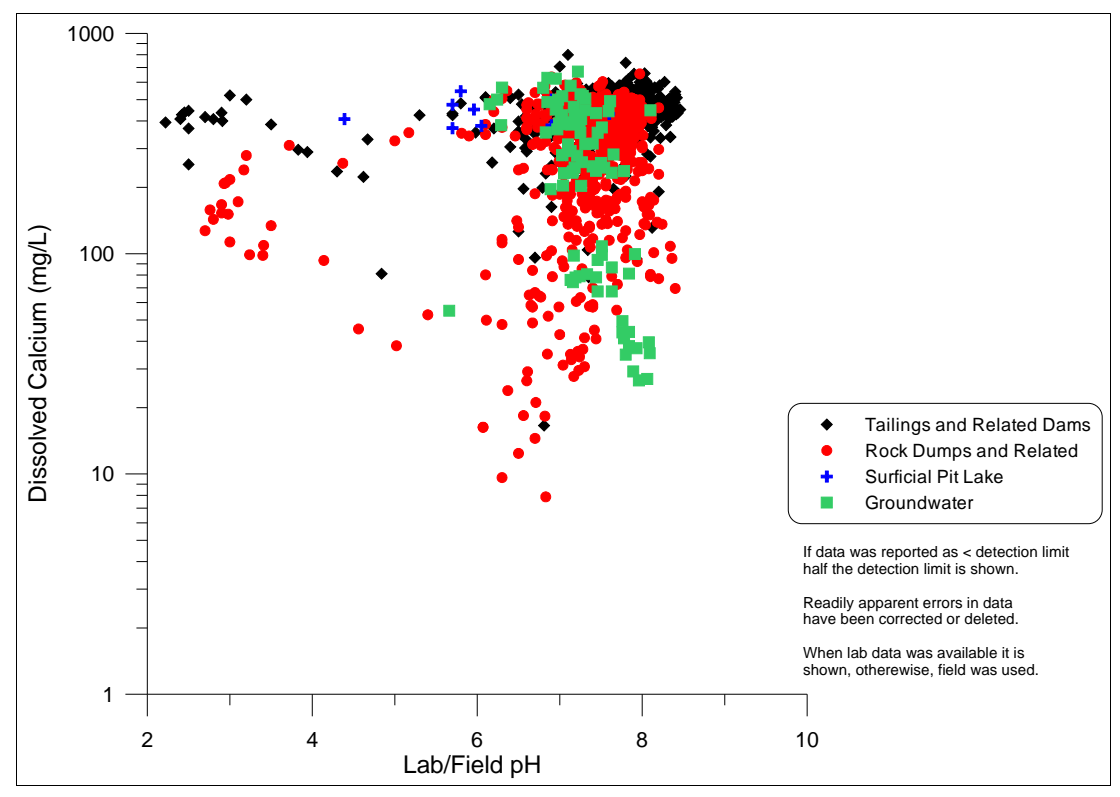


Figure A18-1. Dissolved calcium vs. pH at the Bell Minesite.

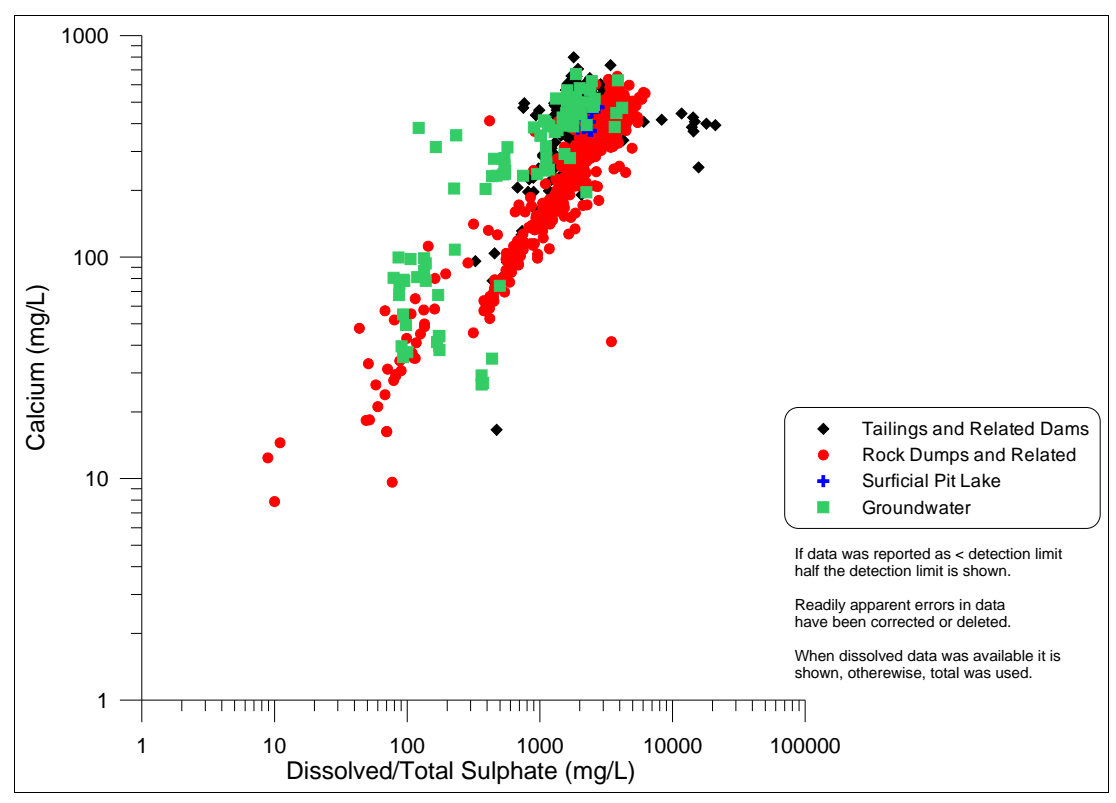


Figure A18-2. Dissolved calcium vs. sulphate at the Bell Minesite.

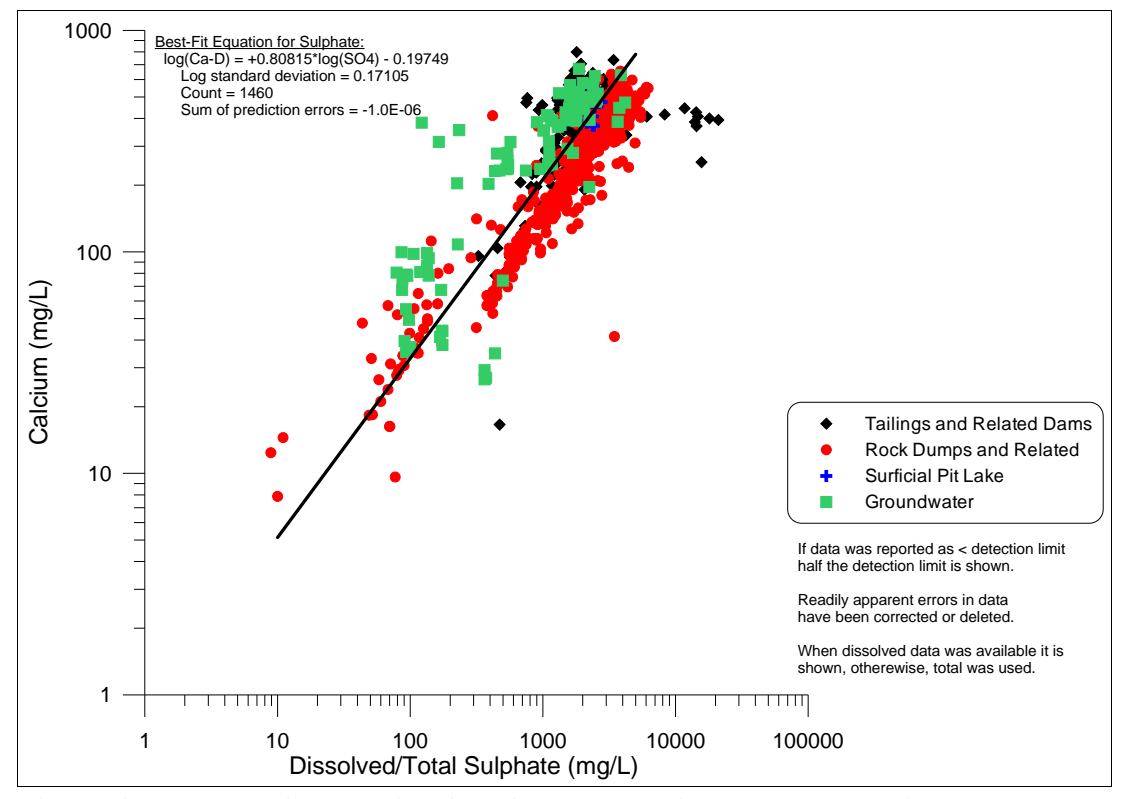


Figure A18-3. Best-fit equation for dissolved calcium vs. sulphate in the 2010 Bell EDCM.

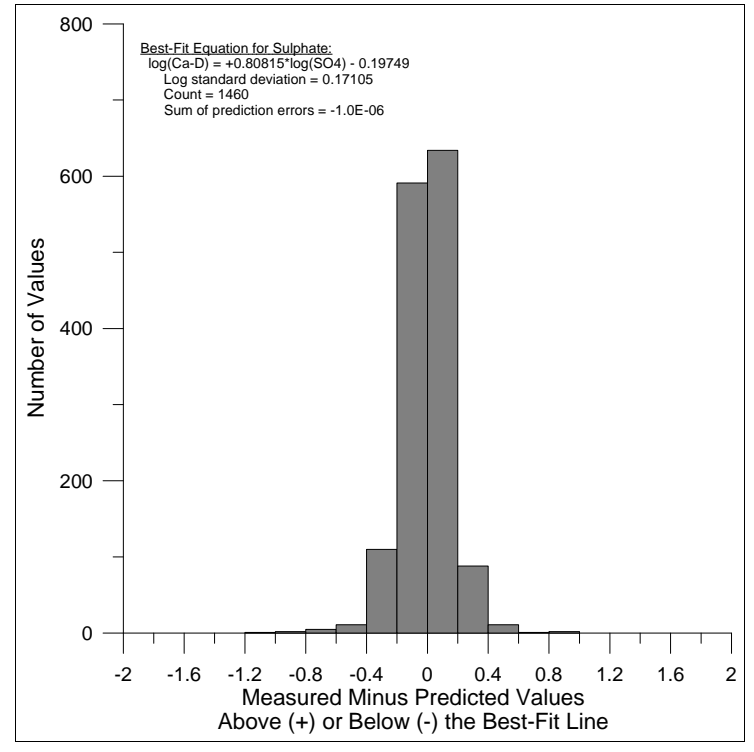


Figure A18-4. Statistical distribution of (measured-calculated) datapoints around the best-fit equation for dissolved calcium.

Appendix A19. Dissolved Chromium (Cr-D)

Notes:

Of the approximately 800 analyses of dissolved chromium in the Bell Minesite database, nearly all were at or below various detection limits. However, at acidic pH (Figure A19-1) and higher sulphate (Figure A19-2), some correlation could be seen with a few above-detection values. Based on only 11 datapoints below pH 4.0 (Figure A19-3), a best-fit equation with pH generally represents those datapoints, which may form a lognormal distribution around that acidic line (Figure A19-4). Above pH 4, dissolved chromium is set at the lowest detection limit of <0.001 mg/L.

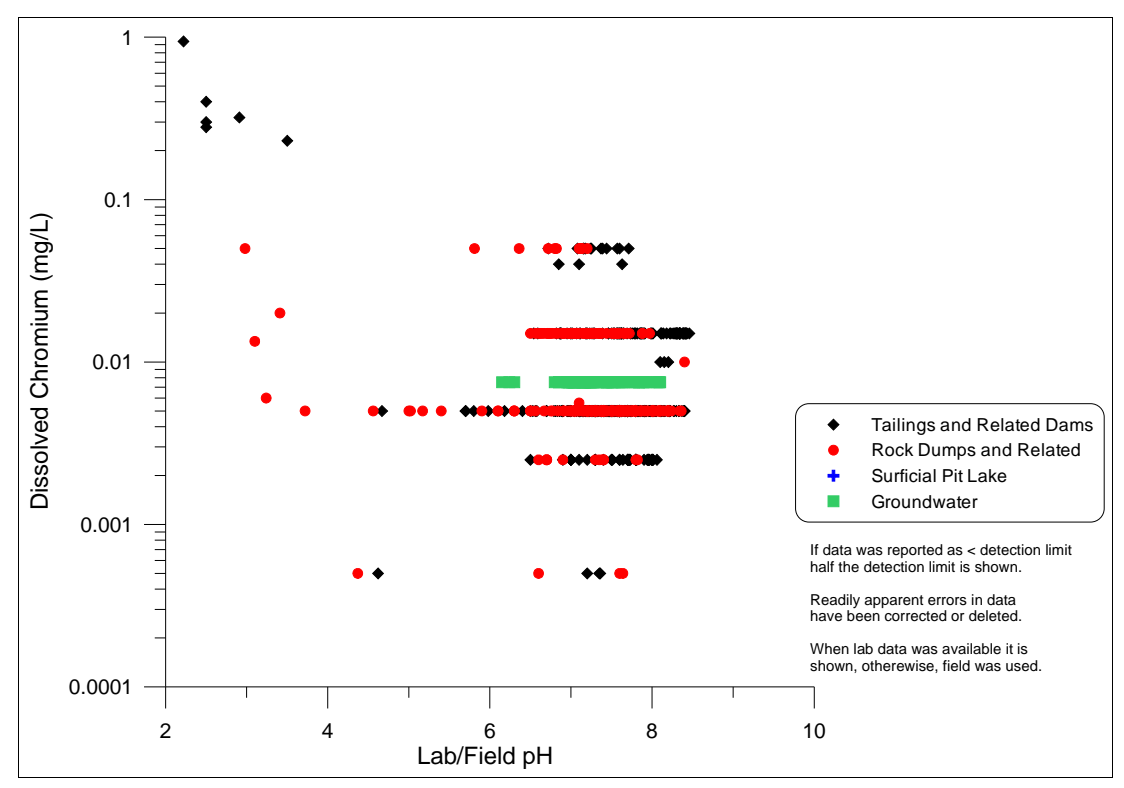


Figure A19-1. Dissolved chromium vs. pH at the Bell Minesite.

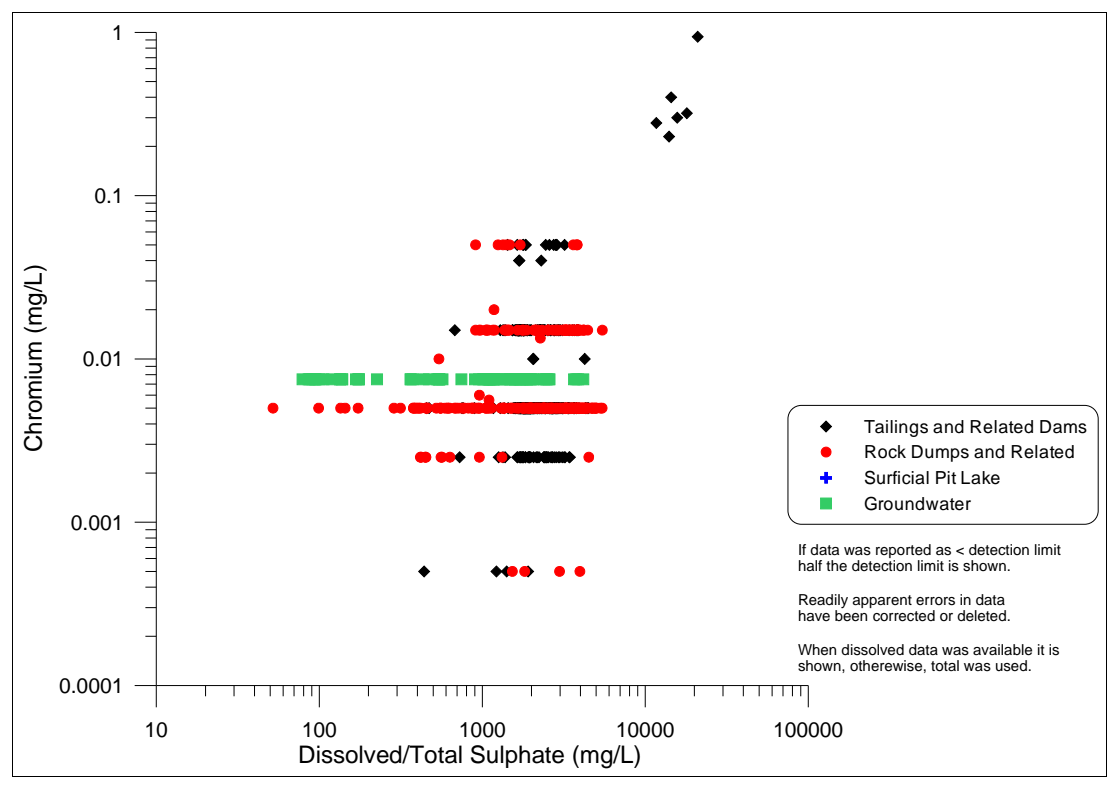


Figure A19-2. Dissolved chromium vs. sulphate at the Bell Minesite.

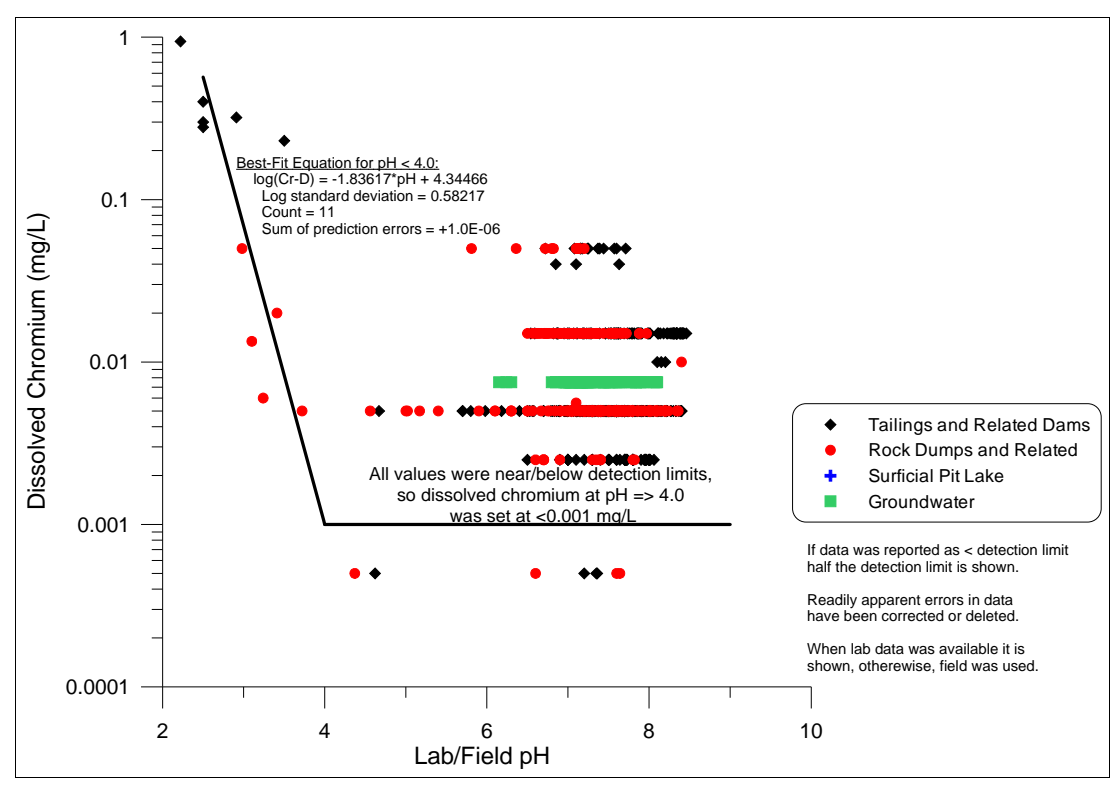


Figure A19-3. Best-fit equations for dissolved chromium vs. pH in the 2010 Bell EDCM.

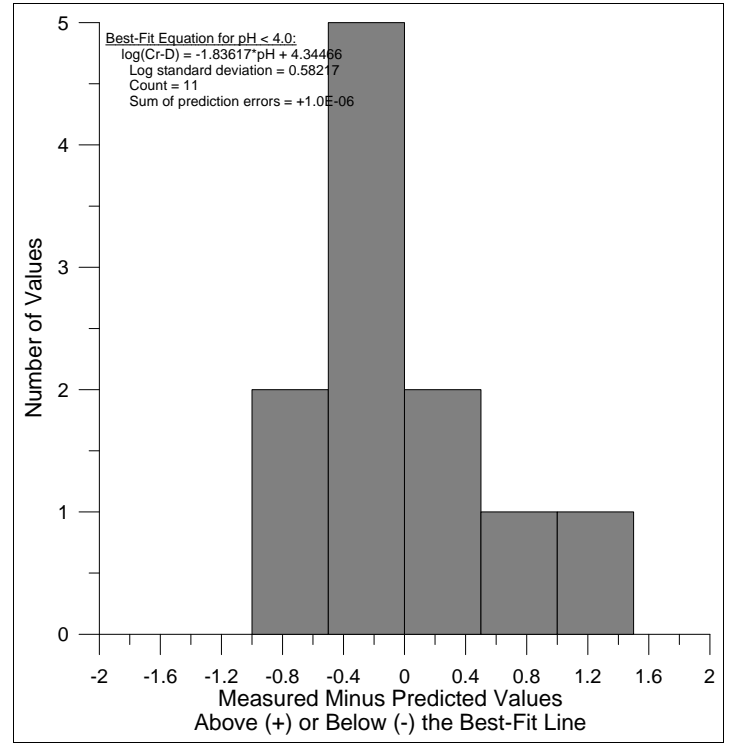


Figure A19-4. Statistical distribution of (measured-calculated) datapoints around the best-fit equation for dissolved chromium below pH 4.0.

Appendix A20. Dissolved Cobalt (Co-D)

Notes:

Across the measured ranges, dissolved cobalt shows better correlation with pH (Figure A20-1) than sulphate (Figure A20-2). Excluding 2009 data which were anomalously low compared to past years and may be erroneous, the best-fit equation relating dissolved cobalt and pH has a slope of roughly -0.38 (Figure A20-3). The 130 datapoints used in this equation form a general lognormal distribution (Figure A20-4).

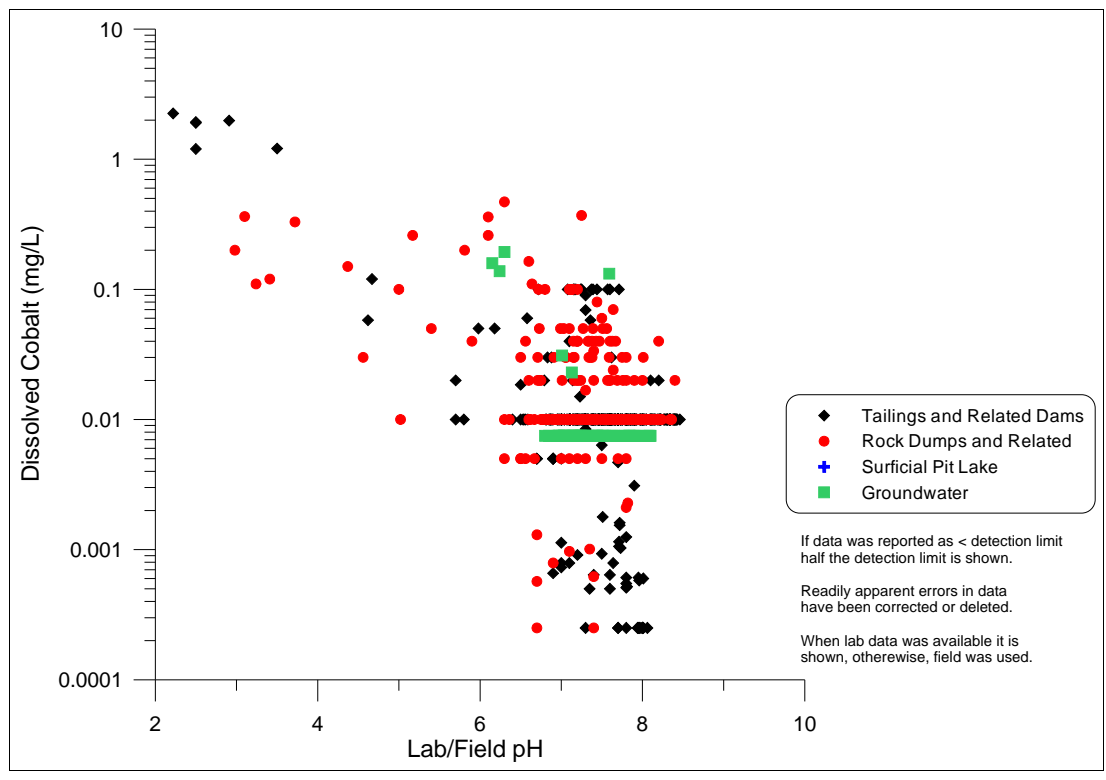


Figure A20-1. Dissolved cobalt vs. pH at the Bell Minesite.

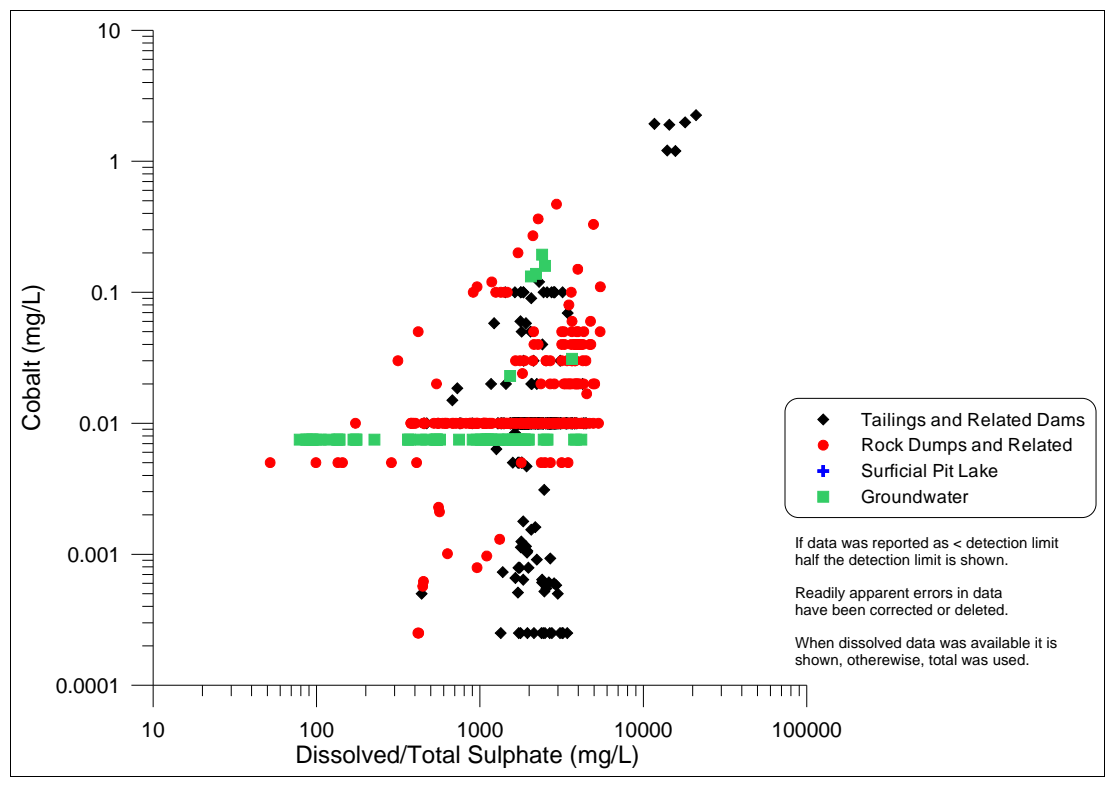


Figure A20-2. Dissolved cobalt vs. sulphate at the Bell Minesite.

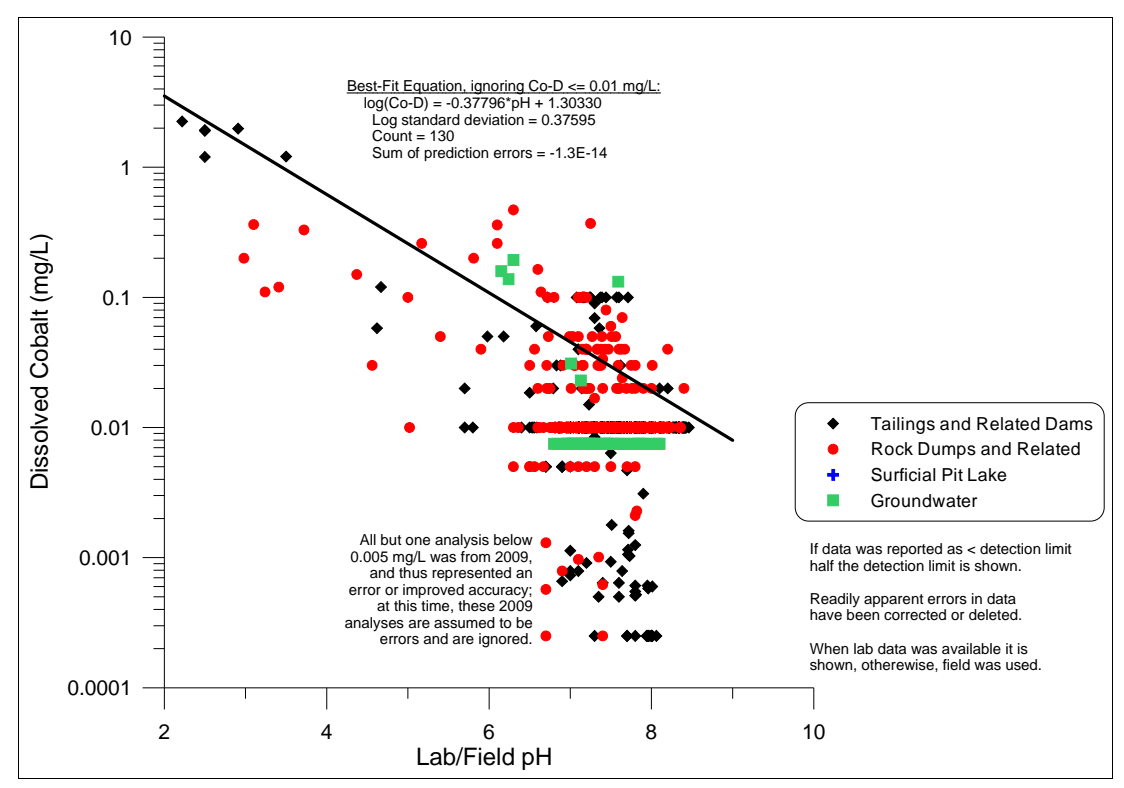


Figure A20-3. Best-fit equation for dissolved cobalt vs. pH in the 2010 Bell EDCM.

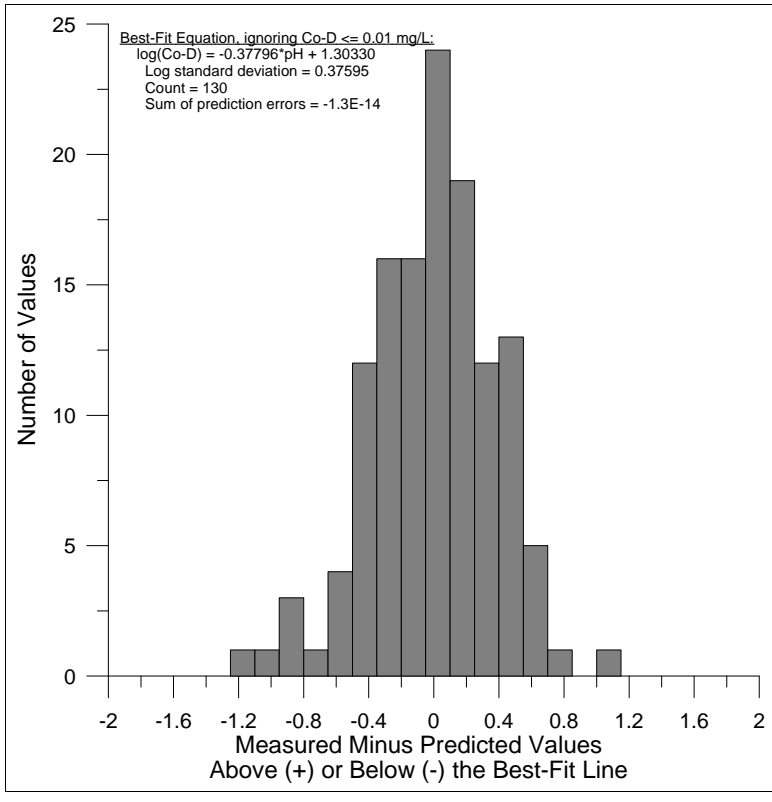


Figure A20-4. Statistical distribution of (measured-calculated) datapoints around the best-fit equation for dissolved cobalt.

Appendix A21. Dissolved Copper (Cu-D)

Notes:

Dissolved copper, with nearly 5500 values spanning decades, is one of the frequently analyzed parameters at the Bell Minesite, in addition to pH, sulphate, dissolved iron, and dissolved zinc.

Dissolved copper correlates better with pH (Figure A21-1) than sulphate (Figure A21-2). The best-fit line for the pH correlation is divided into three segments (Figure A21-3), joining at pH 3.0 and 5.5. Above pH 5.5, dissolved copper does not correlate as well with pH.

The datapoints above and below each of these segments form general lognormal distributions (Figures A21-4 to A21-6). The segment above pH 5.5 has the largest standard deviation of 0.81956, reflecting the weaker correlation at near-neutral pH.

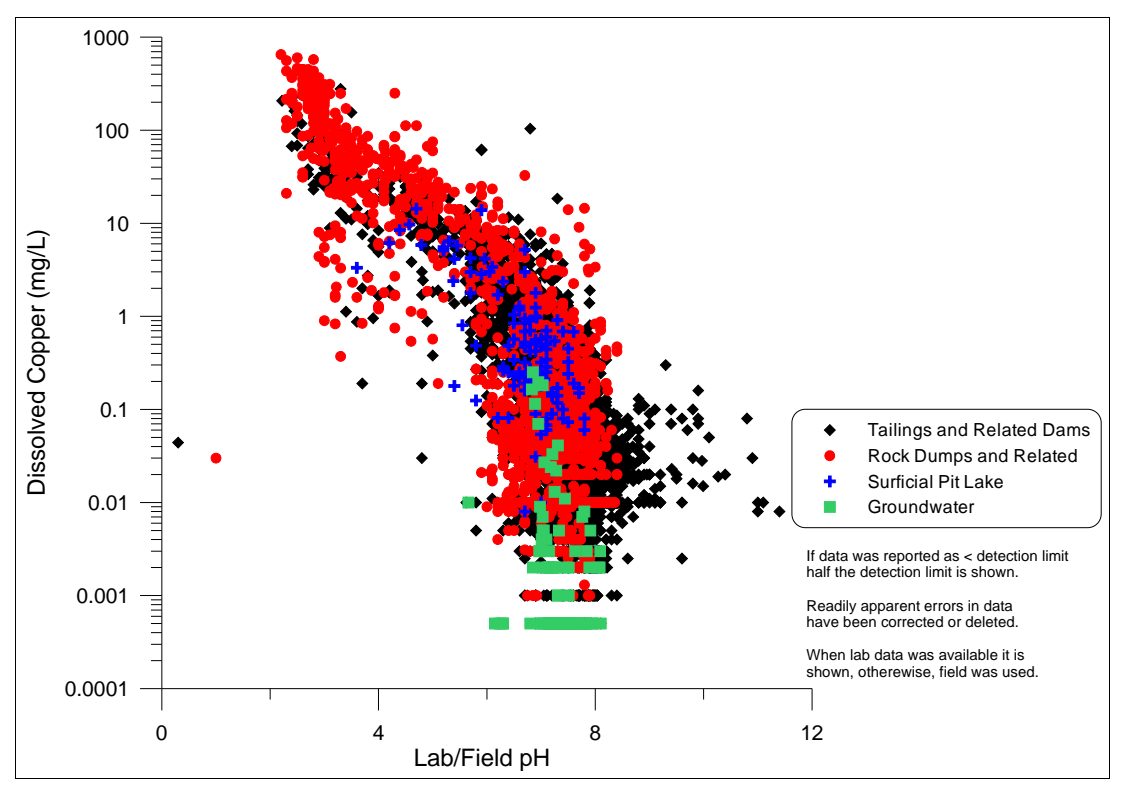


Figure A21-1. Dissolved copper vs. pH at the Bell Minesite.

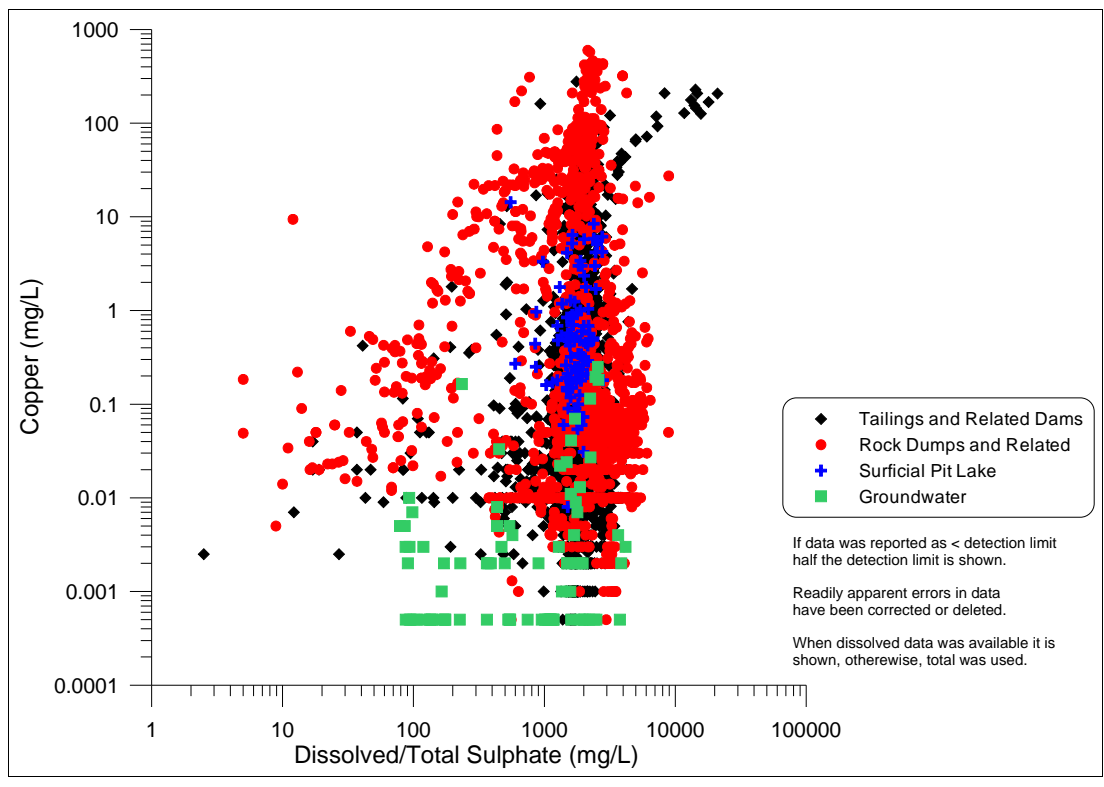


Figure A21-2. Dissolved copper vs. sulphate at the Bell Minesite.

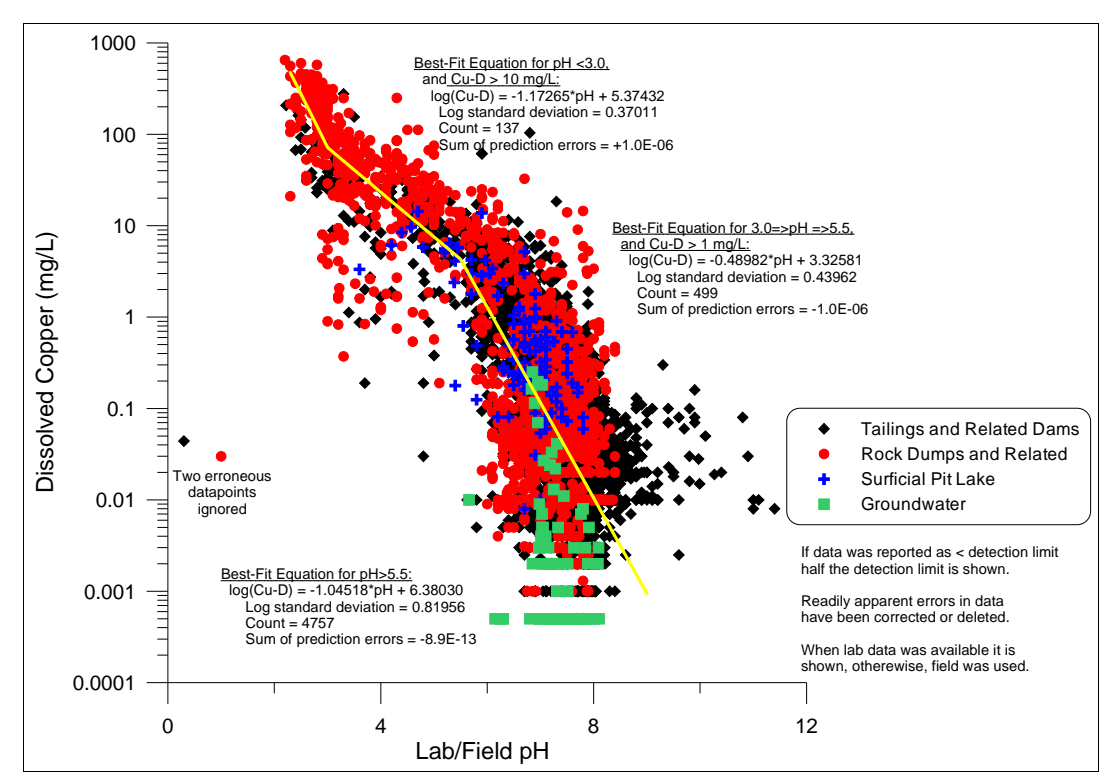


Figure A21-3. Best-fit equations for dissolved copper vs. pH in the 2010 Bell EDCM.

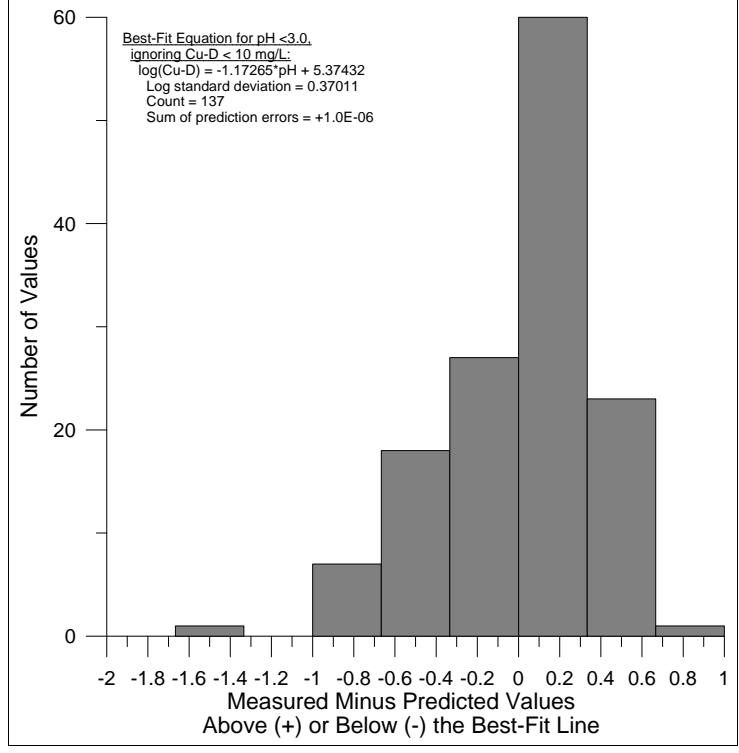


Figure A21-4. Statistical distribution of (measured-calculated) datapoints around the best-fit equation for dissolved copper below pH 3.0.

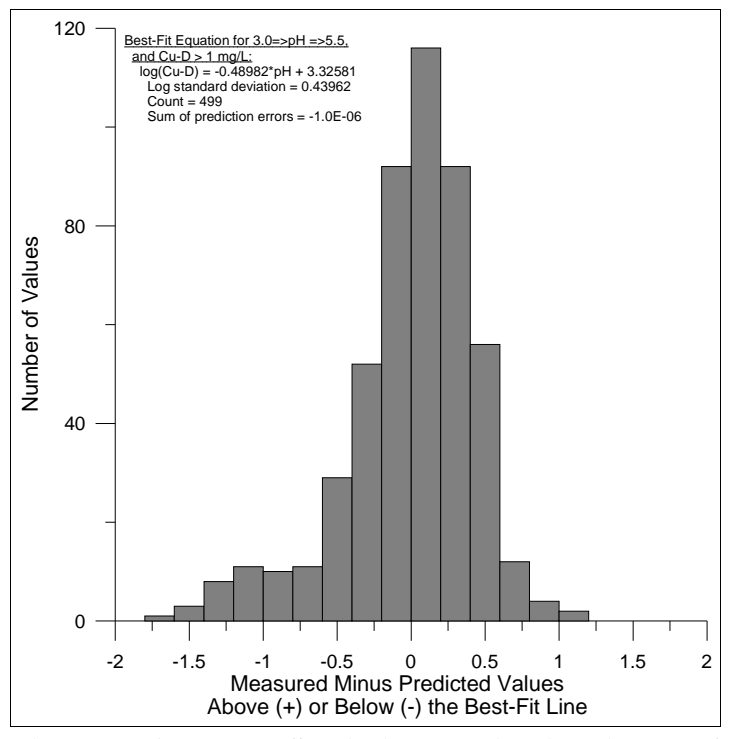


Figure A21-5. Statistical distribution of (measured-calculated) datapoints around the best-fit equation for dissolved copper between pH 3.0 and 5.5.

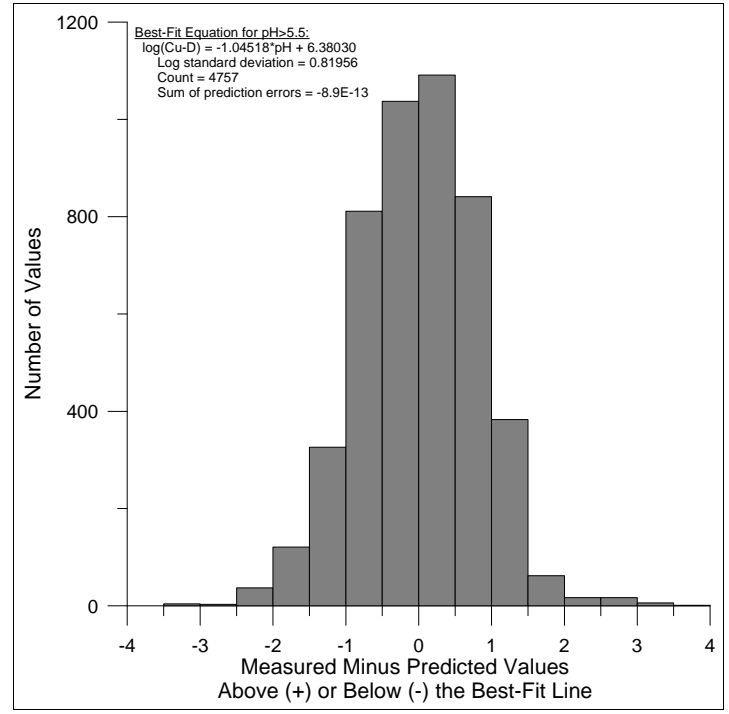


Figure A21-6. Statistical distribution of (measured-calculated) datapoints around the best-fit equation for dissolved copper above pH 5.5.

Appendix A22. Dissolved Iron (Fe-D)

Notes:

Dissolved iron, with nearly 4300 values spanning decades, is one of the frequently analyzed parameters at the Bell Minesite, in addition to pH, sulphate, dissolved copper, and dissolved zinc.

Dissolved iron shows better correlation with pH (Figure A22-1) than with sulphate (Figure A22-2). The best-fit correlation of dissolved iron with pH consists of two segments (Figure A22-3), joined at pH 4.0. Above pH 4.0, the best-fit equation excludes the higher levels of dissolved iron that reflect more reducing (low Eh) conditions, and thus this segment with lower iron applies only to more oxidized drainages. The (measured-calculated) datapoints above and below the two best-fit segments generally form lognormal distributions (Figures A22-4 and A22-5).

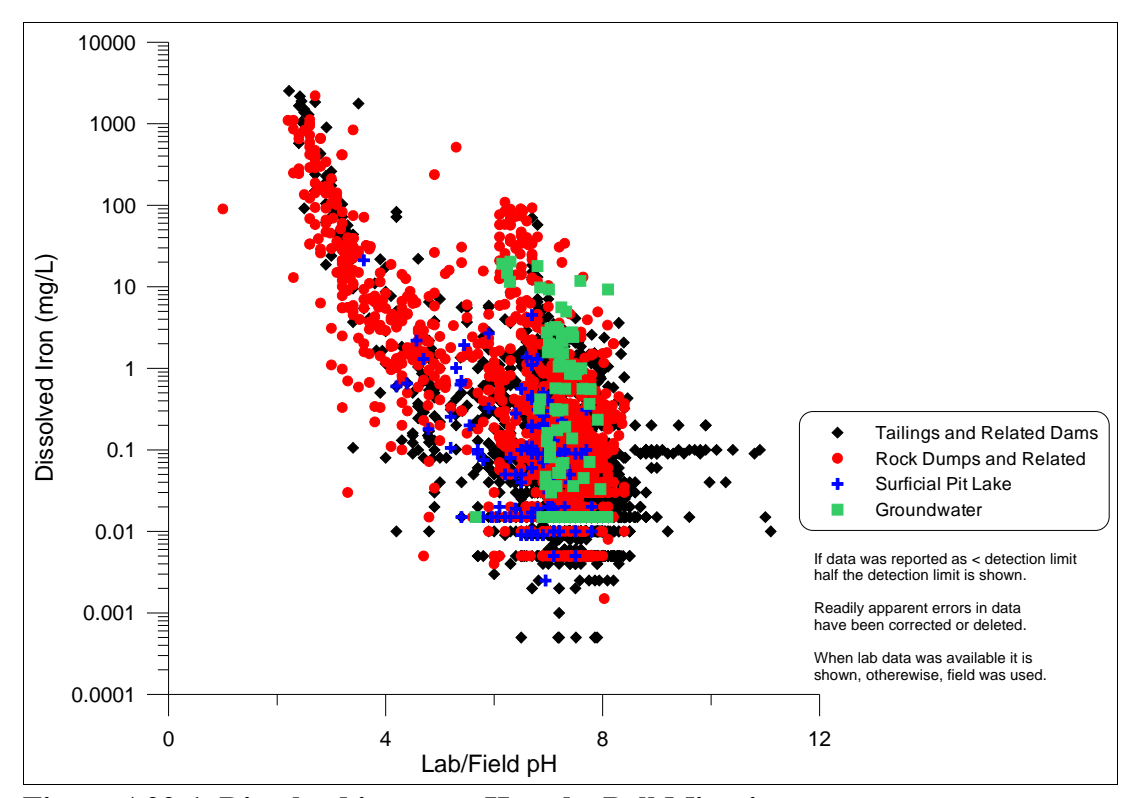


Figure A22-1. Dissolved iron vs. pH at the Bell Minesite.

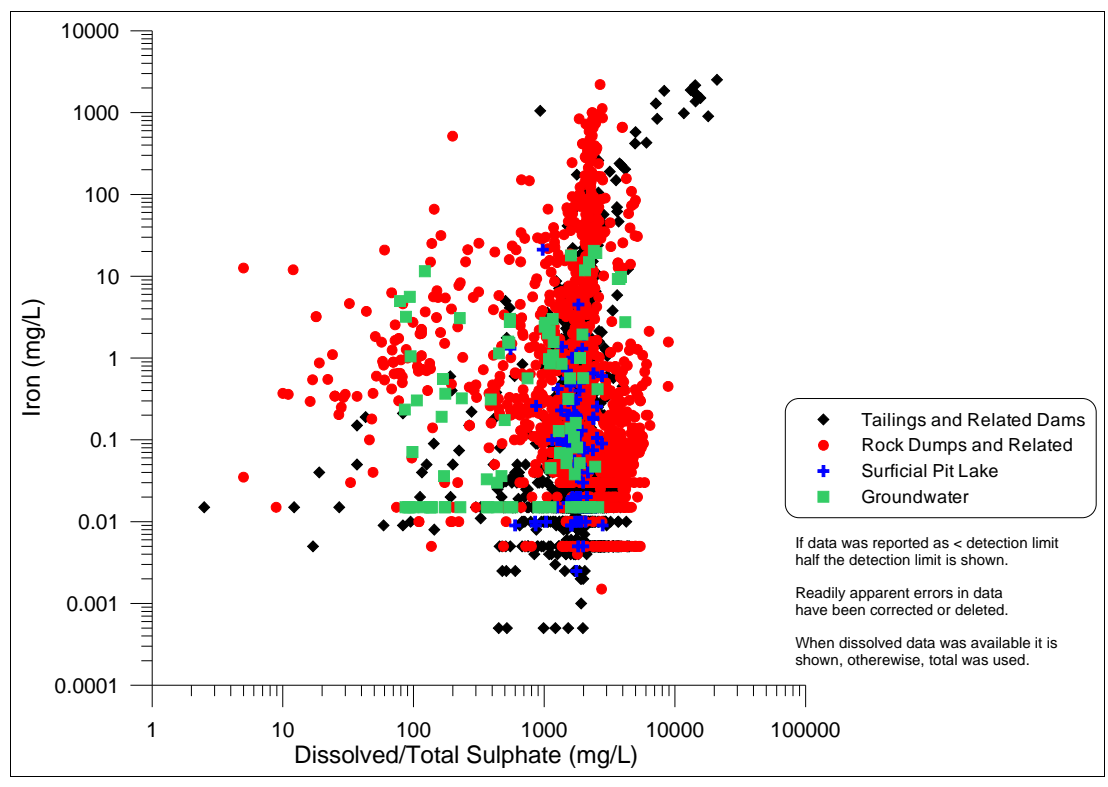


Figure A22-2. Dissolved iron vs. sulphate at the Bell Minesite.

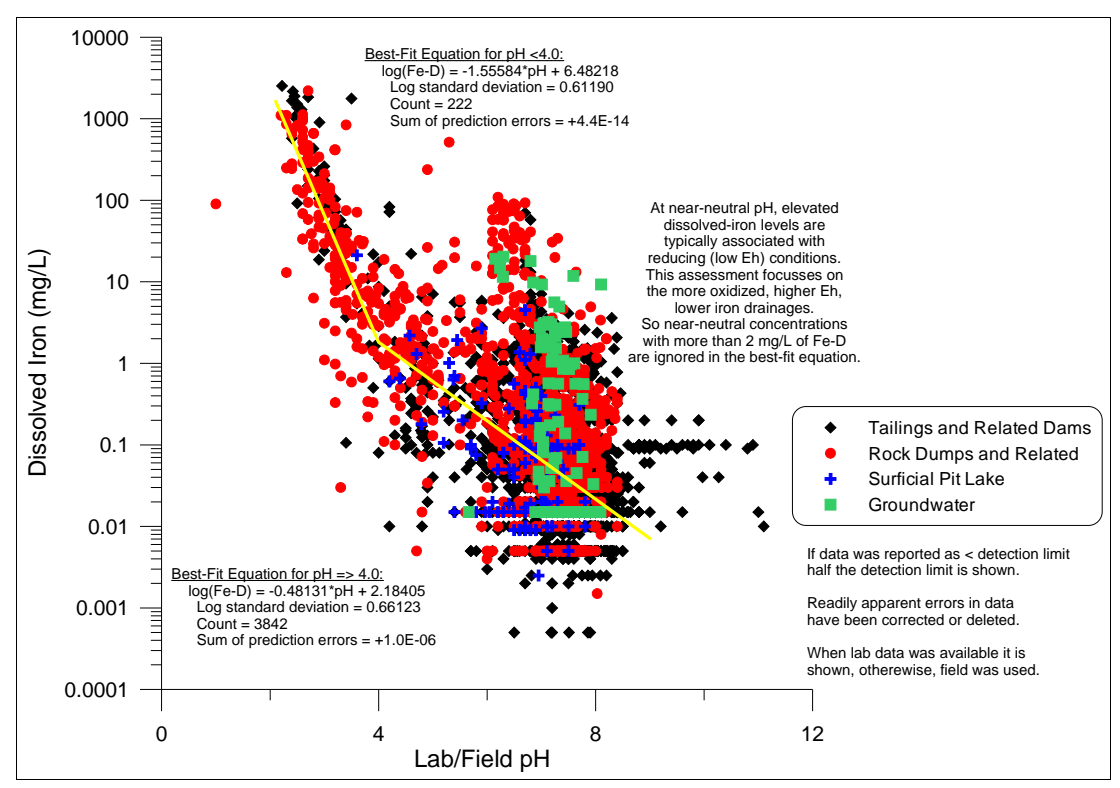


Figure A22-3. Best-fit equations for dissolved iron vs. pH in the 2010 Bell EDCM.

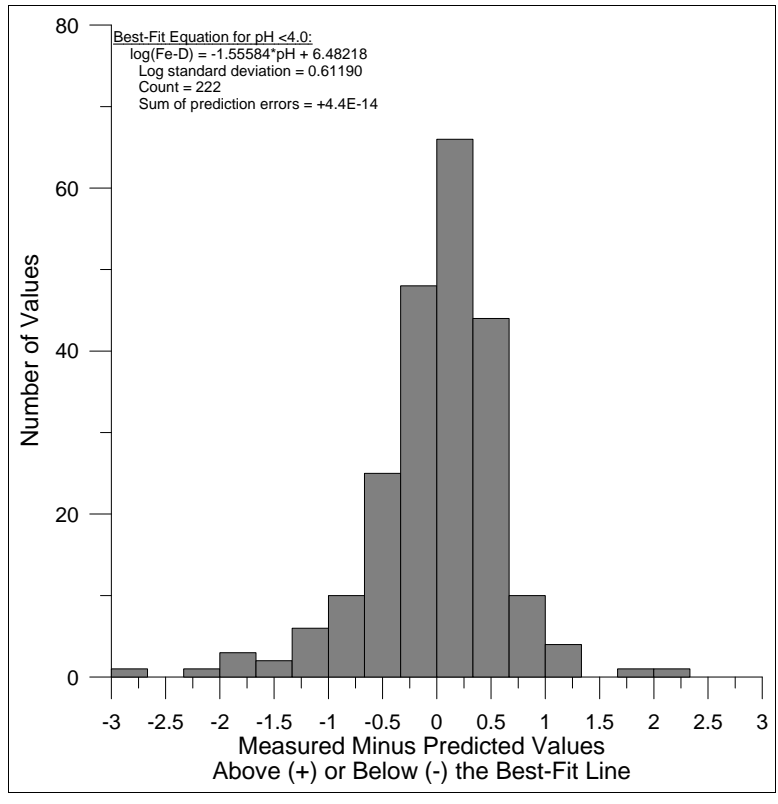


Figure A22-4. Statistical distribution of (measured-calculated) datapoints around the best-fit equation for dissolved iron below pH 4.0.

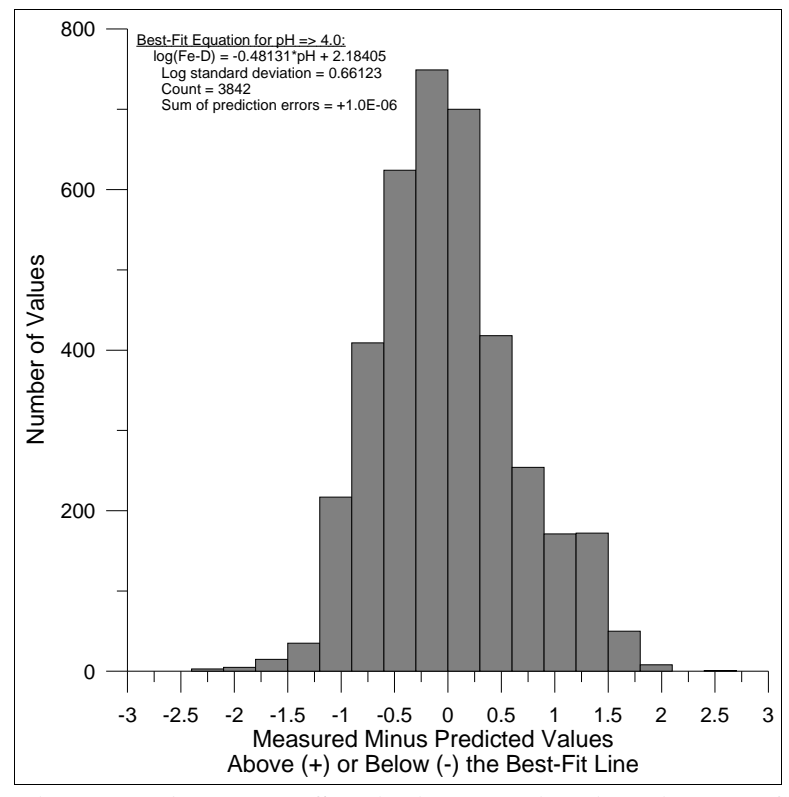


Figure A22-5. Statistical distribution of (measured-calculated) datapoints around the best-fit equation for dissolved iron above pH 4.0.

Appendix A23. Dissolved Lead (Pb-D)

Notes:

Of the nearly 900 analyses for dissolved lead, most were below various detection limits. As a result, any trends with pH (Figure A23-1) and sulphate (Figure A23-2) are not clear. Because of this, and including all below-detection values, dissolved lead is set at an average concentration of 0.009213 mg/L (Figure A23-3), independent of the master parameters. Most of the (measured-calculated) datapoints above and below this constant value display a general lognormal distribution (Figure A23-4), but a secondary peak with nearly 150 below-detection values can be also be seen.

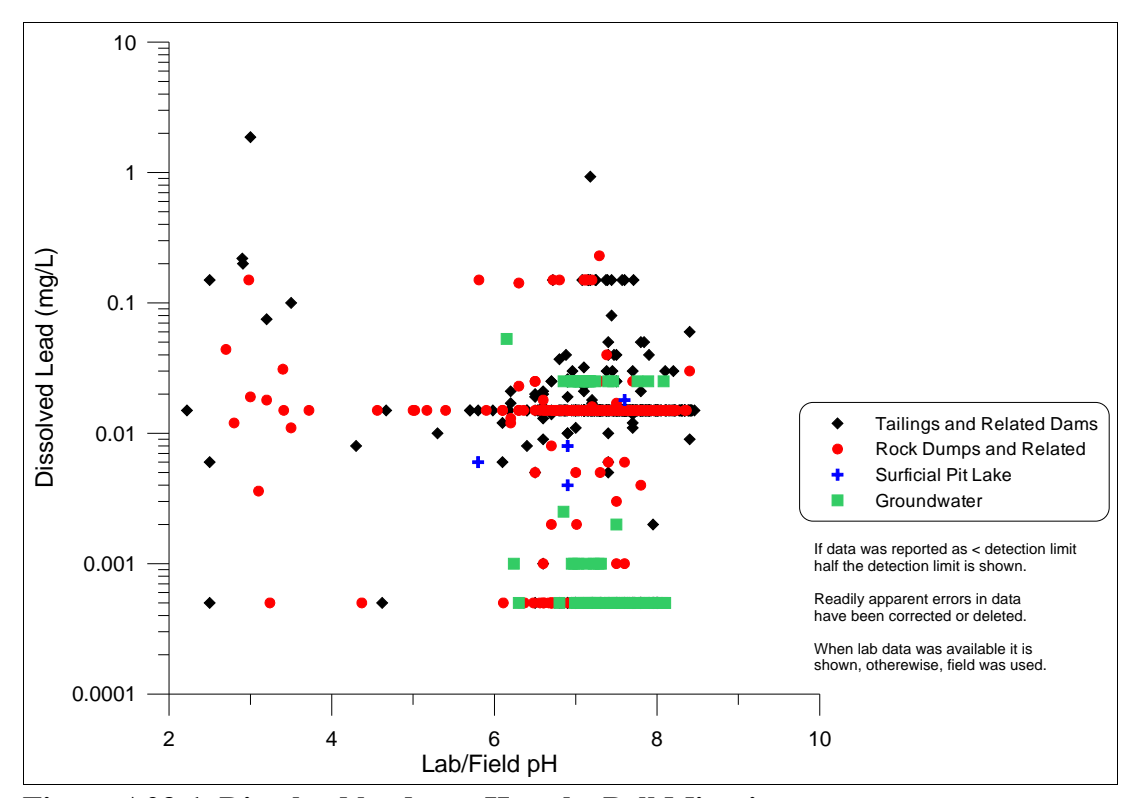


Figure A23-1. Dissolved lead vs. pH at the Bell Minesite.

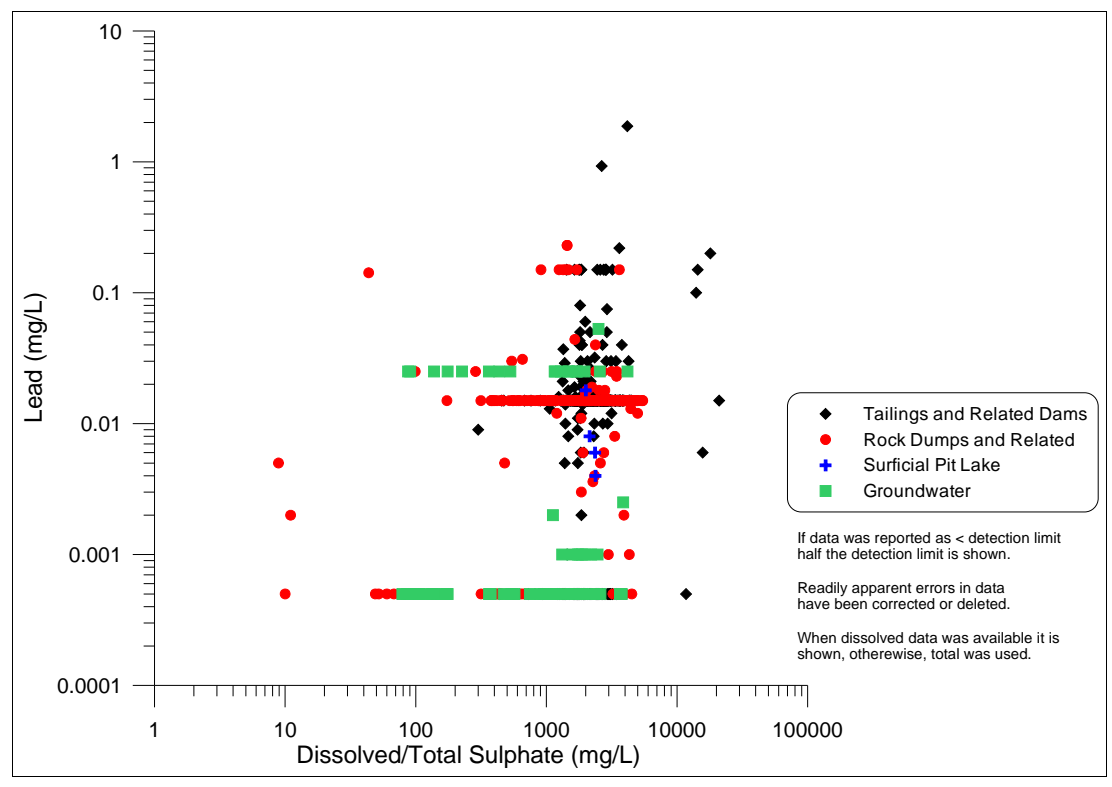


Figure A23-2. Dissolved lead vs. sulphate at the Bell Minesite.

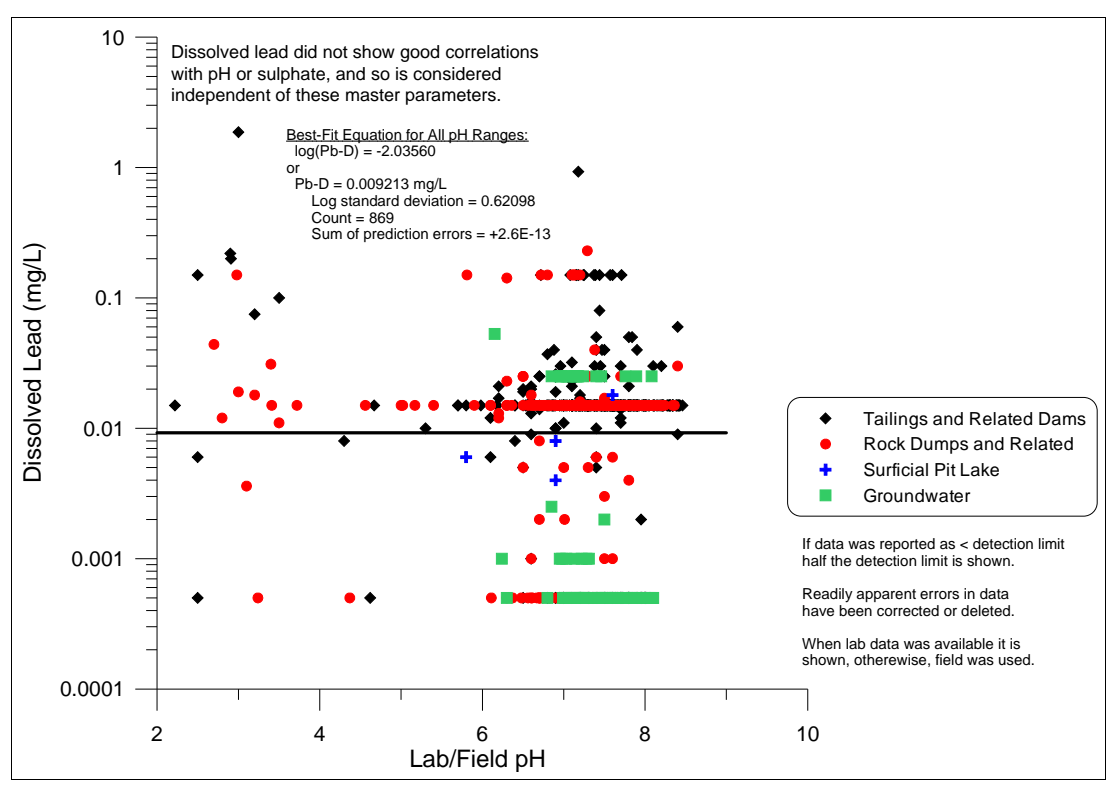


Figure A23-3. Best-fit equation for dissolved lead vs. pH in the 2010 Bell EDCM.

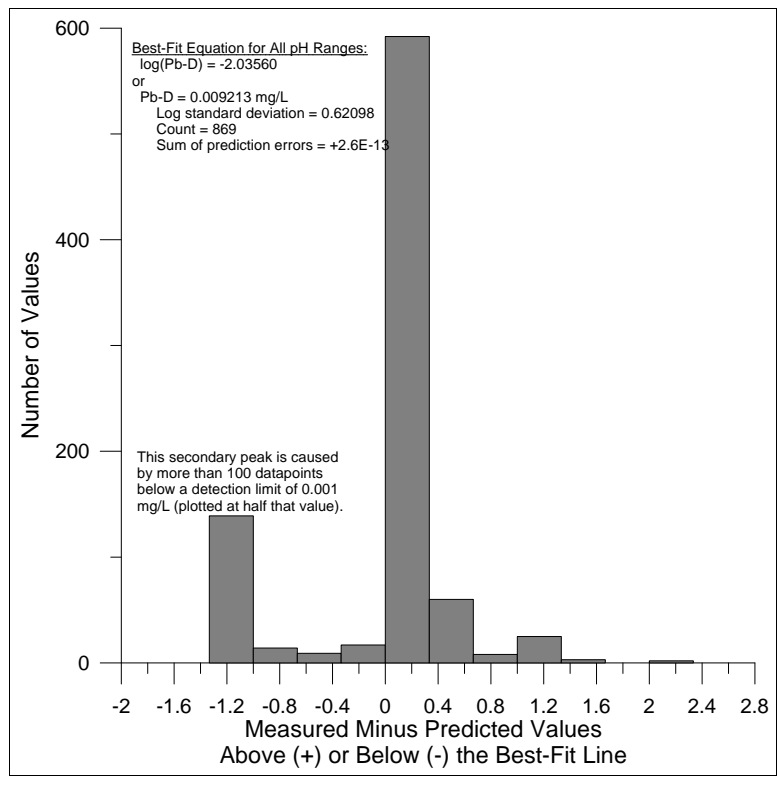


Figure A23-4. Statistical distribution of (measured-calculated) datapoints around the best-fit equation for dissolved lead.

Appendix A24. Dissolved Lithium (Li-D)

Notes:

Only near-neutral drainages at the Bell Minesite have been analyzed for dissolved lithium, and lithium was often below various detection limits. Thus, trends with pH (Figure A24-1) and sulphate (Figure A24-2) are not apparent. Thus, dissolved lithium is simply set at <0.1 mg/L (Figure A24-3).

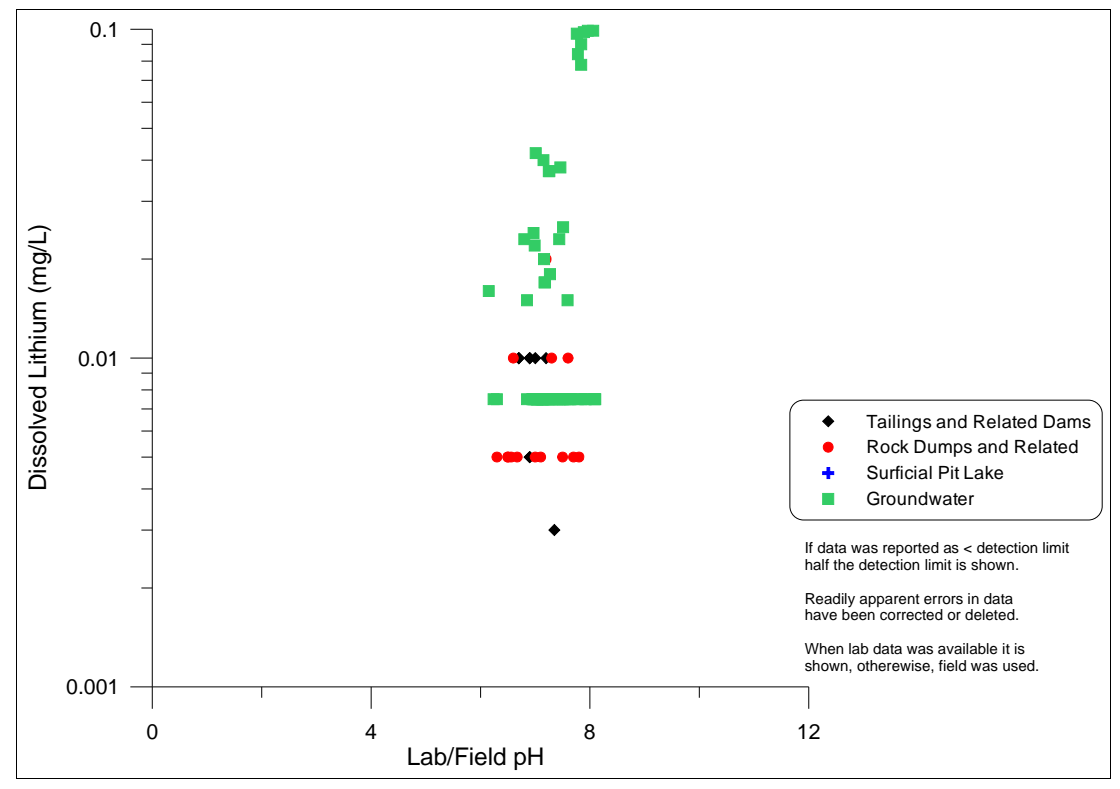


Figure A24-1. Dissolved lithium vs. pH at the Bell Minesite.

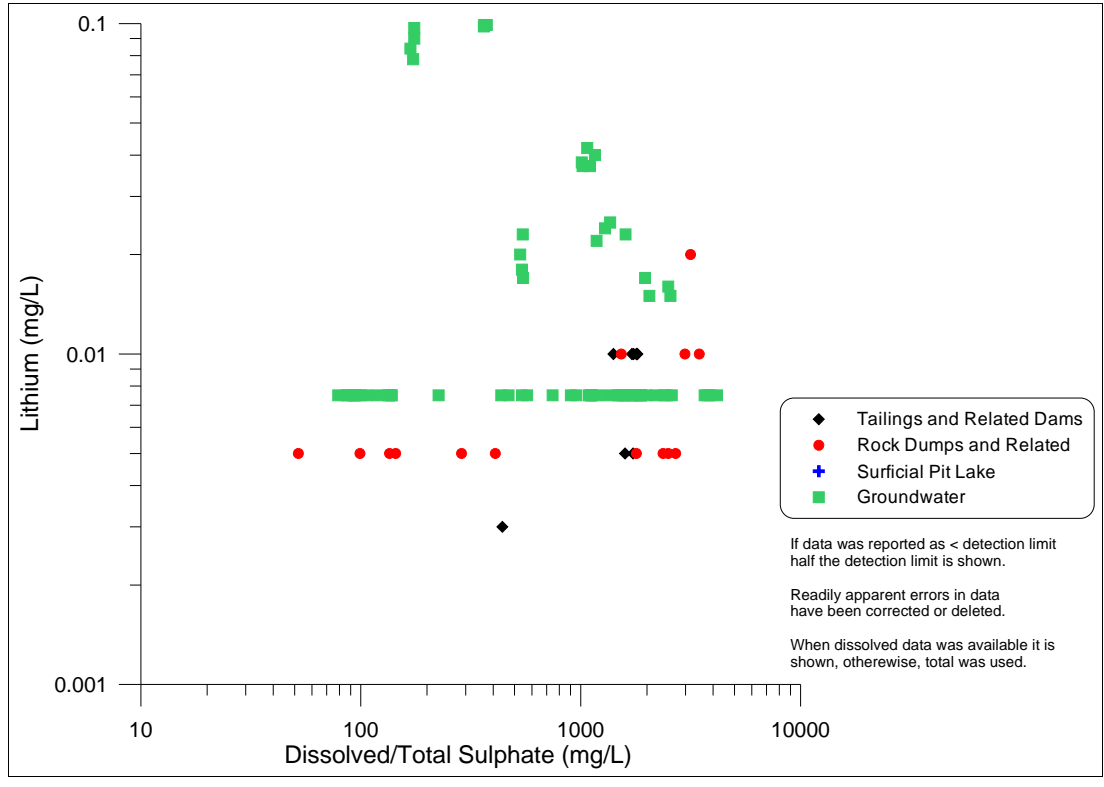


Figure A24-2. Dissolved lithium vs. sulphate at the Bell Minesite.

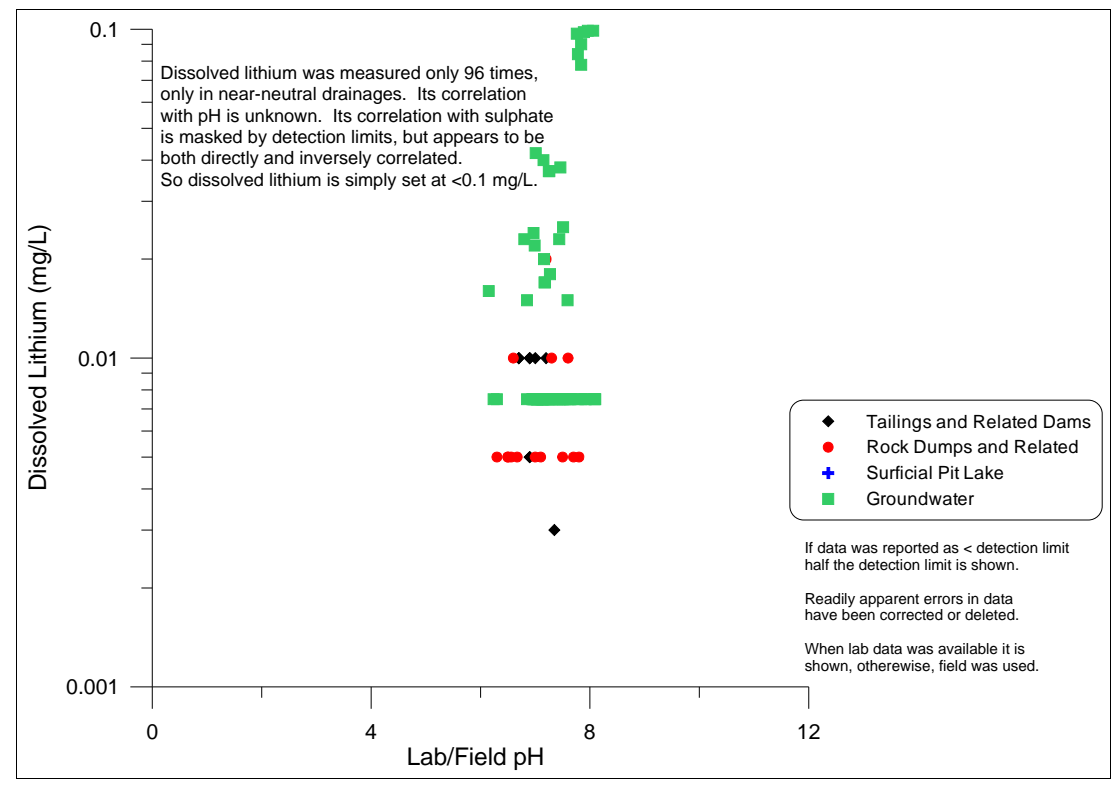


Figure A24-3. Best-fit equations for dissolved cobalt vs. pH in the 2010 Bell EDCM.

Appendix A25. Dissolved Magnesium (Mg-D)

Notes:

More than 1400 analyses of dissolved magnesium correlate much better with the master parameter of sulphate (Figure A25-2) than with pH (Figure A25-1). The best-fit equation has a slope of nearly +1.0 (Figure A25-3). The (measured-calculated) datapoints above and below this equation form a general lognormal distribution (Figure 25-4), with a standard deviation of 0.18773 log cycles.

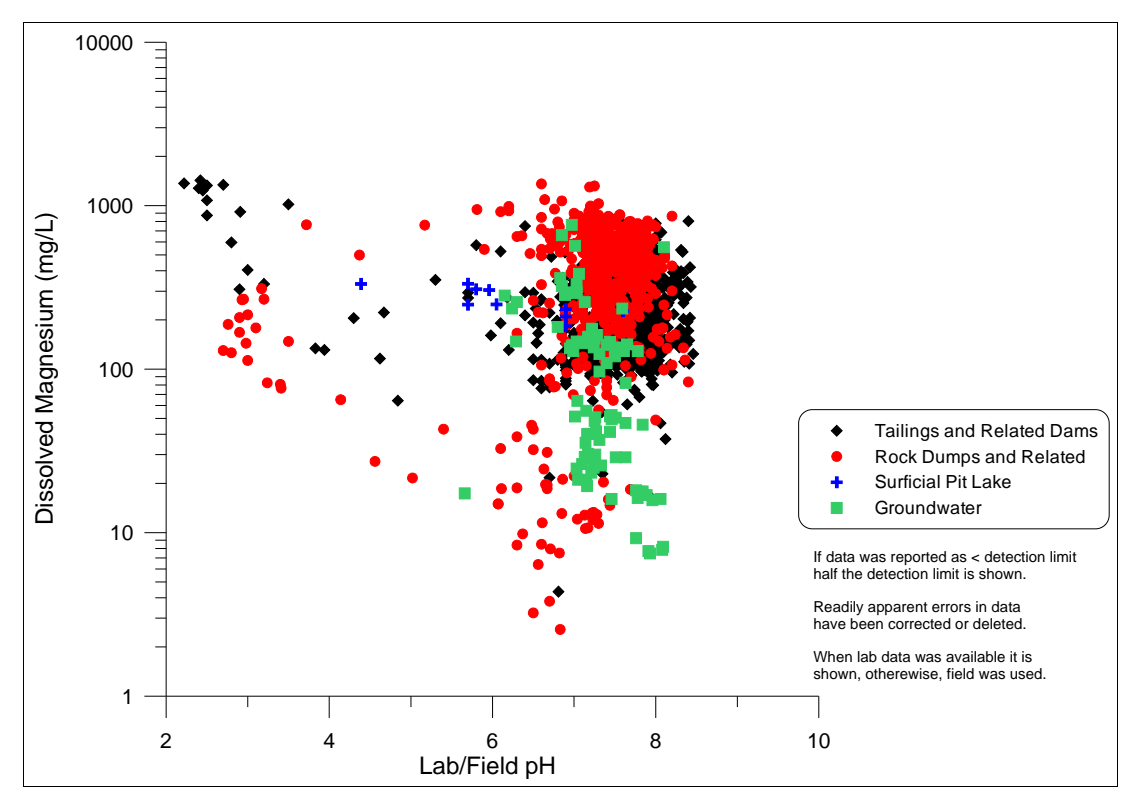


Figure A25-1. Dissolved magnesium vs. pH at the Bell Minesite.

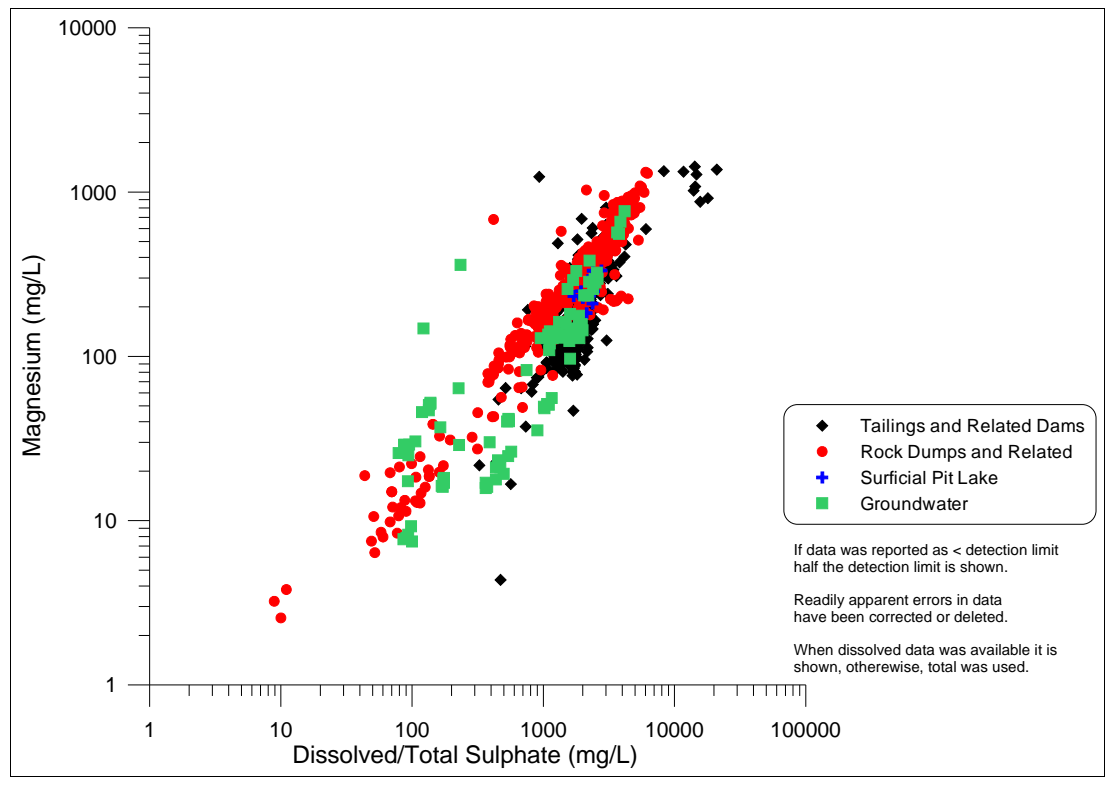


Figure A25-2. Dissolved magnesium vs. sulphate at the Bell Minesite.

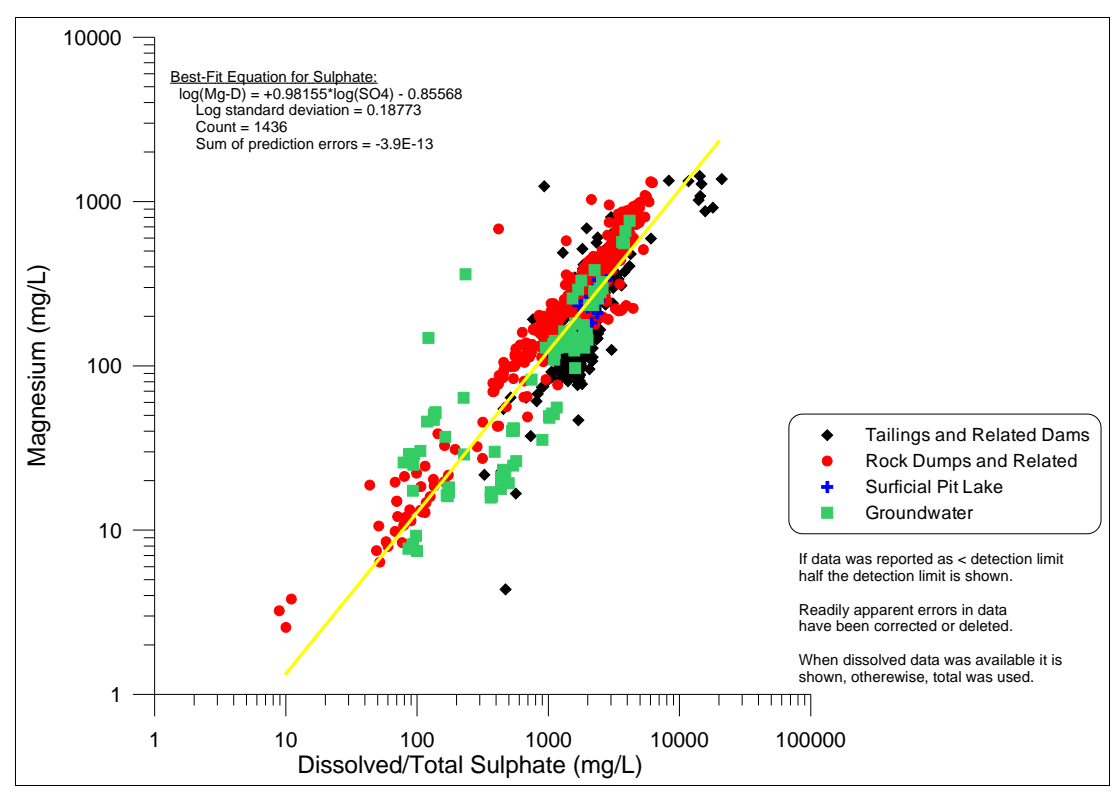


Figure A25-3. Best-fit equation for dissolved magnesium vs. sulphate in the 2010 Bell EDCM.

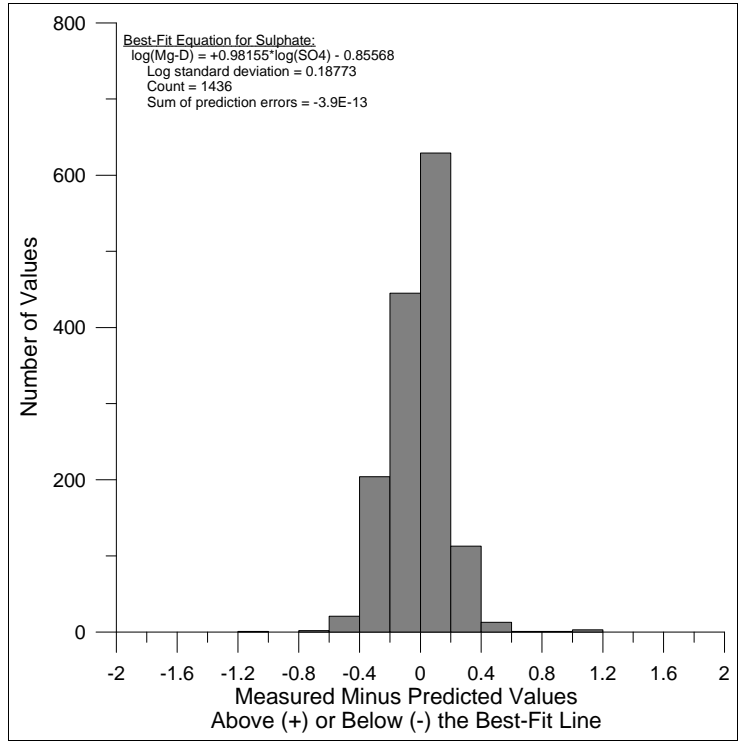


Figure A25-4. Statistical distribution of (measured-calculated) datapoints around the best-fit equation for dissolved magnesium.

Appendix A26. Dissolved Manganese (Mn-D)

Notes:

Based on more than 700 analyses of dissolved manganese in the Bell Minesite database, higher concentrations of manganese show some correlation with pH (Figure A26-1) and sulphate (Figure A26-2). Lower manganese levels are mostly independent of pH and sulphate.

If dissolved manganese below 0.1 mg/L is excluded assuming that mostly reflects dilution, then the best-fit equation reflects undiluted minesite drainage under acidic and near-neutral conditions (Figure A26-3). The (measured-calculated) datapoints above and below this equation form a general lognormal distribution (Figure A26-4), with a standard deviation of 0.45138 log cycles.

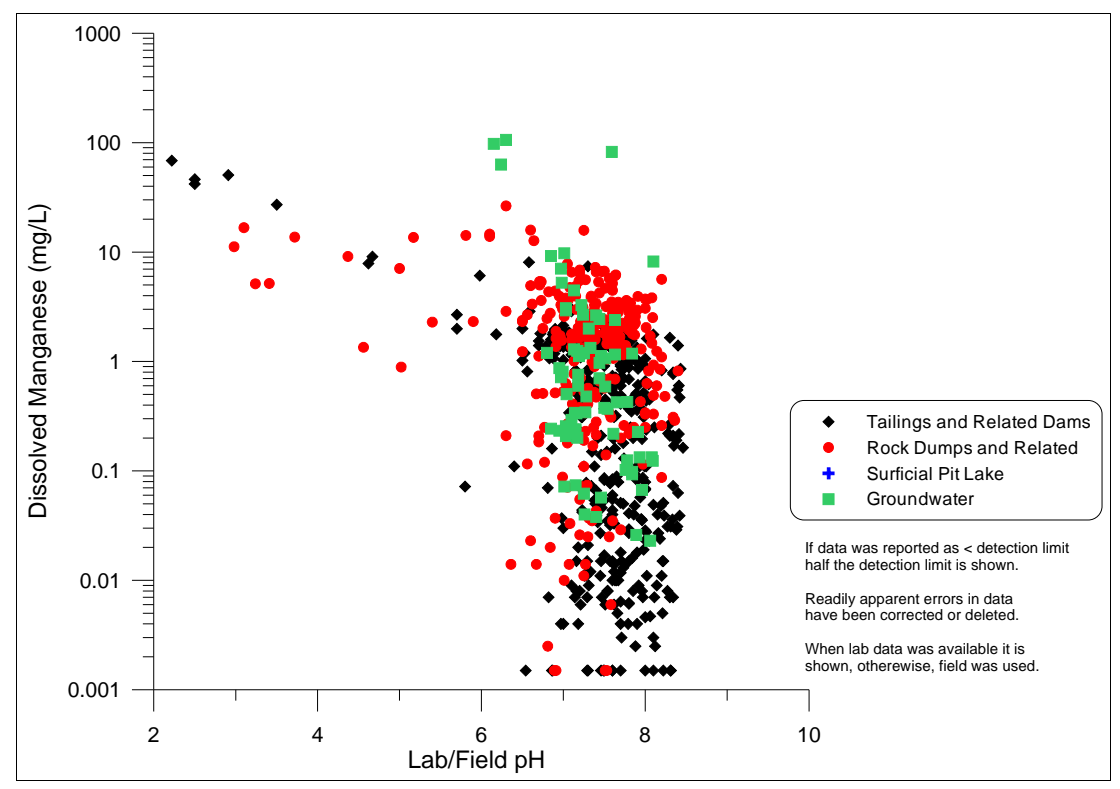


Figure A26-1. Dissolved manganese vs. pH at the Bell Minesite.

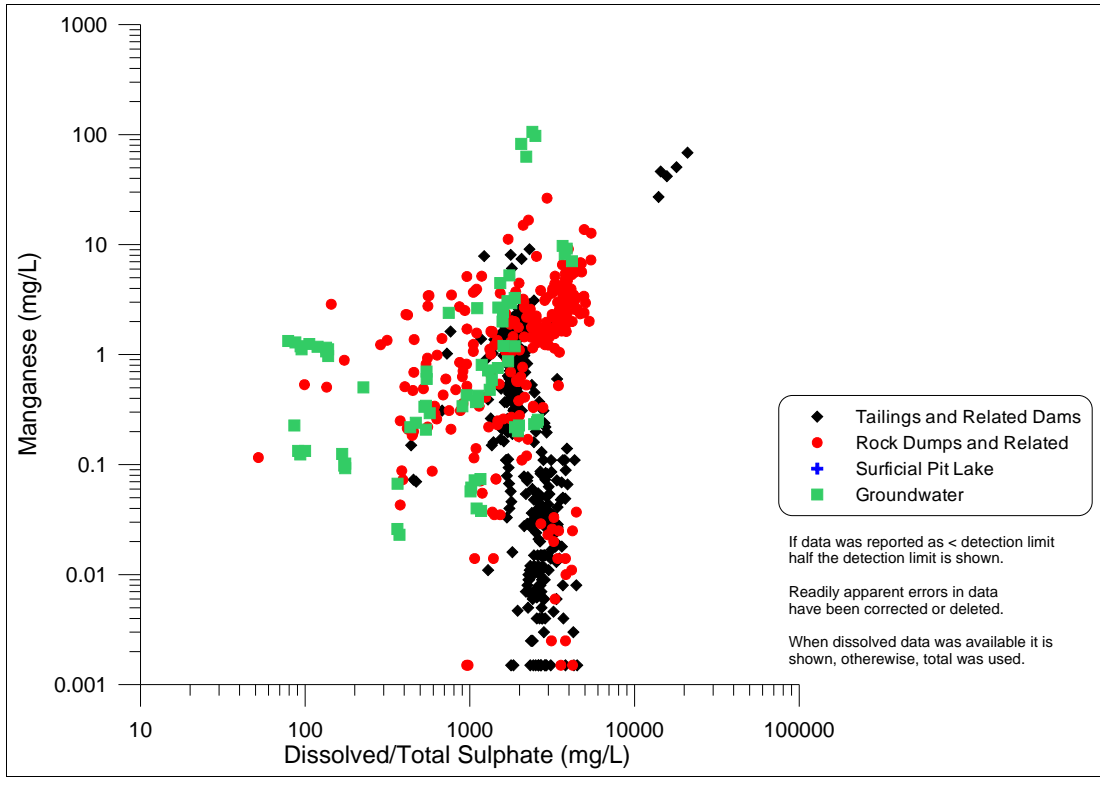


Figure A26-2. Dissolved manganese vs. sulphate at the Bell Minesite.

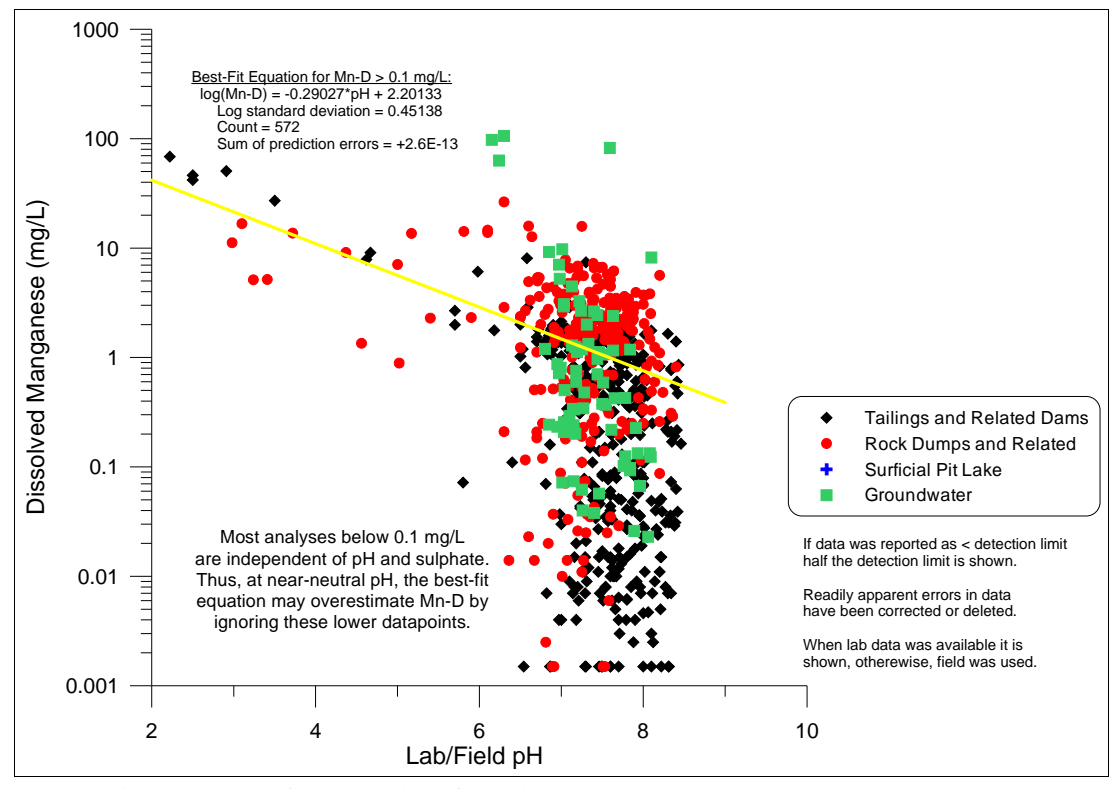


Figure A26-3. Best-fit equation for dissolved manganese vs. pH in the 2010 Bell EDCM.

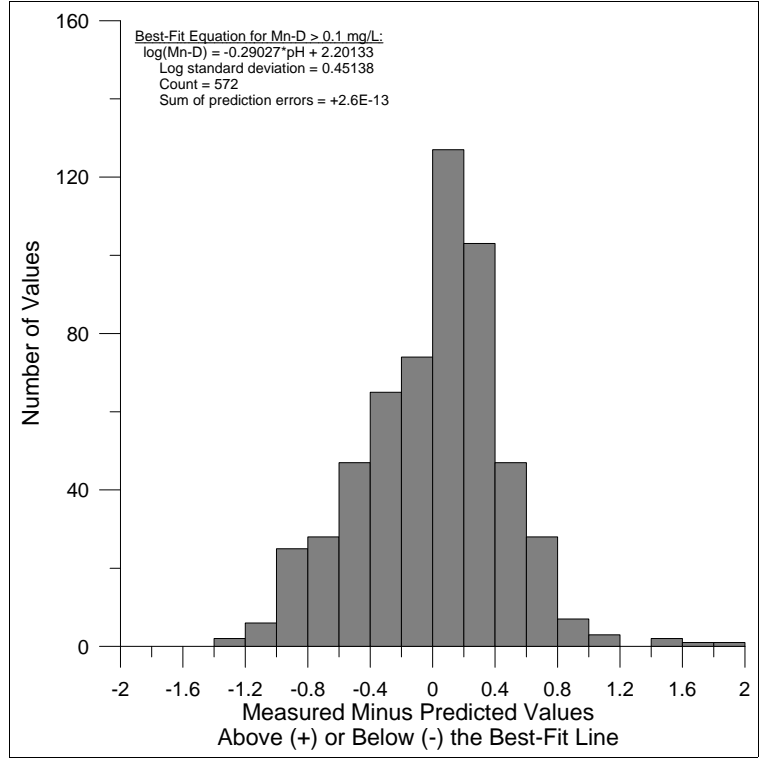


Figure A26-4. Statistical distribution of (measured-calculated) datapoints around the best-fit equation for dissolved manganese.

## MDAG.com Internet Case Study #33: 31 Years of Minesite-Drainage Chemistry...: Bell Minesite Page 131

Appendix A27. Dissolved Mercury (Hg-D)

Notes:

The few dozen analyses for dissolved mercury were below two detection limits. Thus, no trends are apparent with the master parameters of pH (Figure A27-1) and sulphate (Figure A27-2). Therefore, dissolved mercury is set below the detection limit used in 2009, at < 0.0005 mg/L (Figure A27-3).

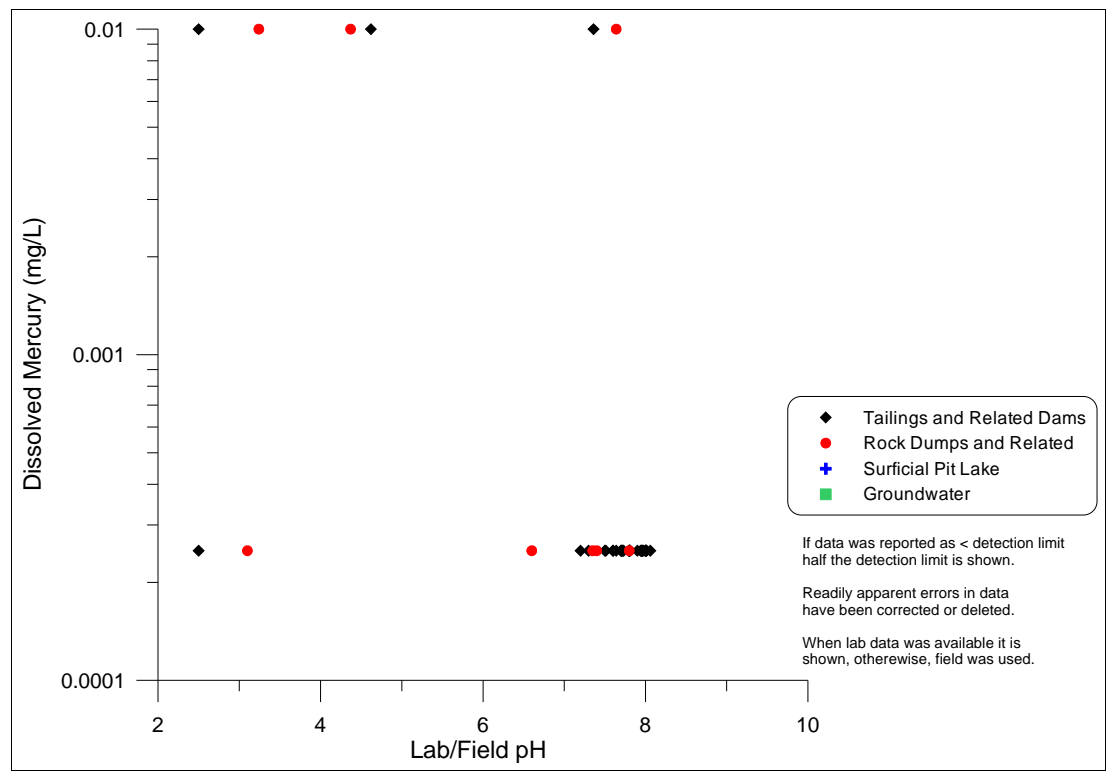


Figure A27-1. Dissolved mercury vs. pH at the Bell Minesite.

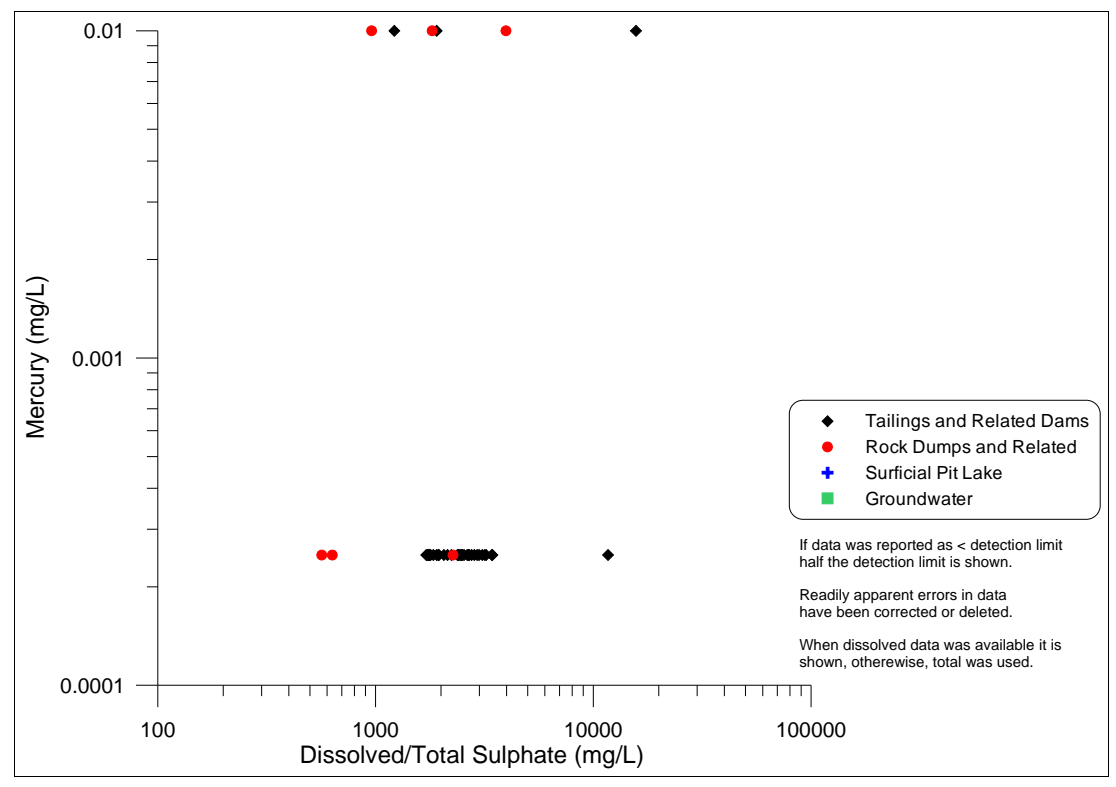


Figure A27-2. Dissolved mercury vs. sulphate at the Bell Minesite.

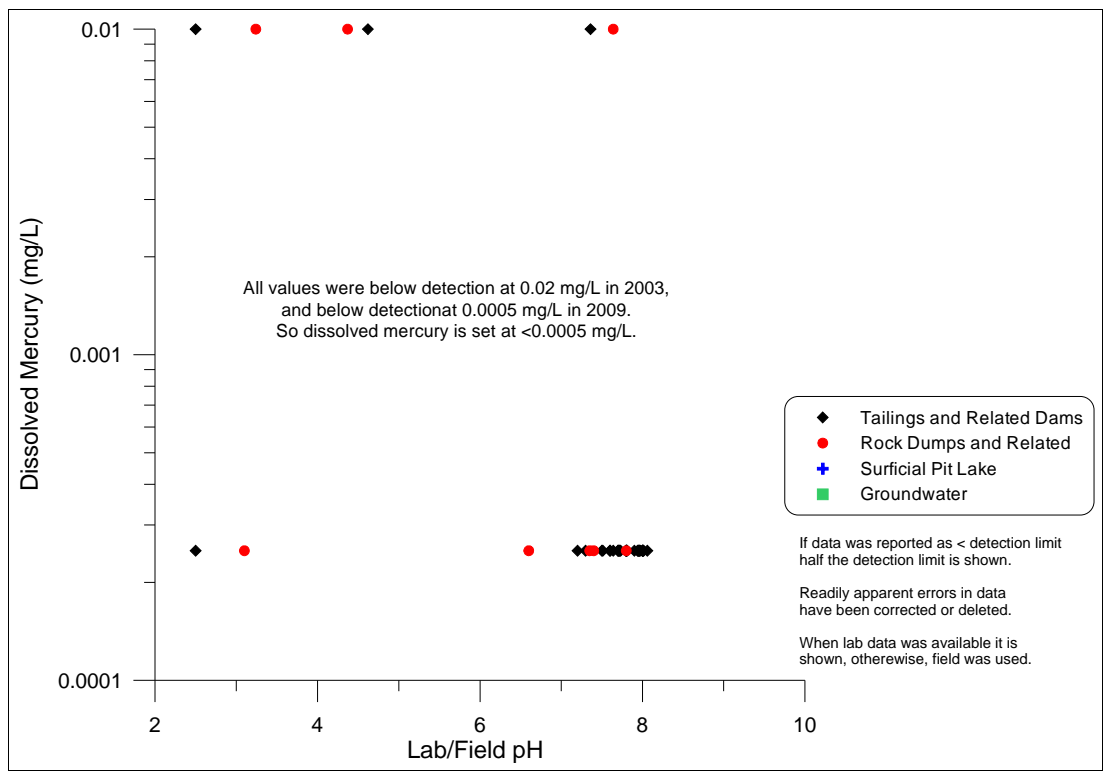


Figure A27-3. Best-fit equation for dissolved mercury in the 2010 Bell EDCM.

Appendix A28. Dissolved Molybdenum (Mo-D)

Notes:

Of the nearly 800 analyses for dissolved molybdenum in the Bell Minesite database, most were below various detection limits and analyses from 2009 were 10-100 times lower than previous levels. As a result, no good correlations were seen with pH (Figure A28-1) or sulphate (Figure A28-2).

However, excluding detection limits and the anomalous 2009 data, a constant value of 0.0640 mg/L can be assigned to dissolved molybdenum (Figure A28-3), independent of pH and sulphate. This is based on only 18 datapoints, which may form a lognormal distribution around the constant value (Figure A28-4) with a standard deviation of 0.27549 log cycles.

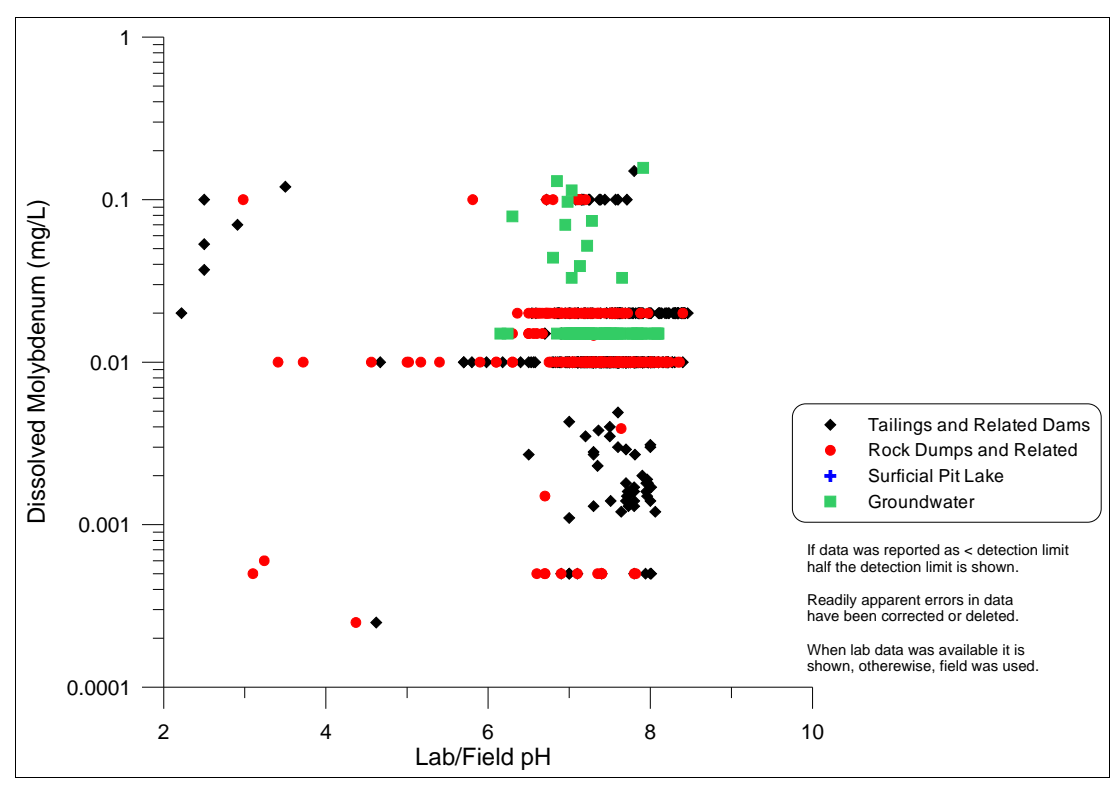


Figure A28-1. Dissolved molybdenum vs. pH at the Bell Minesite.

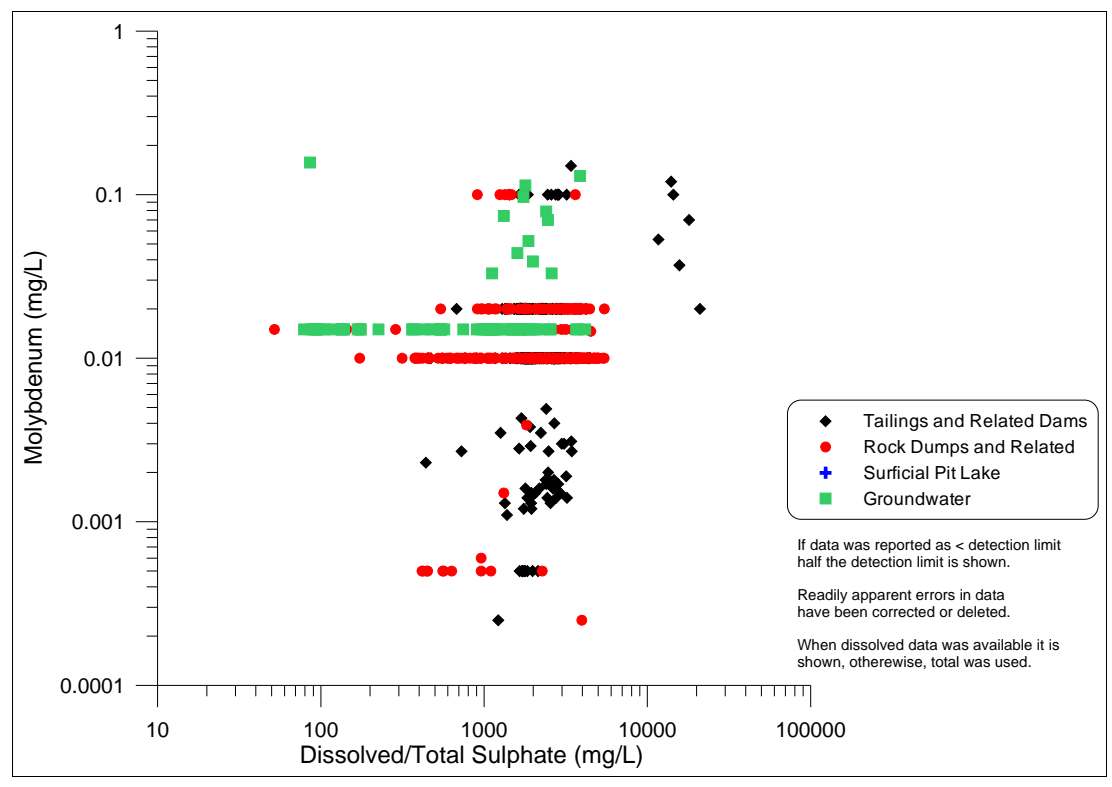


Figure A28-2. Dissolved molybdenum vs. sulphate at the Bell Minesite.

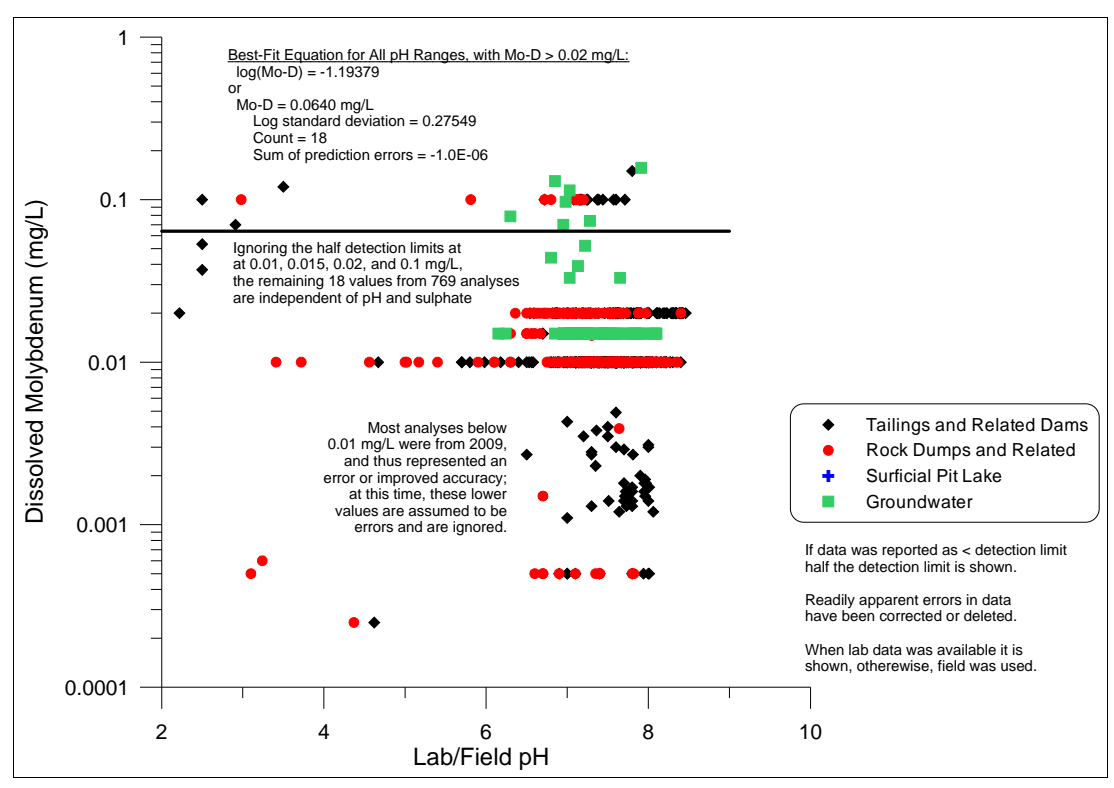


Figure A28-3. Best-fit equation for dissolved molybdenum in the 2010 Bell EDCM.

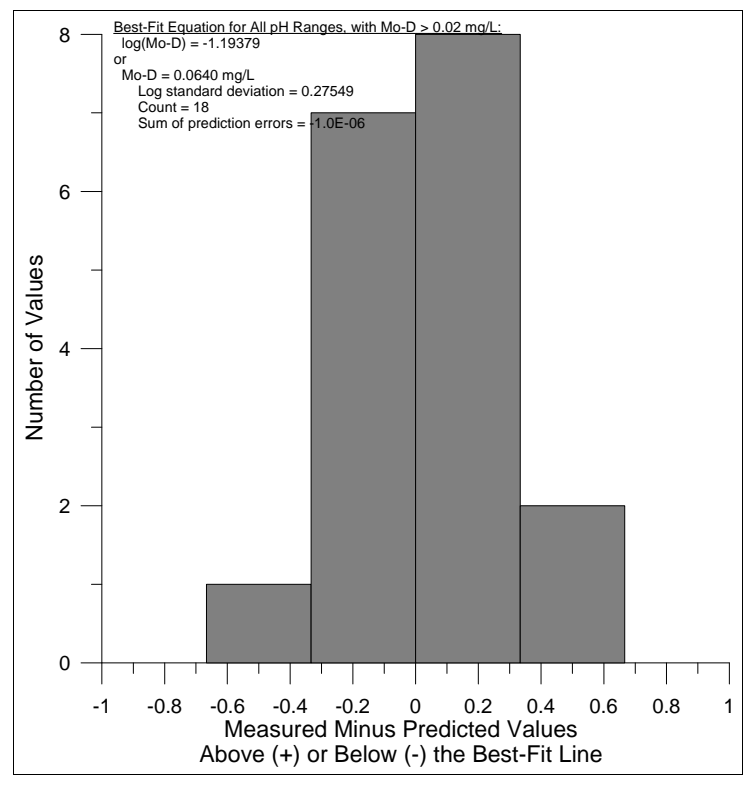


Figure A28-4. Statistical distribution of (measured-calculated) datapoints around the best-fit equation for dissolved molybdenum.

Appendix A29. Dissolved Nickel (Ni-D)

Notes:

Dissolved nickel shows more correlation across the range of measured pH (Figure A29-1) than the range of sulphate (Figure A29-2). The best-fit correlation with pH has a slope of about -0.46 (Figure A29-3). The distribution of (measured-calculated) datapoints above and below this correlation is not symmetrical (Figure A29-4). However, the lognormal standard deviation of 0.40611 log cycles is used as a general indicator of variability around the equation.

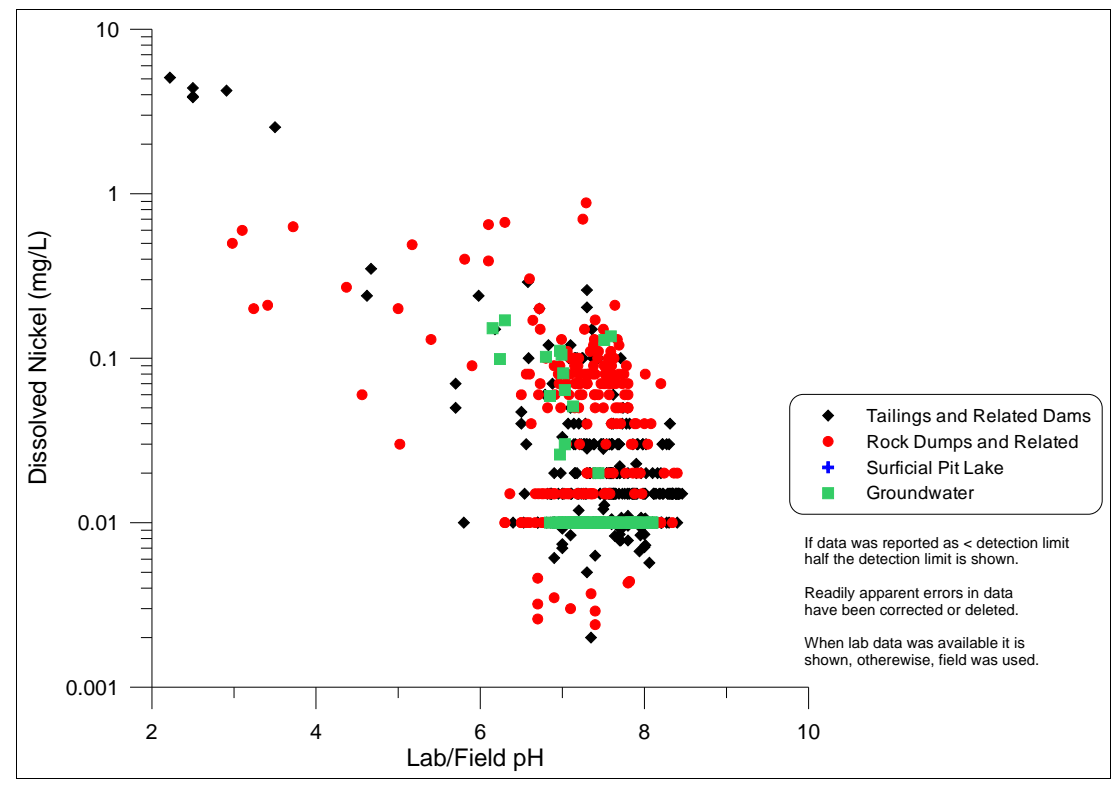


Figure A29-1. Dissolved nickel vs. pH at the Bell Minesite.

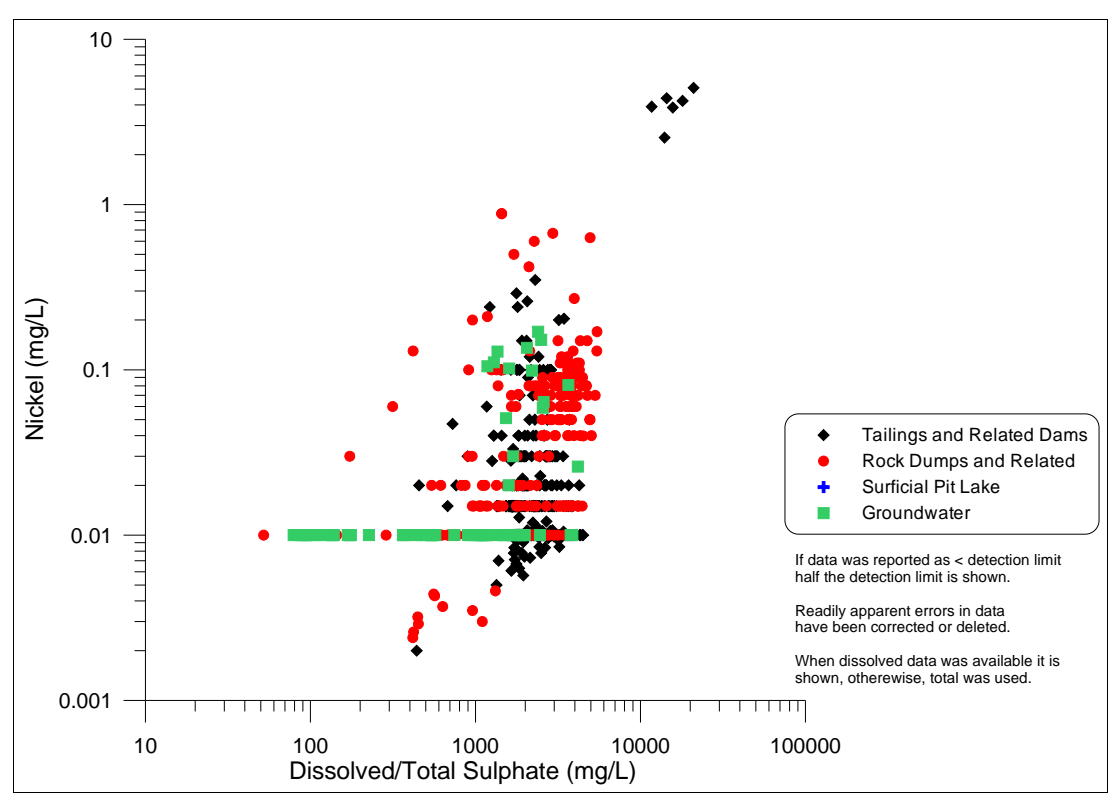


Figure A29-2. Dissolved nickel vs. sulphate at the Bell Minesite.

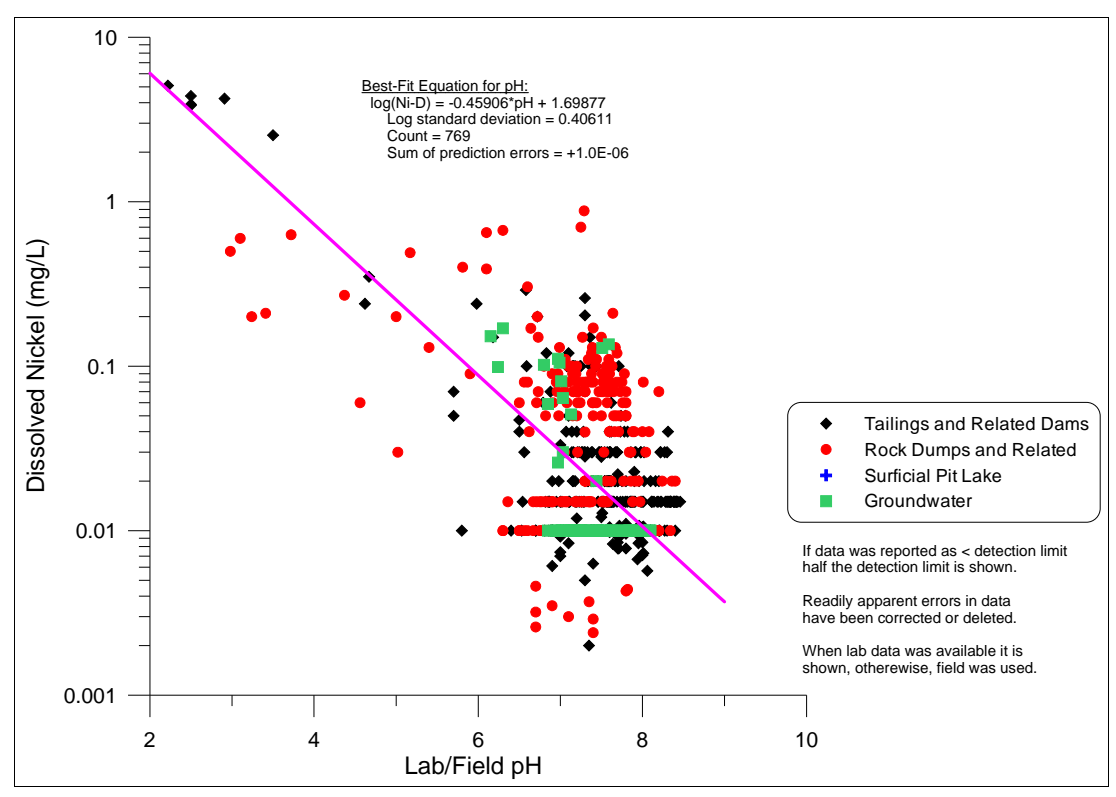


Figure A29-3. Best-fit equation for dissolved nickel vs. pH in the 2010 Bell EDCM.

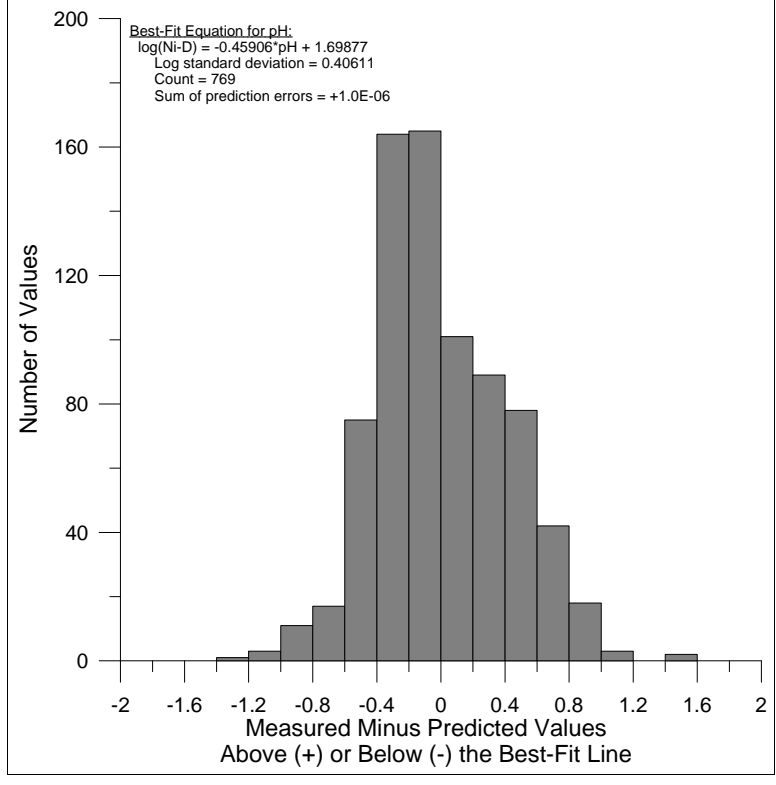


Figure A29-4. Statistical distribution of (measured-calculated) datapoints around the best-fit equation for dissolved nickel.

Appendix A30. Dissolved Phosphorus (P-D)

Notes:

Trends with the 887 analyses of dissolved phosphorus are distorted by changing detection limits through time. Before 1998, all P-D values were <0.7 mg/L and most were <0.06 mg/L. When P-D analyses started again in 2002, detection limits were higher (0.15 and 0.4 mg/l), and several values were above 1 mg/L with acidic samples containing up to 261 mg/L. Because of this, correlations are not clear with the master parameters of pH (Figure A30-1) and sulphate (Figure A30-2).

The best-fit correlation with pH consists of two segments joined at pH 5.0 (Figure A30-3). The acidic segment is based on only 15 datapoints. At near-neutral pH, the trend is distorted by changing detection limits and by a temporal trend, but all data, even below detection, are used for simplicity. This results in a pH-independent, constant value of 0.09467 mg/L above pH 5. The (measured-calculated) values above and below the two segments resemble lognormal distributions (Figures A30-4 and A30-5).

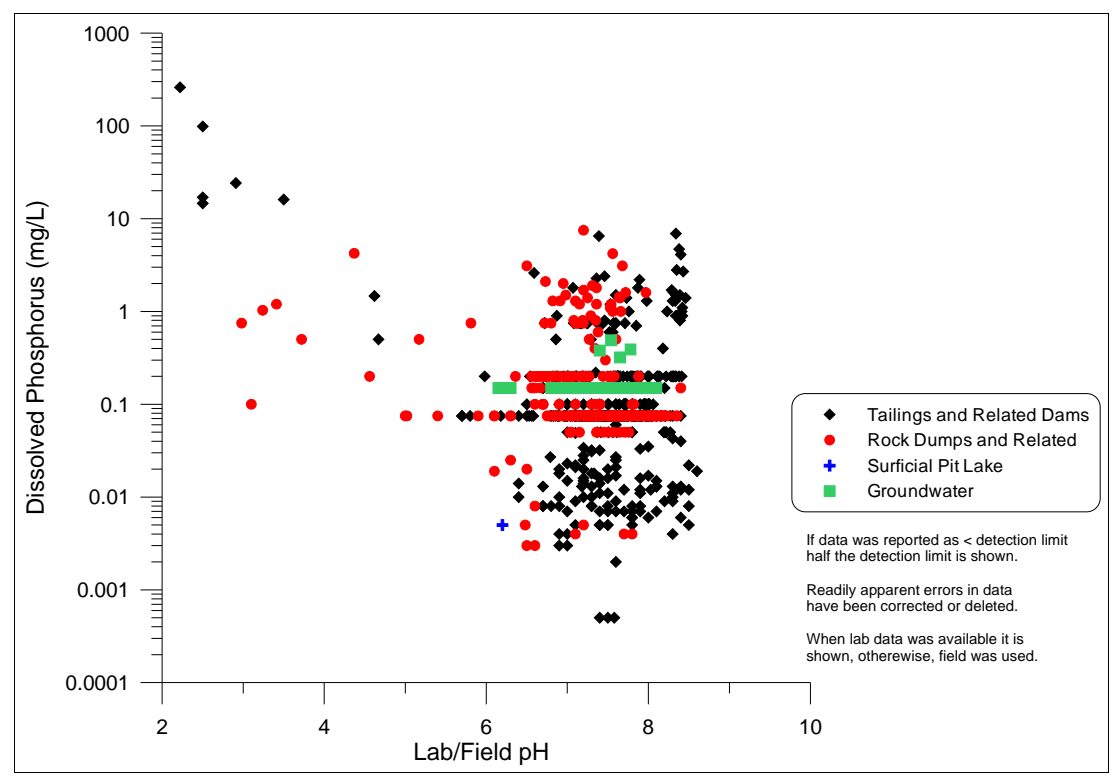


Figure A30-1. Dissolved phosphorus vs. pH at the Bell Minesite.

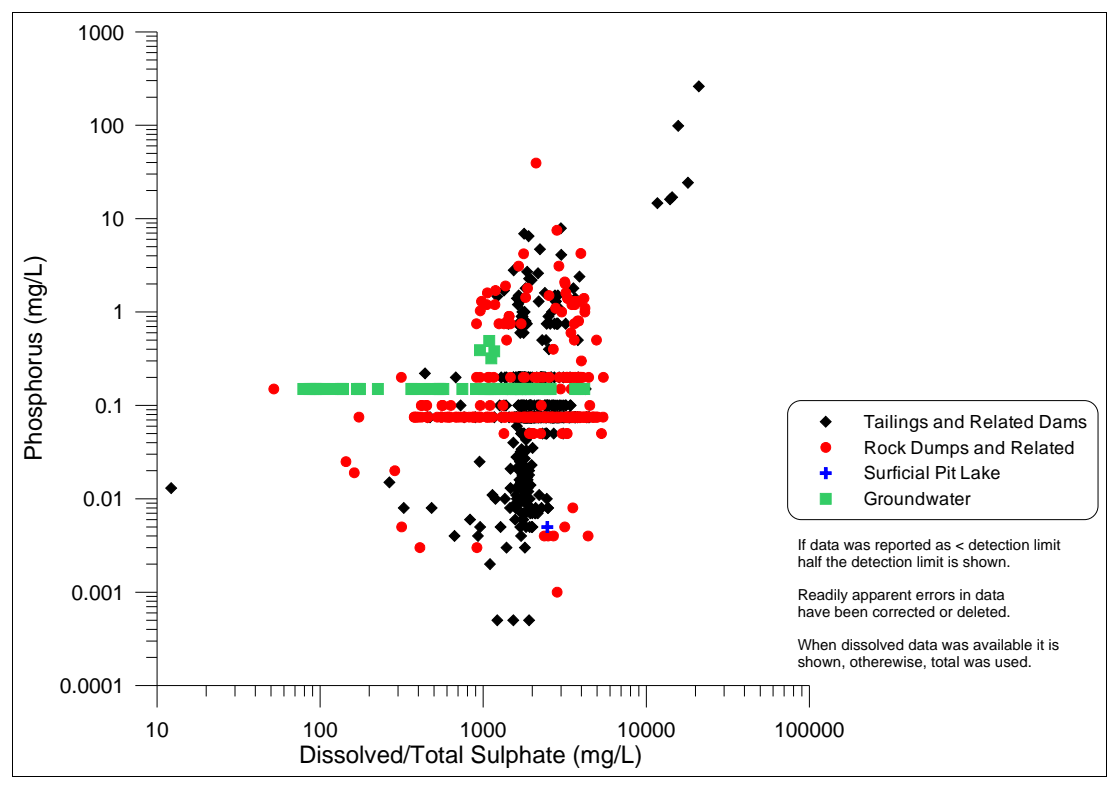


Figure A30-2. Dissolved phosphorus vs. sulphate at the Bell Minesite.

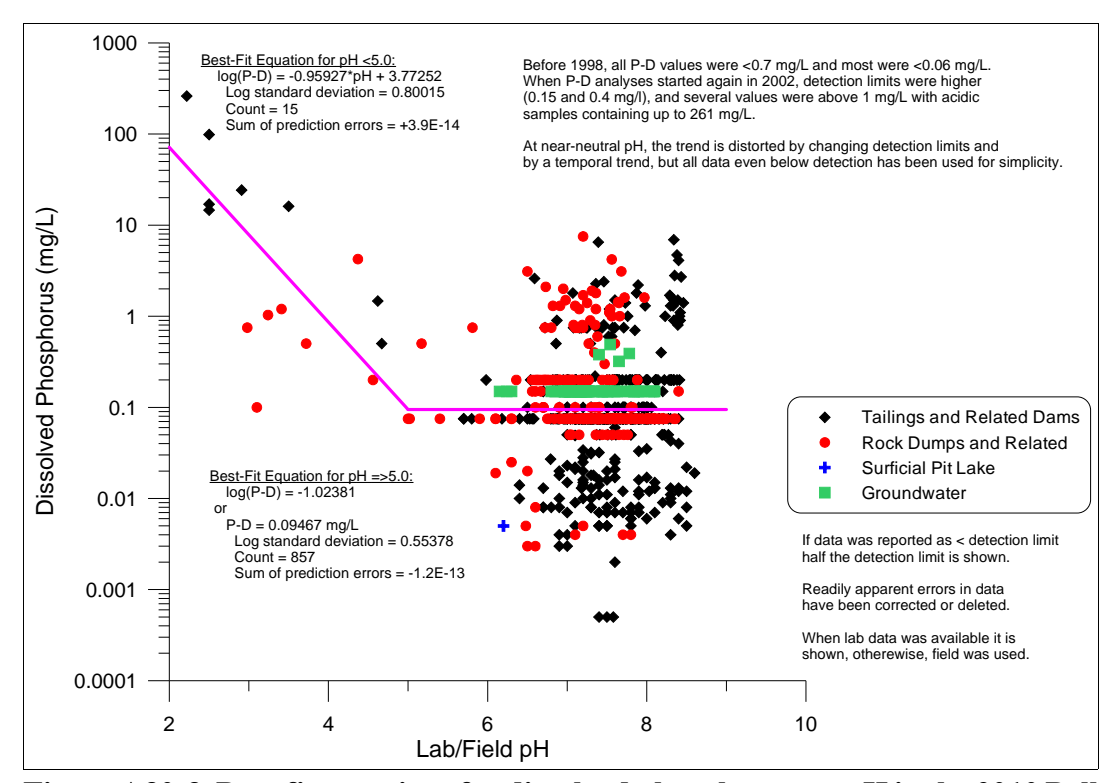


Figure A30-3. Best-fit equations for dissolved phosphorus vs. pH in the 2010 Bell EDCM.

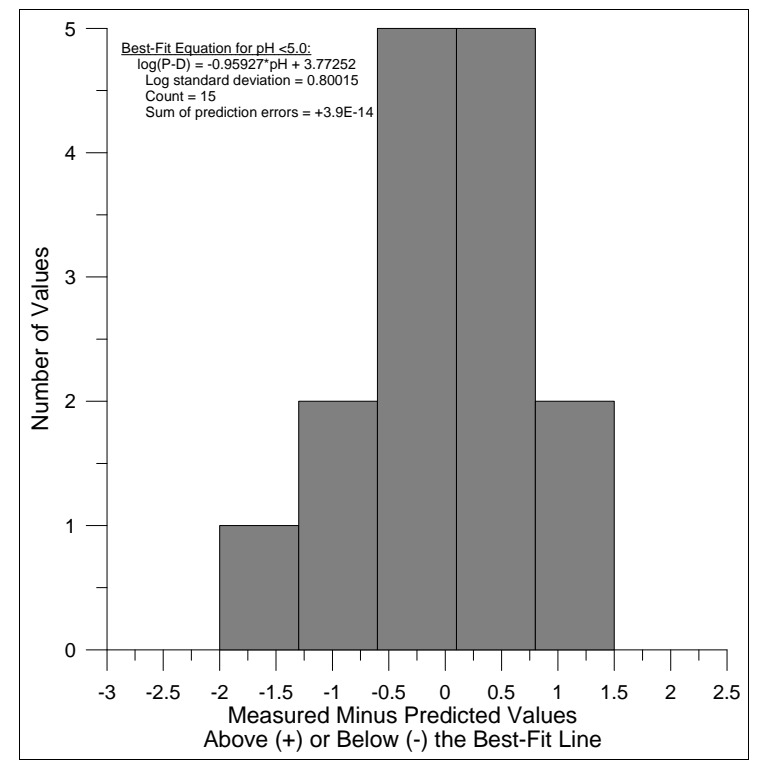


Figure A30-4. Statistical distribution of (measured-calculated) datapoints around the best-fit equation for dissolved phosphorus below pH 5.0.

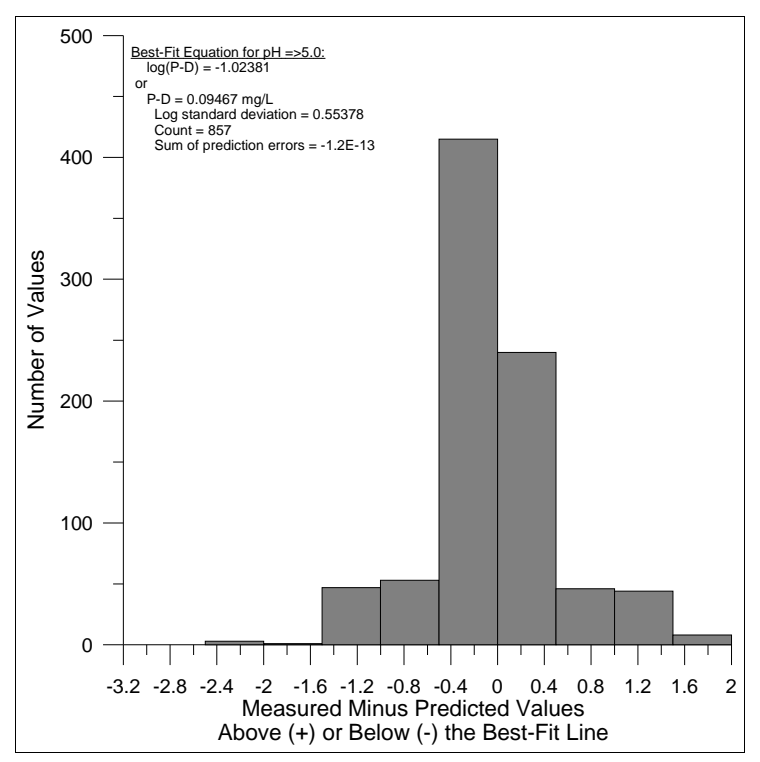


Figure A30-5. Statistical distribution of (measured-calculated) datapoints around the best-fit equation for dissolved phosphorus above pH 5.0.

Appendix A31. Dissolved Potassium (K-D)

Notes:

Dissolved potassium was analyzed 98 times in Bell Minesite drainages, only in near-neutral waters. Thus, any correlation with pH is unknown (Figure A31-1). There may be some correlation with sulphate (Figure A31-2), but it is not substantial. Therefore, dissolved potassium was simply set at <75 mg/L at near-neutral pH (Figure A31-3).

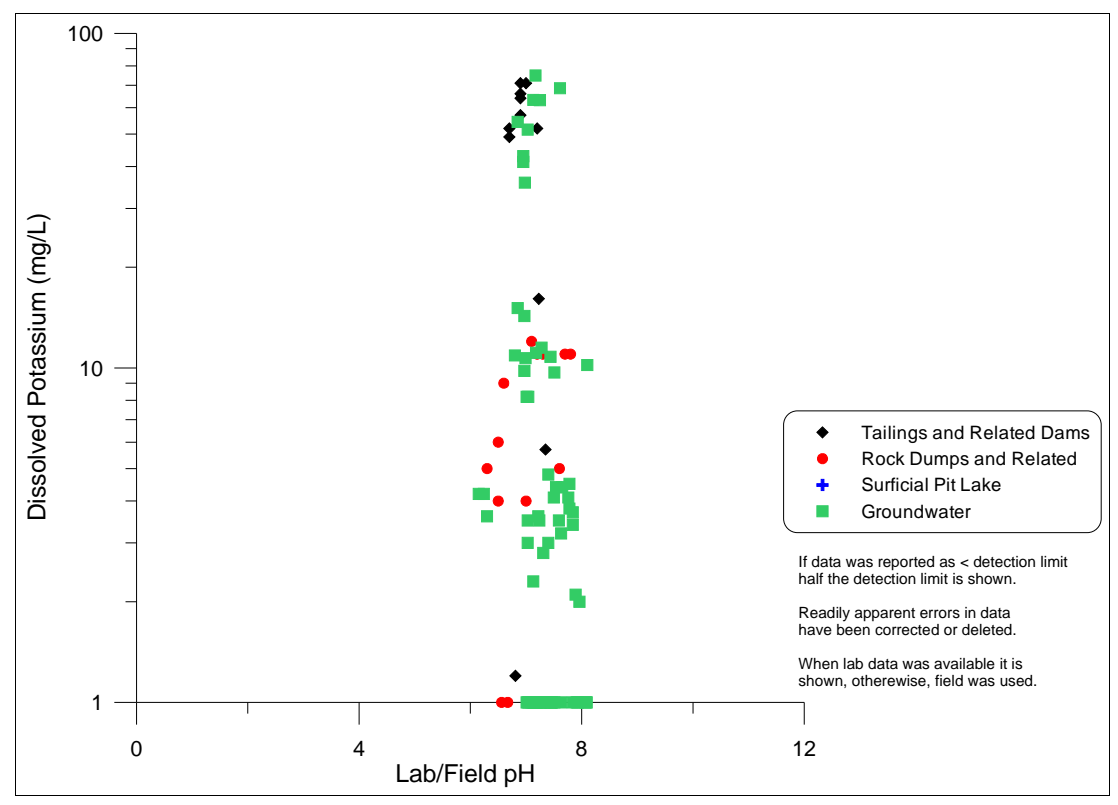


Figure A31-1. Dissolved potassium vs. pH at the Bell Minesite.

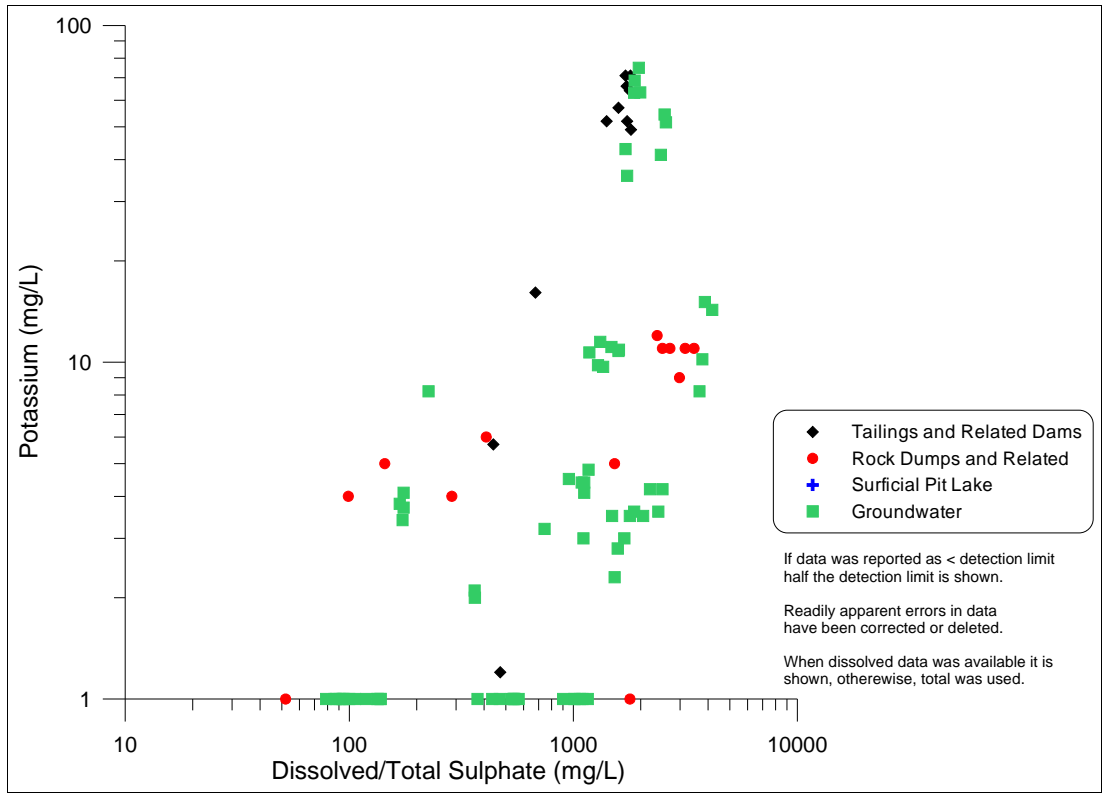


Figure A31-2. Dissolved potassium vs. sulphate at the Bell Minesite.

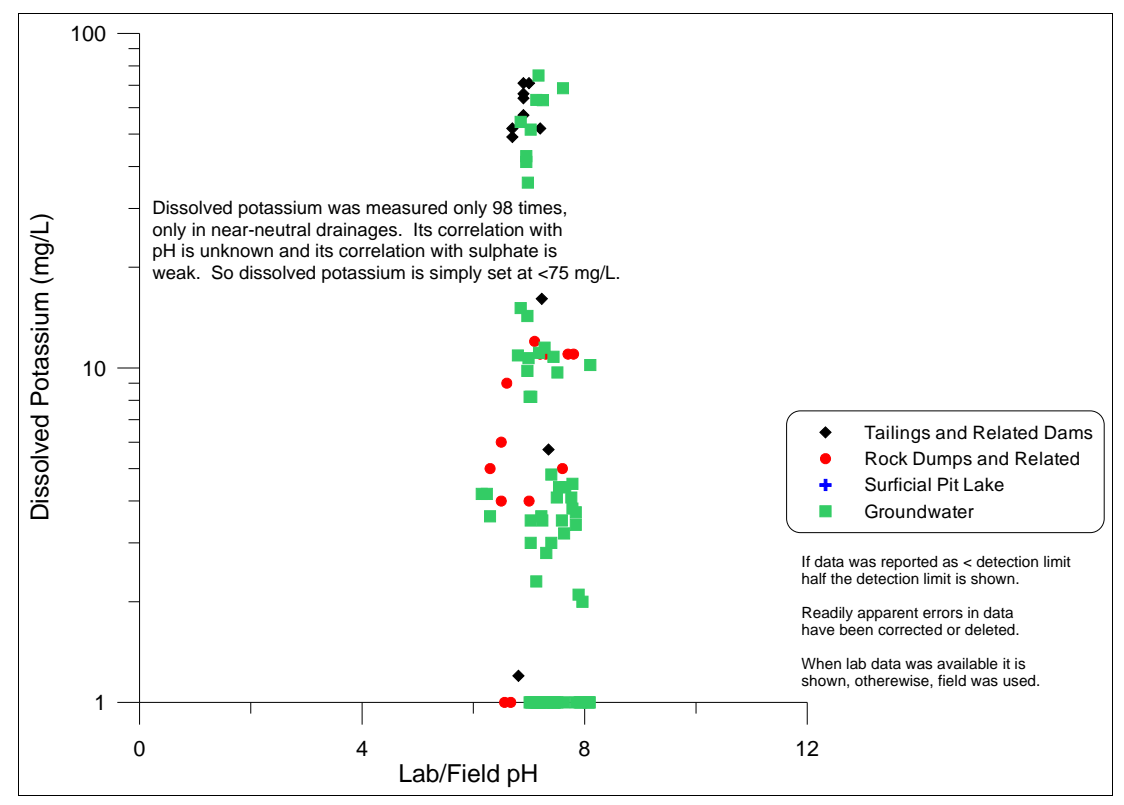


Figure A31-3. Best-fit equation for dissolved potassium in the 2010 Bell EDCM.

Appendix A32. Dissolved Selenium (Se-D)

Notes:

Of the more than 160 analyses for dissolved selenium at the Bell Minesite, most have been at or below various detection limits. As a result, correlations are not apparent with the master parameters of pH (Figure A32-1) and sulphate (Figure A32-2).

Four datapoints less then pH 4.0 (Figure A32-3) were used to define an unconfirmed correlation with dissolved selenium (Figure A32-3). Above pH 4.0, Se-D was set below its lowest detection limit, at <0.0005 mg/L.

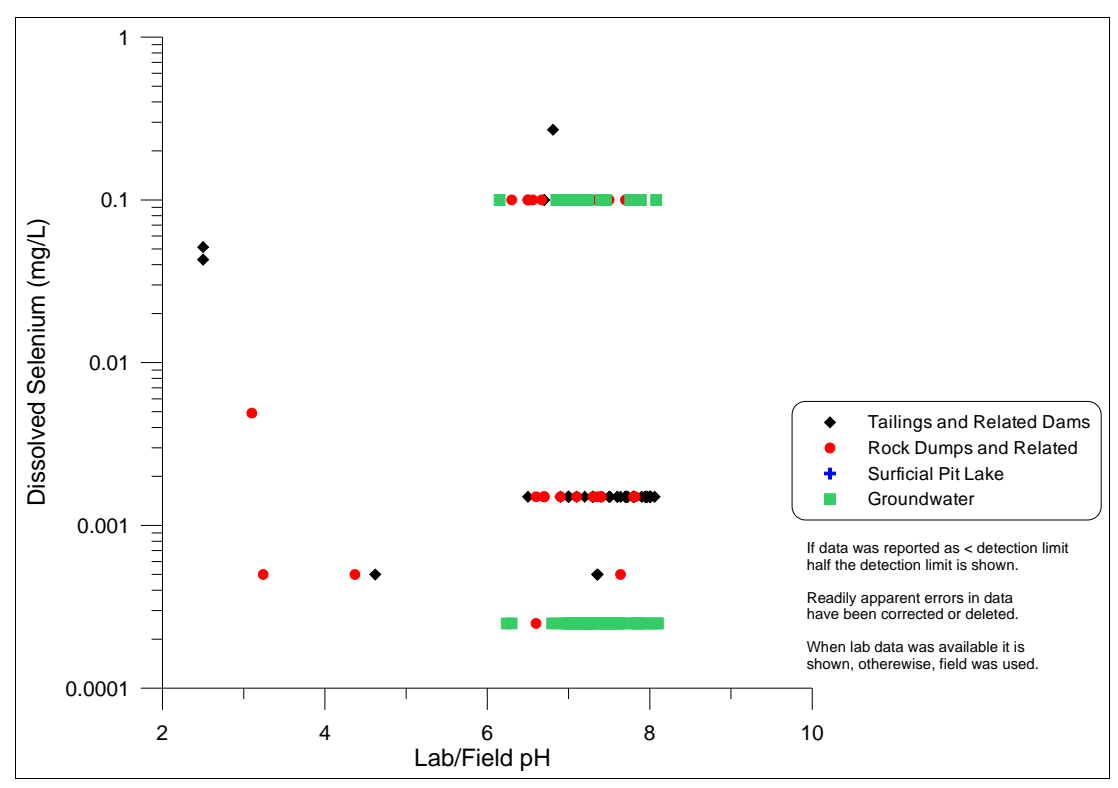


Figure A32-1. Dissolved selenium vs. pH at the Bell Minesite.

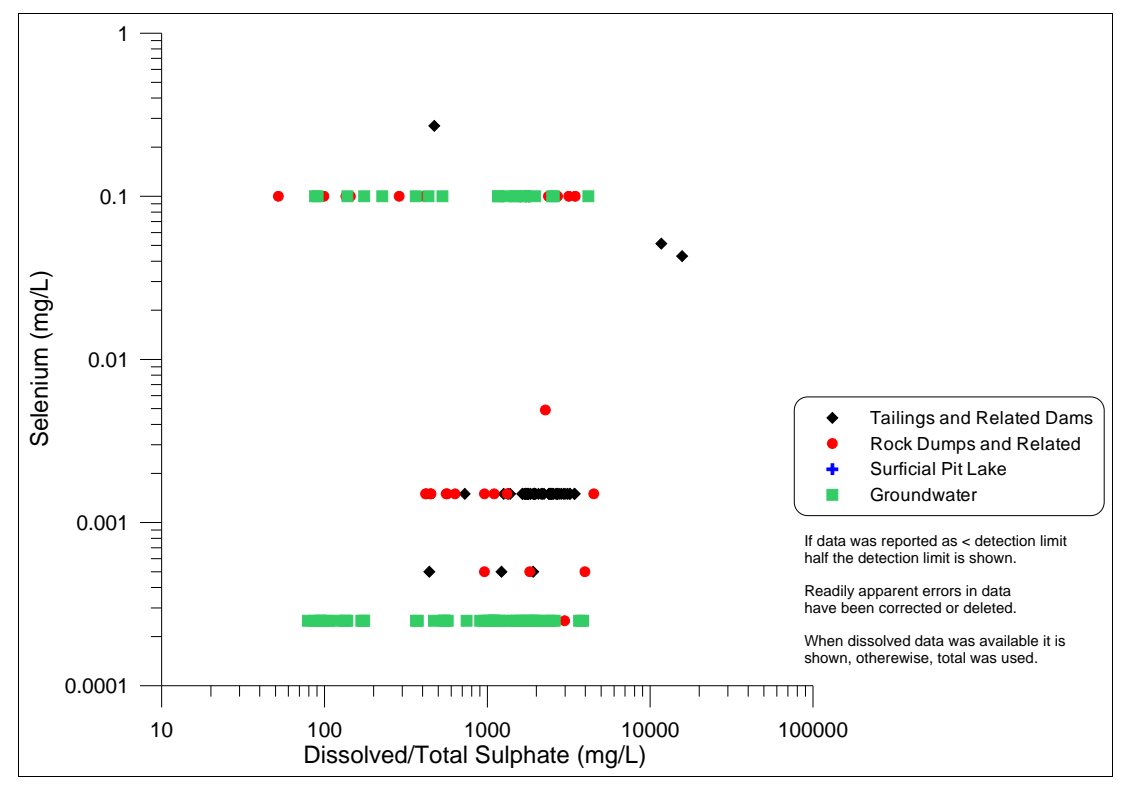


Figure A32-2. Dissolved selenium vs. sulphate at the Bell Minesite.

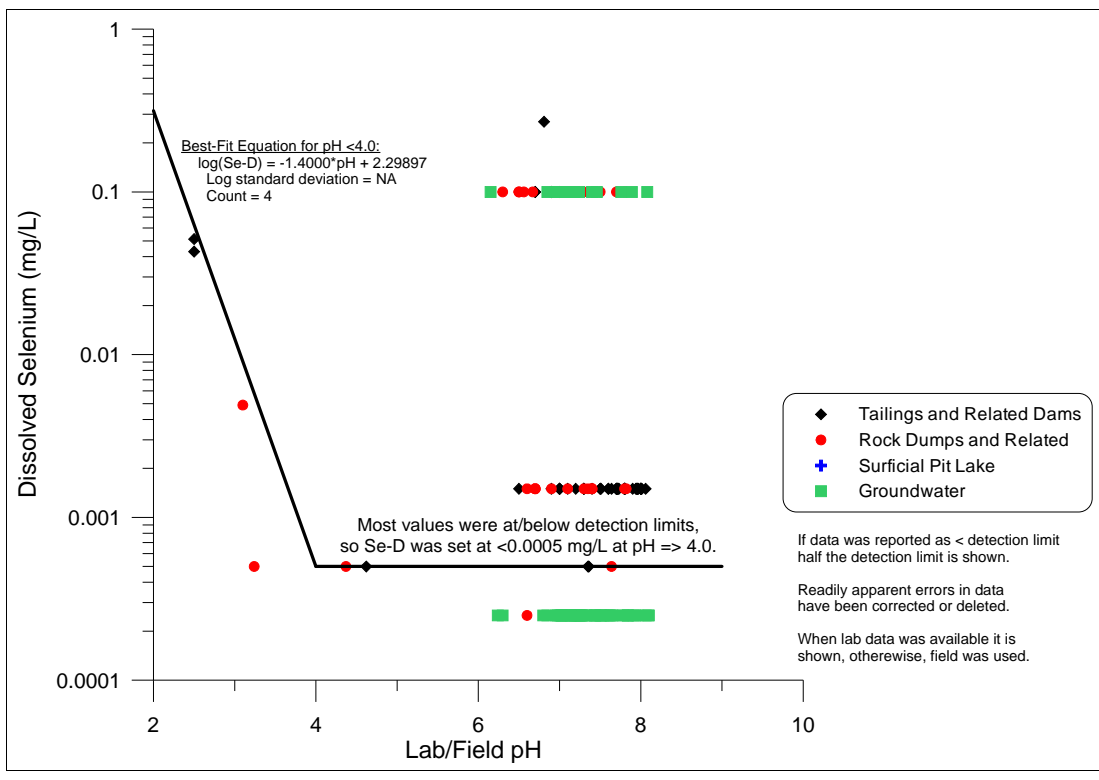


Figure A32-3. Best-fit equations for dissolved selenium vs. pH in the 2010 Bell EDCM.

Appendix A33. Dissolved Silicon (Si-D)

Notes:

Dissolved silicon shows some correlation with pH at acidic values (Figure A33-1) and with sulphate at the few highest sulphate concentrations (Figure A33-2). Lower silicon concentrations are predominantly independent of pH and sulphate.

The best-fit correlation with pH consists of two segments (Figure A33-3), joined at pH 5.0. The acidic segment is based only on 15 datapoints, which may form a lognormal distribution above and below this segment (Figure A33-4). Above pH 5.0, dissolved silicon is nearly independent of pH, with a slope of -0.076, and the 661 datapoints form a general lognormal distribution around this segment (Figure A33-5).

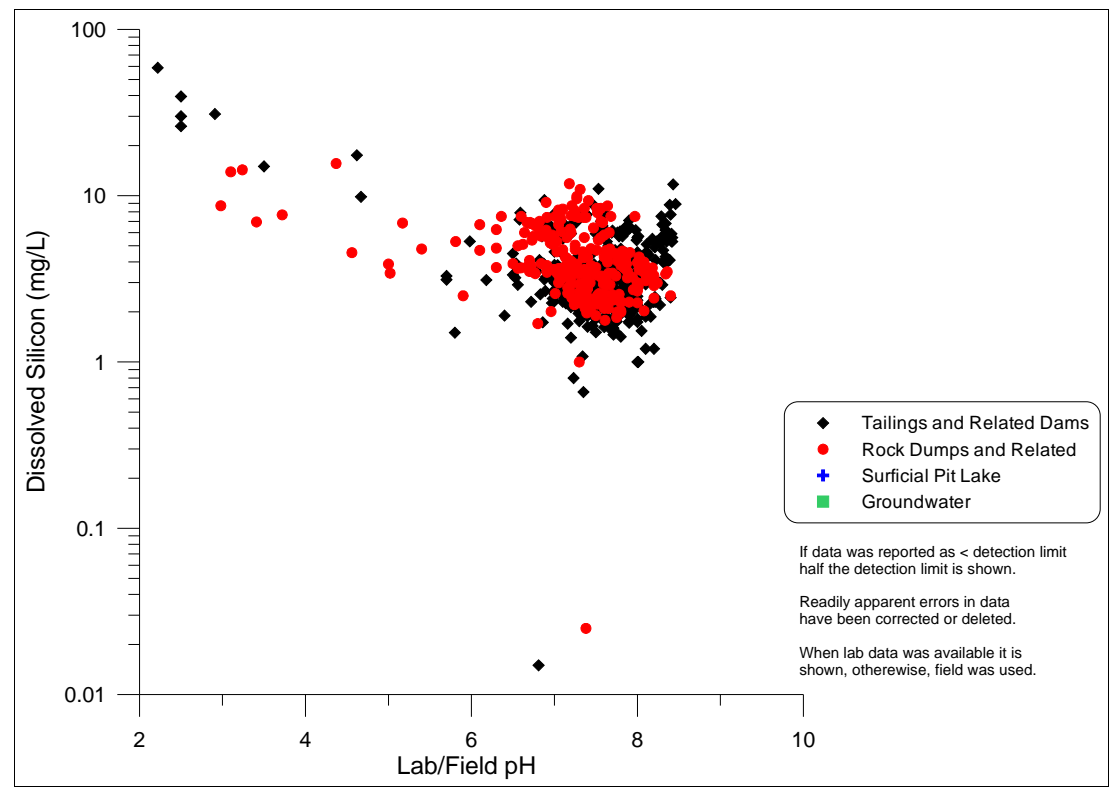


Figure A33-1. Dissolved silicon vs. pH at the Bell Minesite.

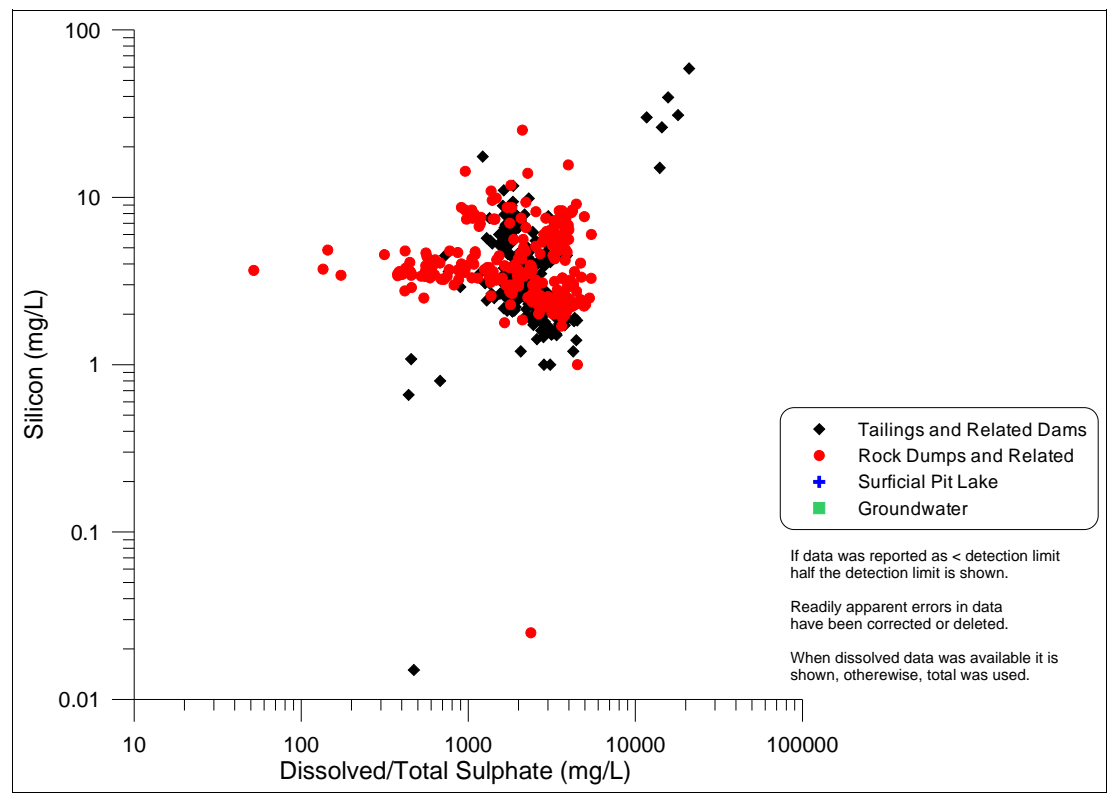


Figure A33-2. Dissolved silicon vs. sulphate at the Bell Minesite.

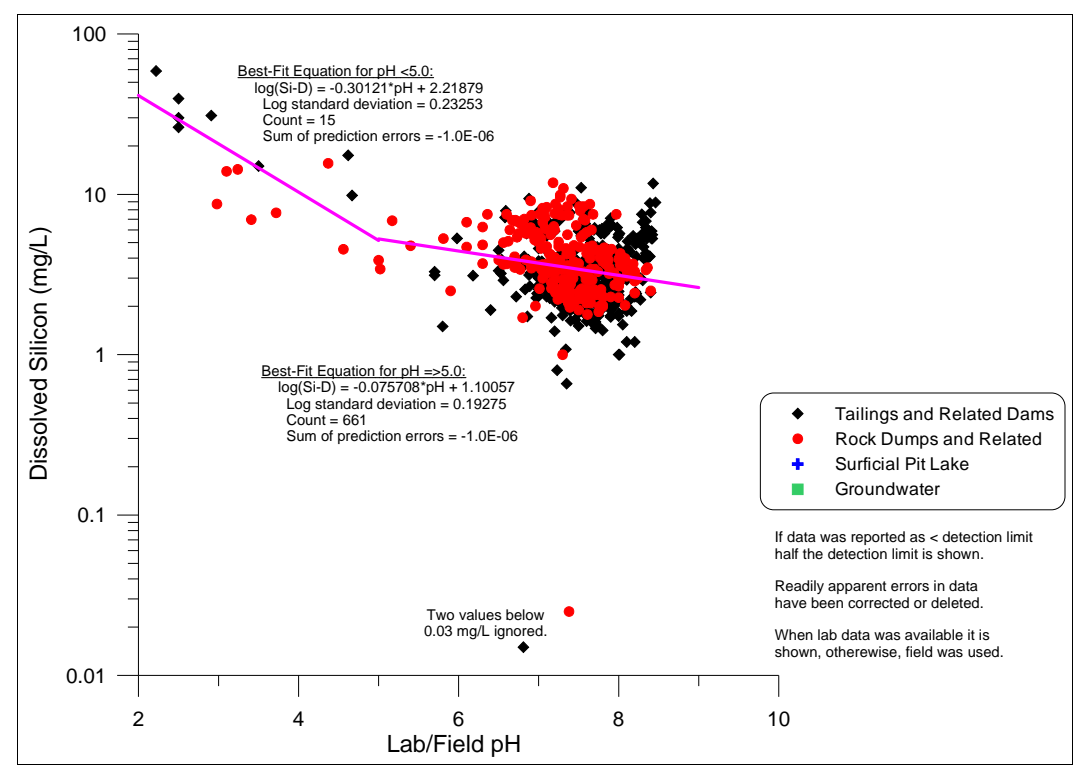


Figure A33-3. Best-fit equations for dissolved silicon vs. pH in the 2010 Bell EDCM.

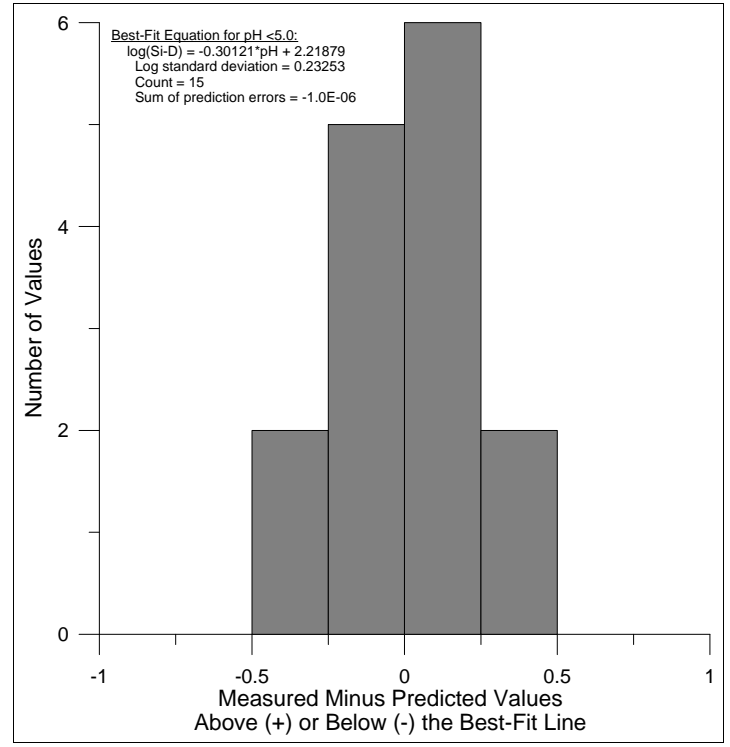


Figure A33-4. Statistical distribution of (measured-calculated) datapoints around the best-fit equation for dissolved silicon below pH 5.0.

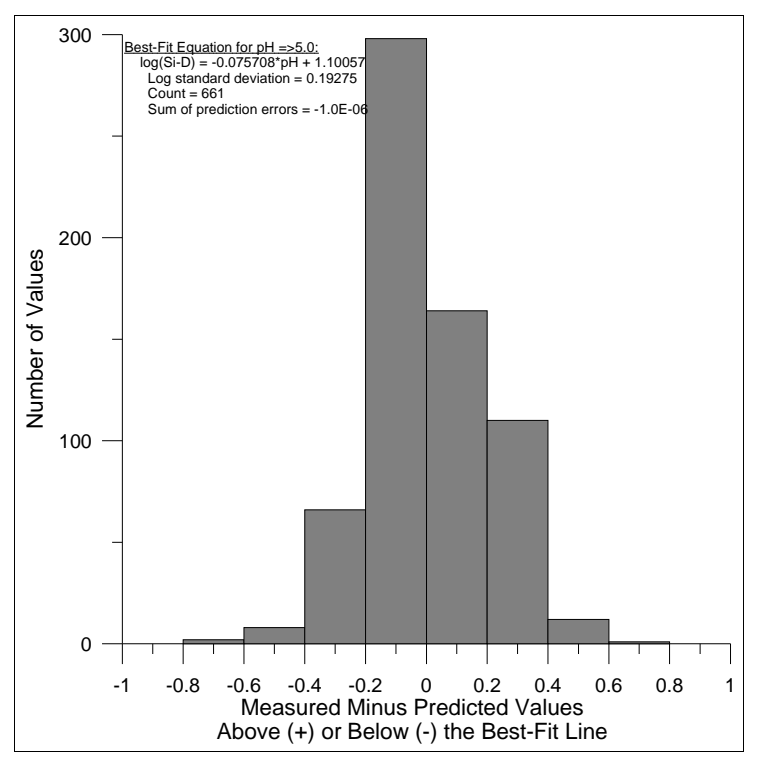


Figure A33-5. Statistical distribution of (measured-calculated) datapoints around the best-fit equation for dissolved silicon above pH 5.0.

Appendix A34. Dissolved Silver (Ag-D)

Notes:

The roughly 800 analyses of dissolved silver in the Bell Minesite database were at or below various detection limits. As a result, no correlations could be seen with pH (Figure 34-1) or sulphate (Figure 34-2). Because of this, dissolved silver is set at less than its lowest detection limit: <0.0001 mg/L (Figure 34-3).

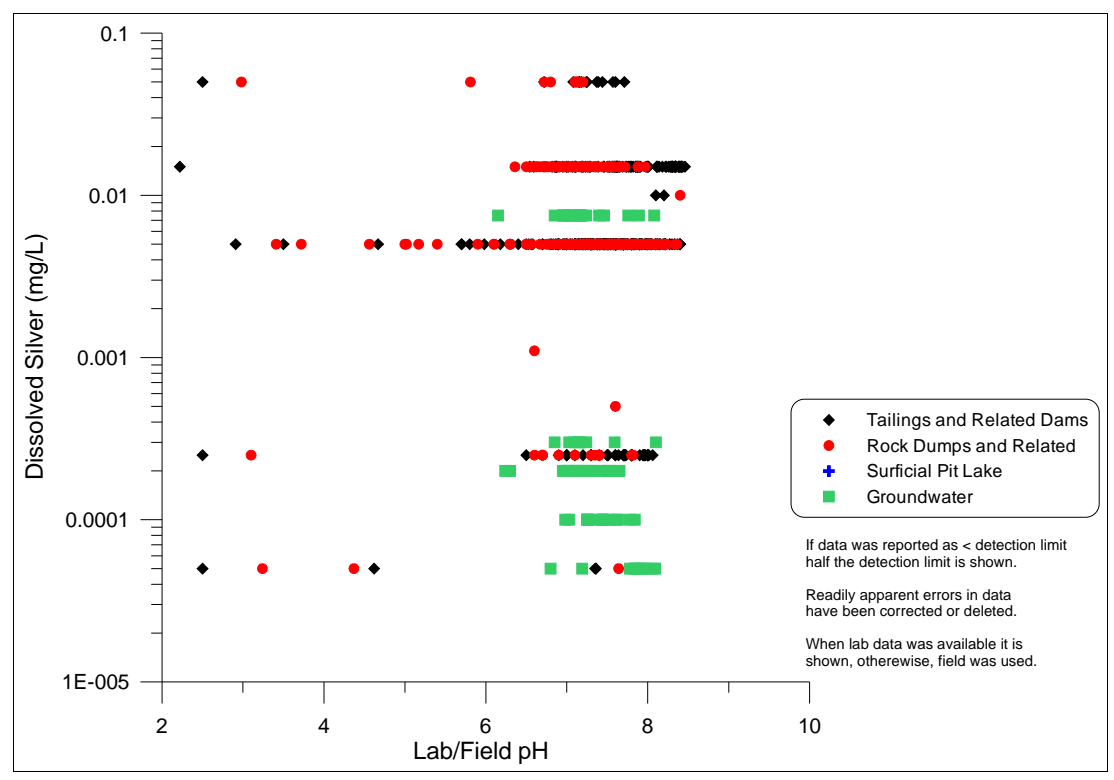


Figure A34-1. Dissolved silver vs. pH at the Bell Minesite.

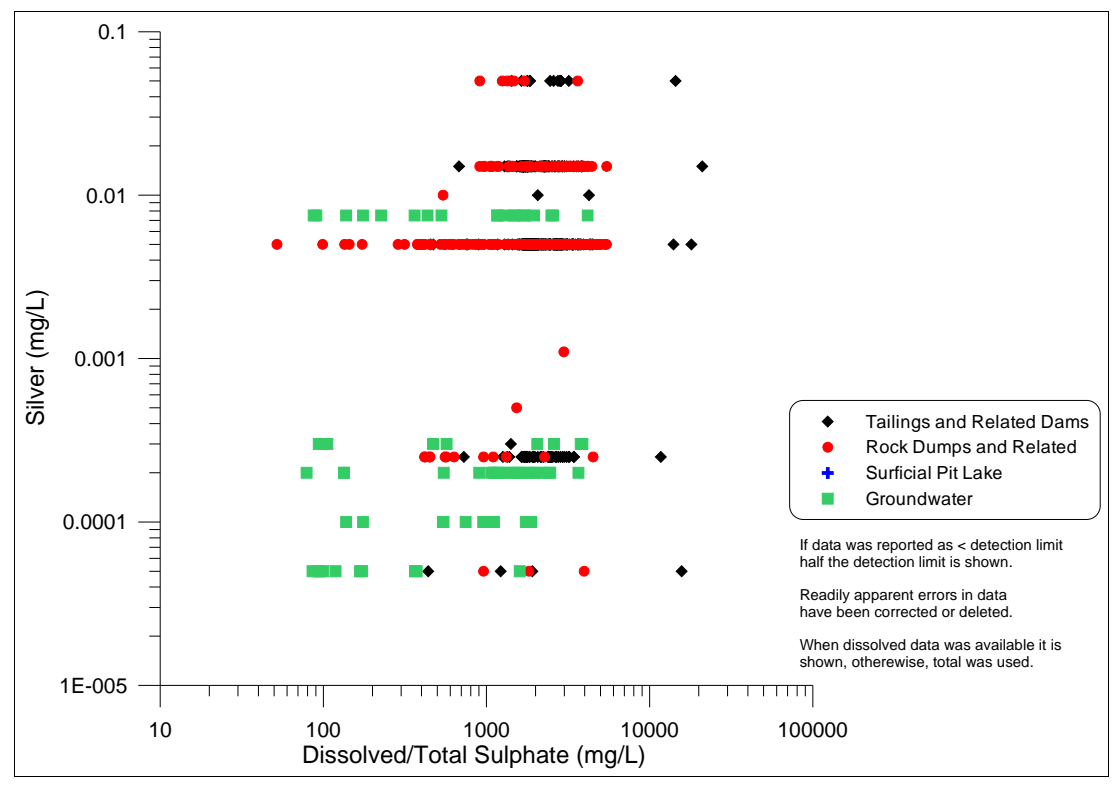


Figure A34-2. Dissolved silver vs. sulphate at the Bell Minesite.

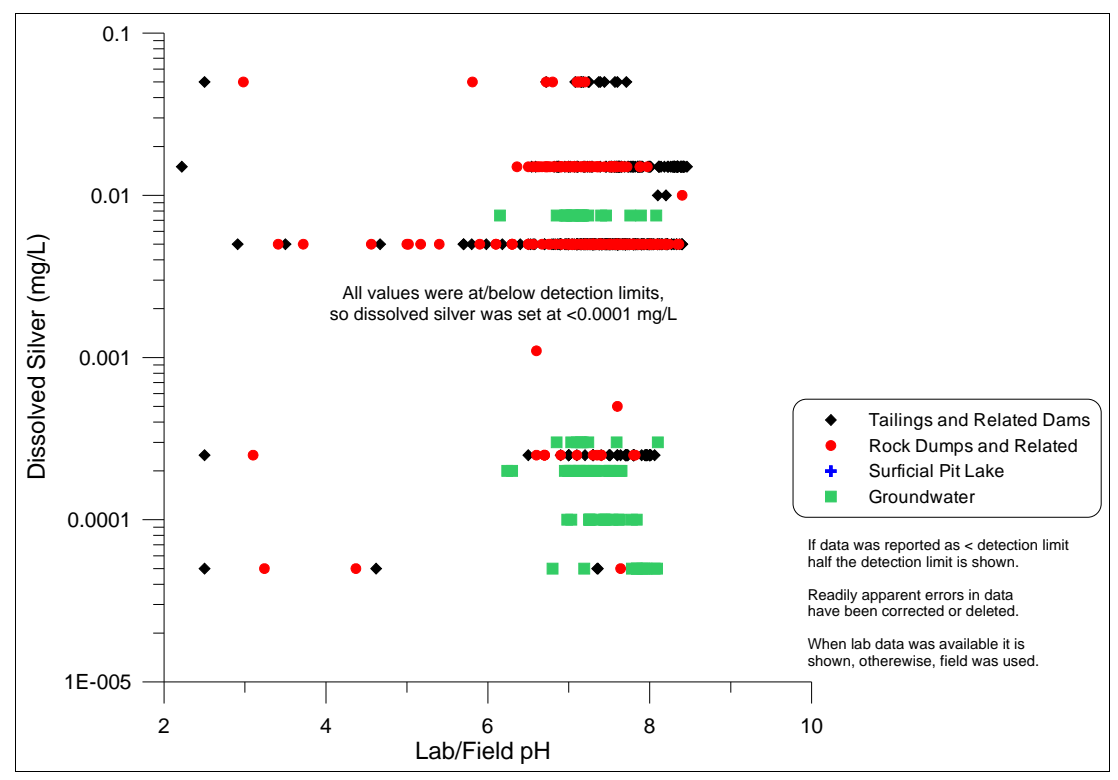


Figure A34-3. Best-fit equation for dissolved silver in the 2010 Bell EDCM.

Appendix A35. Dissolved Sodium (Na-D)

Notes:

The nearly 800 analyses of dissolved sodium in the Bell Minesite database show better correlation with sulphate (Figure A35-2) than with pH (Figure A35-1). However, the correlations with sulphate are location-dependent, so they are separated into one for tailings and associated rock dams (Figure A35-3) and for rock piles and related drainages (Figure A35-5). The hundreds of (measured-calculated) datapoints for each of these location-dependent correlations form general lognormal distributions (Figures A35-4 and A35-6), with standard deviations of 0.17-0.19 log cycles.

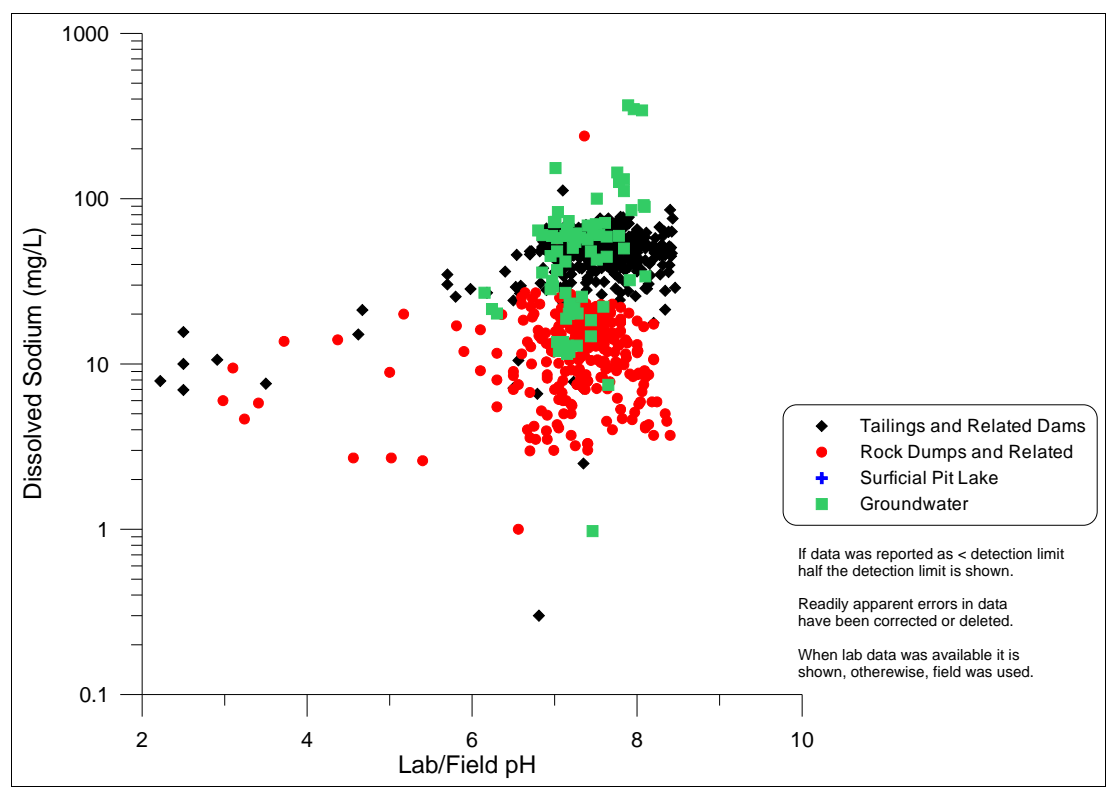


Figure A35-1. Dissolved sodium vs. pH at the Bell Minesite.

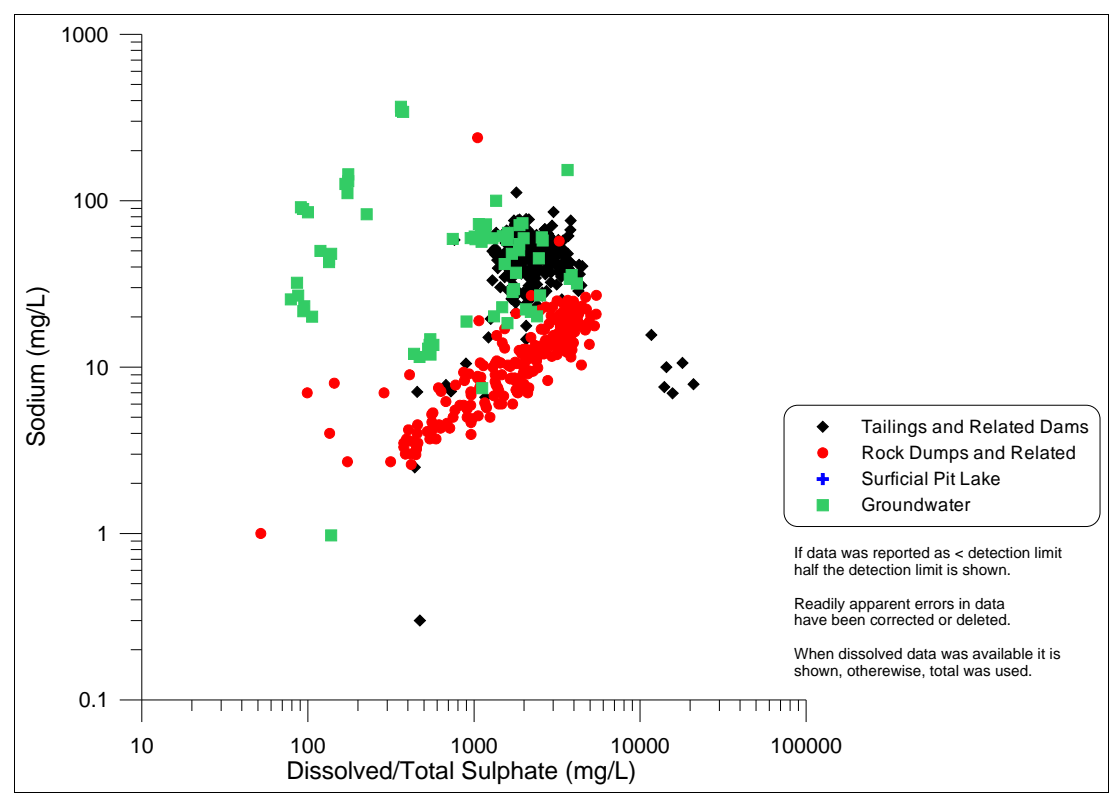


Figure A35-2. Dissolved sodium vs. sulphate at the Bell Minesite.

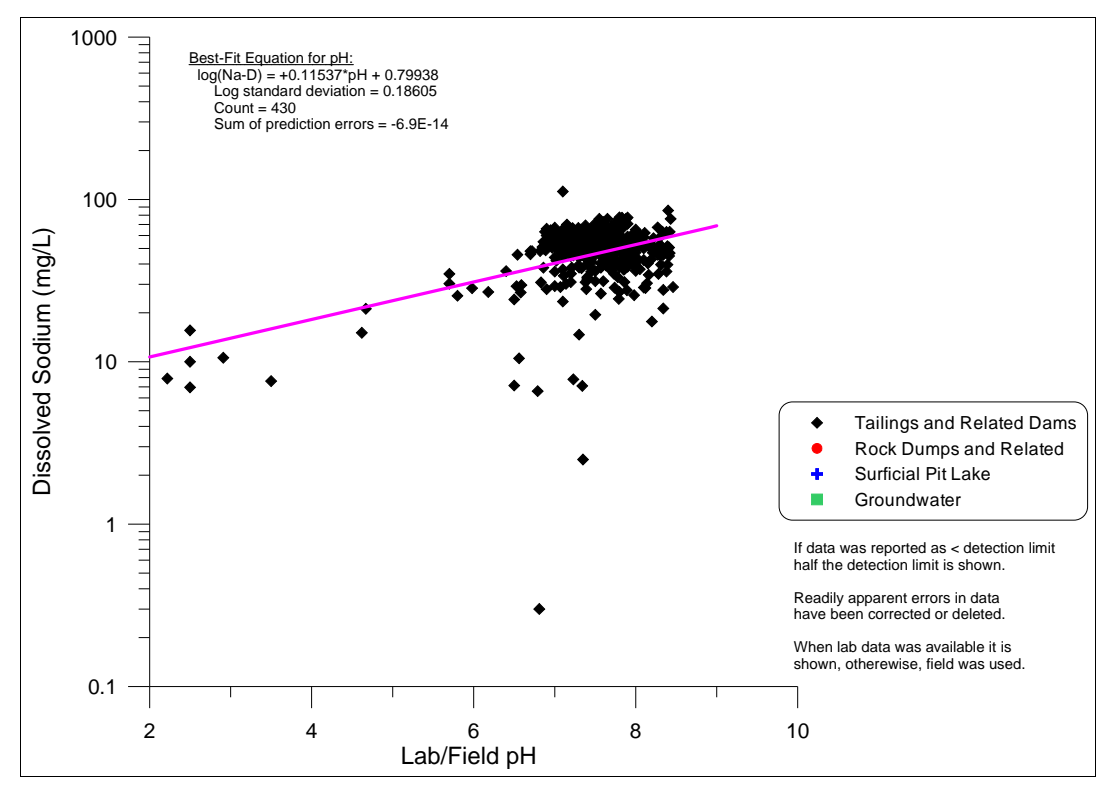


Figure A35-3. Best-fit equations for dissolved sodium vs. pH from tailings and related dams in the 2010 Bell EDCM.

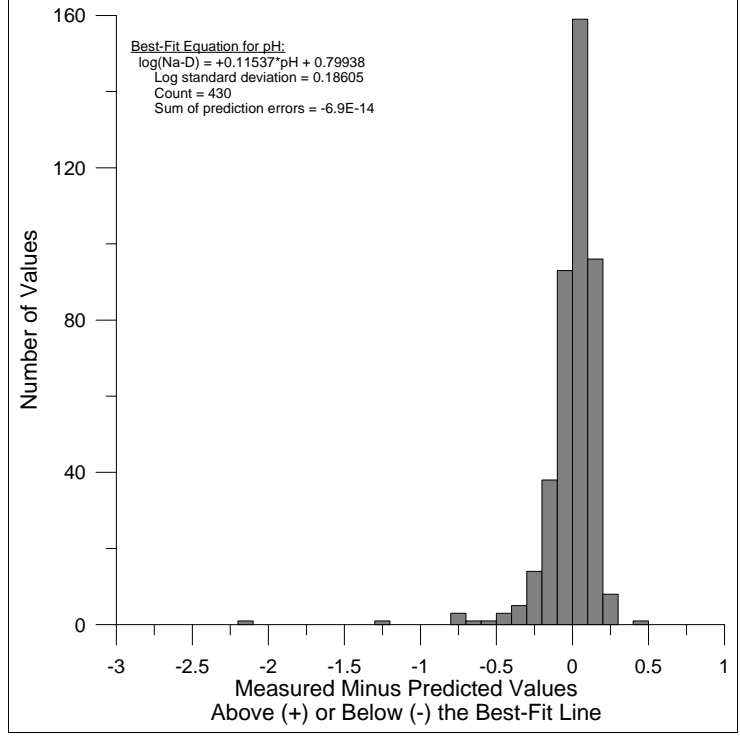


Figure A35-4. Statistical distribution of (measured-calculated) datapoints around the best-fit equation for dissolved sodium from tailings and related dams.

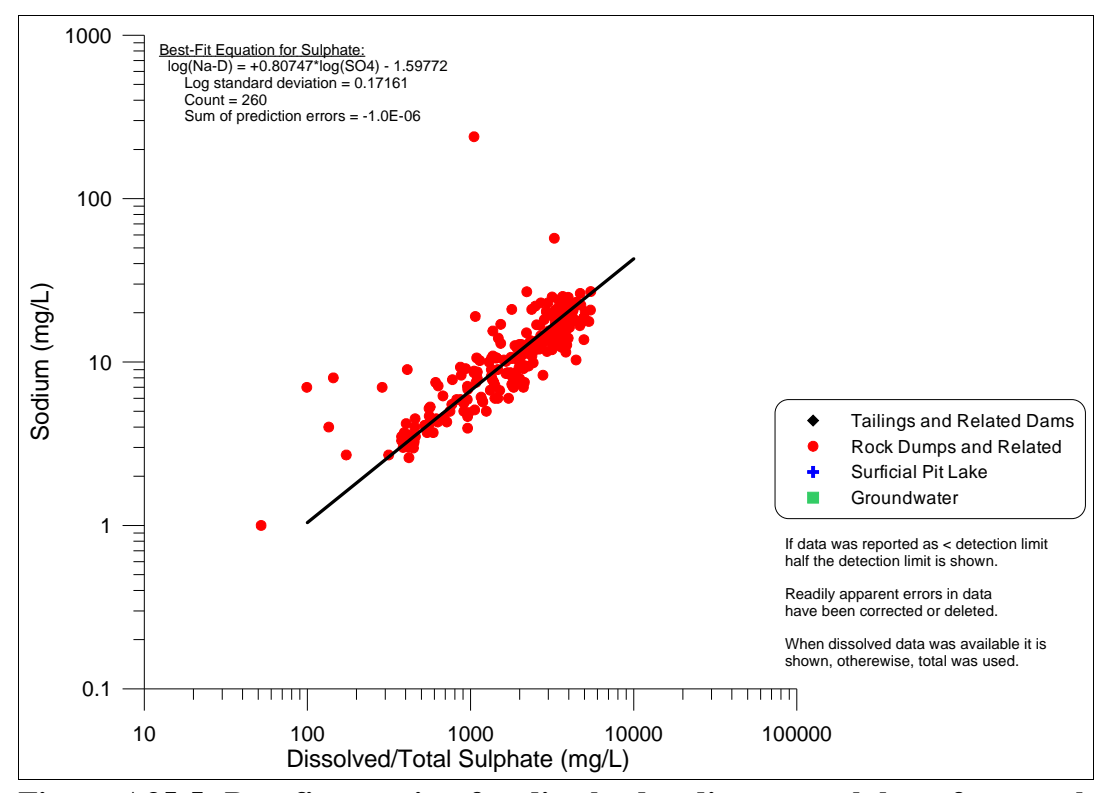


Figure A35-5. Best-fit equation for dissolved sodium vs. sulphate from rock dumps and related drainages in the 2010 Bell EDCM.

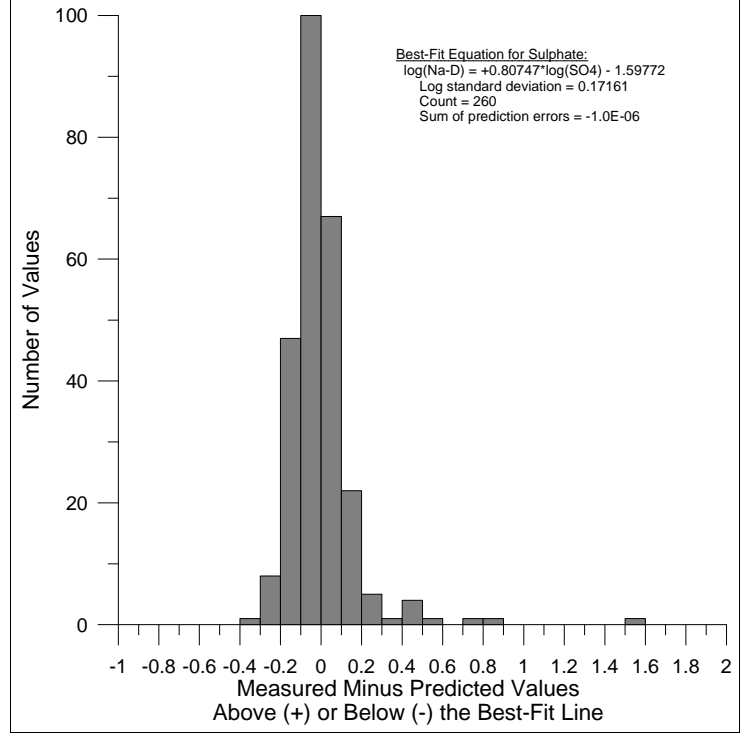


Figure A35-6. Statistical distribution of (measured-calculated) datapoints around the best-fit equation for dissolved sodium from rock dumps and related drainages.

Appendix A36. Dissolved Strontium (Sr-D)

Notes:

Dissolved strontium does not correlate well with the master parameter of pH (Figure A36-1), but correlates with sulphate (Figure A36-2). With sulphate (Figure A36-3), best-fit lines can be developed separately for tailings and surrounding rock dams and for rock piles and related drainages, with the rock-pile best-fit line composed of two segments.

The best-fit equation for tailings and its dams has a relatively steep slope above +2.0 (Figure A36-3). The hundreds of (measured-calculated) datapoints form a general lognormal distribution above and below this equation (Figure A36-4), with a standard deviation of 0.17029 log cycles.

The best-fit equation for rock piles and related drainages has two segments (Figure A36-3), joined at 1700 mg/L of sulphate. The datapoints around these two segments form general lognormal distributions (Figures A36-5 and A36-6).

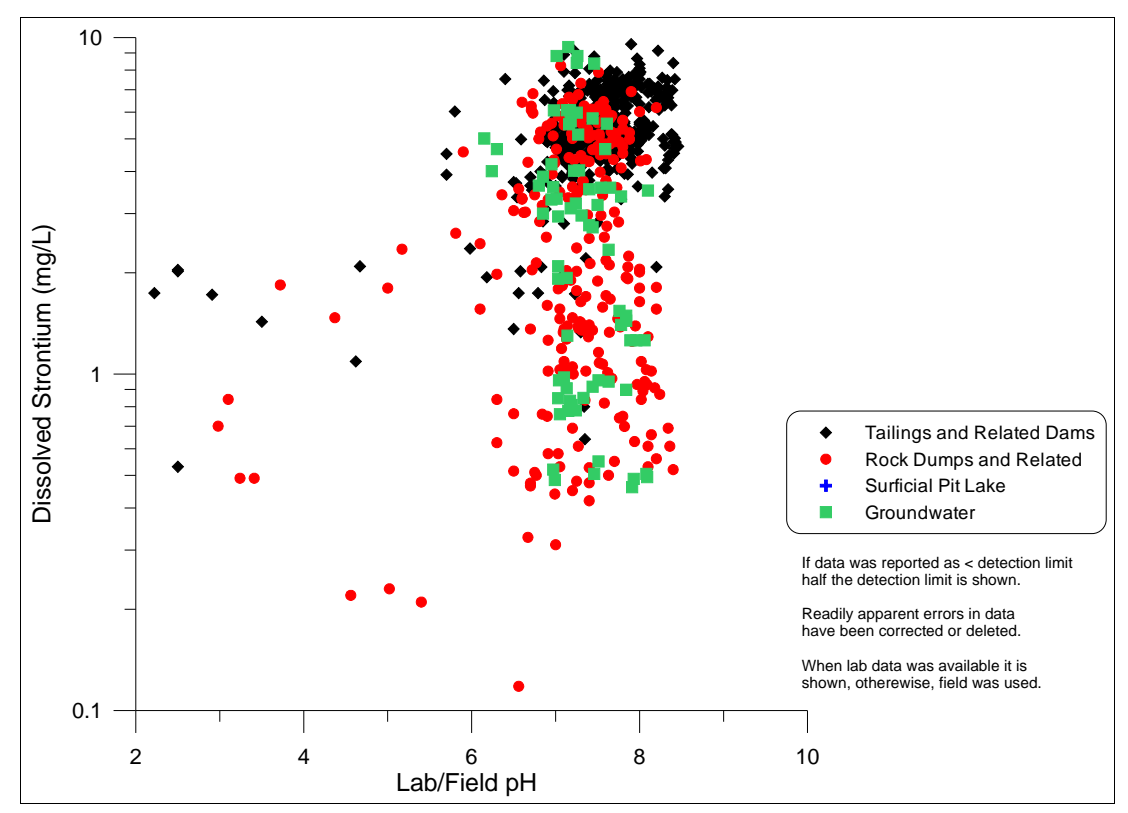


Figure A36-1. Dissolved strontium vs. pH at the Bell Minesite.

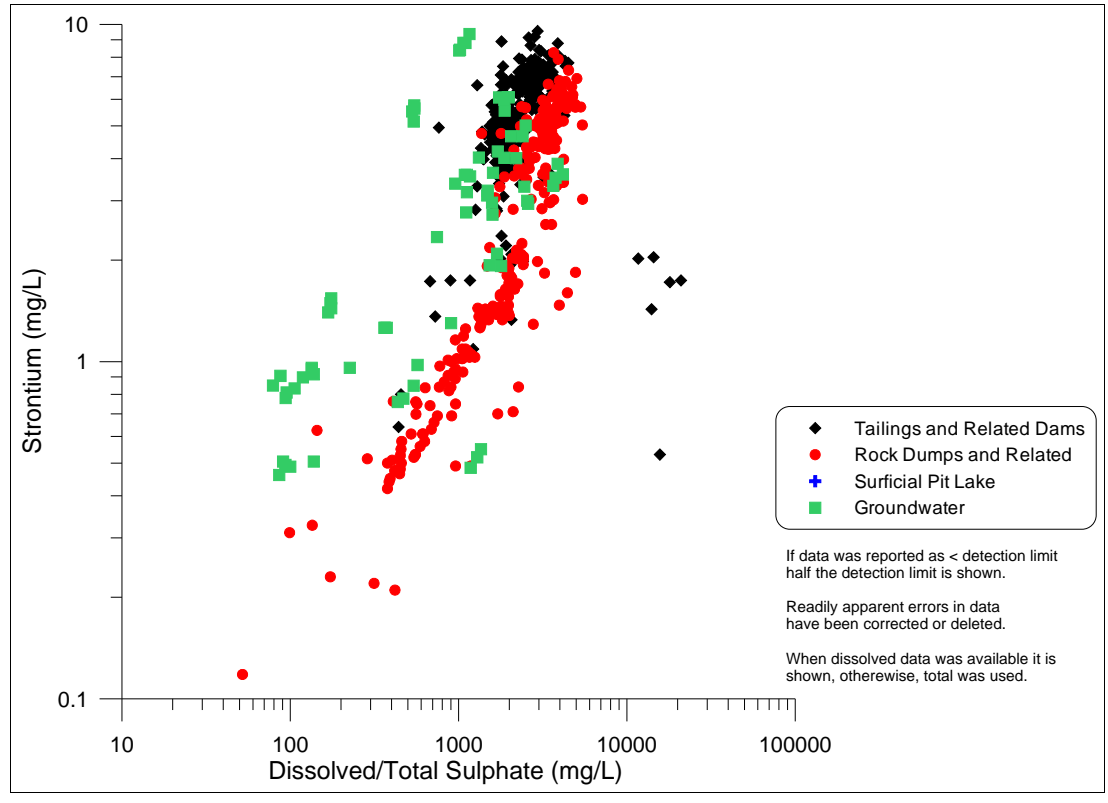


Figure A36-2. Dissolved strontium vs. sulphate at the Bell Minesite.

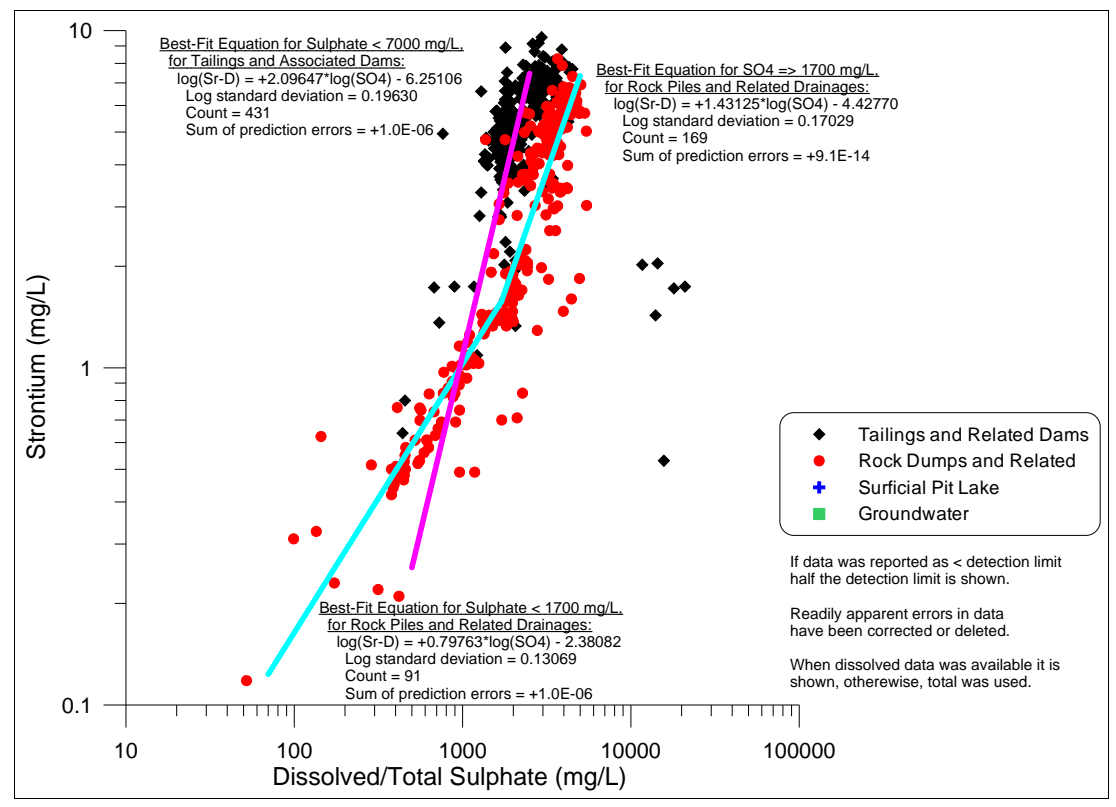


Figure A36-3. Best-fit equations for dissolved strontium vs. sulphate in the 2010 Bell EDCM.

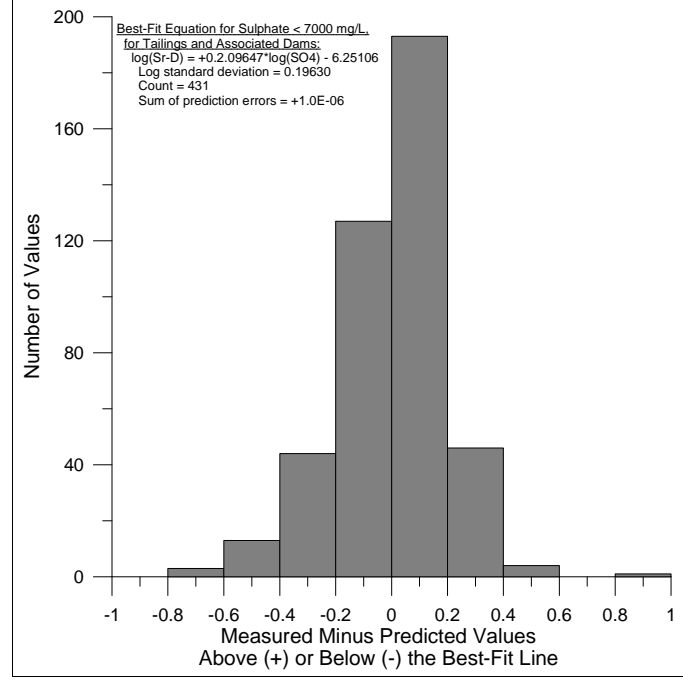


Figure A36-4. Statistical distribution of (measured-calculated) datapoints around the best-fit equation for dissolved strontium from tailings and related dams.

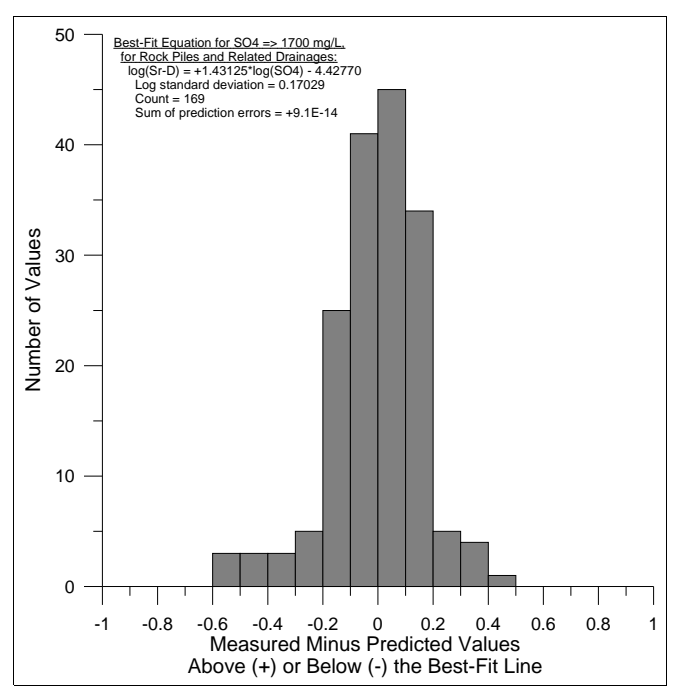


Figure A36-5. Statistical distribution of (measured-calculated) datapoints around the best-fit equation for dissolved strontium from rock piles and related drainages above 1700 mg/L sulphate.

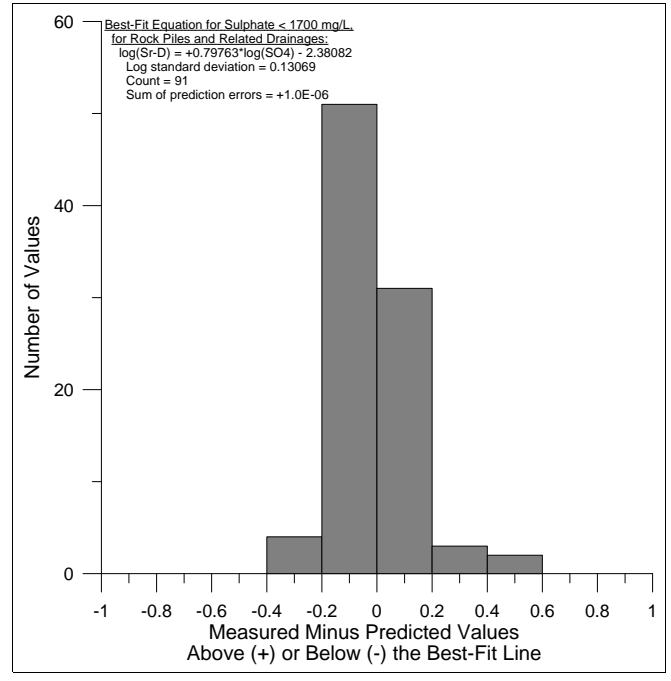


Figure A36-7. Statistical distribution of (measured-calculated) datapoints around the best-fit equation for dissolved strontium from rock piles and related drainages below 1700 mg/L sulphate.

Appendix A37. Dissolved Tellurium (Te-D)

Notes:

All but one of the 68 analyses of dissolved tellurium have been below various detection limits. As a result, there are no apparent correlations with pH (Figure A37-1) or sulphate (Figure A37-2). Thus, dissolved tellurium was set at <0.001 mg/L (Figure A37-3), although it may sometimes be higher at acidic pH.

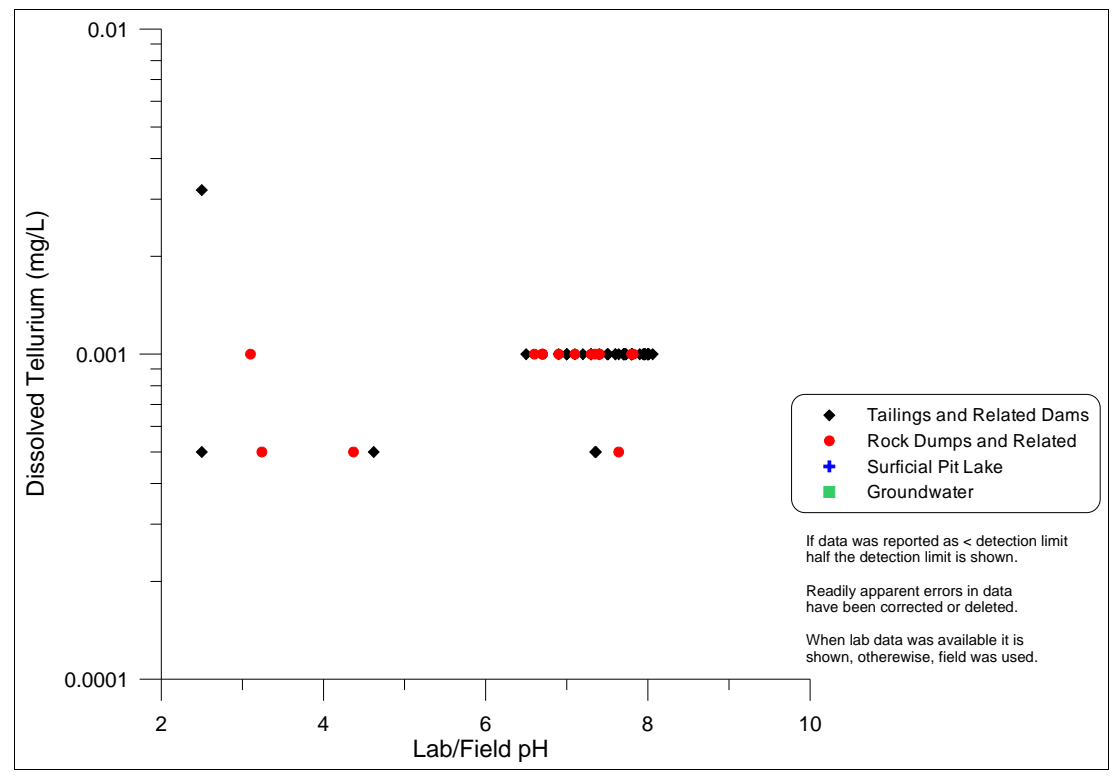


Figure A37-1. Dissolved tellurium vs. pH at the Bell Minesite.

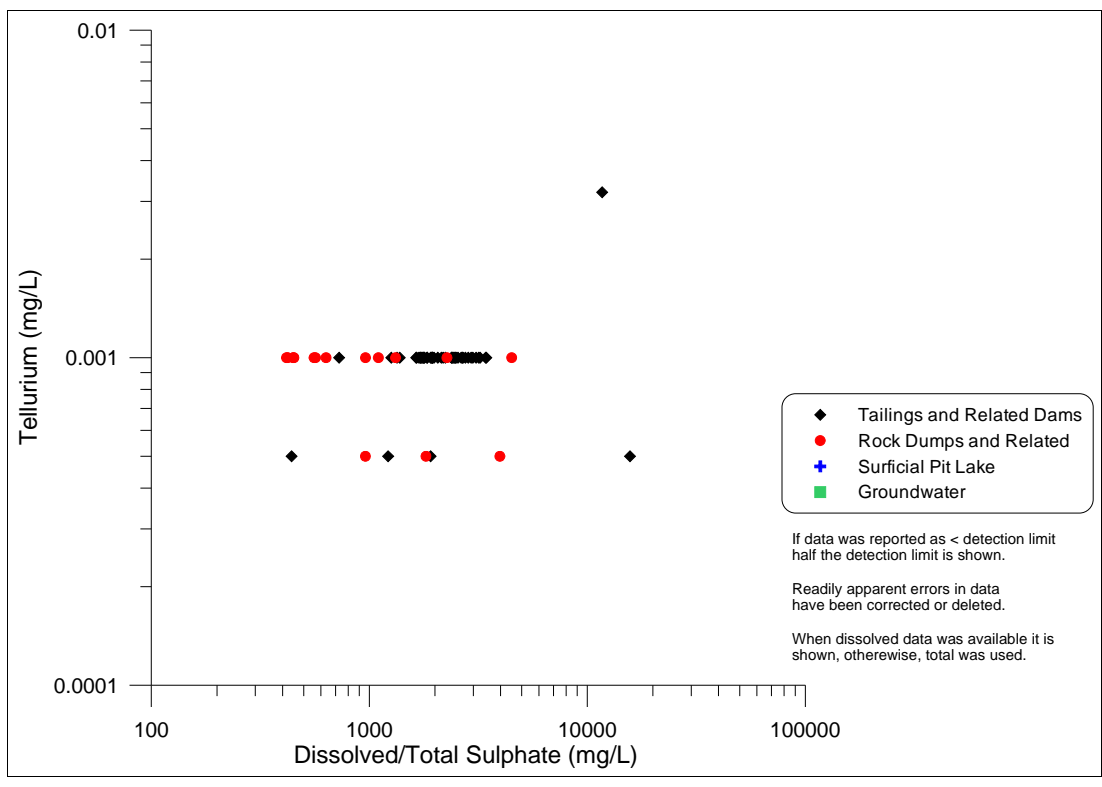


Figure A37-2. Dissolved tellurium vs. sulphate at the Bell Minesite.

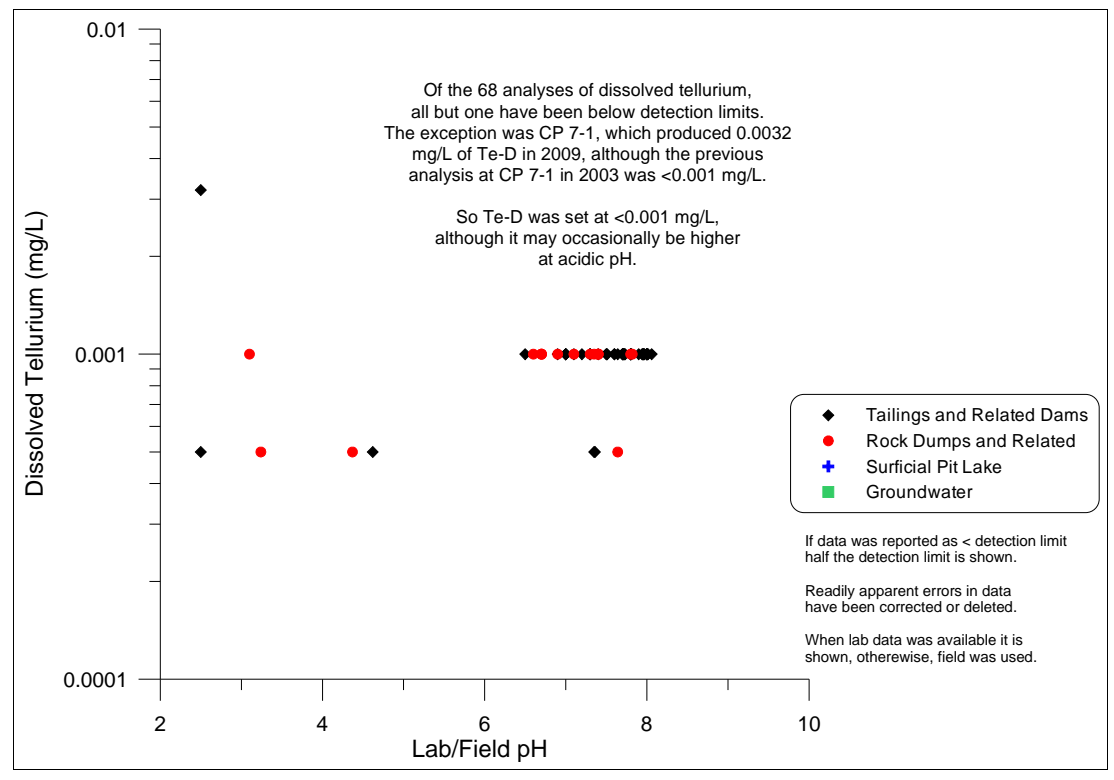


Figure A37-3. Best-fit equation for dissolved tellurium in the 2010 Bell EDCM.

Appendix A38. Dissolved Thallium (Tl-D)

Notes:

Most analyses of dissolved thallium have been below various detection limits, so correlations could not be seen with the master parameters of pH (Figure A38-1) and sulphate (Figure A38-2). The detectable concentrations, above an earlier detection limit of 0.01 mg/L, were reported around closure in 1992 and primarily in groundwater (Figure A38-3). So dissolved thallium is set at <0.0001 mg/L, recognizing it may have been higher in the past in groundwaters.

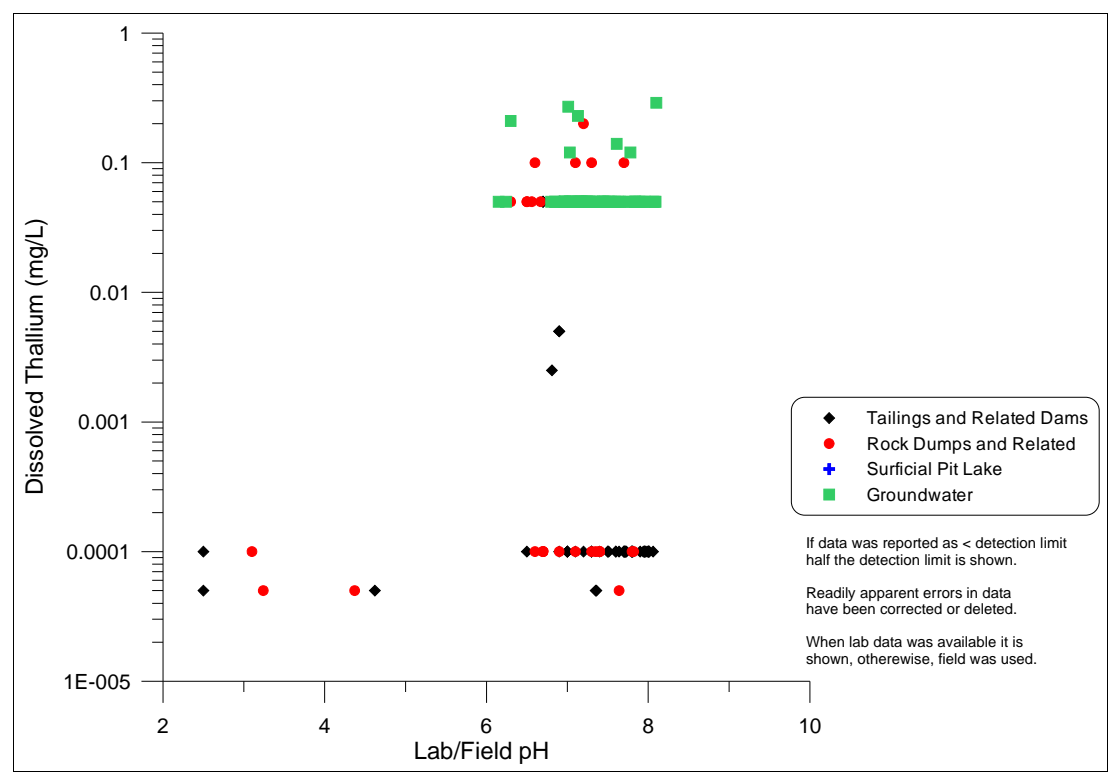


Figure A38-1. Dissolved thallium vs. pH at the Bell Minesite.

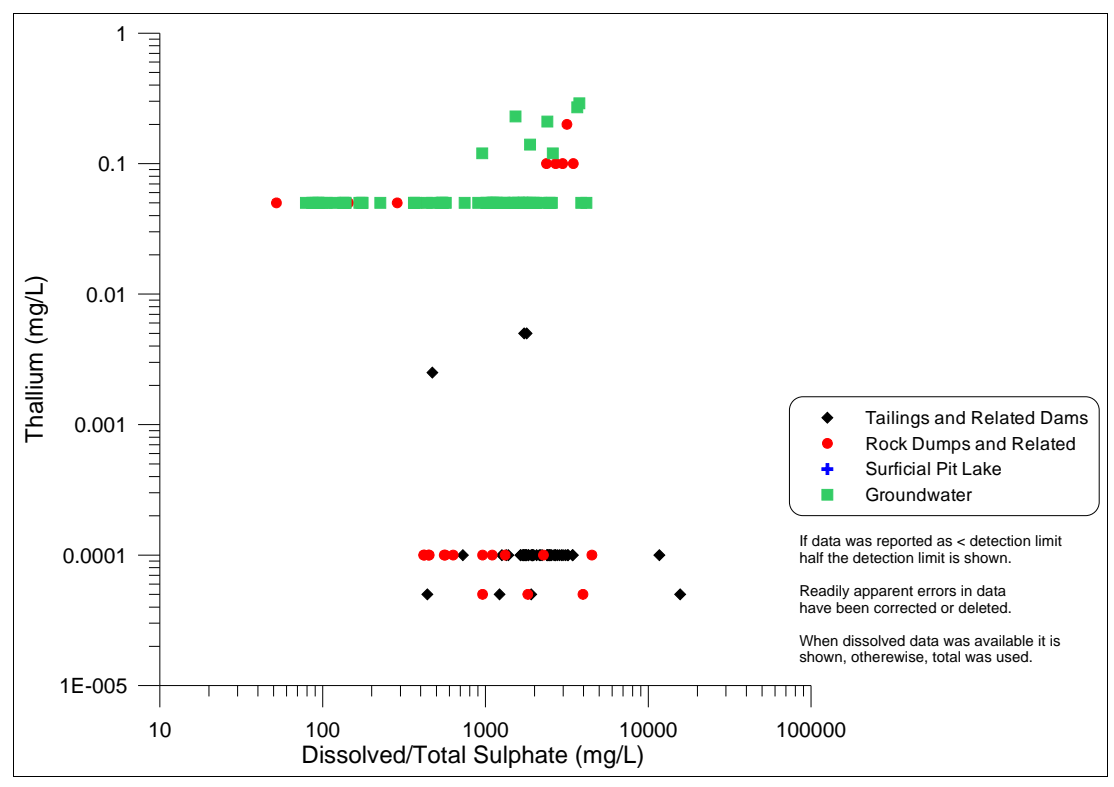


Figure A38-2. Dissolved thallium vs. sulphate at the Bell Minesite.

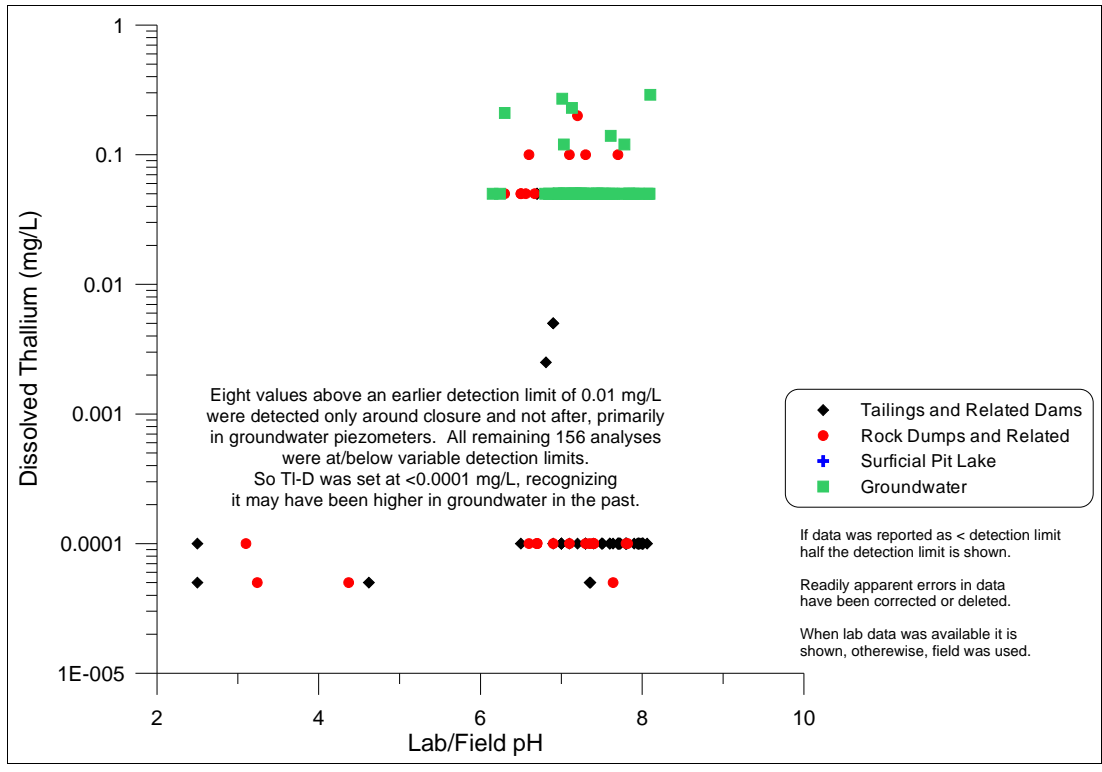


Figure A38-3. Best-fit equation for dissolved thallium in the 2010 Bell EDCM.

Appendix A39. Dissolved Thorium (Th-D)

Notes:

Of the 62 analyses of dissolved thorium in the Bell Minesite database, all but three were below detection. Thus, there was little correlation with pH except the three values at acidic pH (Figure A39-1), and little correlation with sulphate except at the highest sulphate levels (Figure A39-2). Based on the three detectable analyses at acidic pH below pH 3.5 (Figure A39-3), an approximate best-fit equation was given a slope of -2.0. Above pH 3.5, dissolved thorium was set at <0.0005 mg/L.

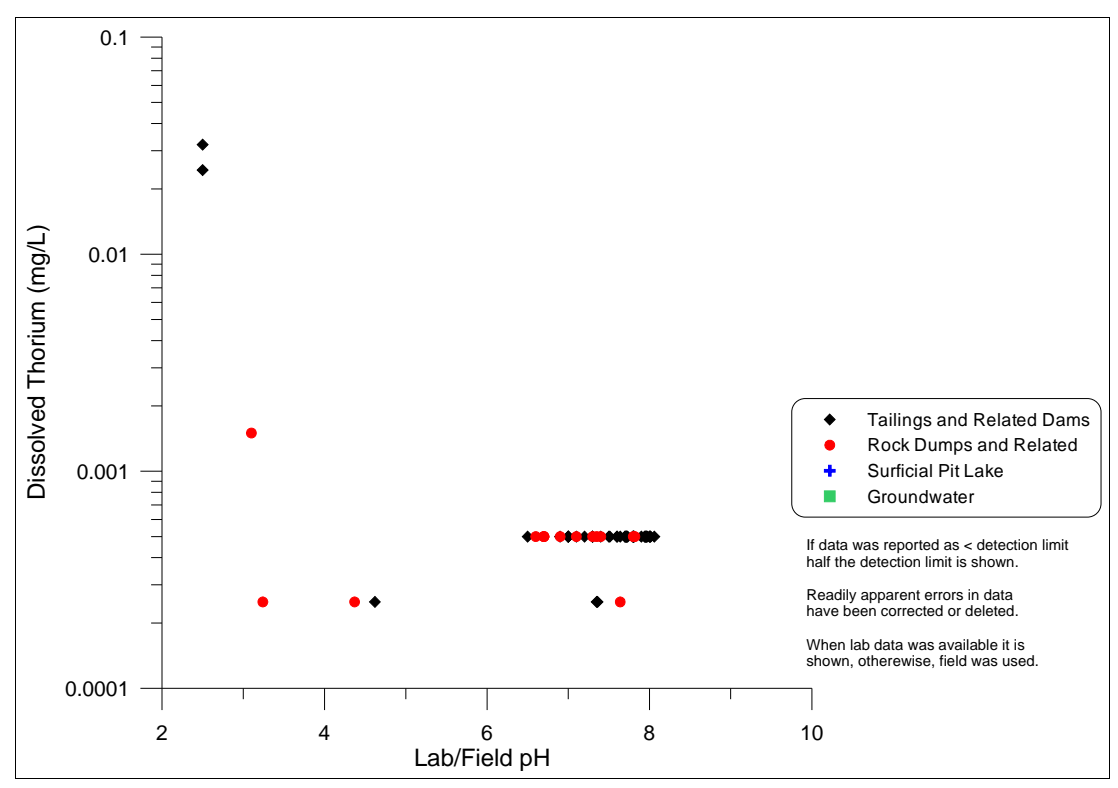


Figure A39-1. Dissolved thorium vs. pH at the Bell Minesite.

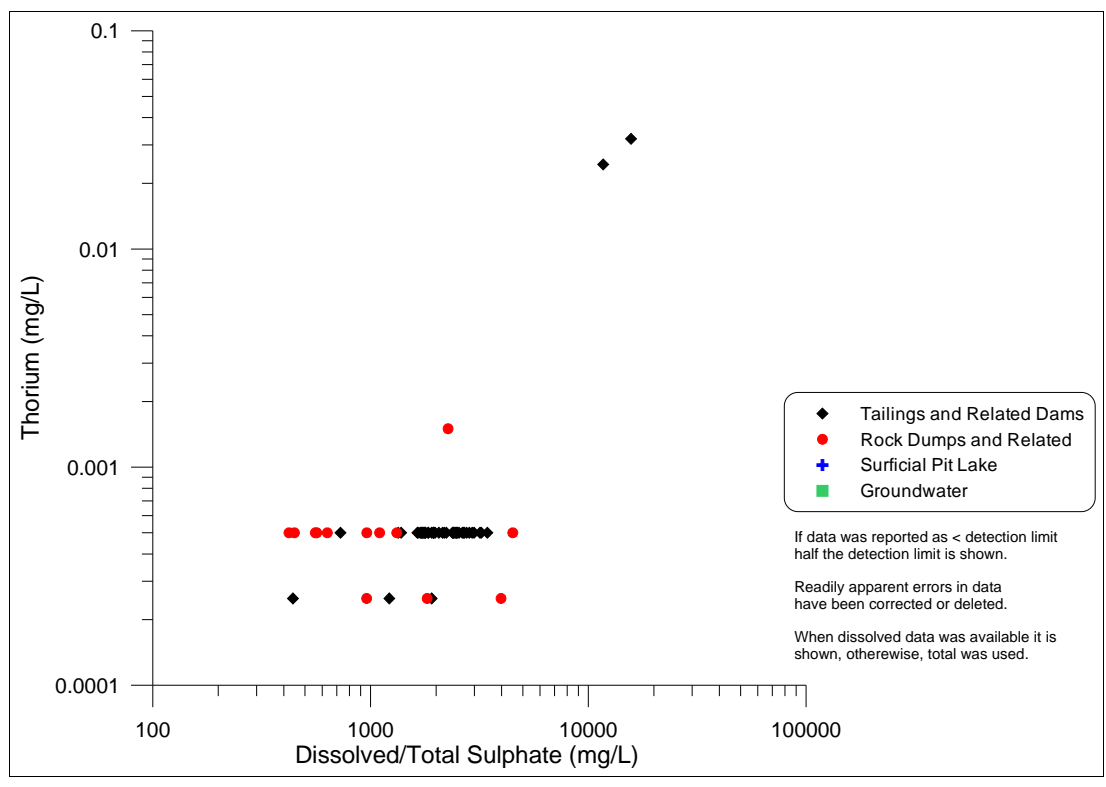


Figure A39-2. Dissolved thorium vs. sulphate at the Bell Minesite.

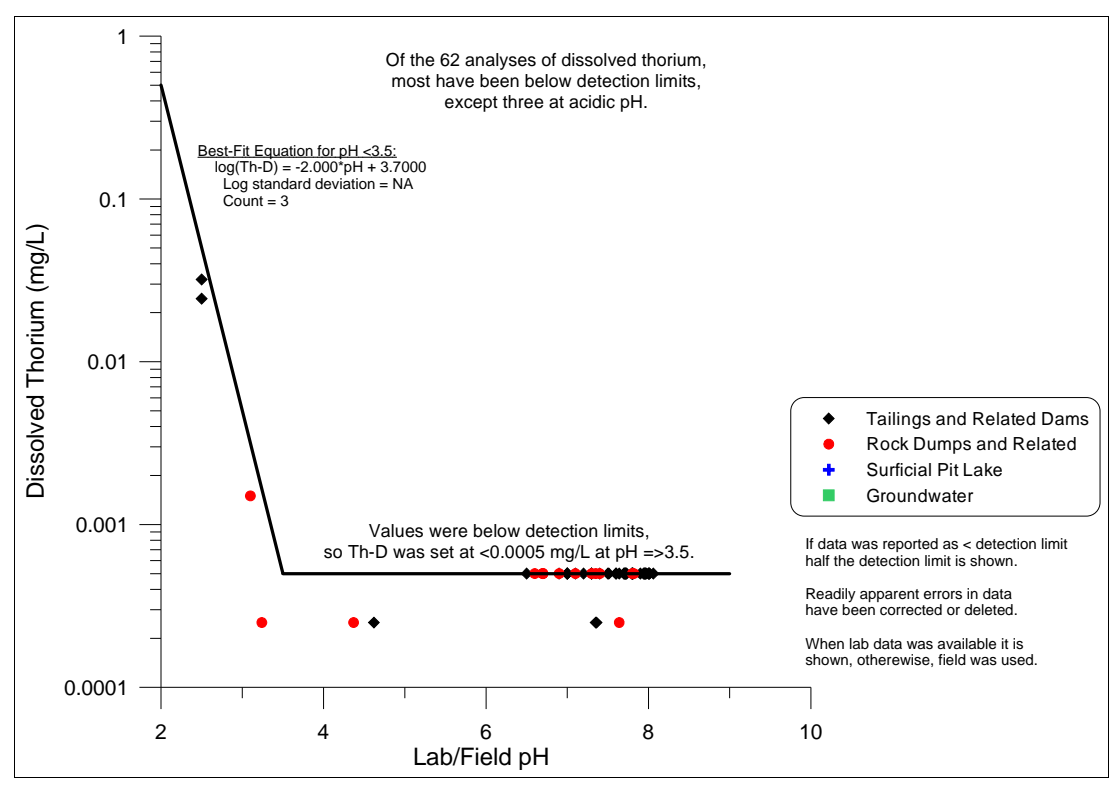


Figure A39-3. Best-fit equations for dissolved thorium vs. pH in the 2010 Bell EDCM.

Appendix A40. Dissolved Tin (Sn-D)

Notes:

Most of the nearly 800 analyses of dissolved tin in the Bell Minesite database are at or below various detection limits that generally decreased through time. As a result, no correlations can be seen with the master parameters of pH (Figure A40-1) and sulphate (Figure A40-2). So dissolved tin was set below its lowest detection limit: <0.001 mg/L (Figure A40-3).

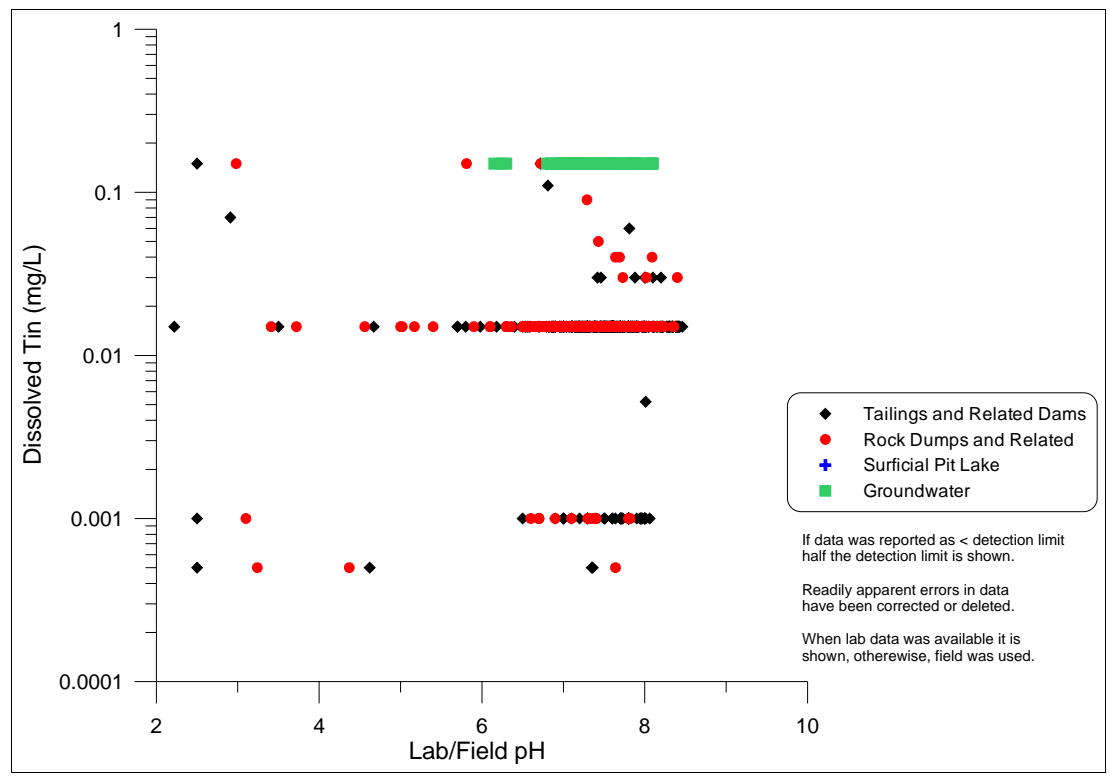


Figure A40-1. Dissolved tin vs. pH at the Bell Minesite.

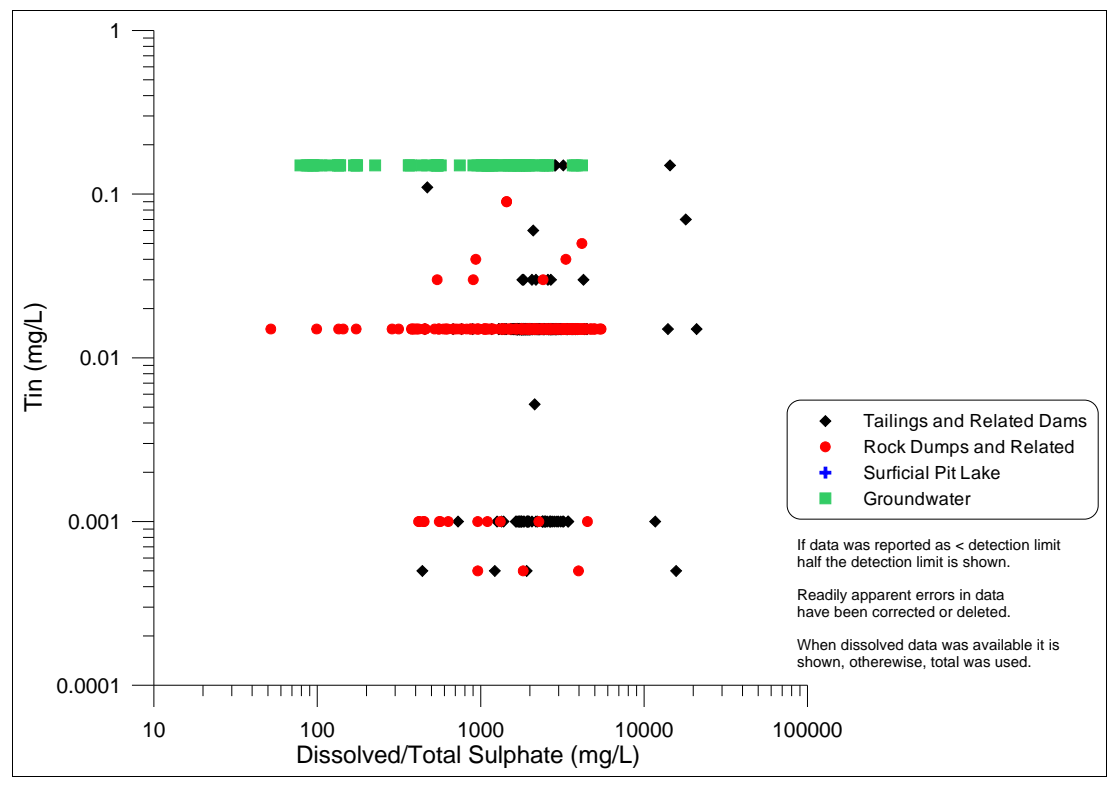


Figure A40-2. Dissolved tin vs. sulphate at the Bell Minesite.

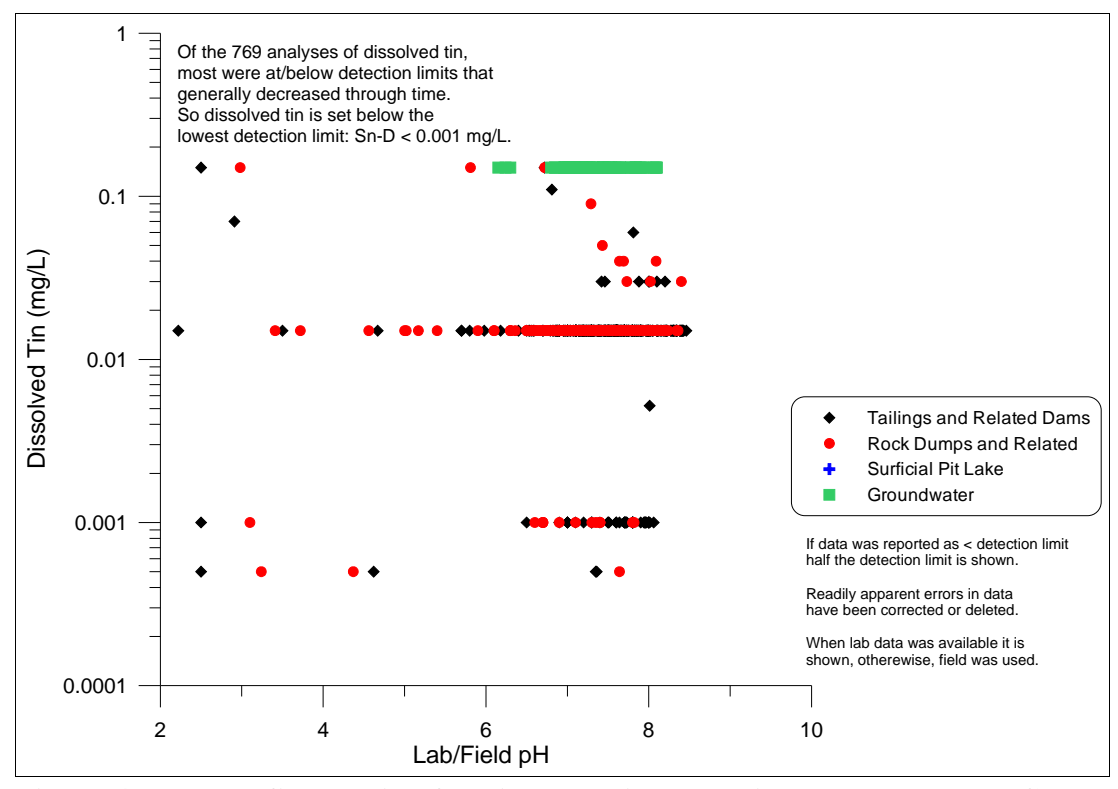


Figure 40-3. Best-fit equation for dissolved tin vs. pH in the 2010 Bell EDCM.

Appendix A41. Dissolved Titanium (Ti-D)

Notes:

Of the nearly 800 analyses for dissolved titanium in the Bell Minesite database, most were at or below various detection limits, particularly below 0.004 mg/L after 2001. As a result, only a few detectable datapoints correlate with pH (Figure A41-1) and sulphate (Figure A41-2).

Excluding the many hundreds of datapoints at or below detection, maximum dissolved titanium correlates with pH at a slope of -0.14162 (Figure A41-3). The (measured-calculated) datapoints above and below this equation generally form a lognormal distribution (Figure A41-4).

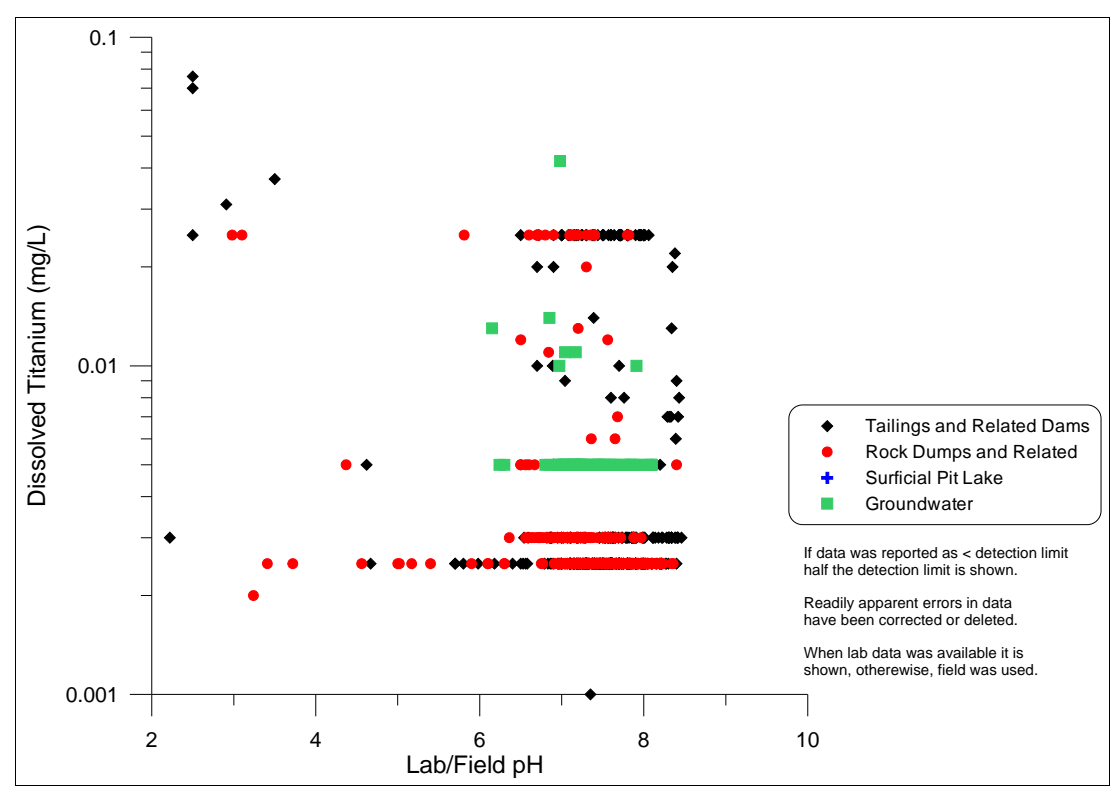


Figure A41-1. Dissolved titanium vs. pH at the Bell Minesite.

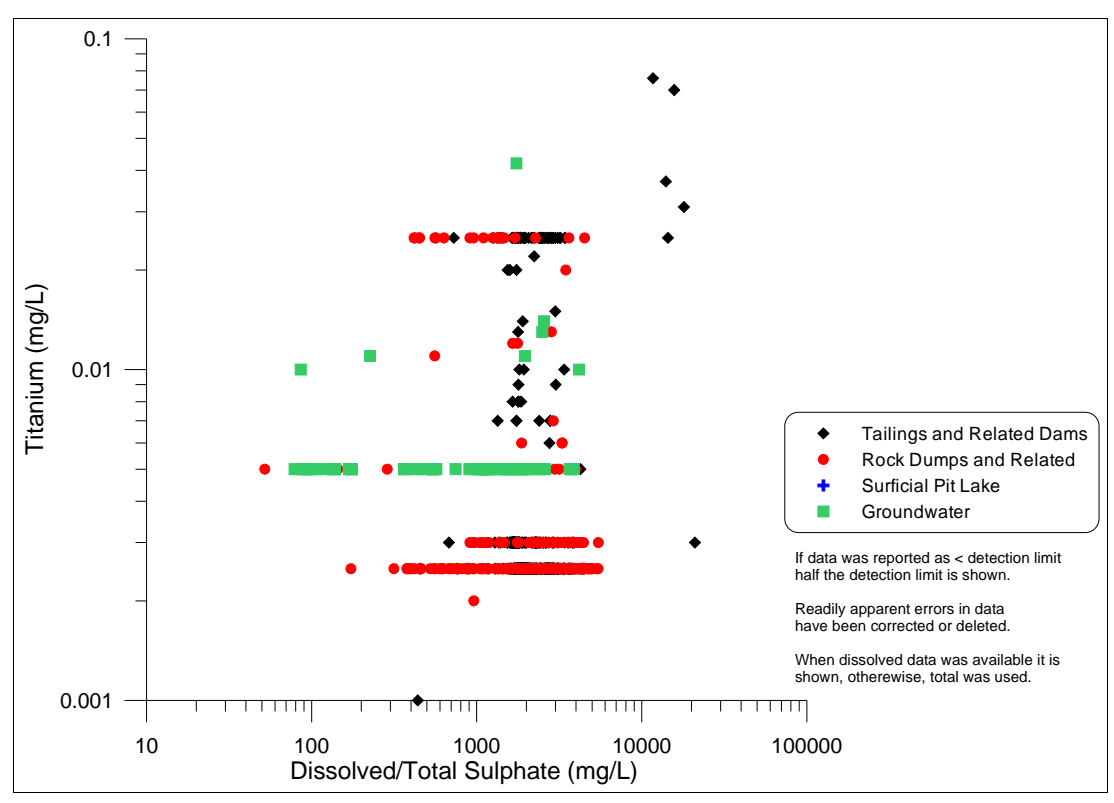


Figure A41-2. Dissolved titanium vs. sulphate at the Bell Minesite.

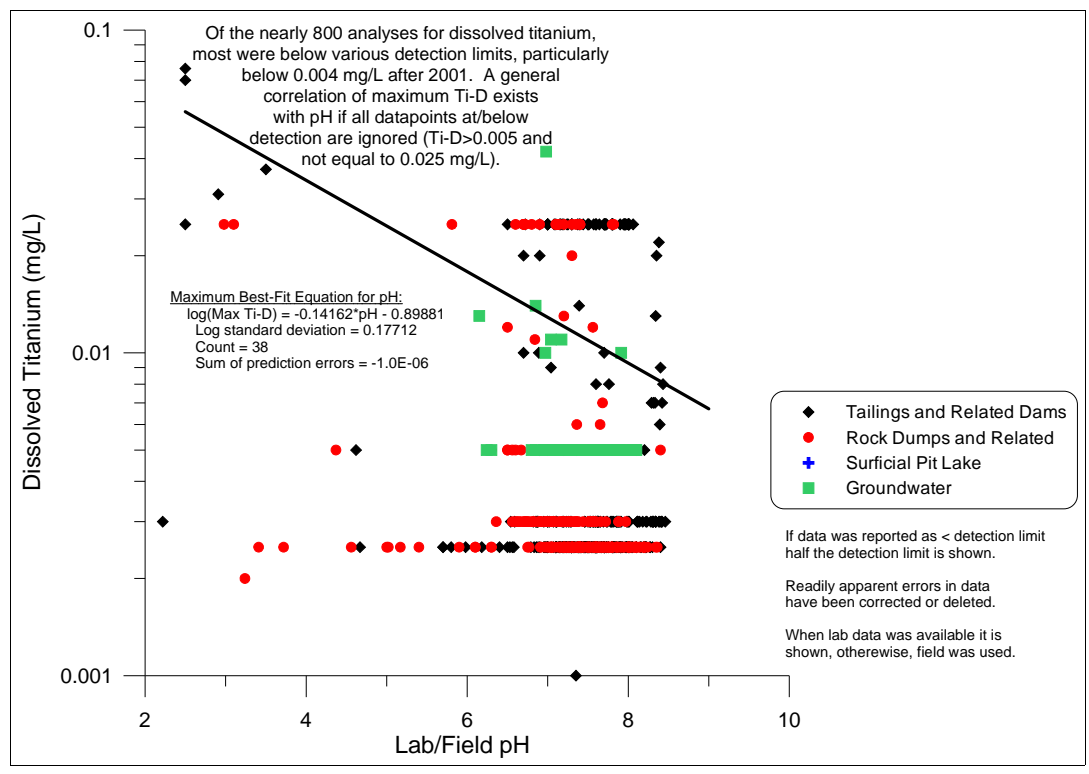


Figure A41-3. Best-fit equation for dissolved titanium vs. pH in the 2010 Bell EDCM.

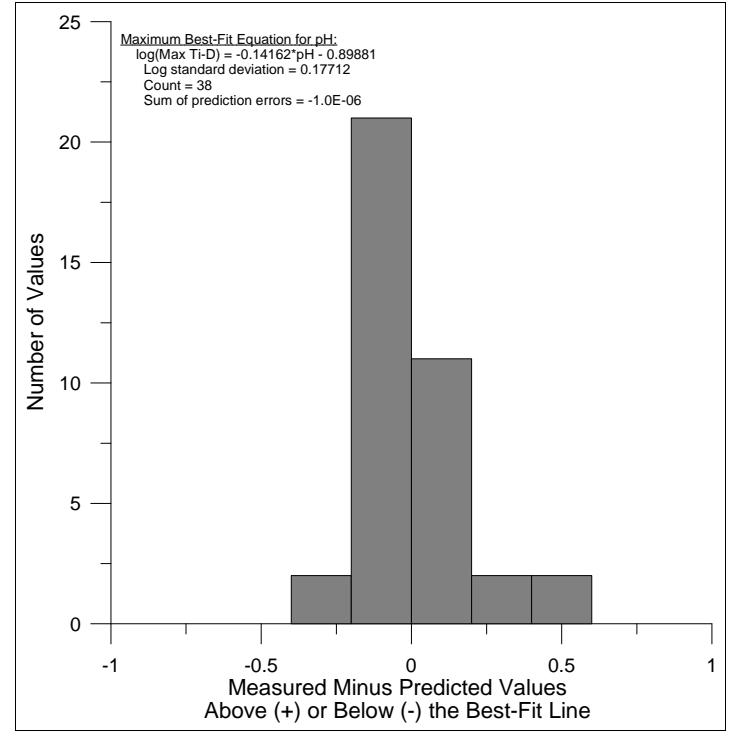


Figure A41-4. Statistical distribution of (measured-calculated) datapoints around the best-fit equation for maximum dissolved titanium.

Appendix A42. Dissolved Tungsten (W-D)

Notes:

Of the 73 analyses for dissolved tungsten in the Bell Minesite database, all were for near-neutral groundwater around mine closure in 1992, and most were at/below detection. As a result, no trends could be seen with the master parameters of pH (Figure A42-1) and sulphate (Figure A42-2). Thus, dissolved tungsten is considered generally undefined at Bell Mine (Figure A42-3).

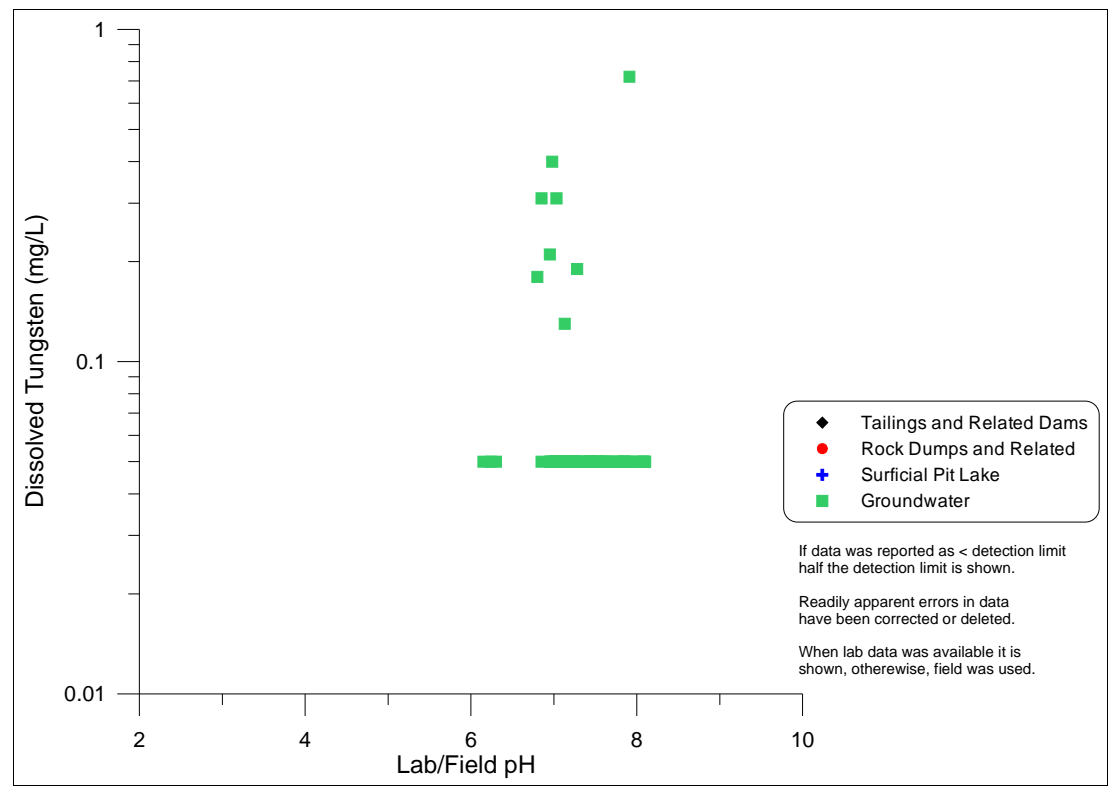


Figure A42-1. Dissolved tungsten vs. pH at the Bell Minesite.

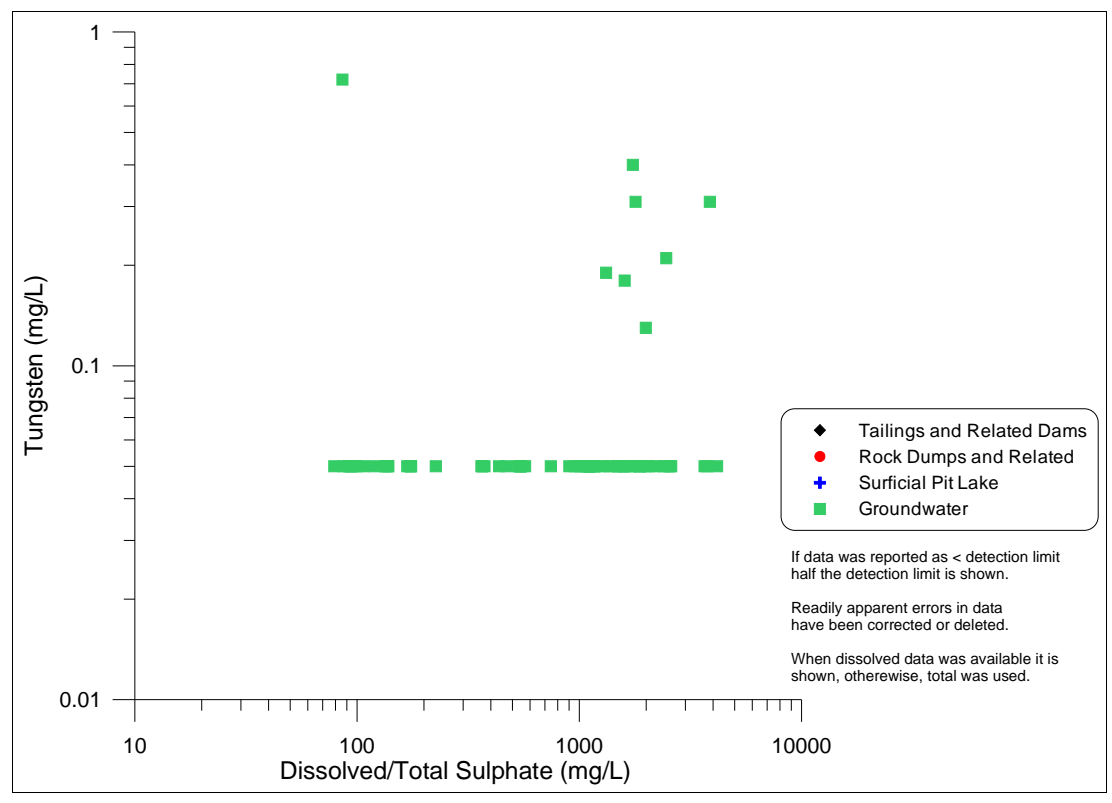


Figure A42-2. Dissolved tungsten vs. sulphate at the Bell Minesite.

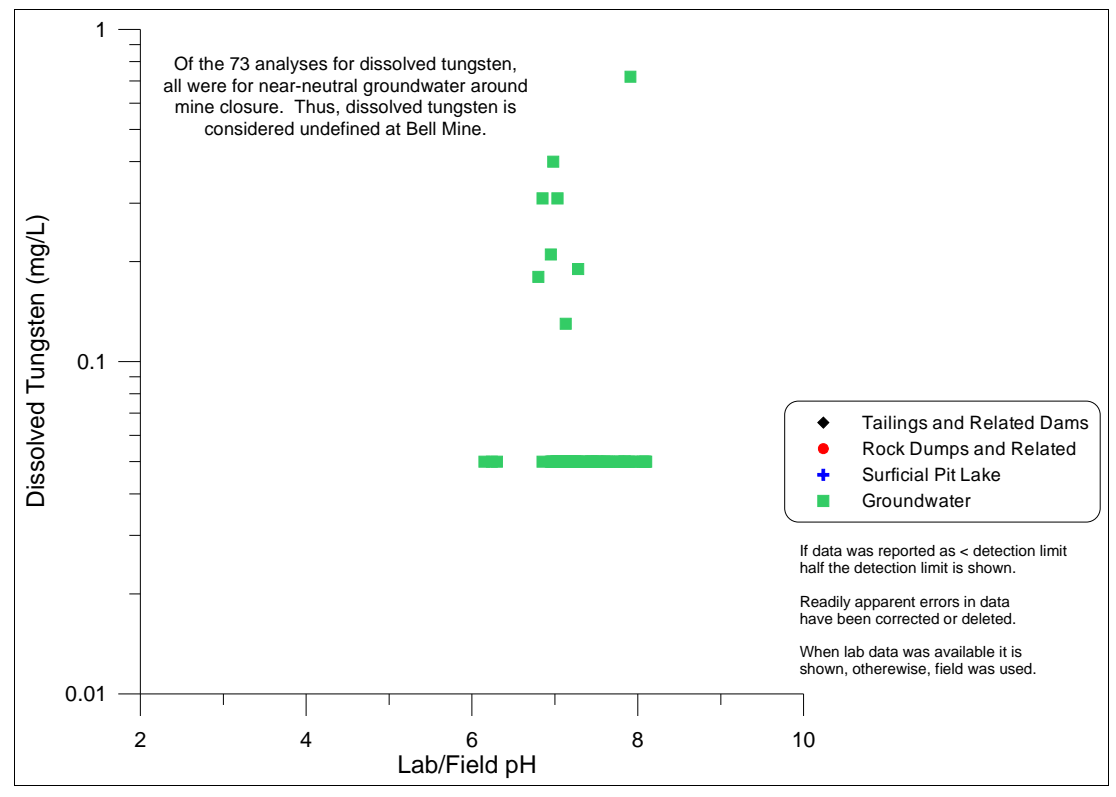


Figure A42-3. Best-fit equation for dissolved tungsten in the 2010 Bell EDCM.

Appendix A43. Dissolved Uranium (U-D)

Notes:

The nearly 70 analyses of dissolved uranium correlate better with sulphate (Figure A43-2) than with pH (Figure A43-1). The direct correlation with sulphate has a slope of roughly +1.3 (Figure A43-3), and the (measured-calculated) datapoints above and below this line form a general lognormal correlation (Figure A43-4).

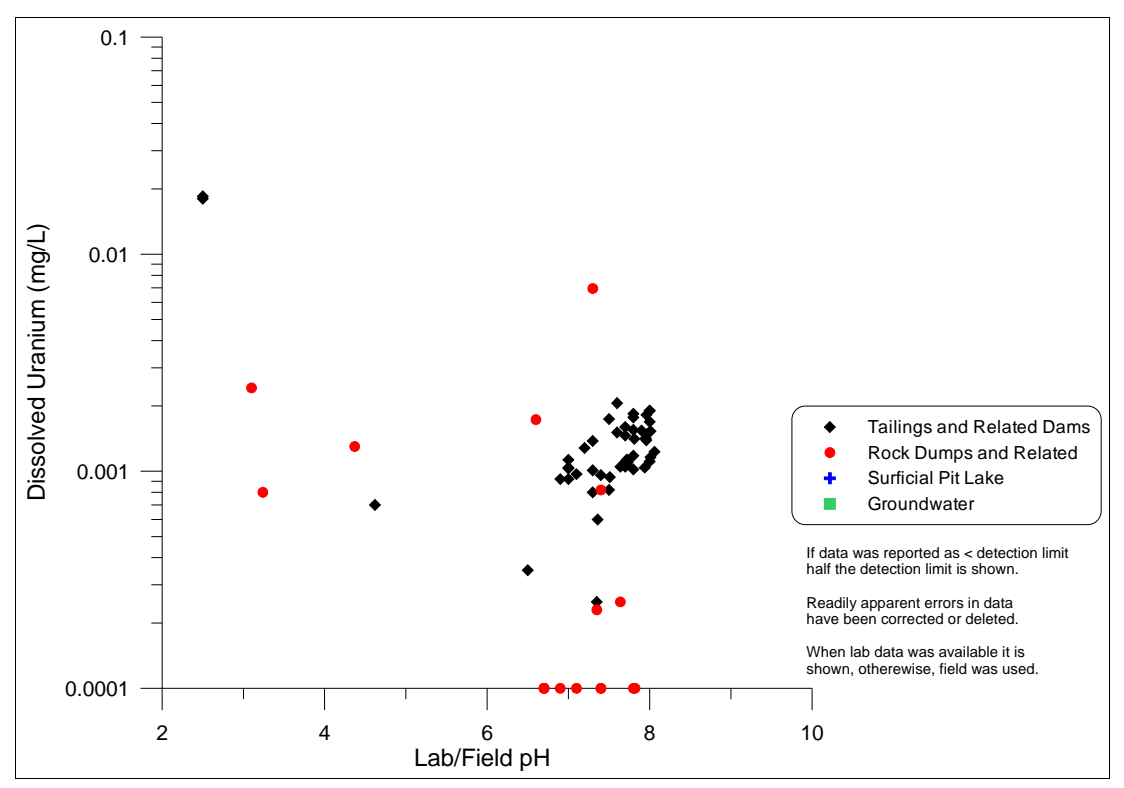


Figure A43-1. Dissolved uranium vs. pH at the Bell Minesite.

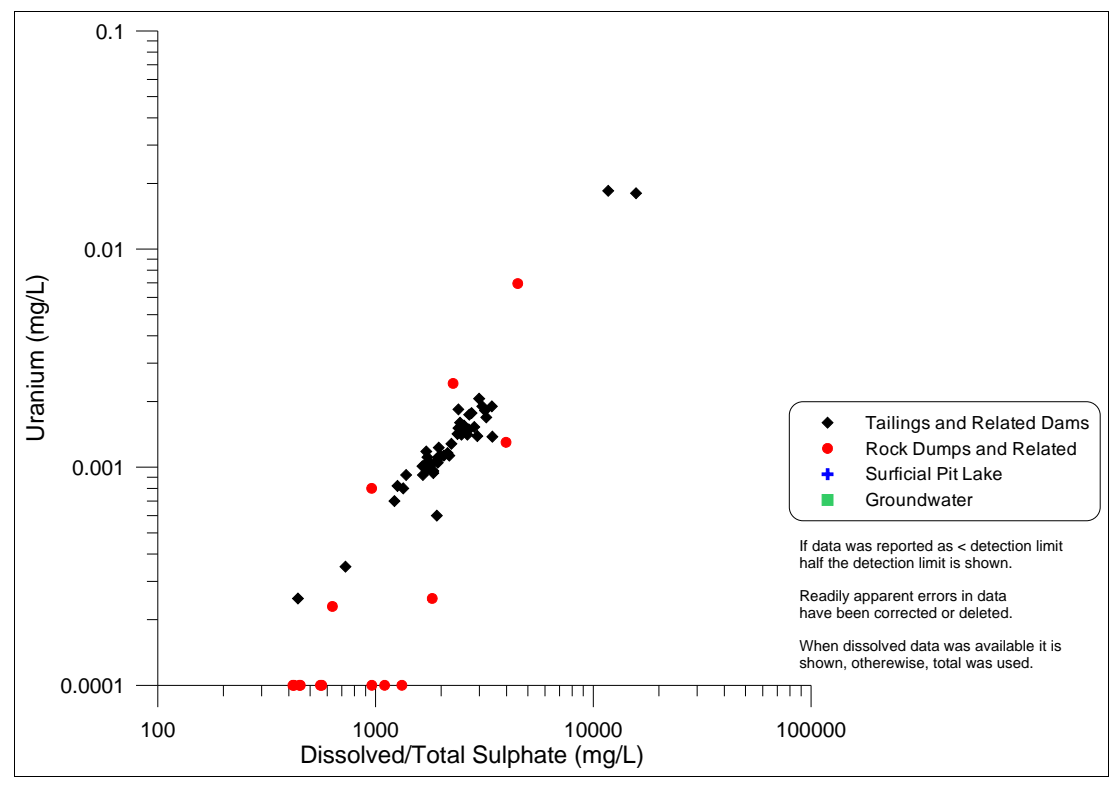


Figure A43-2. Dissolved uranium vs. sulphate at the Bell Minesite.

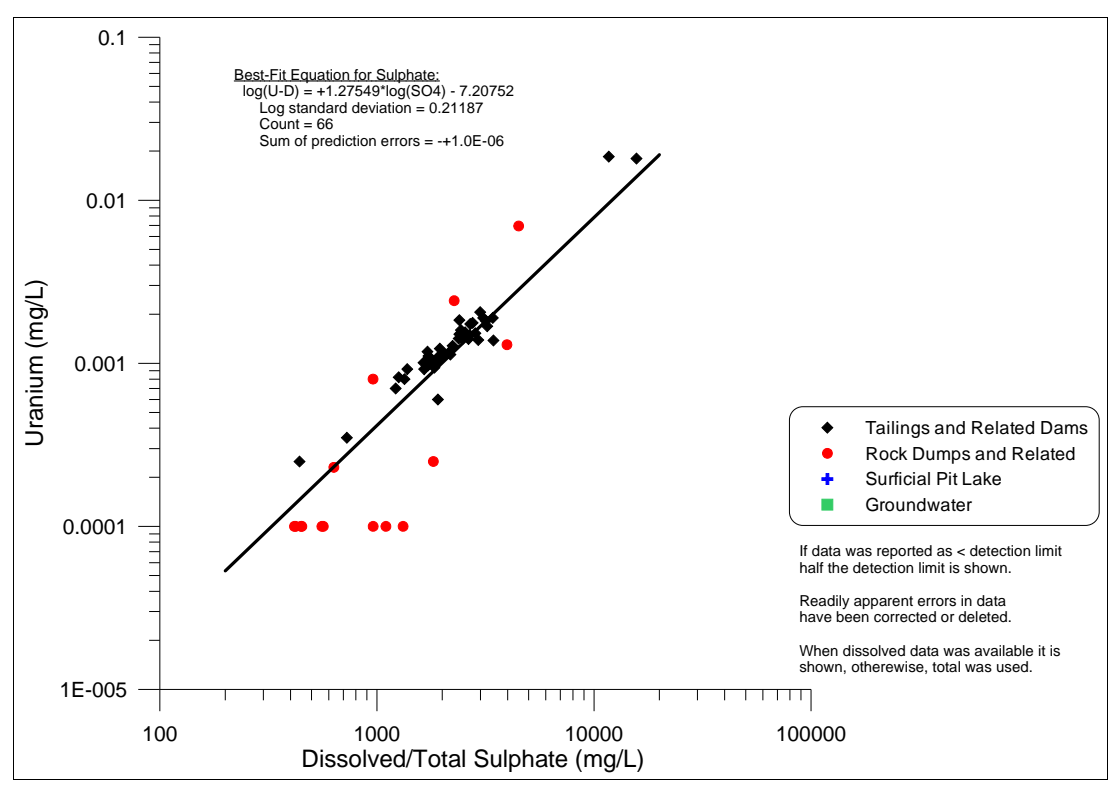


Figure A43-3. Best-fit equation for dissolved uranium vs. sulphate in the 2010 Bell EDCM.

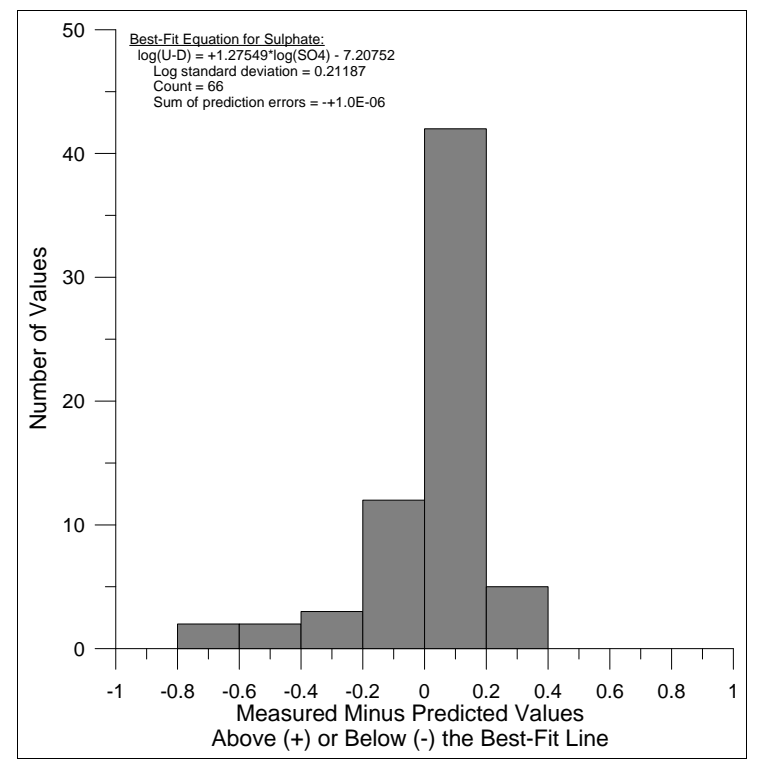


Figure A43-4. Statistical distribution of (measured-calculated) datapoints around the best-fit equation for dissolved uranium.

Appendix A44. Dissolved Vanadium (V-D)

Notes:

Of the nearly 800 analyses for dissolved vanadium in the Bell Minesite database, nearly all were below detection limits. The exceptions were the few at the most acidic pH (Figure A44-1) and highest sulphate (Figure A44-2).

Below pH 3.5 (Figure A44-3), seven datapoints provide an approximate correlation equation with a slope of -1.5. Above pH 3.5, vanadium is set at <0.01 mg/L.

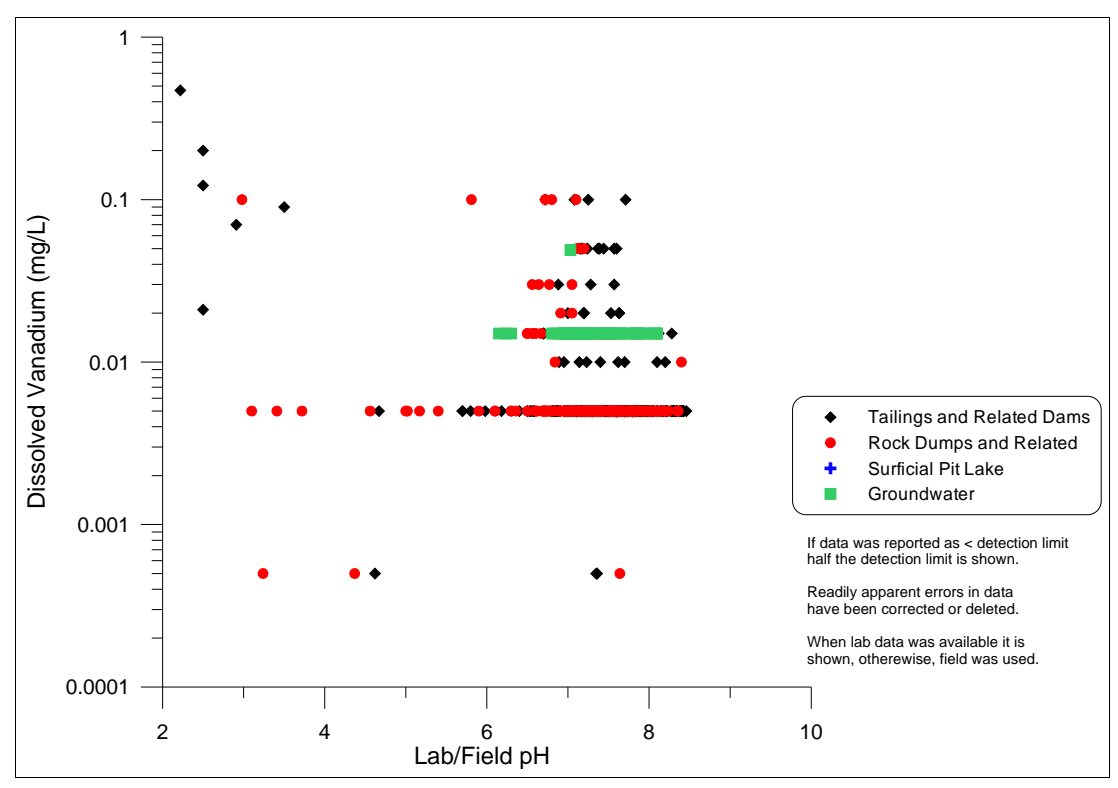


Figure A44-1. Dissolved vanadium vs. pH at the Bell Minesite.

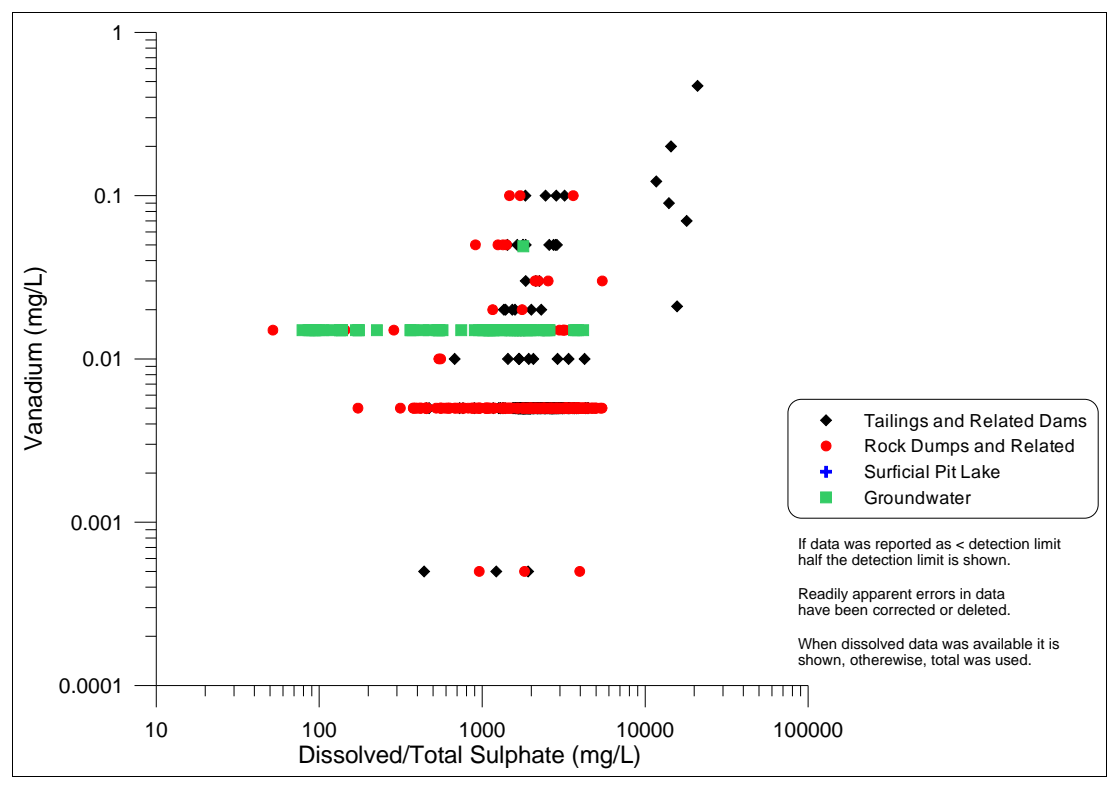


Figure A44-2. Dissolved vanadium vs. sulphate at the Bell Minesite.

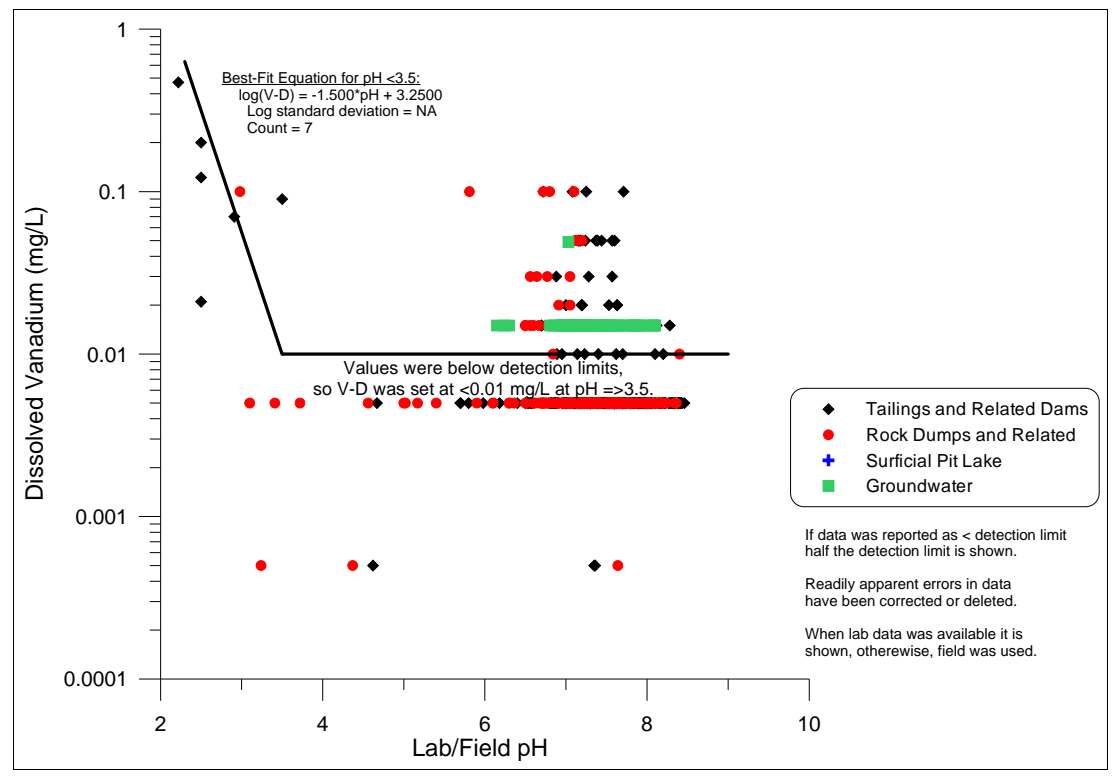


Figure A44-3. Best-fit equations for dissolved vanadium vs. pH in the 2010 Bell EDCM.

Appendix A45. Dissolved Zinc (Zn-D)

Notes:

Dissolved zinc, with roughly 4500 analyses spanning decades, is one of the frequently analyzed parameters at the Bell Minesite, in addition to pH, sulphate, dissolved copper, and dissolved iron.

Some correlation of dissolved zinc can be seen with the master parameters of pH (Figure A45-1) and sulphate (Figure A45-2). The correlation is better with pH, and the resulting best-fit line consists of three segments joined at pH 3.0 and 6.0 (Figure A45-3). The resulting (measured-calculated) datapoints above and below each of these segments form general lognormal distributions (Figures A45-4 to A45-6), with the segment above pH 6.0 having the largest standard deviation of 0.77426 log cycles.

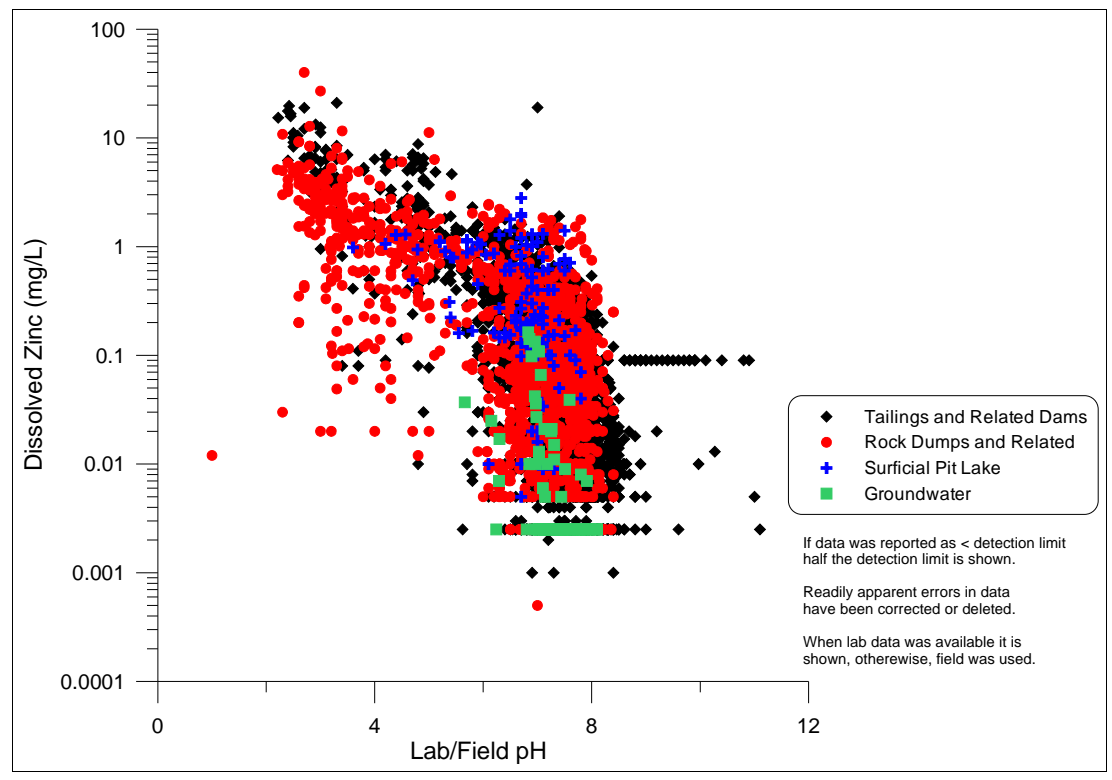


Figure A45-1. Dissolved zinc vs. pH at the Bell Minesite.

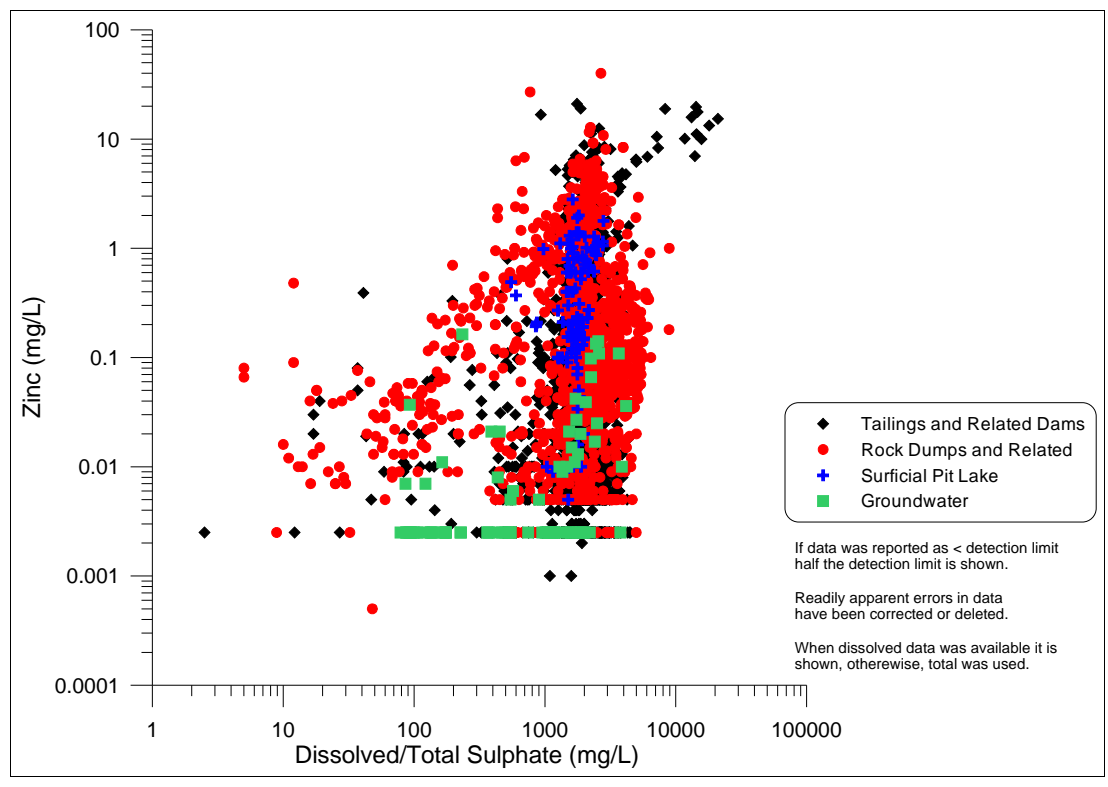


Figure A45-2. Dissolved zinc vs. sulphate at the Bell Minesite.

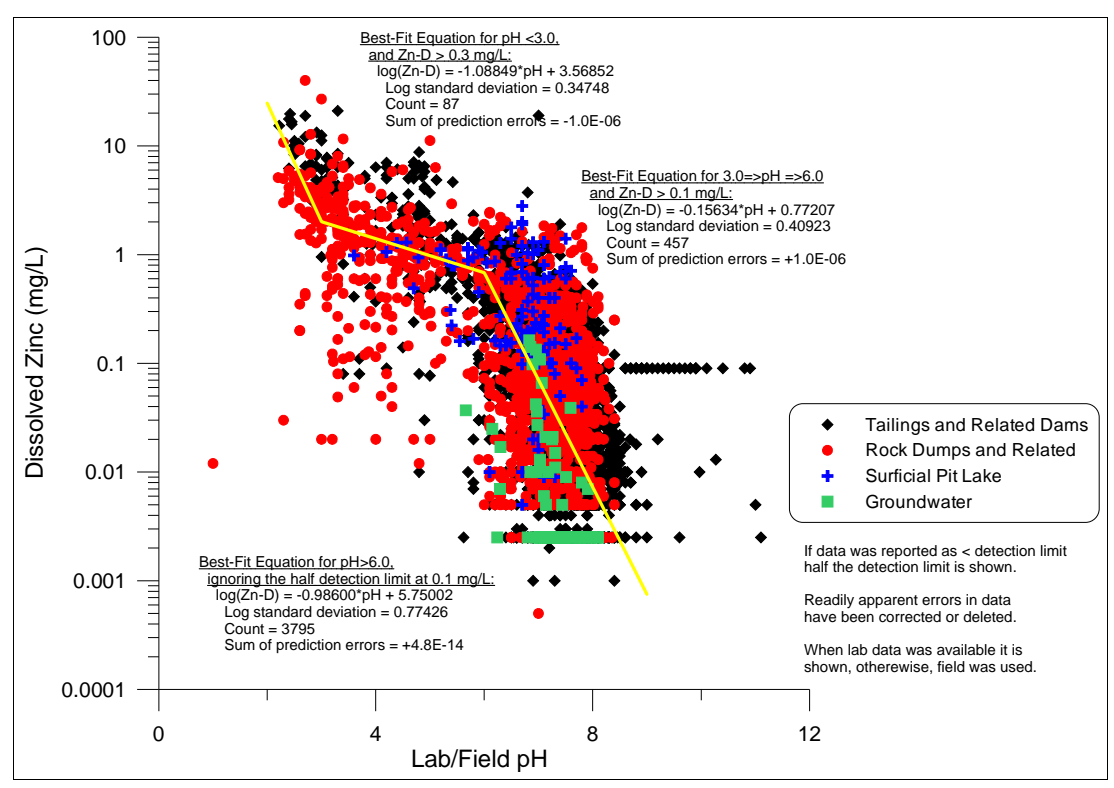


Figure A45-3. Best-fit equations for dissolved zinc vs. pH in the 2010 Bell EDCM.

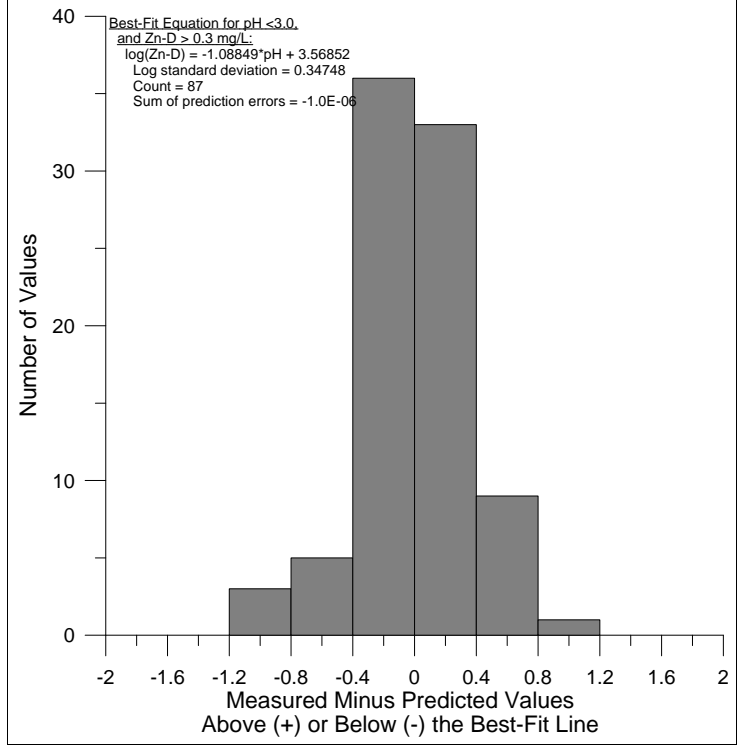


Figure A45-4. Statistical distribution of (measured-calculated) datapoints around the best-fit equation for dissolved zinc below pH 3.0.

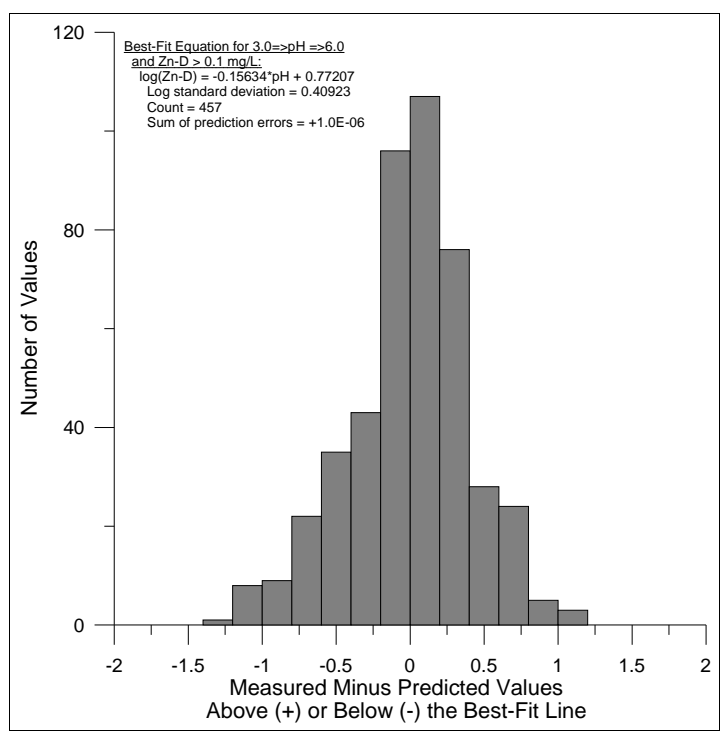


Figure A45-5. Statistical distribution of (measured-calculated) datapoints around the best-fit equation for dissolved zinc between pH 3.0 and 6.0.

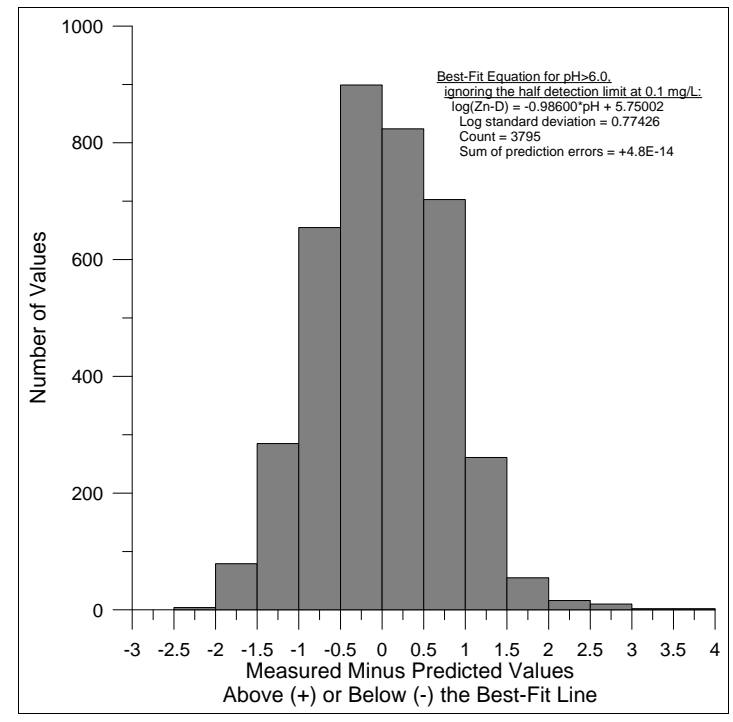


Figure A45-6. Statistical distribution of (measured-calculated) datapoints around the best-fit equation for dissolved zinc above pH 6.0.

Appendix A46. Dissolved Zirconium (Zr-D)

Notes:

The Bell Minesite drainage-chemistry database contains approximately 700 analyses of dissolved zirconium. Most of these were below various detection limits, so no clear correlations can be seen with the master parameters of pH (Figure A46-1) and sulphate (Figure A46-2).

Based on nine datapoints below pH 4.0 (Figure A46-3), an approximate best-fit equation has a slope of -1.5. Above pH 4.0, dissolved zirconium is set below its lowest detection limit: <0.001 mg/L.

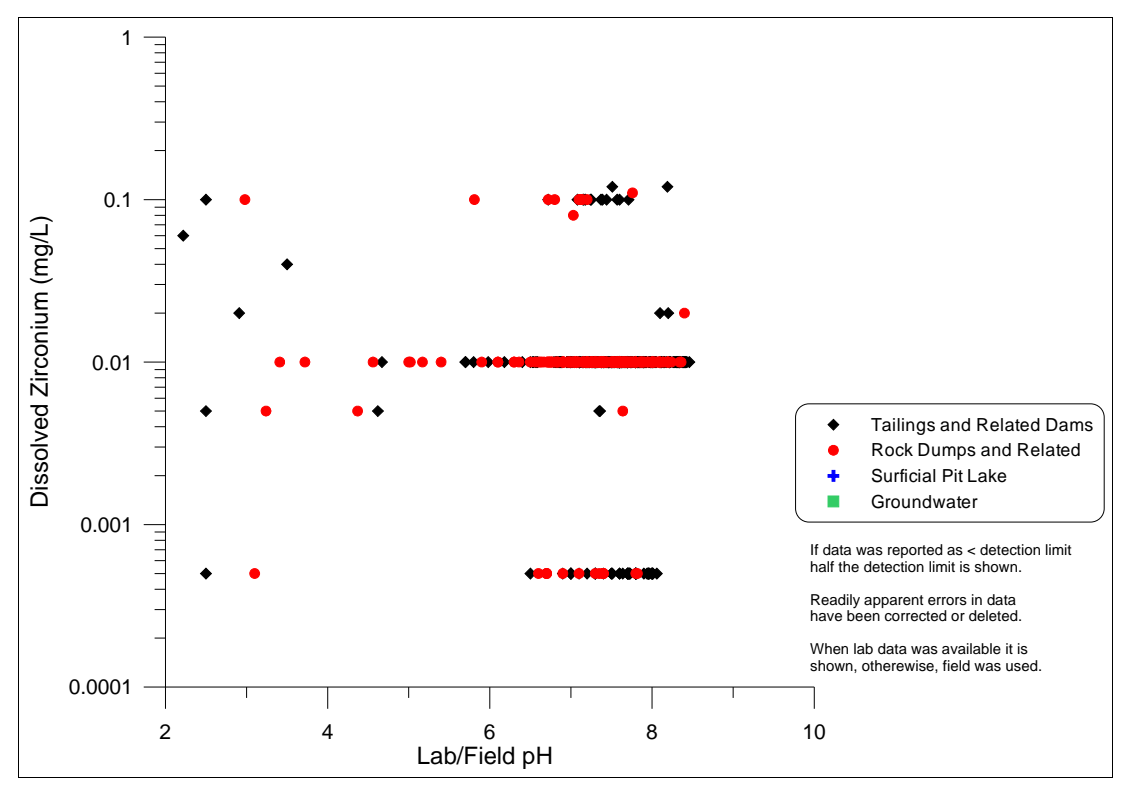


Figure A46-1. Dissolved zirconium vs. pH at the Bell Minesite.

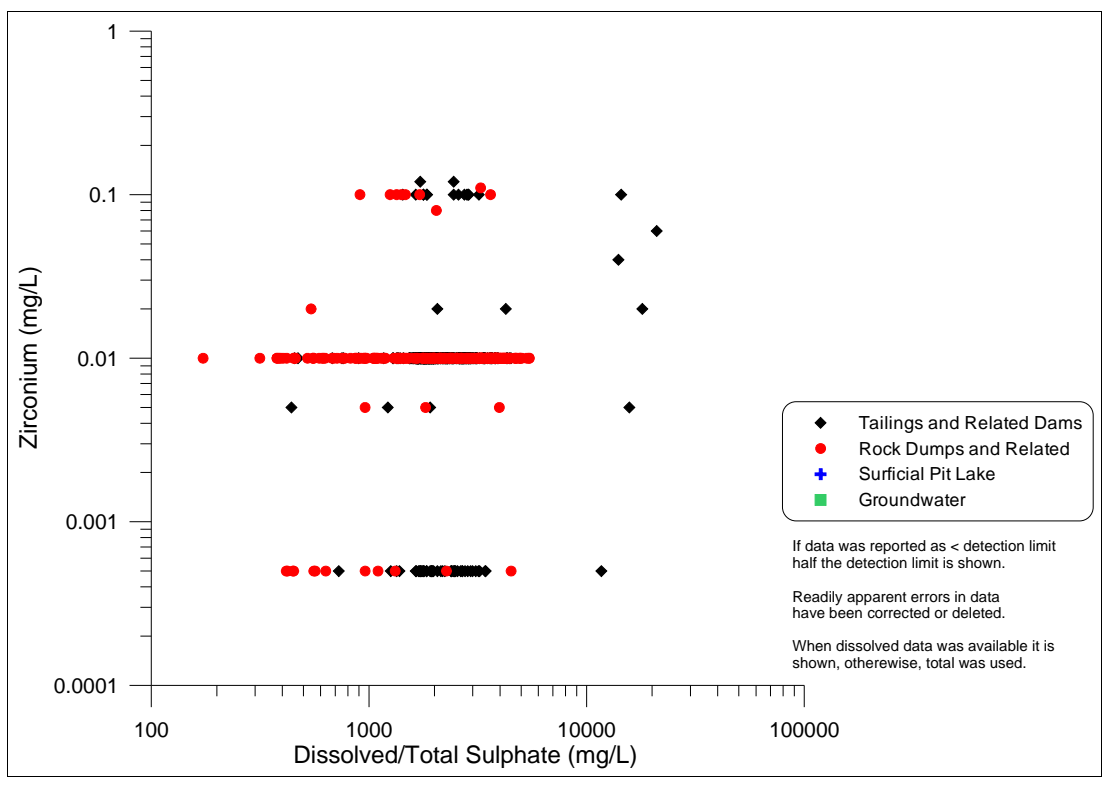


Figure A46-2. Dissolved zirconium vs. sulphate at the Bell Minesite.

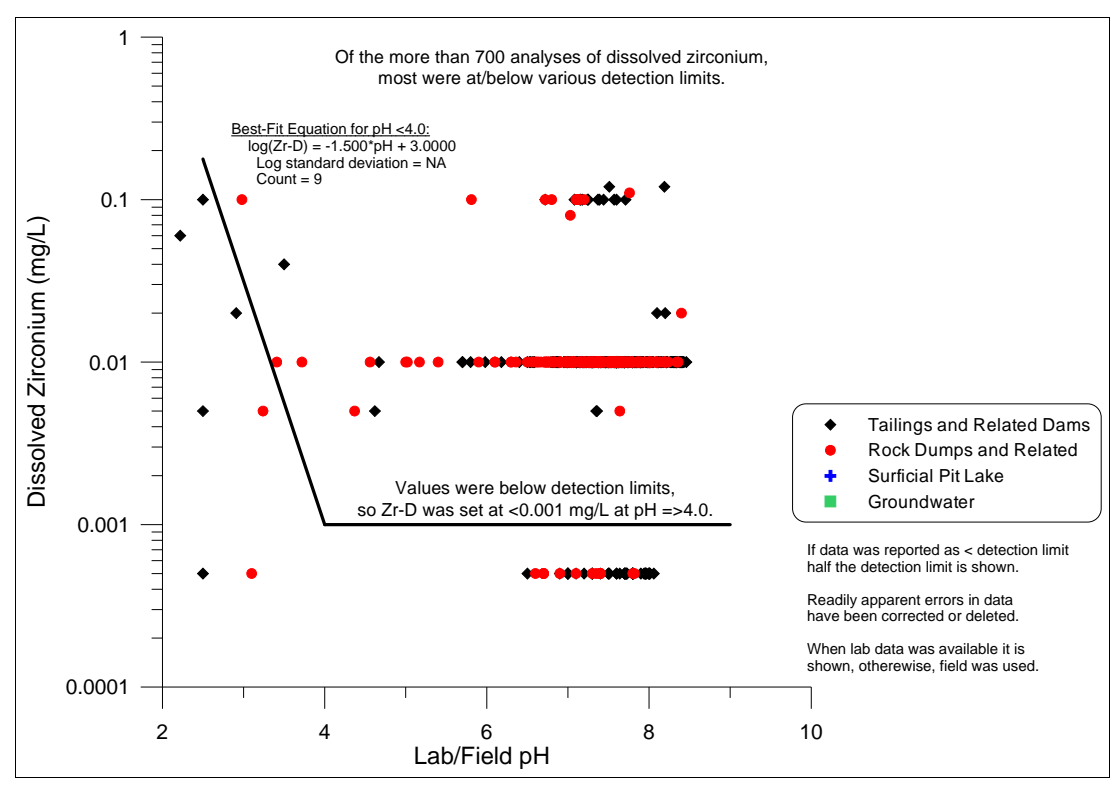


Figure A46-3. Best-fit equations for dissolved zirconium vs. pH in the 2010 Bell EDCM.